

Republic of Iraq
Ministry of Higher Education & Scientific Research
Baghdad University
College of Education for Pure Science / Ibn Al-Haitham



Study of Deformation Parameters for The Elements with Mass Numbers more than 100 ($A > 100$) which Included 30 Elements

A Thesis

Submitted to the Council of Collage of Education for Pure Science / Ibn Al-Haitham - Baghdad University in Partial Fulfillment of the Requirements for the Degree of Master of Science in Physics

By

Haider Abed Alzahera Zghaier
(B.Sc. 1995)

Supervisor

Asst. Prof. Dr. Sameera Ahmed Ebrahiem

2018 A.C.

1439 A.H

بِسْمِ اللّٰهِ الرَّحْمٰنِ الرَّحِیْمِ

﴿... رَبِّ أَوْزِعْنِي أَنْ أَشْكُرَ نِعْمَتَكَ الَّتِي أَنْعَمْتَ عَلَيَّ

وَعَلَىٰ وَالِدَيَّ وَأَنْ أَعْمَلَ صَالِحًا تَرْضَاهُ...﴾

صدق الله العلي العظيم

سورة الأحقاف الآية (15)

Supervisor Certification

I hereby certify that this thesis titled "*Study of Deformation Parameters for The Elements with Mass Numbers more Than 100 ($A > 100$) which Included 30 Elements*" was prepared under my supervision at Department of Physics, College of Education for Pure Science / Ibn Al-Haitham, Baghdad University, as a partial fulfillment of the requirements for the degree of Master of Science in Physics / Nuclear Physics.

Signature : 

Name : *Dr. Sameera Ahmed Ebrahiem*

Scientific position: *Assistant Professor*

Date: / / 2018

PDF Reducer Demo

In view of the available recommendation, I forward this thesis for debate by the examining committee.

Signature: 

Name: *Dr. Kareem Ali Jasim*

Scientific position: *Assistant Professor*

Head of Department of Physics

College of Education for Pure Science / Ibn Al-Haitham

Baghdad University

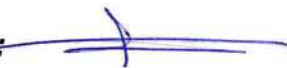
Date: / / 2018

Examining Committee Certification

We hereby certify that we have read this thesis titled "*Study of Deformation Parameters for The Elements with Mass Numbers more Than 100 ($A > 100$) which Included 30 Elements*" and as examining committee, we examined the student (*Haider Abed Alzahera Zghaier*) in its contents and what is related to it, and that in our opinion it is adequate for the partial fulfillment of the requirements for the Degree of Master of Science in Physics.

Signature: 
Name: Dr. Mustafa Kamel Jassim
Scientific position: Assistant Professor
Date: 18/2/2018
(Chairman)

Signature: 
Name: Dr. Intesar H. Hashem
Scientific position: Assistant Professor
Date: / / 2018
(Member)

Signature: 
Name: Dr. Nissan Saud Oraibi
Scientific position: Lecturer
Date: / / 2018
(Member)

Signature: 
Nam: Dr. Sameera Ahmed Ebraheem
Scientific position: Assistant Professor
Date: / / 2018
(Member and Supervisor)

Approved by the University Committee of postgraduate studies.


Prof. Dr. Khalid Fahad Ali
The Dean of College of Education
For Pure Science / Ibn Al-Haitham
Date: / / 2018

Dedication

To whom God has blessed with honor and glory... To the one who taught me tenderness without waiting... To whom I am proud of..... My Father

To the one who were the secret of my success and the fountain of tenderness... My Mother... Thanks for always being there with me.

To who has encouraged me all the way and through her encouragement has made it sure that I give it all it takes to finish the task which I have started..... My Wife.

ACKNOWLEDGEMENT

"Be a scientist ... If you cannot, be educated ... if you cannot, love scientists ... if not, you cannot hate them"

After a journey of research and effort and diligence culminated in the completion of this research, I thank God Almighty on His grace, which gave us, He is the Almighty.

I cannot help except to express my thanks and appreciation for supervisor Dr. "Sameera Ahmed Ebrhiem" for what she gave me of effort, advice and knowledge throughout this research.

I would like to express my thanks to the Dean of the College of Education for Pure Science / Ibn Al-Haitham.

I would like to express my thanks to the Head and the Staff of Department of Physics College of Education for Pure Science / Ibn Al-Haitham University of Baghdad for their help and support.

To those who helped me in my research, and a light that shines upon the darkness that sometimes stood in my way. To those who planted optimism in our path and provided us with assistance, and information, I have all the thanks, in particular my study colleague and my teacher Dr. Ahmed Fadiel for all his help and knowledge.

Although I have conducted this new research by myself, I wouldn't felt the pleasure of hard work and the relief of obtaining the fruitful results without the help, assistance and encouragement of all wonderful people who supported me in this journey

. Finally, I would like to thank my family, my father, my Mother, my wife, brothers and sisters and my friends for their unlimited support in my studies and research.

Haider

ABSTRACT

The present research focus on the study of the even- even nuclei forms with mass numbers greater than 100 ($A > 100$) for (30) elements, which includes the study of deformation parameters β_2 derived from the reduced electric transition probability $B(E2) \uparrow$ based on the energy of the first excited state 2^+ , and deformation parameter δ from intrinsic electric quadrupole moments Q_0 and roots mean square radii $\langle r^2 \rangle^{1/2}$.

The diversity of nuclei forms for selected isotopes and their differences were observed by plotting two-dimensional shapes of single element isotopes in addition to drawing three-dimensional shapes (axially symmetric) to distinguish between them by using semi-major (a) and semi minor (b) axes.

The behavior of deformation parameters (β_2, δ) in even-even nuclei provided good information about magic and closed shell nuclei properties such that, when counted and plotted as a function of neutron number N , spherical shapes with minimum values of these parameters were observed at magic neutron number ($N= 50, 82, \text{ and } 126$).

For sake of comparison, the reduced electric transition $B(E2) \uparrow$ values of the present work and the predicted values of SSANM show a little variation between these results, since the present work is based on using of the Global Best Fit (GBF) equation when compared with the SSANM values, even though they show the same behavior in most of selected elements.

In addition to that, the values of ΔR (the difference between the semi-major and semi-minor axes (a, b)) were calculated using three different methods, and it was found that these results were fairly close.

Roots mean square radii $\langle r^2 \rangle^{1/2}$ were also calculated and compared with theoretical values where the results were in good agreement with the theoretical values.

At the end of our study, it was found that all the nuclei of the isotopes of the selected elements with ($A > 100$) were found to be distorted, which are prolate shapes, this distortion is significant in the regions ($150 \leq A \leq 190$) as well as ($A \geq 220$) except the isotopes that possess protons and / or neutrons equal to the magical numbers where the forms of these nucleuses possess spherically symmetric shapes and have a total angular momentum of zero, and are especially stable.

All the calculations and figures were done using the Matlab program version (8.1) (2013).

Contents

Subject		Page
Abstract		I
Contents		III
List of Abbreviations		VII
List of Tables		IX
List of Figures		XIV
Chapter One: Introduction		
1-1	Introduction	1
1-2	Nuclear Structure	1
1-3	General Properties of Nuclei	2
1-3-1	The Mass Number	2
1-3-2	The Binding Energy	3
1-3-3	Nuclear Radius	3
1-4	Nuclear Models	4
1-4-1	Liquid Drop Model	4
1-4-1-1	Semi Empirical Mass Formula	4
1-4-2	The Shell Model	6
1-4-2-1	Nuclear Magic Number	7
1-4-3	The Collective Model	9
1-5	Previous Studies	10
1-6	The Aim of the Present Work	15

Chapter Two: Theory		
2-1	Nuclear Shape	16
2-2	Nuclear Surface Deformations	16
2-3	Types of Multipole Deformations	18
2-4	The Root Mean Square Charge Radius (Isotopes Shift)	19
2-5	Electric Quadrupole Moment	20
2-6	Quadrupole Deformations	22
2-7	Electromagnetic Transition	24
2-7-1	The Reduced Electric Quadrupole Transition Probability $B(E2) \uparrow$	24
2-7-2	Experimental and Theoretical Predictions of $B(E2) \uparrow$	26
2-7-2-1	Experimental Global Best Fit (GBF)	26
2-7-2-2	Theoretical Predictions	27
Chapter Three: Calculations & Results		
3-1	Calculations	28
3-1-1	The Deformation Parameters(β_2)	28
3-1-2	The Deformation Parameters (δ)	28
3-1-3	Root Mean Square Charge Radius $\langle r^2 \rangle^{1/2}$	29
3-1-4	Semi-Major and Semi-Minor Axis (a, b) and The Deference Between Them ΔR	29
3-2	The Results	29
Chapter Four : Discussions & Conclusions		
4-1	Introduction	96
4-1-1	Zirconium Isotopes $^{102-104}_{40}\text{Zr}$	97
4-1-2	Molybdenum Isotopes $^{102-108}_{42}\text{Mo}$	98
4-1-3	Ruthenium Isotopes $^{102-114}_{44}\text{Ru}$	98

4-1-4	Palladium Isotopes $^{102-118}_{46}\text{Pd}$	99
4-1-5	Cadmium Isotopes $^{102-126}_{48}\text{Cd}$	99
4-1-6	Tin Isotopes $^{102-134}_{50}\text{Sn}$	100
4-1-7	Tellurium Isotopes $^{108-138}_{52}\text{Te}$	101
4-1-8	Barium Isotopes $^{118-148}_{56}\text{Ba}$	101
4-1-9	Cerium Isotopes $^{124-152}_{58}\text{Ce}$	102
4-1-10	Neodymium Isotopes $^{128-156}_{60}\text{Nd}$	102
4-1-11	Samarium Isotopes $^{130-160}_{62}\text{Sm}$	103
4-1-12	Gadolinium Isotopes $^{138-162}_{64}\text{Gd}$	104
4-1-13	Dysprosium Isotopes $^{142-166}_{66}\text{Dy}$	104
4-1-14	Erbium Isotopes $^{144-172}_{68}\text{Er}$	105
4-1-15	Ytterbium Isotopes $^{152-178}_{70}\text{Yb}$	105
4-1-16	Hafnium Isotopes $^{154-184}_{72}\text{Hf}$	106
4-1-17	Tungsten Isotopes $^{162-190}_{74}\text{W}$	107
4-1-18	Osmium Isotopes $^{164-196}_{76}\text{Os}$	108
4-1-19	Platinum Isotopes $^{168-200}_{78}\text{Pt}$	108
4-1-20	Mercury Isotopes $^{176-206}_{80}\text{Hg}$	109
4-1-21	Lead Isotopes $^{182-214}_{82}\text{Pb}$	109
4-1-22	Polonium Isotopes $^{192-218}_{84}\text{Po}$	110
4-1-23	Radon Isotopes $^{198-222}_{86}\text{Rn}$	111
4-1-24	Radium Isotopes $^{206-230}_{88}\text{Ra}$	111
4-1-25	Thorium Isotopes $^{216-234}_{90}\text{Th}$	112
4-1-26	Uranium Isotopes $^{226-240}_{92}\text{U}$	113
4-1-27	Plutonium Isotopes $^{236-246}_{94}\text{Pu}$	113

4-1-28	Curium Isotopes $^{238-250}_{96}\text{Cm}$	114
4-1-29	Californium Isotopes $^{244-252}_{98}\text{Cf}$	114
4-1-30	Fermium Isotopes $^{248-256}_{100}\text{Fm}$	115
4-2	Conclusions	116
4-3	Suggestion and Future Work	116
	References	117
	Appendix	122

List of Abbreviations

Abbreviation	Meaning
Z	<i>Atomic Number</i>
N	<i>Neutron Number</i>
A	<i>Mass Number</i>
m_n, m_p	<i>Mass of Neutron and Proton</i>
c	<i>Velocity of Light</i>
π	<i>Parity</i>
E_γ	<i>Gamma Energy</i>
keV	<i>kilo electron Volt</i>
\hbar	<i>Reduced Blank Constant</i>
B	<i>The Binding Energy</i>
R	<i>Average Nuclear Radius</i>
fm	<i>Fermi</i>
a_v	<i>The Volume Term</i>
a_s	<i>The Surface Term</i>
a_c	<i>The Protons Coulomb Repulsion Term</i>
$\delta(A)$	<i>The Term is a Quantum Pairing Term</i>
S_n & S_p	<i>The Separation Energies of the Proton and Neutron</i>
a, b	<i>Semi- Major and Semi- Minor Axes</i>
ΔR	<i>The Difference Between Semi- Minor and Semi- Major Axes</i>
$R(\theta, \phi, t)$	<i>Indicates the Nuclear Radius in the Direction (θ, ϕ) at Time t</i>
$\alpha_{\lambda\mu}$	<i>The Deformation Variables.</i>
λ	<i>The Multipole or Mode of Nuclear Motion</i>
μ	<i>The Projection of λ on the z-axis</i>
$Y(\theta, \phi)$	<i>The Spherical Harmonic</i>
β_2	<i>Deformation Parameter</i>
δ	<i>Deformation Parameter</i>
$\langle r^2 \rangle^{1/2}$	<i>Root Mean Square Charge Radius</i>
$\langle r^2 \rangle^A$	<i>The Mean Square Charge Radius of Radioactive Isotope A</i>
$\langle r^2 \rangle^{A'}$	<i>The Mean Square Charge Radius of Stable Reference Isotope A'</i>
$\delta \langle r^2 \rangle^{A'A}$	<i>The Radius Change Between Isotopes A and A'</i>
$\rho(r)$	<i>The Charge Density Distribution of the Protons</i>
r	<i>Charge Radius.</i>
Q_0	<i>Intrinsic Quadrupole Moments</i>
J	<i>The Total Nucleus Spin</i>

<i>Abbreviation</i>	<i>Meaning</i>
K	<i>The Projection of J onto the z-axis in the Body Fixed Frame (Symmetry Axis of the Nucleus)</i>
$B(E2) \uparrow$	<i>Reduced Electric Transition Probability</i>
0^+	<i>Ground State</i>
2^+	<i>First Excited State</i>
J_i, J_f	<i>Initial and Final Total Angular Momentum</i>
$\langle J_i K ; 20 J_f K \rangle$	<i>The Clebsch-Gordan Coefficient</i>
τ	<i>The Mean Lifetime</i>
<i>(GBF)</i>	<i>Global Best Fit</i>
<i>(SSANM)</i>	<i>Single Shell Asymptotic Nilsson Model</i>

List of Tables

Tables	Page
Table (3-1): Mass Number (A), Neutron Number (N), Gamma Energy of the First Excited State 2^+ (E_γ), Square Nuclear Average Radius (R^2), Reduced Electric Transition Probability $B(E2)$ \uparrow in unit of e^2b^2 , Intrinsic Quadrupole Moment (Q_o) in unit of barn, and Deformation Parameters (β_2, δ) for $_{40}\text{Zr}$ Isotopes.	30
Table (3-2): Mass Number (A), Neutron Number (N), Gamma Energy of the First Excited State 2^+ (E_γ), Square Nuclear Average Radius (R^2), Reduced Electric Transition Probability $B(E2)$ \uparrow in unit of e^2b^2 , Intrinsic Quadrupole Moment (Q_o) in unit of barn, and Deformation Parameters (β_2, δ) for $_{42}\text{Mo}$ Isotopes.	30
Table (3-3): Mass Number (A), Neutron Number (N), Gamma Energy of the First Excited State 2^+ (E_γ), Square Nuclear Average Radius (R^2), Reduced Electric Transition Probability $B(E2)$ \uparrow in unit of e^2b^2 , Intrinsic Quadrupole Moment (Q_o) in unit of barn, and Deformation Parameters (β_2, δ) for $_{44}\text{Ru}$ Isotopes.	31
Table (3-4) Mass Number (A), Neutron Number (N), Gamma Energy of the First Excited State 2^+ (E_γ), Square Nuclear Average Radius (R^2), Reduced Electric Transition Probability $B(E2)$ \uparrow in unit of e^2b^2 , Intrinsic Quadrupole Moment (Q_o) in unit of barn, and Deformation Parameters (β_2, δ) for $_{46}\text{Pd}$ Isotopes.	31
Table (3-5): Mass Number (A), Neutron Number (N), Gamma Energy of the First Excited State 2^+ (E_γ), Square Nuclear Average Radius (R^2), Reduced Electric Transition Probability $B(E2)$ \uparrow in unit of e^2b^2 , Intrinsic Quadrupole Moment (Q_o) in unit of barn, and Deformation Parameters (β_2, δ) for $_{48}\text{Cd}$ Isotopes.	32
Table (3-6): Mass Number (A), Neutron Number (N), Gamma Energy of the First Excited State 2^+ (E_γ), Square Nuclear Average Radius (R^2), Reduced Electric Transition Probability $B(E2)$ \uparrow in unit of e^2b^2 , Intrinsic Quadrupole Moment (Q_o) in unit of barn, and Deformation Parameters (β_2, δ) for $_{50}\text{Sn}$ Isotopes.	33
Table (3-7): Mass Number (A), Neutron Number (N), Gamma Energy of the First Excited State 2^+ (E_γ), Square Nuclear Average Radius (R^2), Reduced Electric Transition Probability $B(E2)$ \uparrow in unit of e^2b^2 , Intrinsic Quadrupole Moment (Q_o) in unit of barn, and Deformation Parameters (β_2, δ) for $_{52}\text{Te}$ Isotopes.	34
Table (3-8): Mass Number (A), Neutron Number (N), Gamma Energy of the First Excited State 2^+ (E_γ), Square Nuclear Average Radius (R^2), Reduced Electric Transition Probability $B(E2)$ \uparrow in unit of e^2b^2 , Intrinsic Quadrupole Moment (Q_o) in unit of barn, and Deformation Parameters (β_2, δ) for $_{56}\text{Ba}$ Isotopes.	35
Table (3-9): Mass Number (A), Neutron Number (N), Gamma Energy of the First Excited State 2^+ (E_γ), Square Nuclear Average Radius (R^2), Reduced Electric Transition Probability $B(E2)$ \uparrow in unit of e^2b^2 , Intrinsic Quadrupole Moment (Q_o) in unit of barn, and Deformation Parameters (β_2, δ) for $_{58}\text{Ce}$ Isotopes.	36
Table (3-10): Mass Number (A), Neutron Number (N), Gamma Energy of the First Excited State 2^+ (E_γ), Square Nuclear Average Radius (R^2), Reduced Electric Transition Probability $B(E2)$ \uparrow in unit of e^2b^2 , Intrinsic Quadrupole Moment (Q_o) in unit of barn, and Deformation Parameters (β_2, δ) for $_{60}\text{Nd}$ Isotopes.	37
Table (3-11): Mass Number (A), Neutron Number (N), Gamma Energy of the First Excited State 2^+ (E_γ), Square Nuclear Average Radius (R^2), Reduced Electric Transition Probability $B(E2)$ \uparrow in unit of e^2b^2 , Intrinsic Quadrupole Moment (Q_o) in unit of barn, and Deformation Parameters (β_2, δ) for $_{62}\text{Sm}$ Isotopes.	38

Table (3-12): Mass Number (A), Neutron Number (N), Gamma Energy of the First Excited State 2^+ (E_γ), Square Nuclear Average Radius (R^2), Reduced Electric Transition Probability $B(E2)$ ↑ in unit of e^2b^2 , Intrinsic Quadrupole Moment (Q_o) in unit of barn, and Deformation Parameters (β_2, δ) for ^{64}Gd Isotopes.	39
Table (3-13): Mass Number (A), Neutron Number (N), Gamma Energy of the First Excited State 2^+ (E_γ), Square Nuclear Average Radius (R^2), Reduced Electric Transition Probability $B(E2)$ ↑ in unit of e^2b^2 , Intrinsic Quadrupole Moment (Q_o) in unit of barn, and Deformation Parameters (β_2, δ) for ^{66}Dy Isotopes.	40
Table (3-14): Mass Number (A), Neutron Number (N), Gamma Energy of the First Excited State 2^+ (E_γ), Square Nuclear Average Radius (R^2), Reduced Electric Transition Probability $B(E2)$ ↑ in unit of e^2b^2 , Intrinsic Quadrupole Moment (Q_o) in unit of barn, and Deformation Parameters (β_2, δ) for ^{68}Er Isotopes.	41
Table (3-15): Mass Number (A), Neutron Number (N), Gamma Energy of the First Excited State 2^+ (E_γ), Square Nuclear Average Radius (R^2), Reduced Electric Transition Probability $B(E2)$ ↑ in unit of e^2b^2 , Intrinsic Quadrupole Moment (Q_o) in unit of barn, and Deformation Parameters (β_2, δ) for ^{70}Yb Isotopes.	42
Table (3-16): Mass Number (A), Neutron Number (N), Gamma Energy of the First Excited State 2^+ (E_γ), Square Nuclear Average Radius (R^2), Reduced Electric Transition Probability $B(E2)$ ↑ in unit of e^2b^2 , Intrinsic Quadrupole Moment (Q_o) in unit of barn, and Deformation Parameters (β_2, δ) for ^{72}Hf Isotopes.	43
Table (3-17): Mass Number (A), Neutron Number (N), Gamma Energy of the First Excited State 2^+ (E_γ), Square Nuclear Average Radius (R^2), Reduced Electric Transition Probability $B(E2)$ ↑ in unit of e^2b^2 , Intrinsic Quadrupole Moment (Q_o) in unit of barn, and Deformation Parameters (β_2, δ) for ^{74}W Isotopes.	44
Table (3-18): Mass Number (A), Neutron Number (N), Gamma Energy of the First Excited State 2^+ (E_γ), Square Nuclear Average Radius (R^2), Reduced Electric Transition Probability $B(E2)$ ↑ in unit of e^2b^2 , Intrinsic Quadrupole Moment (Q_o) in unit of barn, and Deformation Parameters (β_2, δ) for ^{76}Os Isotopes.	45
Table (3-19): Mass Number (A), Neutron Number (N), Gamma Energy of the First Excited State 2^+ (E_γ), Square Nuclear Average Radius (R^2), Reduced Electric Transition Probability $B(E2)$ ↑ in unit of e^2b^2 , Intrinsic Quadrupole Moment (Q_o) in unit of barn, and Deformation Parameters (β_2, δ) for ^{78}Pt isotopes.	46
Table (3-20) Mass Number (A), Neutron Number (N), Gamma Energy of the First Excited State 2^+ (E_γ), Square Nuclear Average Radius (R^2), Reduced Electric Transition Probability $B(E2)$ ↑ in unit of e^2b^2 , Intrinsic Quadrupole Moment (Q_o) in unit of barn, and Deformation Parameters (β_2, δ) for ^{80}Hg Isotopes.	47
Table (3-21): Mass Number (A), Neutron Number (N), Gamma Energy of the First Excited State 2^+ (E_γ), Square Nuclear Average Radius (R^2), Reduced Electric Transition Probability $B(E2)$ ↑ in unit of e^2b^2 , Intrinsic Quadrupole Moment (Q_o) in unit of barn, and Deformation Parameters (β_2, δ) for ^{82}Pb Isotopes.	48
Table (3-22): Mass Number (A), Neutron Number (N), Gamma Energy of the First Excited State 2^+ (E_γ), Square Nuclear Average Radius (R^2), Reduced Electric Transition Probability $B(E2)$ ↑ in unit of e^2b^2 , Intrinsic Quadrupole Moment (Q_o) in unit of barn, and Deformation Parameters (β_2, δ) for ^{84}Po Isotopes.	49
Table (3-23): Mass Number (A), Neutron Number (N), Gamma Energy of the First Excited State 2^+ (E_γ), Square Nuclear Average Radius (R^2), Reduced Electric Transition Probability $B(E2)$ ↑ in unit of e^2b^2 , Intrinsic Quadrupole Moment (Q_o) in unit of barn, and Deformation Parameters (β_2, δ) for ^{86}Rn Isotopes.	50

Table (3-24): Mass Number (A), Neutron Number (N), Gamma Energy of the First Excited Mass Number (A), Neutron Number (N), Gamma Energy of the First Excited State 2^+ (E_γ), Square Nuclear Average Radius (R^2), Reduced Electric Transition Probability $B(E2)$ ↑ in unit of e^2b^2 , Intrinsic Quadrupole Moment (Q_o) in unit of barn, and Deformation Parameters (β_2, δ) for $_{88}\text{Ra}$ Isotopes.	51
Table (3-25): Mass Number (A), Neutron Number (N), Gamma Energy of the First Excited State 2^+ (E_γ), Square Nuclear Average Radius (R^2), Reduced Electric Transition Probability $B(E2)$ ↑ in unit of e^2b^2 , Intrinsic Quadrupole Moment (Q_o) in unit of barn, and Deformation Parameters (β_2, δ) for $_{90}\text{Th}$ Isotopes.	52
Table (3-26) Mass Number (A), Neutron Number (N), Gamma Energy of the First Excited State 2^+ (E_γ), Square Nuclear Average Radius (R^2), Reduced Electric Transition Probability $B(E2)$ ↑ in unit of e^2b^2 , Intrinsic Quadrupole Moment (Q_o) in unit of barn, and Deformation Parameters (β_2, δ) for $_{92}\text{U}$ Isotopes.	53
Table (3-27): Mass Number (A), Neutron Number (N), Gamma Energy of the First Excited State 2^+ (E_γ), Square Nuclear Average Radius (R^2), Reduced Electric Transition Probability $B(E2)$ ↑ in unit of e^2b^2 , Intrinsic Quadrupole Moment (Q_o) in unit of barn, and Deformation Parameters (β_2, δ) for $_{94}\text{Pu}$ Isotopes.	54
Table (3-28): Mass Number (A), Neutron Number (N), Gamma Energy of the First Excited State 2^+ (E_γ), Square Nuclear Average Radius (R^2), Reduced Electric Transition Probability $B(E2)$ ↑ in unit of e^2b^2 , Intrinsic Quadrupole Moment (Q_o) in unit of barn, and Deformation Parameters (β_2, δ) for $_{96}\text{Cm}$ Isotopes.	54
Table (3-29): Mass Number (A), Neutron Number (N), Gamma Energy of the First Excited State 2^+ (E_γ), Square Nuclear Average Radius (R^2), Reduced Electric Transition Probability $B(E2)$ ↑ in unit of e^2b^2 , Intrinsic Quadrupole Moment (Q_o) in unit of barn, and Deformation Parameters (β_2, δ) for $_{98}\text{Cf}$ Isotopes.	55
Table (3-30): Mass Number (A), Neutron Number (N), Gamma Energy of the First Excited State 2^+ (E_γ), Square Nuclear Average Radius (R^2), Reduced Electric Transition Probability $B(E2)$ ↑ in unit of e^2b^2 , Intrinsic Quadrupole Moment (Q_o) in unit of barn, and Deformation Parameters (β_2, δ) for $_{100}\text{Fm}$ Isotopes.	55
Table (3-31): Mass number (A), Neutron Number (N), Root Mean Square Radii $\langle r^2 \rangle^{1/2}$, Major and minor axes (a, b) and the difference between them (ΔR) by three methods for $_{40}\text{Zr}$ Isotopes.	56
Table (3-32): Mass number (A), Neutron Number (N), Root Mean Square Radii $\langle r^2 \rangle^{1/2}$, Major and minor axes (a, b) and the difference between them (ΔR) by three methods for $_{42}\text{Mo}$ Isotopes.	56
Table (3-33): Mass number (A), Neutron Number (N), Root Mean Square Radii $\langle r^2 \rangle^{1/2}$, Major and minor axes (a, b) and the difference between them (ΔR) by three methods for $_{44}\text{Ru}$ Isotopes.	56
Table (3-34): Mass number (A), Neutron Number (N), Root Mean Square Radii $\langle r^2 \rangle^{1/2}$, Major and minor axes (a, b) and the difference between them (ΔR) by three methods for $_{46}\text{Pd}$ Isotopes.	57
Table (3-35): Mass number (A), Neutron Number (N), Root Mean Square Radii $\langle r^2 \rangle^{1/2}$, Major and minor axes (a, b) and the difference between them (ΔR) by three methods for $_{48}\text{Cd}$ Isotopes.	57
Table (3-36): Mass number (A), Neutron Number (N), Root Mean Square Radii $\langle r^2 \rangle^{1/2}$, Major and minor axes (a, b) and the difference between them (ΔR) by three methods for $_{50}\text{Sn}$ Isotopes.	58

Table (3-37): Mass number (A), Neutron Number (N), Root Mean Square Radii $\langle r^2 \rangle^{1/2}$, Major and minor axes (a, b) and the difference between them (ΔR) by three methods for $_{52}\text{Te}$ Isotopes	58
Table (3-38): Mass number (A), Neutron Number (N), Root Mean Square Radii $\langle r^2 \rangle^{1/2}$, Major and minor axes (a, b) and the difference between them (ΔR) by three methods for $_{56}\text{Ba}$ Isotopes	59
Tables (3-39): Mass number (A), Neutron Number (N), Root Mean Square Radii $\langle r^2 \rangle^{1/2}$, Major and minor axes (a, b) and the difference between them (ΔR) by three methods for $_{58}\text{Ce}$ Isotopes	59
Tables (3-40): Mass number (A), Neutron Number (N), Root Mean Square Radii $\langle r^2 \rangle^{1/2}$, Major and minor axes (a, b) and the difference between them (ΔR) by three methods for $_{60}\text{Nd}$ Isotopes	60
Tables (3-41): Mass number (A), Neutron Number (N), Root Mean Square Radii $\langle r^2 \rangle^{1/2}$, Major and minor axes (a, b) and the difference between them (ΔR) by three methods for $_{62}\text{Sm}$ Isotopes	60
Tables (3-42): Mass number (A), Neutron Number (N), Root Mean Square Radii $\langle r^2 \rangle^{1/2}$, Major and minor axes (a, b) and the difference between them (ΔR) by three methods for $_{64}\text{Gd}$ Isotopes	61
Tables (3-43): Mass number (A), Neutron Number (N), Root Mean Square Radii $\langle r^2 \rangle^{1/2}$, Major and minor axes (a, b) and the difference between them (ΔR) by three methods for $_{66}\text{Dy}$ Isotopes	61
Tables (3-44): Mass number (A), Neutron Number (N), Root Mean Square Radii $\langle r^2 \rangle^{1/2}$, Major and minor axes (a, b) and the difference between them (ΔR) by three methods for $_{68}\text{Er}$ Isotopes	62
Tables (3-45): Mass number (A), Neutron Number (N), Root Mean Square Radii $\langle r^2 \rangle^{1/2}$, Major and minor axes (a, b) and the difference between them (ΔR) by three methods for $_{70}\text{Yb}$ Isotopes.	62
Tables (3-46): Mass number (A), Neutron Number (N), Root Mean Square Radii $\langle r^2 \rangle^{1/2}$, Major and minor axes (a, b) and the difference between them (ΔR) by three methods $_{72}\text{Hf}$ Isotopes.	63
Tables (3-47): Mass number (A), Neutron Number (N), Root Mean Square Radii $\langle r^2 \rangle^{1/2}$, Major and minor axes (a, b) and the difference between them (ΔR) by three methods for $_{74}\text{W}$ Isotopes.	63
Tables (3-48): Mass number (A), Neutron Number (N), Root Mean Square Radii $\langle r^2 \rangle^{1/2}$, Major and minor axes (a, b) and the difference between them (ΔR) by three methods for $_{76}\text{Os}$ Isotopes.	64
Tables (3-49): Mass number (A), Neutron Number (N), Root Mean Square Radii $\langle r^2 \rangle^{1/2}$, Major and minor axes (a, b) and the difference between them (ΔR) by three methods for $_{78}\text{Pt}$ Isotopes.	64
Tables (3-50): Mass number (A), Neutron Number (N), Root Mean Square Radii $\langle r^2 \rangle^{1/2}$, Major and minor axes (a, b) and the difference between them (ΔR) by three methods for $_{80}\text{Hg}$ Isotopes.	65
Tables (3-51): Mass number (A), Neutron Number (N), Root Mean Square Radii $\langle r^2 \rangle^{1/2}$, Major and minor axes (a, b) and the difference between them (ΔR) by three methods for $_{82}\text{Pb}$ Isotopes.	65
Tables (3-52): Mass number (A), Neutron Number (N), Root Mean Square Radii $\langle r^2 \rangle^{1/2}$, Major and minor axes (a, b) and the difference between them (ΔR) by three methods for $_{84}\text{Po}$ Isotopes.	66
Tables (3-53): Mass number (A), Neutron Number (N), Root Mean Square Radii $\langle r^2 \rangle^{1/2}$, Major and minor axes (a, b) and the difference between them (ΔR) by three methods for $_{86}\text{Rn}$ Isotopes.	66

Tables (3-54): Mass number (A), Neutron Number (N), Root Mean Square Radii $\langle r^2 \rangle^{1/2}$, Major and minor axes (a, b) and the difference between them (ΔR) by three methods for $_{88}\text{Ra}$ Isotopes.	67
Tables (3-55): Mass number (A), Neutron Number (N), Root Mean Square Radii $\langle r^2 \rangle^{1/2}$, Major and minor axes (a, b) and the difference between them (ΔR) by three methods for $_{90}\text{Th}$ Isotopes.	67
Tables (3-56): Mass number (A), Neutron Number (N), Root Mean Square Radii $\langle r^2 \rangle^{1/2}$, Major and minor axes (a, b) and the difference between them (ΔR) by three methods for $_{92}\text{U}$ Isotopes.	68
Tables (3-57): Mass number (A), Neutron Number (N), Root Mean Square Radii $\langle r^2 \rangle^{1/2}$, Major and minor axes (a, b) and the difference between them (ΔR) by three methods for $_{94}\text{Pu}$ Isotopes.	68
Tables (3-58): Mass number (A), Neutron Number (N), Root Mean Square Radii $\langle r^2 \rangle^{1/2}$, Major and minor axes (a, b) and the difference between them (ΔR) by three methods for $_{96}\text{Cm}$ Isotopes.	69
Tables (3-59): Mass number (A), Neutron Number (N), Root Mean Square Radii $\langle r^2 \rangle^{1/2}$, Major and minor axes (a, b) and the difference between them (ΔR) by three methods for $_{98}\text{Cf}$ Isotopes.	69
Tables (3-60): Mass number (A), Neutron Number (N), Root Mean Square Radii $\langle r^2 \rangle^{1/2}$, Major and minor axes (a, b) and the difference between them (ΔR) by three methods for $_{100}\text{Fm}$ Isotopes.	69

List of Figures

Figure	Page
Fig. (1.1): Basic components summary of the liquid-drop model.	5
Fig. (1.2): In lead isotopes, the neutron separation energy is a function of N .	7
Fig. (1.3): Shows binding energy per nucleon of nuclei with mass number A .	8
Fig. (1.4): The energy E_1 or E_γ of the first excited state of even-even nuclei.	8
Fig. (1.5): Collective nuclear phenomena known as the giant dipole resonance (a) and the giant quadrupole resonance (b). Protons are the solid circles, neutrons are the open circles	9
Fig. (2.1): A vibrating nucleus with a spherical equilibrium shape.	17
Fig. (2.2): Demonstrates the multipole deformations for $\lambda = 1, \dots, 4$.	19
Fig. (2.3): Represents the isobar as a prolate nucleon collective rotation with radical spin $K= 1/2$.	22
Fig. (2.4): Figure (2.4): A diagrammatic representation of three of a nuclear shapes (a) Spherical, (b) Oblate, (c) Prolate.	23
Fig. (3-1): Represents the relationship of Deformation Parameter (β_2) value of the Present Work as a function of neutron Number for the ^{40}Zr Isotopes.	70
Fig. (3-2): Represents the relationship of Deformation Parameter (β_2) value of the Present Work as a function of neutron Number for the ^{42}Mo Isotopes.	70
Fig. (3-3): Represents the relationship of Deformation Parameter (β_2) value of the Present Work as a function of neutron Number for the ^{44}Ru Isotopes.	71
Fig. (3-4): Represents the relationship of Deformation Parameter (β_2) value of the Present Work as a function of neutron Number for the ^{46}Pd Isotopes.	71
Fig. (3-5): Represents the relationship of Deformation Parameter (β_2) value of the Present Work as a function of neutron Number for the ^{48}Cd Isotopes.	72
Fig. (3-6): Represents the relationship of Deformation Parameter (β_2) value of the Present Work as a function of neutron Number for the ^{50}Sn Isotopes.	72
Fig. (3-7): Represents the relationship of Deformation Parameter (β_2) value of the Present Work as a function of neutron Number for the ^{52}Te Isotopes.	73
Fig. (3-8): Represents the relationship of Deformation Parameter (β_2) value of the Present Work as a function of neutron Number for the ^{56}Ba Isotopes.	73
Fig. (3-9): Represents the relationship of Deformation Parameter (β_2) value of the Present Work as a function of neutron Number for the ^{58}Ce Isotopes.	74

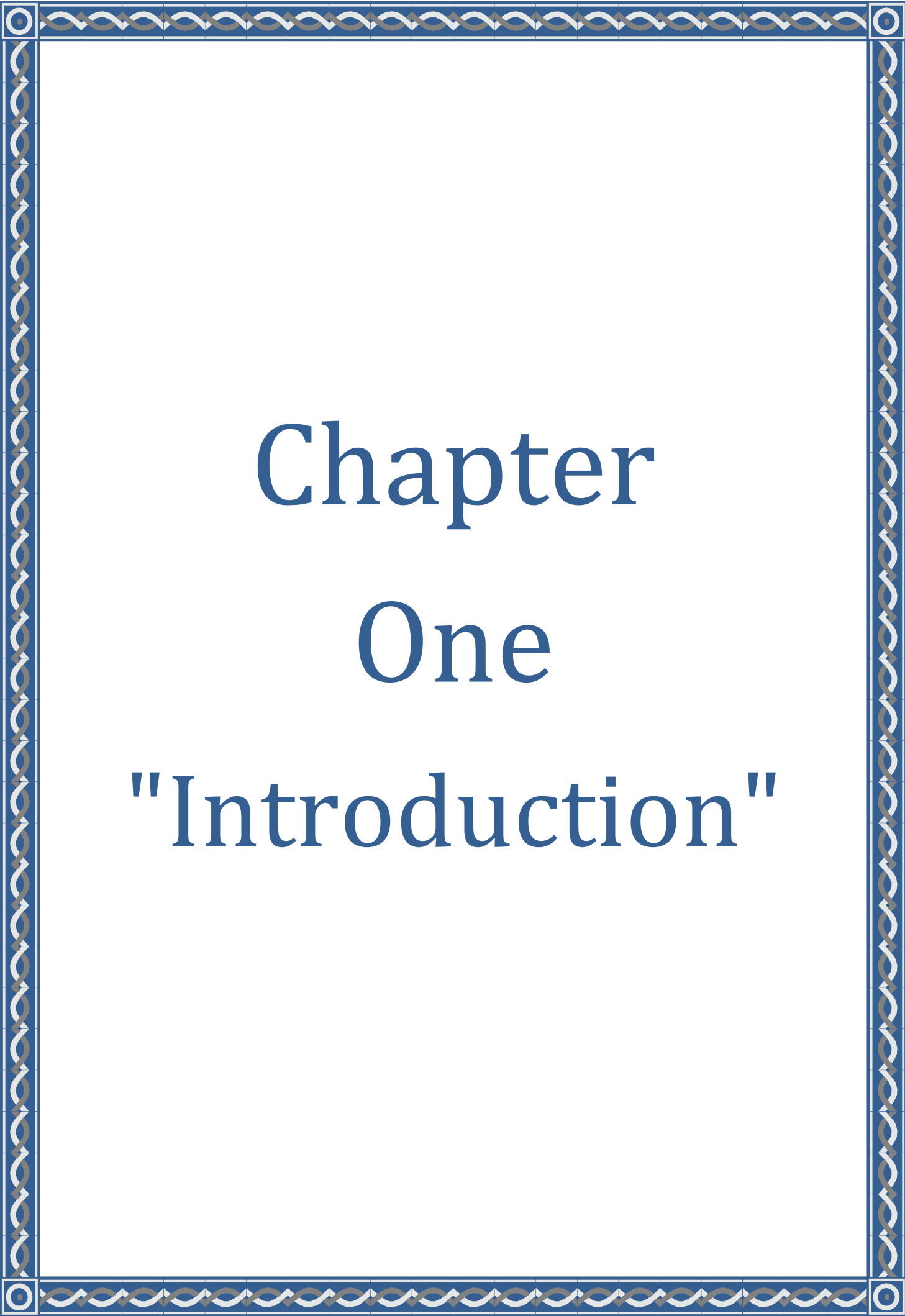
Figure	Page
Fig.(3-10): Represents the relationship of Deformation Parameter (β_2) value of the Present Work as a function of neutron Number for the ^{60}Nd Isotopes.	74
Fig.(3-11): Represents the relationship of Deformation Parameter (β_2) value of the Present Work as a function of neutron Number for the ^{62}Sm Isotopes.	75
Fig.(3-12): Represents the relationship of Deformation Parameter (β_2) value of the Present Work as a function of neutron Number for the ^{64}Gd Isotopes.	75
Fig.(3-13): Represents the relationship of Deformation Parameter (β_2) value of the Present Work as a function of neutron Number for the ^{66}Dy Isotopes.	76
Fig.(3-14): Represents the relationship of Deformation Parameter (β_2) value of the Present Work as a function of neutron Number for the ^{68}Er Isotopes.	76
Fig.(3-15): Represents the relationship of Deformation Parameter (β_2) value of the Present Work as a function of neutron Number for the ^{70}Yb Isotopes.	77
Fig.(3-16): Represents the relationship of Deformation Parameter (β_2) value of the Present Work as a function of neutron Number for the ^{72}Hf Isotopes.	77
Fig.(3-17): Represents the relationship of Deformation Parameter (β_2) value of the Present Work as a function of neutron Number for the ^{74}W Isotopes.	78
Fig.(3-18): Represents the relationship of Deformation Parameter (β_2) value of the Present Work as a function of neutron Number for the ^{76}Os Isotopes.	78
Fig.(3-19): Represents the relationship of Deformation Parameter (β_2) value of the Present Work as a function of neutron Number for the ^{78}Pt Isotopes.	79
Fig.(3-20): Represents the relationship of Deformation Parameter (β_2) value of the Present Work as a function of neutron Number for the ^{80}Hg Isotopes.	79
Fig.(3-21): Represents the relationship of Deformation Parameter (β_2) value of the Present Work as a function of neutron Number for the ^{82}Pb Isotopes.	80
Fig.(3-22): Represents the relationship of Deformation Parameter (β_2) value of the Present Work as a function of neutron Number for the ^{84}Po Isotopes.	80
Fig.(3-23): Represents the relationship of Deformation Parameter (β_2) value of the Present Work as a function of neutron Number for the ^{86}Rn Isotopes.	81
Fig.(3-24): Represents the relationship of Deformation Parameter (β_2) value of the Present Work as a function of neutron Number for the ^{88}Ra Isotopes.	81

Figure	Page
Fig.(3-25): Represents the relationship of Deformation Parameter (β_2) value of the Present Work as a function of neutron Number for the $_{90}\text{Th}$ Isotopes.	82
Fig.(3-26): Represents the relationship of Deformation Parameter (β_2) value of the Present Work as a function of neutron Number for the $_{92}\text{U}$ Isotopes.	82
Fig.(3-27): Represents the relationship of Deformation Parameter (β_2) value of the Present Work as a function of neutron Number for the $_{94}\text{Pu}$ Isotopes.	83
Fig.(3-28): Represents the relationship of Deformation Parameter (β_2) value of the Present Work as a function of neutron Number for the $_{96}\text{Cm}$ Isotopes.	83
Fig.(3-29): Represents the relationship of Deformation Parameter (β_2) value of the Present Work as a function of neutron Number for the $_{98}\text{Cf}$ Isotopes.	84
Fig.(3-30): Represents the relationship of Deformation Parameter (β_2) value of the Present Work as a function of neutron Number for the $_{100}\text{Fm}$ Isotopes.	84
Fig.(3-31): The relationship of deformation parameters (β_2) for (30) elements as a function of mass numbers (A).	85
Fig.(3-32): Shapes of axially symmetric quadrupole deformation for $_{40}\text{Zr}$ isotopes from major (\mathbf{a}) and minor (\mathbf{b}) axes.	86
Fig.(3-33): Shapes of axially symmetric quadrupole deformation for $_{42}\text{Mo}$ isotopes from major (\mathbf{a}) and minor (\mathbf{b}) axes.	86
Fig.(3-34): Shapes of axially symmetric quadrupole deformation for $_{44}\text{Ru}$ isotopes from major (\mathbf{a}) and minor (\mathbf{b}) axes.	86
Fig.(3-35): Shapes of axially symmetric quadrupole deformation for $_{46}\text{Pd}$ isotopes from major (\mathbf{a}) and minor (\mathbf{b}) axes.	87
Fig.(3-36): Shapes of axially symmetric quadrupole deformation for $_{48}\text{Cd}$ isotopes from major (\mathbf{a}) and minor (\mathbf{b}) axes.	87
Fig.(3-37): Shapes of axially symmetric quadrupole deformation for $_{50}\text{Sn}$ isotopes from major (\mathbf{a}) and minor (\mathbf{b}) axes.	87
Fig.(3-38): Shapes of axially symmetric quadrupole deformation for $_{52}\text{Te}$ isotopes from major (\mathbf{a}) and minor (\mathbf{b}) axes.	88
Fig.(3-39): Shapes of axially symmetric quadrupole deformation for $_{56}\text{Ba}$ isotopes from major (\mathbf{a}) and minor (\mathbf{b}) axes.	88
Fig.(3-40): Shapes of axially symmetric quadrupole deformation for $_{58}\text{Ce}$ isotopes from major (\mathbf{a}) and minor (\mathbf{b}) axes.	88
Fig.(3-41): Shapes of axially symmetric quadrupole deformation for $_{60}\text{Nd}$ isotopes from major (\mathbf{a}) and minor (\mathbf{b}) axes.	89
Fig.(3-42): Shapes of axially symmetric quadrupole deformation for $_{62}\text{Sm}$ isotopes from major (\mathbf{a}) and minor (\mathbf{b}) axes.	89
Fig.(3-43): Shapes of axially symmetric quadrupole deformation for $_{64}\text{Gd}$ isotopes from major (\mathbf{a}) and minor (\mathbf{b}) axes.	89
Fig.(3-44): Shapes of axially symmetric quadrupole deformation for $_{66}\text{Dy}$ isotopes from major (\mathbf{a}) and minor (\mathbf{b}) axes.	90
Fig.(3-45): Shapes of axially symmetric quadrupole deformation for $_{68}\text{Er}$ isotopes from major (\mathbf{a}) and minor (\mathbf{b}) axes.	90
Fig.(3-46): Shapes of axially symmetric quadrupole deformation for $_{70}\text{Yb}$ isotopes from major (\mathbf{a}) and minor (\mathbf{b}) axes.	90
Fig.(3-47): Shapes of axially symmetric quadrupole deformation for $_{72}\text{Hf}$ isotopes from major (\mathbf{a}) and minor (\mathbf{b}) axes.	91

Fig.(3-48): Shapes of axially symmetric quadrupole deformation for ${}_{74}\text{W}$ isotopes from major (a) and minor (b) axes.	91
Fig.(3-49): Shapes of axially symmetric quadrupole deformation for ${}_{76}\text{Os}$ isotopes from major (a) and minor (b) axes.	91
Fig.(3-50): Shapes of axially symmetric quadrupole deformation for ${}_{78}\text{Pt}$ isotopes from major (a) and minor (b) axes.	92
Fig.(3-51): Shapes of axially symmetric quadrupole deformation for ${}_{80}\text{Hg}$ isotopes from major (a) and minor (b) axes.	92
Fig.(3-52): Shapes of axially symmetric quadrupole deformation for ${}_{82}\text{Pb}$ isotopes from major (a) and minor (b) axes.	92
Fig.(3-53): Shapes of axially symmetric quadrupole deformation for ${}_{84}\text{Po}$ isotopes from major (a) and minor (b) axes.	93
Fig.(3-54): Shapes of axially symmetric quadrupole deformation for ${}_{86}\text{Rn}$ isotopes from major (a) and minor (b) axes.	93
Fig.(3-55): Shapes of axially symmetric quadrupole deformation for ${}_{88}\text{Ra}$ isotopes from major (a) and minor (b) axes.	93
Fig.(3-56): Shapes of axially symmetric quadrupole deformation for ${}_{90}\text{Th}$ isotopes from major (a) and minor (b) axes.	94
Fig.(3-57): Shapes of axially symmetric quadrupole deformation for ${}_{92}\text{U}$ isotopes from major (a) and minor (b) axes.	94
Fig.(3-58): Shapes of axially symmetric quadrupole deformation for ${}_{94}\text{Pu}$ isotopes from major (a) and minor (b) axes.	94
Fig.(3-59): Shapes of axially symmetric quadrupole deformation for ${}_{96}\text{Cm}$ isotopes from major (a) and minor (b) axes.	95
Fig.(3-60): Shapes of axially symmetric quadrupole deformation for ${}_{98}\text{Hf}$ isotopes from major (a) and minor (b) axes.	95
Fig.(3-61): Shapes of axially symmetric quadrupole deformation for ${}_{100}\text{Fm}$ isotopes from major (a) and minor (b) axes.	95
Fig.(A-1): Axially-symmetric quadrupole deformations, the prolate shape of Nucleus with ($x = y < z$) (where z is the minor axis (b) (symmetric axis) and (x,y) are major axes (a)) for Zr isotopes.	122
Fig.(A-2): Axially-symmetric quadrupole deformations, the prolate shape of Nucleus with ($x = y < z$) (where z is the minor axis (b) (symmetric axis) and (x,y) are major axes (a)) for Mo isotopes.	122
Fig.(A-3): Axially-symmetric quadrupole deformations, the prolate shape of Nucleus with ($x = y < z$) (where z is the minor axis (b) (symmetric axis) and (x,y) are major axes (a)) for Ru isotopes.	123
Fig.(A-4): Axially-symmetric quadrupole deformations, the prolate shape of Nucleus with ($x = y < z$) (where z is the minor axis (b) (symmetric axis) and (x,y) are major axes (a)) for Pd isotopes.	124
Fig.(A-5): Axially-symmetric quadrupole deformations, the prolate shape of Nucleus with ($x = y < z$) (where z is the minor axis (b) (symmetric axis) and (x,y) are major axes (a)) for Cd isotopes.	125-126
Fig.(A-6): Axially-symmetric quadrupole deformations, the prolate shape of Nucleus with ($x = y < z$) (where z is the minor axis (b) (symmetric axis) and (x,y) are major axes (a)) for Sn isotopes.	127-128
Fig.(A-7): Axially-symmetric quadrupole deformations, the prolate shape of Nucleus with ($x = y < z$) (where z is the minor axis (b) (symmetric axis) and (x,y) are major axes (a)) for Te isotopes.	129-130

Fig.(A-8): Axially-symmetric quadrupole deformations, the prolate shape of Nucleus with($x = y < z$) (where z is the minor axis (b) (symmetric axis) and (x,y) are major axes (a)) for Ba isotopes.	131-132
Fig.(A-9): Axially-symmetric quadrupole deformations, the prolate shape of Nucleus with($x = y < z$) (where z is the minor axis (b) (symmetric axis) and (x,y) are major axes (a)) for Ce isotopes.	133-134
Fig.(A-10): Axially-symmetric quadrupole deformations, the prolate shape of Nucleus with($x = y < z$) (where z is the minor axis (b) (symmetric axis) and (x,y) are major axes (a)) for Nd isotopes.	135-136
Fig.(A-11): Axially-symmetric quadrupole deformations, the prolate shape of Nucleus with($x = y < z$) (where z is the minor axis (b) (symmetric axis) and (x,y) are major axes (a)) for Sm isotopes.	137-138
Fig.(A-12): Axially-symmetric quadrupole deformations, the prolate shape of Nucleus with($x = y < z$) (where z is the minor axis (b) (symmetric axis) and (x,y) are major axes (a)) for Gd isotopes.	139-140
Fig.(A-13): Axially-symmetric quadrupole deformations, the prolate shape of Nucleus with($x = y < z$) (where z is the minor axis (b) (symmetric axis) and (x,y) are major axes (a)) for Dy isotopes.	141-142
Fig.(A-14): Axially-symmetric quadrupole deformations, the prolate shape of Nucleus with($x = y < z$) (where z is the minor axis (b) (symmetric axis) and (x,y) are major axes (a)) for Er isotopes.	143-144
Fig.(A-15): Axially-symmetric quadrupole deformations, the prolate shape of Nucleus with($x = y < z$) (where z is the minor axis (b) (symmetric axis) and (x,y) are major axes (a)) for Yb isotopes.	145-146
Fig.(A-16): Axially-symmetric quadrupole deformations, the prolate shape of Nucleus with($x = y < z$) (where z is the minor axis (b) (symmetric axis) and (x,y) are major axes (a)) for Hf isotopes.	147-148
Fig.(A-17): Axially-symmetric quadrupole deformations, the prolate shape of Nucleus with($x = y < z$) (where z is the minor axis (b) (symmetric axis) and (x,y) are major axes (a)) for W isotopes.	149-150
Fig.(A-18): Axially-symmetric quadrupole deformations, the prolate shape of Nucleus with($x = y < z$) (where z is the minor axis (b) (symmetric axis) and (x,y) are major axes (a)) for Os isotopes.	151-152
Fig.(A-19): Axially-symmetric quadrupole deformations, the prolate shape of Nucleus with($x = y < z$) (where z is the minor axis (b) (symmetric axis) and (x,y) are major axes (a)) for Pt isotopes.	153-154
Fig.(A-20): Axially-symmetric quadrupole deformations, the prolate shape of Nucleus with($x = y < z$) (where z is the minor axis (b) (symmetric axis) and (x,y) are major axes (a)) for Hg isotopes.	155-156
Fig.(A-21): Axially-symmetric quadrupole deformations, the prolate shape of Nucleus with($x = y < z$) (where z is the minor axis (b) (symmetric axis) and (x,y) are major axes (a)) for Pb isotopes.	157-158
Fig.(A-22): Axially-symmetric quadrupole deformations, the prolate shape of Nucleus with($x = y < z$) (where z is the minor axis (b) (symmetric axis) and (x,y) are major axes (a)) for Po isotopes.	159-160
Fig.(A-23): Axially-symmetric quadrupole deformations, the prolate shape of Nucleus with($x = y < z$) (where z is the minor axis (b) (symmetric axis) and (x,y) are major axes (a)) for Rn isotopes.	161-162
Fig.(A-24): Axially-symmetric quadrupole deformations, the prolate shape of Nucleus with($x = y < z$) (where z is the minor axis (b) (symmetric axis) and (x,y) are major axes (a)) for Ra isotopes.	163-164

Fig.(A-25): Axially-symmetric quadrupole deformations, the prolate shape of Nucleus with($x = y < z$) (where z is the minor axis (b) (symmetric axis) and (x,y) are major axes (a)) for Th isotopes.	165-166
Fig.(A-26): Axially-symmetric quadrupole deformations, the prolate shape of Nucleus with($x = y < z$) (where z is the minor axis (b) (symmetric axis) and (x,y) are major axes (a)) for U isotopes.	166-167
Fig.(A-27): Axially-symmetric quadrupole deformations, the prolate shape of Nucleus with($x = y < z$) (where z is the minor axis (b) (symmetric axis) and (x,y) are major axes (a)) for Pu isotopes.	168
Fig.(A-28): Axially-symmetric quadrupole deformations, the prolate shape of Nucleus with($x = y < z$) (where z is the minor axis (b) (symmetric axis) and (x,y) are major axes (a)) for Cm isotopes.	169
Fig.(A-29): Axially-symmetric quadrupole deformations, the prolate shape of Nucleus with($x = y < z$) (where z is the minor axis (b) (symmetric axis) and (x,y) are major axes (a)) for Cf isotopes.	170
Fig.(A-30): Axially-symmetric quadrupole deformations, the prolate shape of Nucleus with($x = y < z$) (where z is the minor axis (b) (symmetric axis) and (x,y) are major axes (a)) for Fm isotopes.	171



Chapter One

"Introduction"

1-1 Introduction:

The shape of an atomic nucleus reflects the shell structure of the protons and neutrons of which it is formed. If the shells are completely filled, we speak of a "magic" nucleus, which is spherical in shape. Most nuclei, however, tend to be deformed because their shells are only partially filled. The most commonly encountered shapes are prolate (elongated, cigar shaped and rugby ball) or oblate (flattened, pan cake and cushion); these shapes can change from one nucleus to its neighbor by adding or removing a proton or neutron. In some cases it is sufficient to rearrange the protons or neutrons within the same nucleus to change its shape. The same nucleus can therefore assume different shapes corresponding to states of different energy. If such states come close in energy (one thousandth of the binding energy of the nucleus or so), the different shapes can mix. [1]

It can be observed that there are different shapes of nuclei in the ground state and only few have spherical shape, predominating in the same nucleus. It can simply subdivide deformed nuclei into oblate, prolate and triaxial deformed nuclei depending on the relative pivot values of the ellipsoid shapes. The low energy spectrum part of the spherical nuclei can be explained as surface vibrations expression [2]. Since the nucleons number is changeable from nucleus to another, it has generally been observed one progressive growth of different shapes – spherical, axially quadrupole deformed and smooth shapes with regard to triaxial deformation, octupole shapes [3].

1-2 Nuclear structure:

Nucleons are particles of quantum bound states of the atomic nuclei. There are two types of particles: positive charge (proton) and no charge (neutron) which has the same mass and converted into energy by ($E = mc^2$): [4, 5].

$$m_n c^2 = 939.56 \text{ MeV}, \quad m_p c^2 = 938.27 \text{ MeV} \quad (1.1)$$

i.e. an arrangement mass difference is one part per thousand.

$$(m_n - m_p)c^2 = 1.29 \text{ MeV} \quad (1.2)$$

The mass difference comparing with the mass themselves is very important, as in lots of applications are considered "infinite". It is noted that the mass difference has the same arrangement that is found in electron mass [4].

$$m_e c^2 = 0.511 \text{ MeV} \quad (1.3).$$

Nucleons and electrons are spin 1/2 fermions meaning that their intrinsic angular momentum projected on an arbitrary direction can take on only the values of $\pm \hbar/2$. Having spin 1/2, they must satisfy the Pauli Exclusion Principle (that prevents two identical particles from having the same spatial wave function unless their spins are oppositely aligned) [4].

Nucleons are engaged in nuclei by nuclear powers which are powerful and attractive enough to beat the long-range coulomb propulsion between protons despite of their short range. Comparing with other electromagnetic reactions, it has been noted that the nuclear powers are nuclear reaction according to the strong interaction. It can be seen that the strong reactions of nucleon are similar and caused by the positive charge (protons) and no charge (neutrons) which in turn cause different electromagnetic interactions; this also explains their common name (nucleon) as their masses are equal [4].

1-3 General properties of Nuclei:

1-3-1 The mass number:

The mass number A gives the number of nucleons in the nucleus, in addition to the Z protons, N neutrons that are found in the nucleus, where $A = Z + N$. Atoms can be classified according to the neutrons and protons number in the elements nucleus:

- **Isotopes:** Atoms equalize with atomics numbers, but differ in neutrons numbers N and have practically conforming chemical properties (since these arise from the Z electron). Element isotopes have different nuclear properties, as that is found in Uranium Isotopes [4,6].

- **Isotones:** When atoms are equaled in Neutron number N but different in Atomic Number Z , like ($^{14}_6\text{C}$) and ($^{16}_8\text{O}$), this sort of atoms are seldom to be used [4,6].
- **Isobars:** They are the atoms that have the same mass number A , such as (^3He) and (^3H). These atoms often have similar nuclear properties because protons and neutrons have the same nuclear reactions [4,6].
- **Isomers:** Atoms that have the same number of protons and neutrons in case of atoms are exactly the same but their energy level is different, this happens when the atoms are in state of being stable, for instance, xenon element ($^{131\text{m}}\text{Xe}$) in the transformation state and the xenon (^{131}Xe) in the normal state [6].

1-3-2 The binding energy (B):

This can be determined from atomic masses [4], as it can be measured with much higher accuracy than nuclear masses, the equation below can show this:

$$B(Z, A) = [ZM(^1\text{H}) + (A - Z)M_n - M(A, Z)]. c^2 \quad (1.4)$$

where: $[M(^1\text{H}) = Mp + me]$ is the hydrogen atom mass (the 13.6 eV binding energy of the H-atom is negligible), M_n = the neutron mass, and $M(A, Z)$ = the atom mass with Z electrons whose nucleus A = nucleons.

Nuclides are indicated by ^AX , X considering it is the element chemical symbol e.g. the stable carbon isotopes are classified into ^{12}C and ^{13}C ; whereas the radioactive carbon isotope repeatedly used for isotopic dating is categorized ^{14}C . Occasionally the record ^A_ZX or $^A_Z\text{X}_N$ is used by adding the atomic number Z and probably the neutron number N [5].

1-3-3 Nuclear radius:

It has been noted that the nucleus volume is directly proportional to the nucleons number that forms it, which is its mass number A . This suggests that the nucleons density is nearly similar in the interiors of all nuclei. When a nuclear

radius is R , the correspondent volume is $(\frac{4}{3}\pi R^3)$ and so R^3 is proportional to A . This relation can generally be expressed in reverse formula as in nuclear radius [7].

$$R = R_0 \times A^{1/3} \quad (1.5)$$

where: $R_0 = 1.2$ fm, (A) is the mass number.

This means that the nucleons are not compressed in size in spite of the great efficient powers between them [7].

1-4 Nuclear models :

1-4-1 The liquid drop model:

It has been suggested the first nuclear model since 1935 by Bohr, in depending on the nuclear power low range, with the additively of volumes and binding energies, this model is called liquid-drop model. Nucleons react strongly with their closest neighbors, as what molecules do in a drop of water. Thus, we can describe their properties by the identical quantities, such as, the density, the volume energy, the surface tension and the radius [4].

When the surface tension energy of the nucleus is much bigger than the electrostatic Coulomb repulsion between the protons charged then the nucleus will be steady further, it may be deformed and decayed because of the fission. This has led von Weizsäcker in 1935 to suggest a semi-empirical mass formula based on the liquid-drop model, which might work well for nuclei close to and above the saturation point [8].

1-4-1-1 The semi-empirical mass formula:

The formulation of Weizsäcker can be affirmed as follows in supposing that nuclei are nearly spherical:

$$B(A, Z) = a_V A - a_S A^{2/3} - a_C \frac{Z(Z-1)}{A^{1/3}} - a_a \frac{(N-2Z)^2}{A} + \delta(A) \quad (1.6)$$

The coefficients (a_i) can be selected in order that they can provide better approximation to the spotted binding energies as below:

$$a_V = 15.753 \text{ MeV}, a_S = 17.804 \text{ MeV}, a_C = 0.7103 \text{ MeV}, a_a = 23.69 \text{ MeV}$$

$$\text{And } \delta(A) = \begin{cases} 33.6 A^{-3/4} & \text{if } N \text{ and } Z \text{ are even} \\ -33.6 A^{-3/4} & \text{if } N \text{ and } Z \text{ are odd} \\ 0 & A = N + Z \text{ is odd} \end{cases}$$

- The term a_V (volume) that reflects the closest-neighbor reactions, and in turn may lead to a constant binding energy per nucleon $B/A \sim 16$ MeV .
- The term a_S (surface) can lower the binding energy. Internal nucleons sense the isotropic reactions, while nucleons near the nucleus surface sense the powers that come from the inside only. As a result, this is called surface tension term that is proportional to the area $4\pi R^2 \sim A^{2/3}$.
- The term a_C (protons Coulomb repulsion) that is proportional to Q^2/R , i.e. $\sim Z^2/A^{1/3}$.The term is considered calculable and smaller than the nuclear terms for small values of Z . Neutron increasing over protons are preferred by this term.
- On the contrary, the asymmetry term a_a prefers symmetry between protons and neutrons (isospin). In the electric forces non-attendance, $Z = N$ is energetically preferable.
- Finally, the term $\delta(A)$ is a quantum pairing term [4,9].

The effects of these three terms are clearly seen in Fig. (1.1)

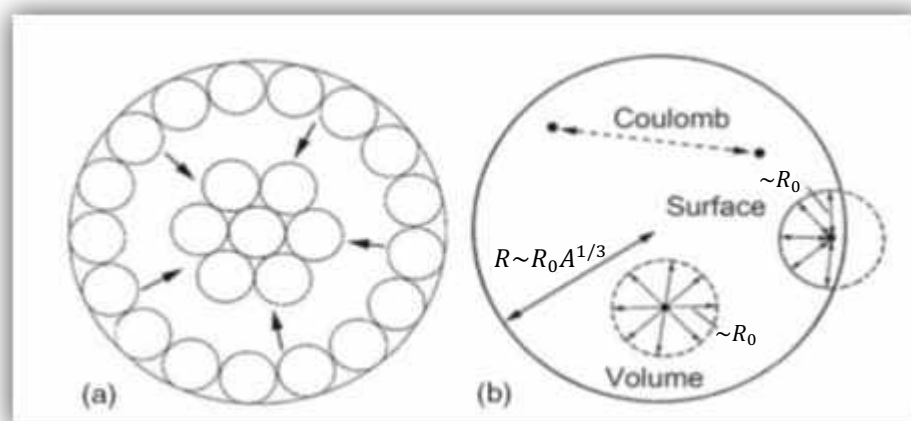


Fig. (1.1): Basic components summary of the liquid-drop model. (a) Describes the volume and surface components. (b) Demonstrates the three major terms in the formulation for binding energies which are the terms of volume, surface and Coulomb [9].

1-4-2 The shell model (the independent-particle models) :

The idea of a Fermi gas has led to the independent-particle model which presumes that nucleons are point particles and free to orbit through the nucleus because of the net attractive power of a potential-well. In this model the nuclear power is presumed to act between nucleons that produce a net potential-well pulls all nucleons toward the nucleus center and not toward other solo nucleons. Nucleons that are influenced by potential-well can be in special quantal energy states, the bulk and holding of which sets the detailed nucleon build-up procedure [9].

A comparable phenomenon takes place in nuclear physics, many experiential signs exhibit that atomic nuclei have a shell-structure and can be built, like atoms, through filling up alternate shells of a functional potential well. For instance, the nuclear analogs of atomic ionization energies are the “separation energies” (S_n and S_p) that are needful for extracting a proton or a neutron from a nucleus

$$S_n = B(Z, N) - B(Z, N - 1), \quad S_p = B(Z, N) - B(Z - 1, N) \quad (1.7)$$

It has been shown abruptions at specific values of N or Z that are known magic numbers. Figure (1.2) demonstrates the neutron separation energy of lead isotope ($Z = 82$) as a function of N where the measured values are shown by the filled points while the prognostic of the Bethe– Weizsäcker formulation is shown by the open points. The stopping at the magic number $N = 126$ [4].

In spite of the liquid drop model of the nucleus has perfectly demonstrated a success in predicting delicate differences in the nuclides mass with other different mass and atomic numbers, any mention of the internal arrangement of the nucleons in the nucleus has been avoided by this model. However, it has been noticed that there are signals for such an implied structure and an abnormally high number of stable nuclides, their proton and/or neutron numbers are equal to the magic numbers [10].

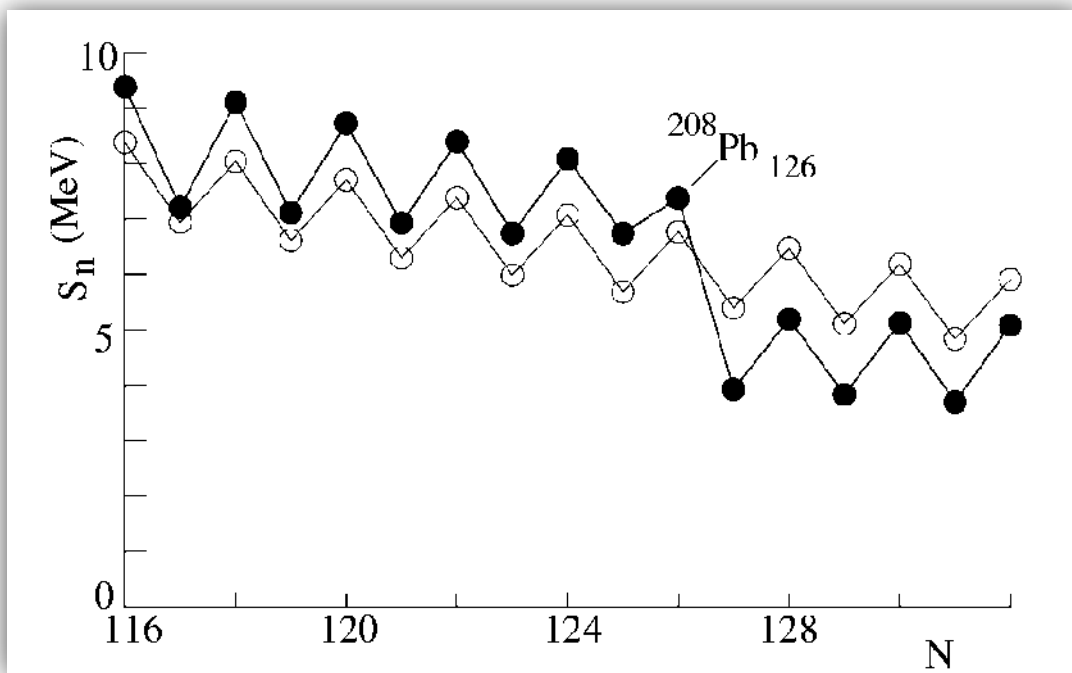


Fig. (1.2): In lead isotopes, the neutron separation energy is a function of N [4].

1-4-2-1 Nuclear magic numbers

It has been reported that nuclides with particular proton and /or neutron numbers are especially stable (Fig. (1.3)) [5].

These numbers (2, 8, 20, 28, 50, 82, 126) are recognized as magic numbers. Nuclei with a magic proton or neutron number have an uncommonly large steady number or very long lived nuclides. A lot of energy is required to extract a neutron from nucleus if it has a magic neutron number, while if the neutron number is increased by one, the separation energy is extremely smaller. The same applies to protons. It is also pointed that much energy is required to trigger such nuclei (Fig. (1.4)) [5].

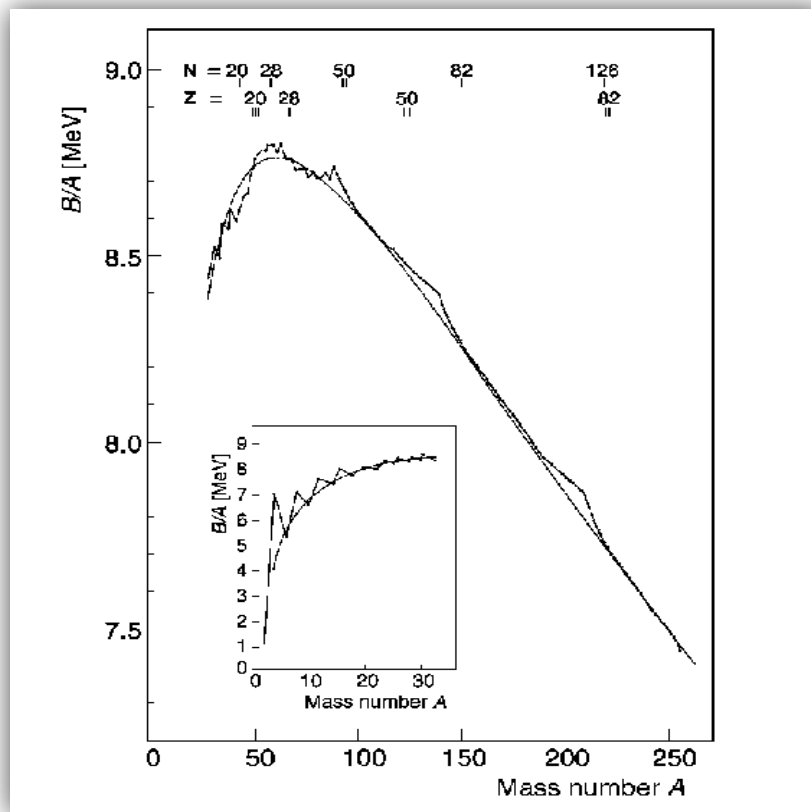


Fig. (1.3): Shows binding energy per nucleon of nuclei with mass number A . [5].

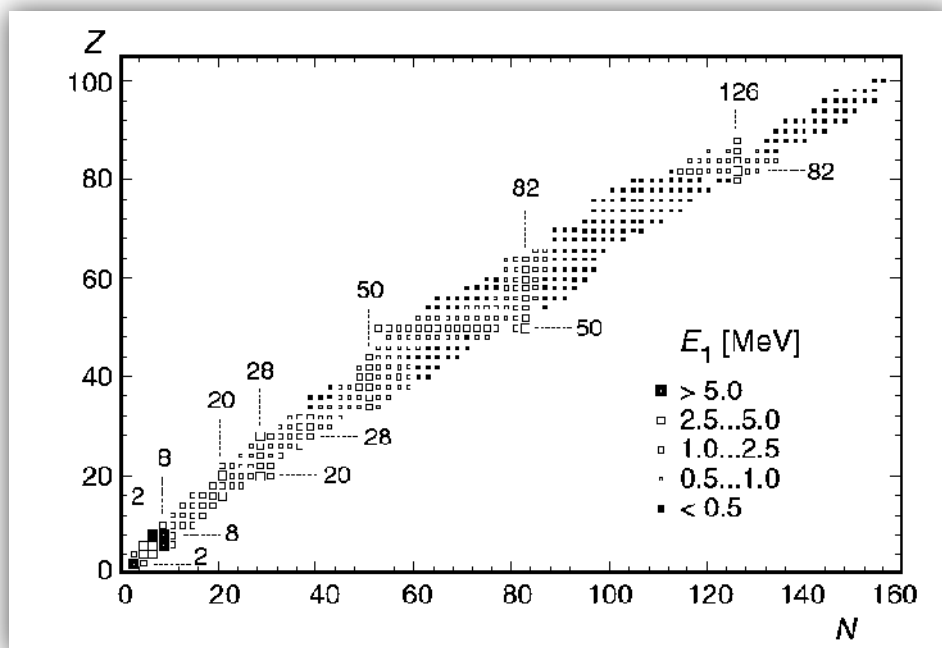


Fig. (1.4): The energy E_1 or E_γ of the first excited state of even-even nuclei. It is noted that it is especially large for nuclei with “magic” proton or neutron number [5].

1-4-3 The collective model :

The liquid drop and shell models are in severe disparity, the first one is based on the strong nucleon reactions with its closest neighbors while the second one is based on the freelance movement of each nucleon uninfluenced by other nucleons. A united or collective model has been suggested in which an individual nucleon reacts with a "core" of other nucleons that is able to make complex deformity and pulses. Though the shell features are kept with this model, the locked shells are deformed by other nucleons. These deformations make orderly spaced excited energy levels over the ground state, levels that have been spotted experimentally [9]. The collective model has concentrated on nuclear phenomena, where all or most nucleons move in concert. Representative of such effects are the huge dipole resonance and the huge quadrupole resonance (Fig. (1.5)). The importance of collective vibrations and rotations lies in the fact that the majority of higher-energy states can be understood only as the statistical effects of many nucleons in motion together. In this regard, the collective model can be an immediate descendant of the liquid-drop model [9].

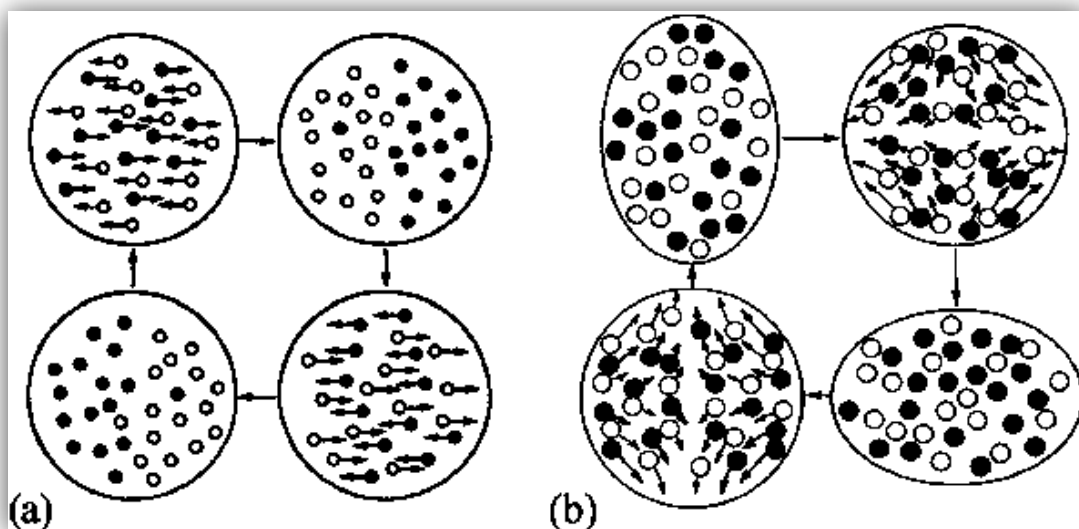


Figure (1.5): Collective nuclear phenomena known as the giant dipole resonance (a) and the giant quadrupole resonance (b). Protons are the solid circles; neutrons are the open circles [5].

1-5 Previous studies

H. Iwasaki, T. Motobayashi and others in 2000 were studied the inelastic proton scattering, exciting the 2^+ states in the neutron-rich with Beryllium isotopes $^{10,12}\text{Be}$ utilizing an inverse kinematics. The deformation lengths for the 2^+ states in ^{10}Be and ^{12}Be was explained to become 1.80 ± 0.25 fm and 2.00 ± 0.23 fm respectively, this indicates that a tendency in a direction to a strong quadrupole deformation can be kept for these nuclei and also the singly-closed shell structure cannot dominate in ^{12}Be [11].

N. Benhamouda, M.R. Oudih, and others in 2001 a microscopic quadrupole moment expression was made in this study. Electric quadrupole moments assurance of the ground states of even-even (Sm) neutron-rich nuclei was implemented [12].

Raman S. et al. in 2001 reported that experimental values for deformation parameters β_2 were collected. Quadrupole moment Q_0 and the diminutive electric quadrupole transmission likelihood $B(E2: 0^+ \rightarrow 2^+)$ between the 0^+ ground state and the first excited state 2^+ , in even-even nuclides [13].

P. G. Bizzeti and A. M. Bizzeti-Sona in 2004 reported that an investigation on the dynamics of nuclear collective motion was done in this study, in the reflection-asymmetric forms case. The studied sample was based on a new parameterization of the octupole and quadrupole independent degrees which is valid for nuclei near the axial symmetry. The nuclei case which has a lasting quadrupole deformation was discussed in some detail and a simple solution was gained at the phase transition critical point between consistent octupole oscillation and a permanent asymmetric shape. Results were matched with experimental data of thorium isotopic chain [14].

S. Chmel, S. Frauendorf, and H. Hubel in 2007 reported that tilt angles, deformation parameters, angular moment, reduced magnetic dipole and electric quadrupole transition possibility at the framework of the tilted-axis cranking model for shears bands in the neutron-deficient Pb isotopes (^{193}Pb to ^{202}Pb) metrication were calculated [15].

Boboshin I. et al. in 2007 reported that the deformation parameters were gained by two different processes: nuclear quadrupole moments Q (Q -type data) and miniature transference likelihood $B(E2: 0^+ \rightarrow 2^+)$ (B-type data). The nuclides were divided into two groups : group1 (Ti, Cr, Zr, Nd, Sm, Gd, Dy, Er, W, Os, Ra), group2 (C, Si, Ar, Ca, Fe, Ni, Zn, Ge, Se, Kr, Sr, Mo, Ru, Pd, Cd, Sn, Te, Ba, Yb, Hf, Pt, Pb). For all isotopes of “group 1” nuclei in good admission was seen for both types data, whereas for isotopes of (group 2) (B-type) β_2 data values are greater than (Q -type) [16].

A. Al-Sayed in 2009 the analyze of the nearest neighbor spacing distributions of low-lying 2^+ levels of even-even nuclei were done by researcher, and he classified the nuclei into groups realized by the quadrupole deformation parameter. For each group, the calculation of the nearest neighbor spacing distributions was done by using of the Bayesian inference method. By comparing these distributions to a formula that describes the transition to chaos by varying a tuning parameter. Results showed that these parameters depend in a non-trivial way on the nuclear deformation, and takes small values indicating regularity in strongly deformed nuclei and especially in those having an oblate deformation [17].

Ikuko Hamamot and Ben R. Mottelson in 2009 reported in this study, it was demonstrated nearly whole prolate domination over oblate disfigurement in the ground states of deformation even-even nuclei, this is related to the splitting of high ℓ (surface) orbits in the Nilsson's diagram: on the oblate side, the strongly appearance of numerous passages which can minimize the moving out of the low orbits, while on the prolate side there are the same reactions that increase the fanning out [18].

César Barbero, Jorge G. Hirsch and Alejandro E. Mariano in 2012 reported that the capability of three diverse Liquid Drop Mass (LDM) formulations for describing nuclei nuclear masses in several deformation zones was analyzed. Dividing the 2149 measured nuclear types into eight groups with same quadrupole

deformations. It was shown that the prolate deformed nuclei masses are preferable described than with the spherical ones [19].

S. Mohammadi in 2012 reported that a special computing code to calculate nuclear quadrupole moments against deformation parameter δ was developed. Some heavy nuclei results were compared with 2001 experimental data which showed that when increasing neutron number, the deformation parameter δ will increase too in some isotopes. This means that there will be more deformation from spherical shape [20].

A. G. Smith, J. L. Durell, W. R. Phillips, and W. Urban in 2012 reported that the extracted transition quadrupole moments were compared with different new theoretical methods, as well as with lower spin measurements and data interpretation was also done within the situation of prolate-oblate shape competition in this area [21].

Azad M. Kareem in 2014 reported that the study calculated the reduced transition possibility values $B(E2) \uparrow$ of gamma transmission among the Yarest bands states of some deformed even – even nuclei, the quadrupole moments values (Q_0) and moments of inertia (ϑ) for the bands states as a rotational frequency squared function ($\hbar^2\omega^2$). The results were the observation of different behavior of $2\vartheta/\hbar^2$ and Q_0 with $\hbar^2\omega^2$ for different isotopes of the same element [22].

B. Pritychenko, M. Birch, M. Horoi, and B. Singh in 2014: reported that it was studied a cooperative for assessing $B(E2) \uparrow$ for $0^+ \rightarrow 2^+$ transmission, the subset of $B(E2) \uparrow$ recommended values for relevance nuclei to the double-beta disintegration issue , assessment policies of experiential data and systematics. It was also studied the future plans for fulfillment of the $B(E2: 0^+ \rightarrow 2^+)$ assessment project [23]

K. A. Gado in 2014 reported that the study has developed a specific computing code for counting of nuclear quadrupole moments against deformation parameter β_2 , and it has seen that for some even-even nuclei the deformation parameter

increases when increasing number of neutrons which means more deformation occurs[24].

M. Haberichter, P. H. C. Lau, and N. S. Manton in 2015 were calculated the reduction of electromagnetic transition $B(E2)$ power for light nuclei with mass numbers: $B = 8, 12, 16, 20, 24$ and 32 , using Skyrme method and it was found out that the expected transmission powers were of the correct arrangement of proportion and the computed substantial quadrupole moments and matched the experientially spotted effective nuclear shapes. Regarding the Hoyle state, a large $B(E2) \uparrow$ value of $0.0521 e^2 b^2$ was predicted. For Oxygen-16, a quantitative realizing of the ground state rotational band and the rotational excitations of the second spin-0 state, were gained [25].

P. Möllera, A. J. Sierka, T. Ichikawab and H. Sagawac, in 2015: reported that it was worked on tabulating the atomic mass increasing and binding energies, ground-state shell-plus-pairing rectification, ground-state microscopic rectification, and nuclear ground-state deformations for (9318) nuclei with range of ^{16}O to $A = 339$. It was obtained the same model results but with quite amended treating of deformation and slightly of the accession that was necessary earlier, because of the limitations in computer power [26].

F. Ertuğral, Ali Kuliev, and Ekber Guliyev in 2015 reported that the quadrupole moments of the $^{166-180}\text{Hf}$, $^{180-186}\text{W}$ and $^{152-168}\text{Sm}$ isotopic chains were studies and that showed the disfigurements parameter were fundamentally used in literature overvalue in the real deformation parameters values β_2 by 10% for the well-deformed rare-earth nuclei. The theoretical values of the quadrupole moments results were well agreed with the former theoretical works which were only done for Sm isotopes [27].

Rusul Saad Hadi in 2015 reported that the search focused on studying of electromagnetic properties for even-even nuclei of ($_{50}\text{Sn}$, $_{48}\text{Cd}$ and $_{46}\text{Pd}$), and study the structure for nucleus through converting the adopted values for the transition of $E2 \downarrow$ to $B(E2) \uparrow e^2 b^2$ which in turn helped in calculating the deformation

parameters β . The good comparisons for the present calculation to the values of the $B(E2) \uparrow e^2 b^2$ and β with most recent values of experimental and theoretical was done [28].

B. Pritychenko, M. Birch, B. Singh, and M. Horoi in 2016: reported that gathering and assessing the experiential results of $E2$ transmission possibilities or $B(E2)$ values for the known first 2^+ cases in 447 even-even nuclei. The preferred $B(E2)$ values were compared with overall shell model calculating for the chosen nuclei group, where theoretical procedures like this can be adjustable [29].

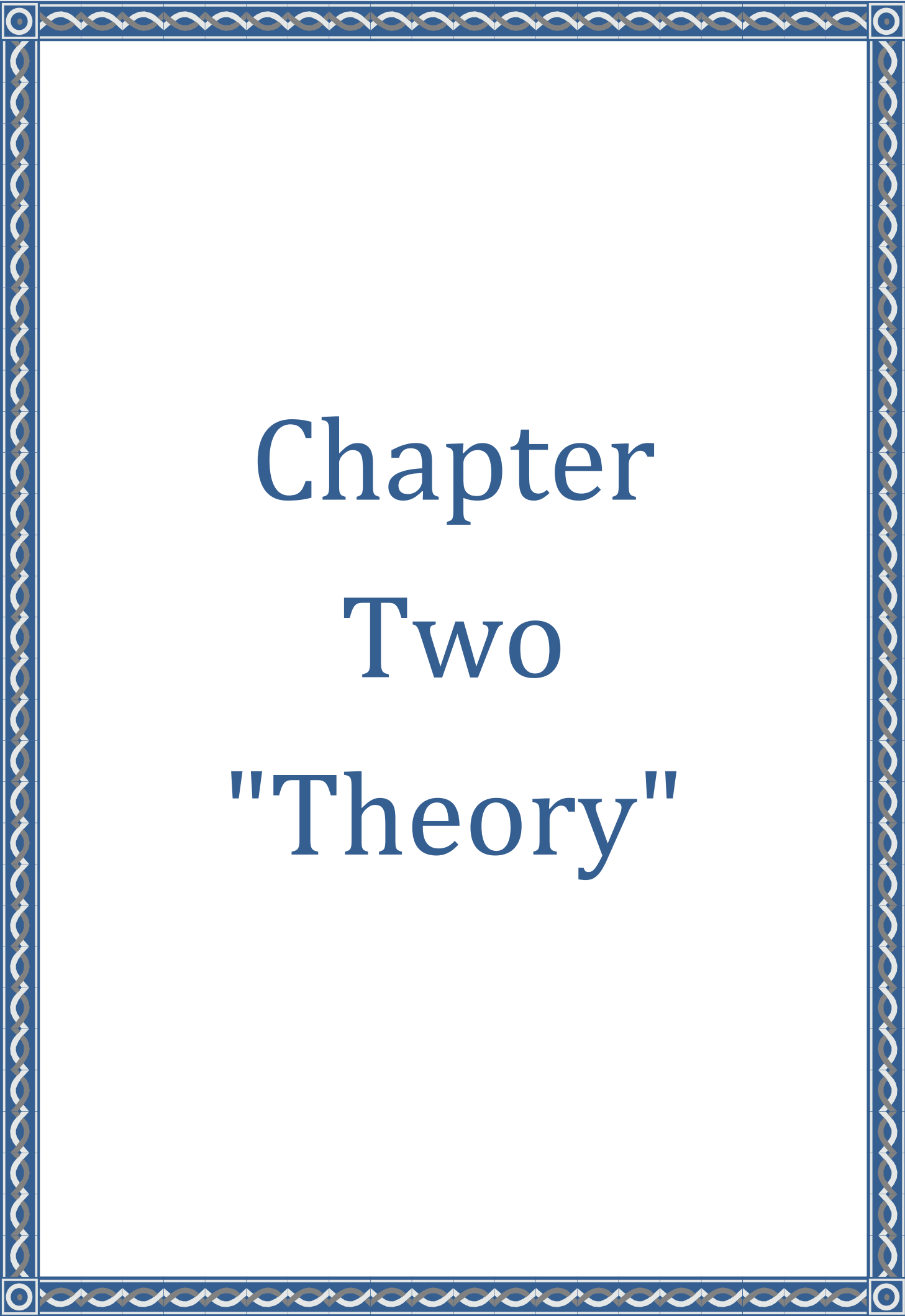
Hussain Jani Hassan in 2016 reported that the disfigurements parameters in this study were calculated using two different procedures (β_2, δ) for some even-even nuclei like, (${}_{20}\text{Ca}$ $38 \leq A \leq 48$, ${}_{36}\text{Kr}$ $74 \leq A \leq 92$, ${}_{54}\text{Xe}$ $118 \leq A \leq 140$, and ${}_{82}\text{Pb}$ $204 \leq A \leq 210$). It was noticed that the light shape for (${}_{20}\text{Ca}$) and medium for (${}_{36}\text{Kr}$) nuclide had significant disfigure in shape when neutrons number were away from magic number, while the heavy nuclei (${}_{54}\text{Xe}$) and (${}_{82}\text{Pb}$) were less deformed in shape, though neutrons number were near from magic number [30].

1-6 The aim of the present work:

This work is presently aimed to determine the nucleus shape for the even-even isotopes with the mass numbers more than 100 ($A > 100$) using (30) element and their Isotopes. The work has been divided as below:

- Calculating nucleus quadrupole deformation parameter β_2 from reduced transition probability $B(E2) \uparrow$ from the ground to the first excited states ($0^+ \rightarrow 2^+$) which is obtained from the energy of the first excited state of the isotopes, and comparing it with the deformation parameter β_2 which obtained of the predicted value $B(E2) \uparrow$ for (SSANM).
- Calculating nucleus quadrupole deformation parameters δ from intrinsic quadrupole moments Q_0 .

These deformation parameters led to understand the nuclei shape distance from spherical shape (oblate and prolate shape) through calculating the major and minor ellipsoid axis (a, b).



Chapter Two "Theory"

2-1 Nuclear shape :

The nuclear shape is generally spherical when nuclei are stable. This attempt is to lower the surface energy. However, small parts from spheres are observed, in the area $150 < A < 190$. These deformations can only be quantified by using the ratio [31]:

$$\delta = \frac{\Delta R}{R} \quad (2.1)$$

where: R is the nuclear average radius and ΔR is the difference between semi-minor and semi-major axes.

$$\Delta R = (b - a) \quad (2.2)$$

For a sphere $\Delta R = 0$.

One of the nuclear deformation reasons is the competition between the Coulomb and nuclear powers. Since the Coulomb power intensity proportional inversely to the distance square, so the nucleus try to decrease its total energy and increase its binding energy through placing protons as far away as possible from each other. Furthermore, the nuclear force attempts to hold the shape to be spherical in order that the low-range attracting can be more efficient. Due to nuclear powers strength, then light nuclei could be spherical on the whole [31].

2-2 Nuclear surface deformations:

The collective motion can be explained as nuclear surface vibrations and rotations in the geometrical collective model that was firstly suggested by Bohr and Mottelson [32], where a nucleus modeled like a charged liquid drop and the moving nuclear surface may be expressed quite generally by an extension in spherical consistent with time-dependent shape parameters that are considered as coefficients[33,34]:

$$R(\theta, \phi, t) = R \left[1 + \sum_{\lambda=0}^{\infty} \sum_{\mu=-\lambda}^{\lambda} \alpha_{\lambda\mu}(t) Y(\theta, \phi) \right] \quad (2.3)$$

where: $R(\theta, \phi, t)$ indicates the nuclear radius in the direction (θ, ϕ) at time t as shown in figure (2.1). R is the average nucleus radius, $\alpha_{\lambda\mu}$ are the deformation variables, λ determines the multipole or mode of nuclear motion, μ is the projection of λ on the z -axis, and $Y(\theta, \phi)$ is the spherical harmonic.

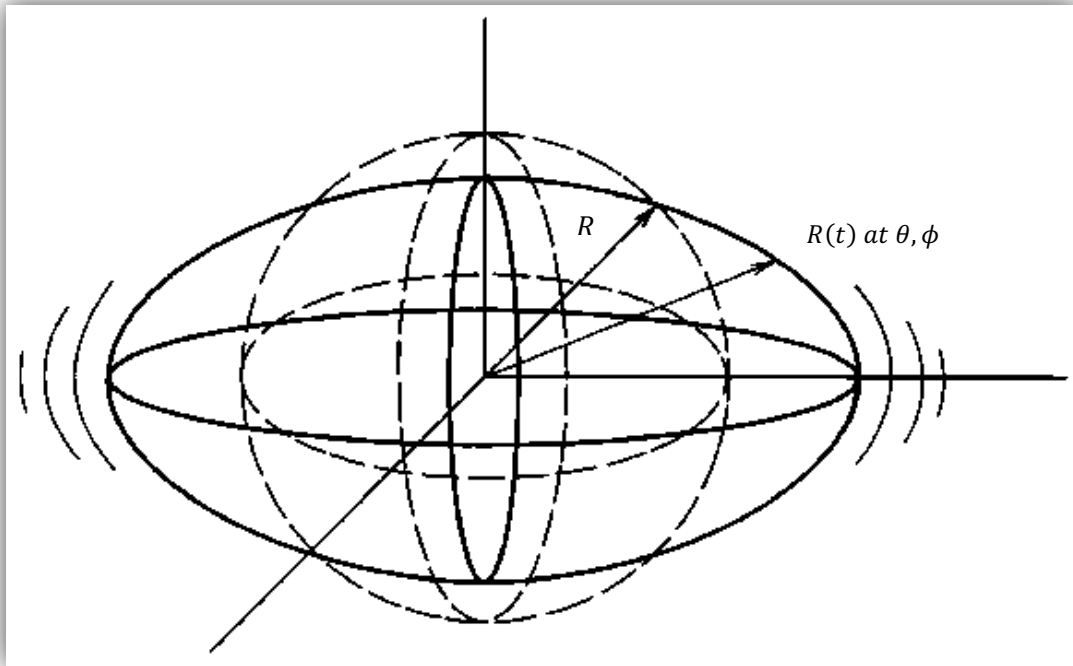


Figure (2.1): A vibrating nucleus with a spherical equilibrium shape. The time-dependent coordinate $R(t)$ locates a point on the surface in the direction (θ, ϕ) [34].

The surface coordinates are determined by λ and μ as functions of θ and ϕ respectively. For axially symmetric nuclei, nuclear radius can be expressed as [33,34]:

$$R(\theta, \phi) = R [1 + \beta_2 Y_{20}(\theta, \phi)] \quad (2.4)$$

The quadrupole deformation parameter $\beta_2 (= \alpha_{20})$, is related to the spheroid axes [34, 35]:

$$\beta_2 = \frac{4}{3} \sqrt{\frac{\pi}{5}} \frac{\Delta R}{R} = 1.06 \frac{\Delta R}{R} = 1.06 \delta \quad (2.5)$$

where R is the average radius $R = 1.2 A^{1/3}$ and ΔR is the difference between both of the semi-major and semi minor axes. As long as the value of β_2 is larger, the nucleus becomes more deformed.

2-3 Types of multipole deformations:

The nuclear surface general extension (2.3) can permit for qualitative deformities. This section explains the physical concept of the different multi pole arrangements and their application will be as λ values increasing.

- The monopole mode, $\lambda = 0$. Here, the spherical harmonic $Y_{00}(\Omega)$ is constant, in order that a non-disappearing value of α_{00} agrees with the sphere radius changing. The related excitement can be the so-called breath mode of the nucleus. Due to the great amount of energy that is required to compress the nuclear material, yet, this mode is away and has too high energy to be vital for the low-energy spectrum. The deformation parameter α_{00} may be utilized to repeal the overall density alteration that is presented as a side effect in the other multipole deformations [36].
- While dipole deformations, $\lambda = 1$ is applied to the lowest arranging, non-corresponding to a nucleus deformation but sort of a mass center transferring. Therefore, lowest order $\lambda = 1$ corresponds only to the nucleus translation and has to be ignored for nuclear excitement[36].
- For quadrupole deformations the modes with $\lambda = 2$ turn to become the most important nucleus collective excitements [36].
- Further, for the octupole deformations, $\lambda = 3$, the essential asymmetric modes of the nucleus related with negative-parity bands. The octupole-deformed shape seems somewhat like a pear [36].
- Finally, for hexadecupole deformations, $\lambda = 4$, which is the highest angular momentum, there is no evidence for pure hexadecupole excitement in spectrum. This sounds to have an important role as a mixture to quadrupole excitations and for the ground-state shape of heavy nuclei [36].

An illustration of the multipole deformations for the lowest four angular momenta is given in Fig. (2.2).

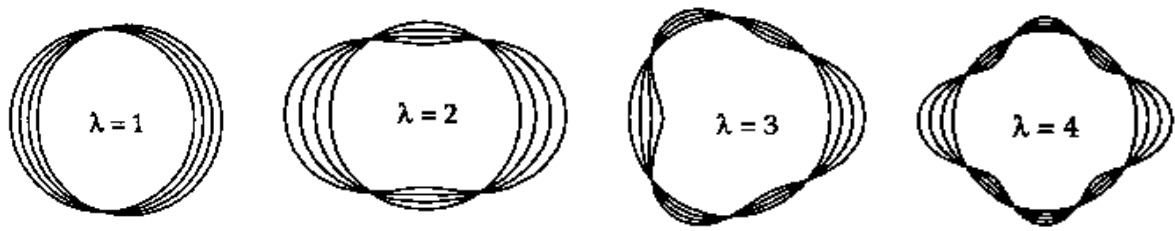


Figure.(2.2): demonstrates the multipole deformations for $\lambda = 1, \dots, 4$ [36].

2-4 The root mean square charge radius (isotopes shift):

The root mean square (rms) nuclear charge radius $R = \langle r^2 \rangle^{1/2}$, with one another nuclear ground-state properties, is considered the key of nuclear materials information which refer to stated nuclear structure effectiveness, for instance: shell closures and a deformation starting. Nuclear quantities, for example charge radius and nuclear moments are reachable through experimentations depending on the nucleus reaction with the electromagnetic field that is generated by the electrons or muons surrounding the nucleus (or with an external electromagnetic field) [37]. There are four measures methods: Transition energies measurement in muonic atoms (μ^-), elastic electron scattering experimentations (e^-), K_α x-ray isotope shifts and optical isotope shifts (KIS, OIS). The first two methods provide information about R and the second ones work on the isotopic changing $\langle r^2 \rangle$. Both pair methods are integral: integrating the data on the rms radius R of a stable reference isotope A' with the radius changing $\delta \langle r^2 \rangle^{A'A} = \langle r^2 \rangle^A - \langle r^2 \rangle^{A'}$ between A' and a radioactive isotope A , one can find the $R(A)$ -value of any isotope A in a long isotopic sequence by using simple relation [38]:

$$R^2(A) = R^2(A') + \delta \langle r^2 \rangle^{A'A} \quad (2.6)$$

As the nucleus borders are not well clarified, so there is no possibility of determining its radius in exact way. It can alternatively work with the average radius which is known as the mean square charge radius [39]:

$$\langle r^2 \rangle = \frac{\int \rho(r)r^2 d^3r}{\int \rho(r)d^3r} \quad (2.7)$$

where: $\rho(r)$ refers to the charge density distribution of the protons.

Isotope shifts consist of information on this quantity changing as a function of neutron number. Because the nucleuses have a long charge distribution which is able to change from one isotope to another and not from being a point charge, the isotope shifts occur. This is traditionally called “nuclear volume shift” or “field shift. It can obtain information about different radius from the isotope shifts measurement [40].

The root of mean square (rms) radius, $\langle r^2 \rangle^{1/2}$, is deduced directly from the distribution of scattered electrons; for a uniformly charged sphere, the squared charge distribution radius $\langle r^2 \rangle$ [16,34]:

$$\langle r^2 \rangle = 0.6 (1.2 A^{\frac{1}{3}})^2 \quad \text{for } A > 100 \quad (2.8)$$

2-5 Electric quadrupole moment:

The charge distribution in a nucleus can be described in terms of electric multipole moments and pursued from the classical electrostatics thoughts [41]. Some nuclei have permanent quadrupole moments which may experimentally be measured. These nuclei are expected to have elliptical shape with a symmetrical axis. This proposition, has classically led to define the intrinsic quadrupole moment as the following equation [20]:

$$Q_0 = \int d^3\rho(r)(3z^2 - r^2) \quad (2.9)$$

where: $\rho(r)$ is radial charge density of the proton, and (r) is charge radius.

The similarity axis can be the z -axis which is defined with regard with the body-fixed frame. If the charge density is concentrated along the z -direction (the particle symmetry axis), the term proportional to $(3z^2)$ dominates, Q_0 is positive and the particle is prolate (cigar-shaped). If the charge density is concentrated in the equatorial plane vertical to z , the term proportional to (r^2) prevads, Q_0 is negative, and the particle is oblate (pancake-shaped). According to the angular momentum selection rules, a spin ($J = 1/2$) nucleus, for example: the nucleon have no a spectroscopic quadrupole moment; yet, it may have a radical quadrupole moment [42]. If Q_0 is considered to be calculated for a homogeneously charged ellipsoid with charge Ze and semi-axes (a and b). With b pointing along the z axis, Q_0 will be [43]:

$$Q_0 = \frac{2}{5}Z(a^2 - b^2) \quad (2.10)$$

If the deviation from sphericity is not very large, the average radius: $R = 1/2 (a + b)$ and $\Delta R = (b - a)$ from equation (2.2) can be presented and with $\delta = \Delta R/R$, from equation (2.1), the quadrupole moment is [43]:

$$Q_0 = \frac{4}{5}ZR^2\delta \quad (2.11)$$

From eq. (2.8) and eq. (2.11), the nucleus quadrupole deformation parameter values δ become as follow [16, 44]:

$$\delta = 0.75 Q_0/(Z\langle r^2 \rangle) \quad (2.12)$$

The semi-axes a and b are gained from the two following equations [44].

$$a = \sqrt{\langle r^2 \rangle (1.66 - \frac{2\delta}{0.9})} \quad (2.13)$$

$$b = \sqrt{5\langle r^2 \rangle - 2a^2} \quad (2.14)$$

The spectroscopic quadrupole moment Q_s of a nuclear state with spin J is a deviation measure of the nuclear charge allocation from sphericity for $K = 0$ bands, and concerned to the radical quadrupole moment Q_0 by [40]:

$$Q_s = \frac{3K^2 - J(J - 1)}{J(J + 1)(2J + 3)} Q_0 \quad (2.15)$$

where: (J) is the total angular momentum (nucleus spin), and (K) is the projection of J onto the z -axis in the body fixed frame (symmetry axis of the nucleus) as shown in the Fig (2.3).

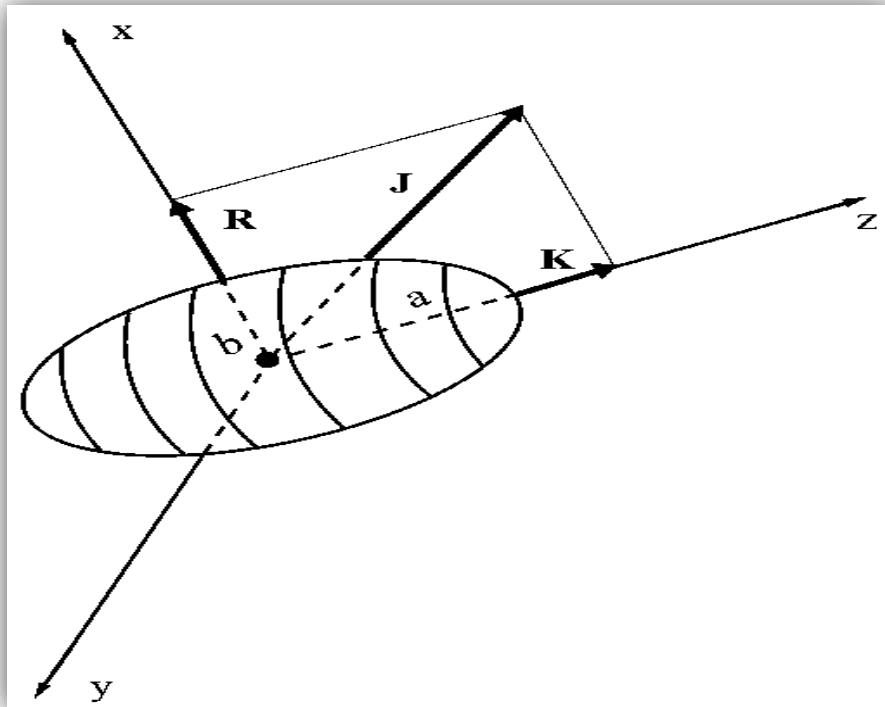


Figure (2.3): Represents the isobar as a prolate nucleon collective rotation with intrinsic spin $K = 1/2$. The collective orbital angular momentum is indicated by R [42].

2-6 Quadrupole deformations:

The quadrupole deformation parameter is one of the main features in nuclei deformation. It provides a significant effectiveness on a nuclear properties number: the excited spectrum levels, the electric and magnetic multi-pole moments and the

nuclear reactions cross sections. The third one is important especially in case of very small cross sections ($<1\mu\text{b}$), for example, new trans-Uranium elements composition when low bombing particles energies which must be used to inhibit the synchronous fission interaction. Thus, various nuclear processes investigating needs information on the quadrupole deformation parameters [45].

In general, nuclei with Z or N far from a magic number are deformed. The so-called quadrupole is the most ordinary deformations where the nucleus may have a prolate or oblate shape. A quadrupole deformation holds one symmetry axis (z axis), as [4]

An illustration of the nucleus shapes are given in Fig (2.4).

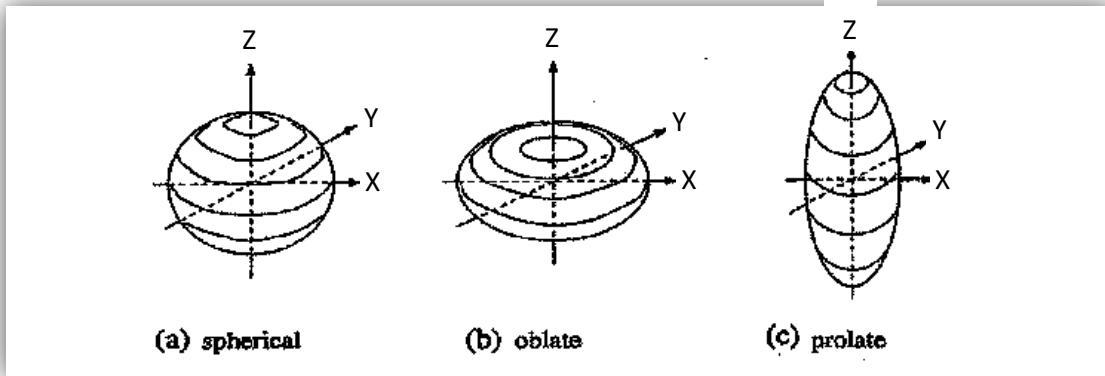


Figure (2.4): A diagrammatic representation of three of a nuclear shapes (a) Spherical, (b) Oblate, (c) Prolate. The z -axis donates to the symmetry axis of the oblate and prolate shapes [28].

It is notorious that the axially symmetric deformed nucleus shape is explained by the deformation parameter (β_2) which is connected to the quadrupole moment (Q_0) and represents the homogeneous charge distribution [35, 46].

$$Q_0 = \frac{3ZR^2}{\sqrt{5\pi}} (\beta_2 + 0.36\beta_2^2 + \dots) \quad (2.16)$$

where Z is the atomic number, $R = 1.2 \times A^{1/3}$ fm, and β_2 the deformation parameter and ($\beta_2 < 1$).

Generally in literature during the determination of the experimental value of (β_2) deformation parameter in the first approximation is assumed as ($\beta_2^2 \ll 1$) and by neglecting the (β_2^2) term in the equation. (2.16) as [47]:

$$Q_0 = \frac{3ZR^2}{\sqrt{5\pi}} \beta_2 \quad (2.17)$$

2-7 Electromagnetic transition:

The nucleus interaction with an external electromagnetic field led to the transition. The charge division couples with the external field that brings “electric” transitions. Electromagnetic transmissions compose the disintegration controlling mode for low-lying excited states in nuclei, especially for the light ones. The major cause is that nucleon emission which is much faster process than γ -decay; this cannot be happened till the excitation energy is above nucleon separation energies. These are the arrangement of (8 -10) MeV for neutrons and a bit lower for protons because of Coulomb repulsion [31].

2-7-1 The reduced electric quadrupole transition probability ($E2$) \uparrow :

Radioactive electromagnetic transformations between nuclear states are a perfect path to achieve nuclear structure and to experiment nuclear structure models [32]. $B(E2) \uparrow$ Transmission plays a definitive role to determine the lifetimes of nuclear states average, the nuclear deformation parameter, the volume of essential electric quadrupole moments and the energy of low-lying nuclei levels. Great quadrupole moments and transmissions forces refer to the collective effects in which many nucleons can participate [13]. For a nuclear state, let J be the total angular momentum and K its dropping on the body-fixed 3-axis. The reduced electric quadrupole transmission strength $B(E2) \uparrow$ from an initial state J_i to a final state J_f can be gained from the intrinsic Quadrupole moment Q_0 via [31]:

$$B(E2 : J_i \rightarrow J_f) = \frac{5}{16\pi} e^2 Q_0^2 \langle J_i K ; 20 | J_f K \rangle^2 \quad (2.18)$$

where: $\langle J_i K ; 20 | J_f K \rangle^2$ the Clebsch-Gordan coefficient rules the angular moment coupling.

For $K = 0$, $J_i = J$ and $J_f = J - 2$, with the Clebsch-Gordan coefficient in (2.16) facilitates to:

$$\langle J 0 ; 20 | (J - 2) 0 \rangle^2 = \frac{3J(J - 1)}{2(2J + 1)(2J - 1)} \quad (2.19)$$

The reduced transmission rate for disintegration between adjacent members of a $K = 0$ band becomes:

$$B(E2 : J \rightarrow J - 2) = \frac{15}{32\pi} e^2 Q_0^2 \frac{J(J - 1)}{(2J + 1)(2J - 1)} \quad (2.20)$$

Instead of that, for electromagnetic excitation from J to $J + 2$

$$B(E2 : J \rightarrow J + 2) = \frac{15}{32\pi} e^2 Q_0^2 \frac{(J + 1)(J + 2)}{(2J + 1)(2J + 3)} \quad (2.21)$$

From here the reduced electric quadrupole transition probability, $B(E2) \uparrow$, from the spin 0^+ ground state to the first excited spin 2^+ state is specified by[25]:

$$B(E2 : 0^+ \rightarrow 2^+) = \frac{5}{16\pi} e^2 Q_0^2 \quad (2.22)$$

where $B(E2) \uparrow$ is electric quadrupole transition probability in the unit of $(e^2 b^2)$ and Q_0 is Intrinsic quadrupole moment in barn unit barn .

Be noted that electromagnetic excitation $B(E2) \uparrow$ and nuclear state disintegration of $B(E2) \downarrow$ are concerning by [32].

$$B(E2 : J_f \rightarrow J_i) = \frac{2J_i + 1}{2J_f + 1} B(E2 : J_i \rightarrow J_f) \quad (2.23)$$

The $B(E2) \uparrow$ value is related to the mean lifetime (τ) via [25]:

$$\tau(1 + \alpha) = \tau_\gamma = 40.81 \times 10^{-13} E_\gamma^{-5} [B(E2) \uparrow / e^2 b^2]^{-1} \quad (2.24)$$

where (E) is the first excited state energy 2^+ in (keV) units, $B(E2) \uparrow$ in ($e^2 b^2$), (τ) is the mean lifetime in (ps) unit, and (α) is the total internal conversion coefficient.

The $B(E2) \uparrow$ values are requisite experimental quantities that have no dependence on nuclear models. A quantity, in which the model is thought to be depended on, is perfectly useful as it is the deformation parameter β_2 . Presuming a uniform charge distribution out to the distance $R(\theta, \phi)$ and zero charge beyond, β_2 is associated to $B(E2) \uparrow$ by the formulation [48]:

$$\beta_2 = (4\pi / 3ZR^2) [B(E2) \uparrow / e^2]^{1/2} \quad (2.25)$$

where R^2 equals to:

$$R^2 = \left(1.2 \times 10^{-13} A^{1/3} \text{ cm}\right)^2 = 0.0144A^{2/3} \text{ barn} \quad (2.26)$$

2-7-2 Experimental and theoretical predications of $B(E2) \uparrow$:

2-7-2-1 Experimental global best fit (GBF)

In accordance with the global systematic, the energy existence E_γ (keV) of the 2^+ state is whole that is required of creating a prediction for the corresponding τ_γ (ps) and hence $B(E2) \uparrow$ ($e^2 b^2$) value. When the indicators of E_γ and A were permitted to change, It was found previously that [13]:

$$\tau_\gamma = 1.25 \times 10^{14} E_\gamma^{-4.0} Z^{-2} A^{0.69} \quad (2.27)$$

where E_γ is the energy of the first excited state in unit keV, (Z) is the atomic number, and (A) is mass number.

From Eqs. (2.24) and (2.27), we converted the τ_γ to $B(E2) \uparrow$, and this expression equals to [13]:

$$B(E2) \uparrow = 3.26 \times E_\gamma^{-1.0} A^{-0.69} \quad (2.28)$$

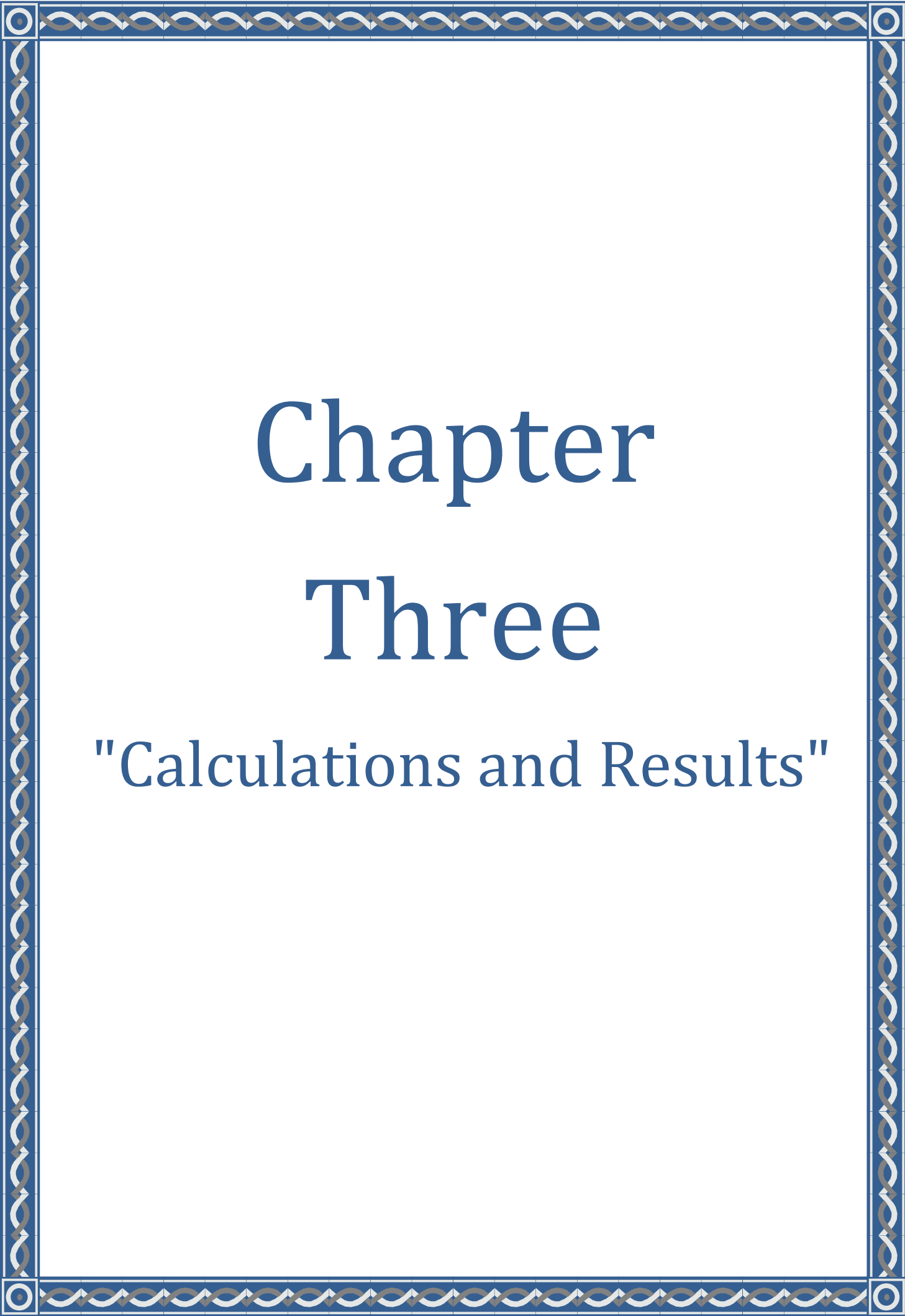
If the indicator of A is given as $(-2/3)$ (instead of -0.69), then:

$$B(E2) \uparrow = 2.6 \times E_\gamma^{-1} Z^2 A^{-\frac{2}{3}} \quad (2.29)$$

2-7-2-2 Theoretical predictions

In order that the $B(E2) \uparrow$ values can be predicted, many theoretical model are presented depending on these models: single-shell asymptotic Nilsson, finite-range droplet, Woods-Saxon, relativistic mean-field, extended Thomas-Fermi Strutinsky-Integral, Hartree-Fock+BCS, and dynamical microscopic [49].

- Single Shell Asymptotic Nilsson Model (SSANM): For knowing the $B(E2) \uparrow$ SSANM is the theoretical method which is depends on a single shell-deformed nucleus. This model type was suggested considering $B(E2) \uparrow$ values (in units of $e^2 b^2$) [13].



Chapter Three

"Calculations and Results"

3-1 Calculations:

In the present review, we computed many parameters for the even-even nuclei with mass numbers greater than 100 ($A > 100$) for (30) elements and their Isotopes which are (${}_{40}\text{Zr}$, ${}_{42}\text{Mo}$, ${}_{44}\text{Ru}$, ${}_{46}\text{Pd}$, ${}_{48}\text{Cd}$, ${}_{50}\text{Sn}$, ${}_{52}\text{Te}$, ${}_{56}\text{Ba}$, ${}_{58}\text{Ce}$, ${}_{60}\text{Nd}$, ${}_{62}\text{Sm}$, ${}_{64}\text{Gd}$, ${}_{66}\text{Dy}$, ${}_{68}\text{Er}$, ${}_{70}\text{Yb}$, ${}_{72}\text{Hf}$, ${}_{74}\text{W}$, ${}_{76}\text{Os}$, ${}_{78}\text{Pt}$, ${}_{80}\text{Hg}$, ${}_{82}\text{Pb}$, ${}_{84}\text{Po}$, ${}_{86}\text{Rn}$, ${}_{88}\text{Ra}$, ${}_{90}\text{Th}$, ${}_{92}\text{U}$, ${}_{94}\text{Pu}$, ${}_{96}\text{Cm}$, ${}_{98}\text{Cf}$, ${}_{100}\text{Fm}$), these Parameters are required for our study:

3-1-1 The deformation parameters (β_2)

Deformation parameters (β_2) derived from reduced electric transition probability $B(E2) \uparrow$ for even-even nucleus of the isotopes were counted using the equation (2.25). This equation contains many parameters which must be obtained:

- 1- Atomic Number Z , The mass number A , neutron number N , and the energies of the first excited states 2^+ , E_γ (keV), which obtained from ref. [50]
- 2- Reduced electric transition probabilities $B(E2) \uparrow: 0^+ \rightarrow 2^+$ from the ground 0^+ to the first excited 2^+ states are calculated by using equation (2.29).
- 3- Nuclear radius average R^2 is calculated using equation (2.26).

All these values were tabulated in tables (3.1)..... (3.30) respectively and the values of (β_2) were compared with the deformation parameters values resulting from the predicted values of $B(E2) \uparrow$ for (SSANM) Ref. [13]

3-1-2 The deformation parameters (δ)

The other method for calculation of deformation parameter (δ) is by using the intrinsic quadrupole moments (Q_0), equation (2.12). To evaluate this, the following variables must be available:

- 1- The mean square charge radius $\langle r^2 \rangle$ which is obtained from equation (2.8) for $A > 100$.
- 2- Intrinsic quadrupole moments (Q_0) of nuclei were calculated from the equation (2.17).

These values also previewed in tables from (3.1) to (3.30).

3-1-3 Root mean square charge radius $\langle r^2 \rangle^{1/2}$:

These values were obtained from values of $\langle r^2 \rangle$ and tabulated in tables from (3-31) to (3-60) and compared with the theoretical values of Ref. [51].

3-1-4 Semi-major and Semi-minor axis (a , b) and the difference between them ΔR :

The Semi-major axis (a) and Semi minor axis (b) were counted using Eq. (2.13) and (2.14) respectively. And these values previewed in the tables from (3-31) to (3-60). The difference ΔR between (a) and (b) was counted also by using three methods Eq. (2.1), (2.2), and (2.5) and tabulated in the same tables.

3-1-4 Figures were drowning to describe the relation between β_2 for the present work as a function of neutron numbers N , figures (3-1).....(3-30)

3-1-5 Figure was also drowning to describe the relation between β_2 for the present work as a function of mass numbers A , figure (3-31) .

3-1-6 The elliptical shapes of the isotopes of elements were drawn using semi major and semi minor axes to determine the shapes of the selected isotopes, figures (3-32).....(3-61) and figures (A-1)....(A-30).

3-2 The Results:

All the results that mentioned above are tabulates in tables and figures as follow:

Table (3-1): Mass Number of Isotopes (A), Neutron Number (N), Gamma Energy of the First Excited State 2^+ (E_γ), Square Nuclear Average Radius (R^2), Reduced Electric Transition Probability $B(E2)\uparrow$ in unit of e^2b^2 , Intrinsic Quadrupole Moment (Q_o) in unit of barn, and Deformation Parameters (β_2, δ) for ${}_{40}\text{Zr}$ Isotopes.

(Z)	(A)	(N)	E_γ (keV) [50]	Theoretical Value			Present Work			
				$B(E2)\uparrow e^2b^2$ For SSANM [13]	β_2	R^2 (barn)	$B(E2)\uparrow e^2b^2$	Q_o (barn)	β_2	δ
40	102	62	151.77 13	1.164	0.3594	0.3144	1.2556	3.5528	0.3733	0.3364
	104	64	140.3 10	1.162	0.3545	0.3185	1.3407	3.6713	0.3808	0.3431

Table (3-2): Mass Number of Isotopes (A), Neutron Number (N), Gamma Energy of the First Excited State 2^+ (E_γ), Square Nuclear Average Radius (R^2), Reduced Electric Transition Probability $B(E2)\uparrow$ in unit of e^2b^2 , Intrinsic Quadrupole Moment (Q_o) in unit of barn, and Deformation Parameters (β_2, δ) for ${}_{42}\text{Mo}$ Isotopes.

(Z)	(A)	(N)	E_γ (keV) [50]	Theoretical Value			Present Work			
				$B(E2)\uparrow e^2b^2$ For SSANM [13]	β_2	R^2 (barn)	$B(E2)\uparrow e^2b^2$	Q_o (barn)	β_2	δ
42	102	60	296.597 12	1.135	0.3228	0.3144	0.7083	2.6685	0.2670	0.2406
	104	62	192.3 2	1.103	0.3289	0.3185	1.0785	3.2927	0.3252	0.2931
	106	64	171.548 8	1.102	0.3246	0.3225	1.1937	3.4641	0.3378	0.3044
	108	66	192.9 10	1.084	0.3180	0.3266	1.0484	3.2465	0.3127	0.2818

Table (3-3): Mass Number of Isotopes (A) , Neutron Number (N), Gamma Energy of the First Excited State 2^+ (E_γ) , Square Nuclear Average Radius (R^2), Reduced Electric Transition Probability $B(E2)\uparrow$ in unit of e^2b^2 , Intrinsic Quadrupole Moment (Q_o) in unit of barn, and Deformation Parameters (β_2, δ) for ^{44}Ru Isotopes.

(Z)	(A)	(N)	E_γ (keV) [50]	Theoretical Value		Present Work				
				$B(E2)\uparrow e^2b^2$ For SSANM [13]	β_2	R^2 (barn)	$B(E2)\uparrow e^2b^2$	Q_o (barn)	β_2	δ
44	102	58	475.079 24	0.769	0.2656	0.3144	0.4853	2.2089	0.2110	0.1901
	104	60	358.02 7	0.886	0.2814	0.3185	0.6357	2.5280	0.2348	0.2148
	106	62	270.07 4	0.951	0.2878	0.3225	0.8321	2.8923	0.2693	0.2426
	108	64	242. 24 7	0.950	0.2841	0.3266	0.9163	3.0350	0.2790	0.2514
	110	66	240.71 10	0.932	0.2780	0.3306	0.9109	3.0261	0.2748	0.2477
	112	68	236.66 17	0.912	0.2717	0.3346	0.9154	3.0336	0.2722	0.2453

Table (3-4): Mass Number of Isotopes (A) , Neutron Number (N), Gamma Energy of the First Excited State 2^+ (E_γ) , Square Nuclear Average Radius (R^2), Reduced Electric Transition Probability $B(E2)\uparrow$ in unit of e^2b^2 , Intrinsic Quadrupole Moment (Q_o) in unit of barn, and Deformation Parameters (β_2, δ) for ^{46}Pd Isotopes.

(Z)	(A)	(N)	E_γ (keV) [50]	Theoretical Value		Present Work				
				$B(E2)\uparrow e^2b^2$ For SSANM [13]	β_2	R^2 (barn)	$B(E2)\uparrow e^2b^2$	Q_o (barn)	β_2	δ
46	102	56	556.43 4	0.494	0.2036	0.3144	0.4529	2.1338	0.1949	0.1757
	104	58	555.81 4	0.619	0.2250	0.3185	0.4476	2.1212	0.1913	0.1724
	106	60	511.851 23	0.728	0.2409	0.3225	0.4799	2.1964	0.1956	0.1762
	108	62	433.938 5	0.789	0.2477	0.3266	0.5590	2.3707	0.2085	0.1879
	110	64	372.81 6	0.788	0.2445	0.3306	0.6411	2.5387	0.2205	0.1987
	112	66	348.79 17	0.771	0.2390	0.3346	0.6789	2.6124	0.2242	0.2021
	114	68	332.50 24	0.752	0.2332	0.3386	0.7038	2.6599	0.2256	0.2033
	116	70	340.6 3	0.732	0.2275	0.3425	0.6791	2.6129	0.2191	0.1974
	118	72	378.4 2	0.626	0.2080	0.3464	0.6043	2.4649	0.2043	0.1841

Table (3-5): Mass Number of Isotopes (A), Neutron Number (N), Gamma Energy of the First Excited State 2^+ (E_γ), Square Nuclear Average Radius (R^2), Reduced Electric Transition Probability $B(E2)\uparrow$ in unit of e^2b^2 , Intrinsic Quadrupole Moment (Q_o) in unit of barn, and Deformation Parameters (β_2, δ) for ${}_{48}\text{Cd}$ Isotopes.

(Z)	(A)	(N)	E_γ (keV) [50]	Theoretical Value		Present Work				
				$B(E2)\uparrow e^2b^2$ For SSANM [13]	β_2	R^2 (barn)	$B(E2)\uparrow e^2b^2$	Q_o (barn)	β_2	δ
48	102	54	776.55 14	0.257	0.1407	0.3144	0.3534	1.8848	0.1650	0.1487
	104	56	658.0 4	0.336	0.1658	0.3185	0.4117	2.0343	0.1758	0.1584
	106	58	632.64 4	0.478	0.1871	0.3225	0.4228	2.0616	0.1759	0.1585
	108	60	632.986 16	0.577	0.2030	0.3266	0.4173	2.0482	0.1726	0.1556
	110	62	657.7638 1	0.634	0.2102	0.3306	0.3967	1.9970	0.1663	0.1498
	112	64	617.250 10	0.632	0.2073	0.3346	0.4175	2.0487	0.1685	0.1519
	114	66	558.456 2	0.617	0.2025	0.3386	0.4562	2.1416	0.1741	0.1569
	116	68	513.490 15	0.600	0.1974	0.3425	0.4905	2.2205	0.1784	0.1608
	118	70	487.77 8	0.581	0.1920	0.3464	0.5105	2.2654	0.1800	0.1622
	120	72	505.9 2	0.484	0.1733	0.3503	0.4867	2.2120	0.1738	0.1566
	122	74	569.45 8	0.359	0.1476	0.3542	0.4277	2.0735	0.1611	0.1452
	124	76	613.33 18	0.250	0.1219	0.3581	0.3928	1.9871	0.1527	0.1376
126	78	652 2	0.161	0.0967	0.3619	0.3656	1.9170	0.1458	0.1314	

Table (3-6): Mass Number of Isotopes (A), Neutron Number (N), Gamma Energy of the First Excited State 2^+ (E_γ), Square Nuclear Average Radius (R^2), Reduced Electric Transition Probability $B(E2)\uparrow$ in unit of e^2b^2 , Intrinsic Quadrupole Moment (Q_o) in unit of barn, and Deformation Parameters (β_2, δ) for ${}_{50}\text{Sn}$ isotopes.

(Z)	(A)	(N)	E_γ (keV) [50]	Theoretical Value		Present Work				
				$B(E2)\uparrow e^2b^2$ For SSANM [13]	β_2	R^2 (barn)	$B(E2)\uparrow e^2b^2$	Q_o (barn)	β_2	δ
50	102	52	1472.22	0.051	0.0602	0.3144	0.2023	1.4260	0.1199	0.1080
	104	54	1260.13	0.116	0.0896	0.3185	0.2332	1.5313	0.1271	0.1145
	106	56	1207.75	0.195	0.1147	0.3225	0.2403	1.5543	0.1273	0.1147
	108	58	1206.0710	0.281	0.1360	0.3266	0.2376	1.5457	0.1251	0.1127
	110	60	1211.8915	0.361	0.1523	0.3306	0.2336	1.5325	0.1225	0.1104
	112	62	1256.857	0.407	0.1597	0.3346	0.2226	1.4959	0.1181	0.1064
	114	64	1299.927	0.406	0.1577	0.3386	0.2127	1.4622	0.1141	0.1028
	116	66	1293.5608	0.394	0.1535	0.3425	0.2113	1.4573	0.1124	0.1013
	118	68	1229.66616	0.379	0.1489	0.3464	0.2197	1.4862	0.1134	0.1021
	120	70	1171.3419	0.365	0.1445	0.3503	0.2281	1.5143	0.1142	0.1029
	122	72	1140.553	0.286	0.1265	0.3542	0.2317	1.5261	0.1138	0.1026
	124	74	1131.73917	0.190	0.1020	0.3581	0.2310	1.5238	0.1124	0.1013
	126	76	1141.154	0.111	0.0771	0.3619	0.2266	1.5094	0.1102	0.0993
	128	78	1168.834	0.035	0.0527	0.3657	0.2190	1.4836	0.1072	0.0966
	130	80	1221.265	0.017	0.0296	0.3695	0.2074	1.4440	0.1032	0.0930
132	82	4041.14	Sph	-----	0.3733	0.0620	0.7898	0.0559	0.0504	
134	84	725.2	0.060	0.0344	0.3771	0.3424	1.8553	0.1300	0.1171	

Table (3-7): Mass Number of Isotopes (A), Neutron Number (N), Gamma Energy of the First Excited State 2^+ (E_γ), Square Nuclear Average Radius (R^2), Reduced Electric Transition Probability $B(E2)\uparrow$ in unit of e^2b^2 , Intrinsic Quadrupole Moment (Q_o) in unit of barn, and Deformation Parameters (β_2, δ) for $_{52}\text{Te}$ Isotopes.

(Z)	(A)	(N)	E_γ (keV) [50]	Theoretical Value		Present Work				
				$B(E2)\uparrow e^2b^2$ For SSANM [13]	β_2	R^2 (barn)	$B(E2)\uparrow e^2b^2$	Q_o (barn)	β_2	δ
52	108	56	625.4 10	0.618	0.1939	0.3266	0.4957	2.2323	0.1737	0.1565
	110	58	657.7 2	0.770	0.2138	0.3306	0.4656	2.1635	0.1663	0.1498
	112	60	689.01 20	0.903	0.2288	0.3346	0.4391	2.1011	0.1595	0.1438
	114	62	708.9 2	0.978	0.2353	0.3386	0.4218	2.0593	0.1545	0.1393
	116	64	678.92 3	0.977	0.2325	0.3425	0.4354	2.0921	0.1552	0.1398
	118	66	605.706 20	0.957	0.2275	0.3464	0.4825	2.2023	0.1615	0.1455
	120	68	560.438 20	0.934	0.2222	0.3503	0.5156	2.2769	0.1651	0.1488
	122	70	564.117 14	0.911	0.2171	0.3542	0.5066	2.2568	0.1619	0.1459
	124	72	602.731 3	0.782	0.1989	0.3581	0.4691	2.1716	0.1541	0.1388
	126	74	666.338 12	0.612	0.1741	0.3619	0.4198	2.0543	0.1442	0.1300
	128	76	743.30 10	0.458	0.1491	0.3657	0.3724	1.9349	0.1344	0.1211
	130	78	839.494 17	0.328	0.1248	0.3695	0.3263	1.8113	0.1245	0.1122
	132	80	973.90 10	0.220	0.1012	0.3733	0.2785	1.6731	0.1139	0.1026
	134	82	1279.04 10	0.112	0.0715	0.3771	0.2099	1.4527	0.0979	0.0882
	136	84	605.91 10	0.346	0.1244	0.3808	0.4387	2.1002	0.1401	0.1236
138	86	443.1 10	0.558	0.1565	0.3845	0.5941	2.4440	0.1615	0.1455	

Table (3-8): Mass Number of Isotopes (A), Neutron Number (N), Gamma Energy of the First Excited State 2^+ (E_γ), Square Nuclear Average Radius (R^2), Reduced Electric Transition Probability $B(E2)\uparrow$ in unit of e^2b^2 , Intrinsic Quadrupole Moment (Q_o) in unit of barn, and Deformation Parameters (β_2, δ) for ${}_{56}\text{Ba}$ Isotopes.

(Z)	(A)	(N)	E_γ (keV) [50]	Theoretical Value		Present Work				
				$B(E2)\uparrow e^2b^2$ For SSANM [13]	β_2	R^2 (barn)	$B(E2)\uparrow e^2b^2$	Q_o (barn)	β_2	δ
56	118	62	194.2	1.882	0.2962	0.3464	1.7452	4.1886	0.2852	0.2570
	120	64	183.5	1.881	0.2928	0.3503	1.8314	4.2908	0.2889	0.2604
	122	66	196.13	1.854	0.2875	0.3542	1.6903	4.1222	0.2745	0.2474
	124	68	229.8910	1.821	0.2819	0.3581	1.4263	3.7867	0.2495	0.2248
	126	70	256.097	1.787	0.2763	0.3619	1.2668	3.5687	0.2326	0.2096
	128	72	284.098	1.595	0.2583	0.3657	1.1300	3.3705	0.2174	0.1959
	130	74	357.388	1.336	0.2340	0.3695	0.8890	2.9896	0.1909	0.1720
	132	76	464.58824	1.092	0.2094	0.3733	0.6770	2.6088	0.1649	0.1486
	134	78	604.723019	0.874	0.1854	0.3771	0.5149	2.2752	0.1423	0.1283
	136	80	818.51512	0.682	0.1622	0.3808	0.3767	1.9459	0.1205	0.1086
	138	82	1435.81810	0.468	0.1331	0.3845	0.2126	1.4621	0.0897	0.0808
	140	84	602.353	0.907	0.1835	0.3883	0.5021	2.2466	0.1365	0.1230
	142	86	359.59614	1.256	0.2139	0.3919	0.8331	2.8939	0.1742	0.1570
	144	88	199.3265	1.634	0.2417	0.3956	1.4889	3.8689	0.2307	0.2079
	146	90	181.055	1.886	0.2573	0.3993	1.6242	4.0409	0.2388	0.2152
148	92	141.710	2.115	0.2700	0.4029	2.0565	4.5469	0.2662	0.2399	

Table (3-9): Mass Number of Isotopes (A), Neutron Number (N), Gamma Energy of the First Excited State 2^+ (E_γ), Square Nuclear Average Radius (R^2), Reduced Electric Transition Probability $B(E2)\uparrow$ in unit of e^2b^2 , Intrinsic Quadrupole Moment (Q_o) in unit of barn, and Deformation Parameters (β_2, δ) for ${}_{58}\text{Ce}$ Isotopes.

(Z)	(A)	(N)	E_γ (keV) [50]	Theoretical Value		Present Work				
				$B(E2)\uparrow e^2b^2$ For SSANM [13]	β_2	R^2 (barn)	$B(E2)\uparrow e^2b^2$	Q_o (barn)	β_2	δ
58	124	66	142 10	2.355	0.3095	0.3581	2.4770	4.9901	0.3174	0.2860
	126	68	169.59 3	2.318	0.3038	0.3619	2.0520	4.5419	0.2859	0.2576
	128	70	207.3 10	2.279	0.2981	0.3657	1.6612	4.0866	0.2545	0.2293
	130	72	253.99 19	2.057	0.2803	0.3695	1.3419	3.6729	0.2264	0.2040
	132	74	325.54 16	1.753	0.2561	0.3733	1.0364	3.2278	0.1969	0.1775
	134	76	409.12 10	1.466	0.2319	0.3771	0.8164	2.8649	0.1731	0.1559
	136	78	552.20 11	1.205	0.2082	0.3808	0.5989	2.4538	0.1468	0.1323
	138	80	788.744 8	0.973	0.1853	0.3845	0.4152	2.0432	0.1210	0.1091
	140	82	1596.227 25	0.707	0.1564	0.3883	0.2032	1.4294	0.0839	0.0756
	142	84	641.286 9	1.245	0.2056	0.3919	0.5011	2.2444	0.1304	0.1175
	144	86	397.441 9	1.661	0.2353	0.3956	0.8010	2.8377	0.1634	0.1472
	146	88	258.46 3	2.104	0.2624	0.3993	1.2205	3.5028	0.1998	0.1801
	148	90	158.468 5	2.398	0.2776	0.4029	1.9726	4.4532	0.2518	0.2269
	150	92	97.1 10	2.663	0.2899	0.4065	3.1907	5.6636	0.3173	0.2860
152	94	81.7 10	2.888	0.2993	0.4101	3.7588	6.1471	0.3414	0.3076	

Table (3-10): Mass Number of Isotopes (A), Neutron Number (N), Gamma Energy of the First Excited State 2^+ (E_γ), Square Nuclear Average Radius (R^2), Reduced Electric Transition Probability $B(E2)\uparrow$ in unit of e^2b^2 , Intrinsic Quadrupole Moment (Q_o) in unit of barn, and Deformation Parameters (β_2, δ) for ${}_{60}\text{Nd}$ Isotopes.

(Z)	(A)	(N)	E_γ (keV) [50]	Theoretical Value		Present Work				
				$B(E2)\uparrow e^2b^2$ For SSANM [13]	β_2	R^2 (barn)	$B(E2)\uparrow e^2b^2$	Q_o (barn)	β_2	δ
60	128	68	133.66 7	2.797	0.3192	0.3657	2.7572	5.2648	0.3170	0.2856
	130	70	158 2	2.754	0.3135	0.3695	2.3085	4.8174	0.2870	0.2587
	132	72	212.62 18	2.504	0.2959	0.3733	1.6981	4.1317	0.2437	0.2196
	134	74	294.30 16	2.160	0.2721	0.3771	1.2146	3.4943	0.2040	0.1839
	136	76	373.6 3	1.832	0.2481	0.3808	0.9473	3.0861	0.1784	0.1608
	138	78	520.1 3	1.533	0.2248	0.3845	0.6739	2.6029	0.1490	0.1343
	140	80	773.73	1.236	0.2021	0.3883	0.4487	2.1238	0.1204	0.1085
	142	82	1575.83 15	0.951	0.1737	0.3919	0.2182	1.4812	0.0832	0.0750
	144	84	696.513 5	1.579	0.2217	0.3956	0.4891	2.2175	0.1234	0.1112
	146	86	453.77 5	2.056	0.2507	0.3993	0.7439	2.7348	0.1508	0.1359
	148	88	301.702 16	2.560	0.2772	0.4029	1.1088	3.3387	0.1825	0.1644
	150	90	130.21 8	2.891	0.2920	0.4065	2.5463	5.0594	0.2740	0.2469
	152	92	72.51 19	3.189	0.3040	0.4101	4.5323	6.7501	0.3624	0.3266
	154	94	70.8 1	3.441	0.3130	0.4137	4.6015	6.8014	0.3620	0.3262
156	96	66.9 10	3.657	0.3199	0.4173	4.8280	6.9668	0.3676	0.3313	

Table (3-11): Mass Number of Isotopes (A), Neutron Number (N), Gamma Energy of the First Excited State 2^+ (E_γ), Square Nuclear Average Radius (R^2), Reduced Electric Transition Probability $B(E2)\uparrow$ in unit of e^2b^2 , Intrinsic Quadrupole Moment (Q_o) in unit of barn, and Deformation Parameters (β_2, δ) for ${}_{62}\text{Sm}$ Isotopes.

(Z)	(A)	(N)	E_γ (keV) [50]	Theoretical Value		Present Work				
				$B(E2)\uparrow e^2b^2$ For SSANM [13]	β_2	R^2 (barn)	$B(E2)\uparrow e^2b^2$	Q_o (barn)	β_2	δ
62	130	68	122 3	3.143	0.3241	0.3695	3.1923	5.6650	0.3267	0.2944
	132	70	131 2	3.096	0.3184	0.3733	2.9429	5.4392	0.3105	0.2798
	134	72	163 2	2.824	0.3011	0.3771	2.3415	4.8518	0.2742	0.2471
	136	74	254.91 16	2.451	0.2777	0.3808	1.4826	3.9606	0.2160	0.1947
	138	76	346.9 3	2.093	0.2542	0.3845	1.0789	3.2933	0.1825	0.1644
	140	78	530.7 1	1.764	0.2311	0.3883	0.6985	2.6499	0.1454	0.1311
	142	80	768 2	1.467	0.2088	0.3919	0.4781	2.1924	0.1192	0.1074
	144	82	1660.2 4	1.122	0.1809	0.3956	0.2191	1.4842	0.0799	0.0720
	146	84	747.115 13	1.815	0.2280	0.3993	0.4825	2.2023	0.1175	0.1059
	148	86	550.265 23	2.337	0.2563	0.4029	0.6491	2.5546	0.1351	0.1217
	150	88	333.863 9	2.886	0.2823	0.4065	1.0604	3.2650	0.1711	0.1542
	152	90	121.7817 2	3.246	0.2968	0.4101	2.8815	5.3822	0.2796	0.2520
	154	92	81.976 18	3.570	0.3085	0.4137	4.2435	6.5315	0.3364	0.3031
	156	94	75.89	3.844	0.3174	0.4173	4.5445	6.7592	0.3451	0.3110
	158	96	72.8 10	4.078	0.3242	0.4209	4.6974	6.8719	0.3479	0.3135
160	98	70.6 10	4.307	0.3304	0.4244	4.8033	6.9490	0.3489	0.3144	

Table (3-12): Mass Number of Isotopes (A), Neutron Number (N), Gamma Energy of the First Excited State 2^+ (E_γ), Square Nuclear Average Radius (R^2), Reduced Electric Transition Probability $B(E2)\uparrow$ in unit of e^2b^2 , Intrinsic Quadrupole Moment (Q_o) in unit of barn, and Deformation Parameters (β_2, δ) for ${}_{64}\text{Gd}$ Isotopes.

(Z)	(A)	(N)	E_γ (keV) [50]	Theoretical Value		Present Work				
				$B(E2)\uparrow e^2b^2$ For SSANM [13]	β_2	R^2 (barn)	$B(E2)\uparrow e^2b^2$	Q_o (barn)	β_2	δ
64	138	74	220.19 18	2.557	0.2722	0.3845	1.8053	4.2602	0.2287	0.2061
	140	76	328.6 10	2.184	0.2491	0.3883	1.2020	3.4762	0.1848	0.1665
	142	78	515.3 1	1.841	0.2266	0.3919	0.7593	2.7628	0.1455	0.1311
	144	80	743.0 10	1.530	0.2046	0.3956	0.5217	2.2902	0.1195	0.1077
	146	82	1971.97 22	1.169	0.1772	0.3993	0.1948	1.3993	0.0723	0.0652
	148	84	784.430 16	1.894	0.2236	0.4029	0.4852	2.2086	0.1132	0.1020
	150	86	638.045 14	2.439	0.2514	0.4065	0.5912	2.4380	0.1238	0.1116
	152	88	344.2789 11	3.013	0.2770	0.4101	1.0861	3.3043	0.1663	0.1499
	154	90	123.0714 10	3.389	0.2912	0.4137	3.0118	5.5026	0.2745	0.2474
	156	92	88.9666 14	3.728	0.3028	0.4173	4.1307	6.4441	0.3188	0.2872
	158	94	79.510 2	4.014	0.3116	0.4209	4.5829	6.7877	0.3329	0.3000
	160	96	75.26 1	4.259	0.3183	0.4244	4.8013	6.9475	0.3379	0.3045
	162	98	71 7	4.499	0.3244	0.4279	5.0474	7.1233	0.3436	0.3096

Table (3-13): Mass Number of Isotopes (A), Neutron Number (N), Gamma Energy of the First Excited State 2^+ (E_γ), Square Nuclear Average Radius (R^2), Reduced Electric Transition Probability $B(E2)\uparrow$ in unit of e^2b^2 , Intrinsic Quadrupole Moment (Q_o) in unit of barn, and Deformation Parameters (β_2, δ) for ${}_{66}\text{Dy}$ Isotopes.

(Z)	(A)	(N)	E_γ (keV) [50]	Theoretical Value		Present Work				
				$B(E2)\uparrow e^2b^2$ For SSANM [13]	β_2	R^2 (barn)	$B(E2)\uparrow e^2b^2$	Q_o (barn)	β_2	δ
66	142	76	315.9 4	2.228	0.2417	0.3919	1.3172	3.6390	0.1858	0.1675
	144	78	492.5 3	1.874	0.2196	0.3956	0.8374	2.9014	0.1468	0.1323
	146	80	682.9 3	1.554	0.1982	0.3993	0.5981	2.4522	0.1229	0.1108
	148	82	1677.3 10	1.183	0.1713	0.4029	0.2413	1.5576	0.0774	0.0697
	150	84	803.4 5	1.929	0.2168	0.4065	0.4993	2.2405	0.1103	0.0994
	152	86	613.81 7	2.491	0.2442	0.4101	0.6478	2.5520	0.1246	0.1122
	154	88	334.58 8	3.083	0.2694	0.4137	1.1782	3.4416	0.1665	0.1500
	156	90	137.83 3	3.474	0.2835	0.4173	2.8355	5.3391	0.2561	0.2308
	158	92	98.9180 10	3.825	0.2949	0.4209	3.9175	6.2750	0.2985	0.2690
	160	94	86.7882 4	4.122	0.3036	0.4244	4.4278	6.6718	0.3147	0.2836
	162	96	80.660 2	4.376	0.3102	0.4279	4.7249	6.8920	0.3224	0.2905
	164	98	73.392 5	4.625	0.3164	0.4314	5.1505	7.1957	0.3338	0.3008
	166	100	76.587 1	4.869	0.3220	0.4349	4.8959	7.0156	0.3229	0.2909

Table (3-14): Mass Number of Isotopes (A), Neutron Number (N), Gamma Energy of the First Excited State 2^+ (E_γ), Square Nuclear Average Radius (R^2), Reduced Electric Transition Probability $B(E2)\uparrow$ in unit of e^2b^2 , Intrinsic Quadrupole Moment (Q_o) in unit of barn, and Deformation Parameters (β_2, δ) for ${}_{68}\text{Er}$ Isotopes.

(Z)	(A)	(N)	E_γ (keV) [50]	Theoretical Value		Present Work				
				$B(E2)\uparrow e^2b^2$ For SSANM [13]	β_2	R^2 (barn)	$B(E2)\uparrow e^2b^2$	Q_o (barn)	β_2	δ
68	144	76	330.10	2.261	0.2341	0.3956	1.3261	3.6512	0.1793	0.1616
	148	80	646.63	1.569	0.1915	0.4029	0.6645	2.5847	0.1246	0.1123
	150	82	1578.8718	1.188	0.1652	0.4065	0.2697	1.6467	0.0787	0.0709
	152	84	808.2710	1.953	0.2099	0.4101	0.5222	2.2913	0.1085	0.0978
	154	86	560.010	2.532	0.2369	0.4137	0.7472	2.7408	0.1287	0.1160
	156	88	344.516	3.143	0.2617	0.4173	1.2042	3.4794	0.1620	0.1460
	158	90	192.153	3.545	0.2756	0.4209	2.1408	4.6392	0.2142	0.1930
	160	92	125.81	3.907	0.2869	0.4244	3.2426	5.7095	0.2614	0.2355
	162	94	102.043	4.214	0.2955	0.4279	3.9647	6.3133	0.2866	0.2583
	164	96	91.402	4.476	0.3021	0.4314	4.3902	6.6434	0.2992	0.2696
	166	98	80.5777	4.734	0.3081	0.4349	4.9398	7.0470	0.3148	0.2836
	168	100	79.8041	4.987	0.3138	0.4384	4.9480	7.0528	0.3125	0.2816
	170	102	78.59122	5.073	0.3140	0.4419	4.9849	7.0791	0.3112	0.2805
	172	104	77.04	4.917	0.3067	0.4454	5.0483	7.1240	0.3108	0.2800

Table (3-15): Mass Number of Isotopes (A), Neutron Number (N), Gamma Energy of the First Excited State 2^+ (E_γ), Square Nuclear Average Radius (R^2), Reduced Electric Transition Probability $B(E2)\uparrow$ in unit of e^2b^2 , Intrinsic Quadrupole Moment (Q_o) in unit of barn, and Deformation Parameters (β_2, δ) for ${}_{70}\text{Yb}$ Isotopes.

(Z)	(A)	(N)	E_γ (keV) [50]	Theoretical Value		Present Work				
				$B(E2)\uparrow e^2b^2$ For SSANM [13]	β_2	R^2 (barn)	$B(E2)\uparrow e^2b^2$	Q_o (barn)	β_2	δ
70	152	82	1531.4 5	1.189	0.1591	0.4101	0.2921	1.7136	0.0789	0.0711
	154	84	821.3 2	1.972	0.2031	0.4137	0.5399	2.3298	0.1063	0.0958
	156	86	536.4 1	2.566	0.2297	0.4173	0.8196	2.8704	0.1298	0.1170
	158	88	358.2 1	3.195	0.2542	0.4209	1.2169	3.7977	0.1569	0.1413
	160	90	243.1 1	3.609	0.2679	0.4244	1.7782	4.2280	0.1880	0.1694
	162	92	166.85 4	3.982	0.2790	0.4279	2.5694	5.0824	0.2241	0.2020
	164	94	123.36 4	4.299	0.2876	0.4314	3.4469	5.8866	0.2575	0.2320
	166	96	102.37 3	4.569	0.2941	0.4349	4.1203	6.4359	0.2793	0.2517
	168	98	87.73 1	4.836	0.3001	0.4384	4.7696	6.9245	0.2981	0.2686
	170	100	84.25474 8	5.097	0.3057	0.4419	4.9273	7.0381	0.3006	0.2709
	172	102	78.7427 5	5.186	0.3060	0.4454	5.2313	7.2519	0.3073	0.2769
	174	104	76.471 1	5.025	0.2989	0.4488	5.3453	7.3305	0.3083	0.2778
	176	106	82.13 2	4.866	0.2919	0.4522	4.9392	7.0466	0.2941	0.2650
	178	108	84 3	4.659	0.2835	0.4557	4.7930	6.9415	0.2875	0.2591

Table (3-16): Mass Number of Isotopes (A), Neutron Number (N), Gamma Energy of the First Excited State 2^+ (E_γ), Square Nuclear Average Radius (R^2), Reduced Electric Transition Probability $B(E2)\uparrow$ in unit of e^2b^2 , Intrinsic Quadrupole Moment (Q_o) in unit of barn, and Deformation Parameters (β_2, δ) for ${}_{72}\text{Hf}$ Isotopes.

(Z)	(A)	(N)	E_γ (keV) [50]	Theoretical Value		Present Work				
				$B(E2)\uparrow e^2b^2$ For SSANM [13]	β_2	R^2 (barn)	$B(E2)\uparrow e^2b^2$	Q_o (barn)	β_2	δ
72	154	82	1513 2	0.973	0.1387	0.4137	0.3101	1.7655	0.0783	0.0706
	156	84	858 2	1.706	0.1821	0.4173	0.5421	2.3344	0.1026	0.0925
	158	86	476.36 11	2.273	0.2084	0.4209	0.9681	3.1197	0.1360	0.1226
	160	88	389.6 10	2.880	0.2326	0.4244	1.1738	3.4352	0.1485	0.1338
	162	90	285.0 10	3.281	0.2463	0.4279	1.5914	3.9998	0.1715	0.1545
	164	92	211.05 5	3.645	0.2574	0.4314	2.1315	4.6291	0.1969	0.1774
	166	94	158.5 3	3.954	0.2660	0.4349	2.8154	5.3201	0.2244	0.2022
	168	96	124.0 2	4.220	0.2726	0.4384	3.5701	5.9909	0.2507	0.2259
	170	98	100.80 17	4.481	0.2787	0.4419	4.3572	6.6184	0.2748	0.2476
	172	100	95.22 4	4.738	0.2843	0.4454	4.5768	6.7831	0.2795	0.2518
	174	102	90.985 19	4.825	0.2847	0.4488	4.7530	6.9125	0.2826	0.2547
	176	104	88.351 24	4.667	0.2779	0.4522	4.8576	6.9881	0.2835	0.2555
	178	106	93.180 1	4.511	0.2712	0.4557	4.5713	6.7790	0.2730	0.2460
	180	108	93.326 2	4.307	0.2630	0.4591	4.5302	6.7485	0.2697	0.2431
	182	110	97.79 9	4.109	0.2550	0.4625	4.2917	6.5685	0.2606	0.2348
184	112	107.4 5	3.910	0.2469	0.4658	3.8793	6.2449	0.2460	0.2217	

Table (3-17): Mass Number of Isotopes (A), Neutron Number (N), Gamma Energy of the First Excited State 2^+ (E_γ), Square Nuclear Average Radius (R^2), Reduced Electric Transition Probability $B(E2)\uparrow$ in unit of e^2b^2 , Intrinsic Quadrupole Moment (Q_o) in unit of barn, and Deformation Parameters (β_2, δ) for ${}_{74}W$ Isotopes.

(Z)	(A)	(N)	E_γ (keV) [50]	Theoretical Value		Present Work				
				$B(E2)\uparrow e^2b^2$ For SSANM [13]	β_2	R^2 (barn)	$B(E2)\uparrow e^2b^2$	Q_o (barn)	β_2	δ
74	162	88	450.2 3	2.381	0.2041	0.4279	1.0642	3.2708	0.1365	0.1230
	164	90	331.6 3	2.755	0.2178	0.4314	1.4330	3.7956	0.1571	0.1415
	166	92	251.7 2	3.096	0.2290	0.4349	1.8728	4.3390	0.1781	0.1605
	168	94	199.3 2	3.387	0.2376	0.4384	2.3463	4.8567	0.1978	0.1782
	170	96	156.85 14	3.638	0.2443	0.4419	2.9579	5.4531	0.2203	0.1985
	172	98	123.2 1	3.885	0.2505	0.4454	3.7366	6.1290	0.2457	0.2214
	174	100	113.0 1	4.130	0.2563	0.4488	4.0426	6.3750	0.2536	0.2285
	176	102	109.08 9	4.213	0.2569	0.4522	4.1561	6.4639	0.2552	0.2299
	178	104	106.06	4.062	0.2504	0.4557	4.2423	6.5306	0.2559	0.2306
	180	106	103.557 7	3.914	0.2439	0.4591	4.3126	6.5845	0.2561	0.2307
	182	108	100.1060 1	3.720	0.2361	0.4625	4.4286	6.6724	0.2576	0.2321
	184	110	111.208 4	3.532	0.2284	0.4658	3.9575	6.3076	0.2417	0.2178
	186	112	122.33 7	3.344	0.2206	0.4692	3.5719	5.9924	0.2280	0.2055
	188	114	143 2	2.973	0.2065	0.4726	3.0339	5.5227	0.2086	0.1880
190	116	205 2	2.502	0.1881	0.4759	2.1014	4.5963	0.1724	0.1554	

Table (3-18): Mass Number of Isotopes (A), Neutron Number (N), Gamma Energy of the First Excited State 2^+ (E_γ), Square Nuclear Average Radius (R^2), Reduced Electric Transition Probability $B(E2)\uparrow$ in unit of e^2b^2 , Intrinsic Quadrupole Moment (Q_o) in unit of barn, and Deformation Parameters (β_2, δ) for ${}_{76}\text{Os}$ Isotopes.

(Z)	(A)	(N)	E_γ (keV) [50]	Theoretical Value		Present Work				
				$B(E2)\uparrow e^2b^2$ For SSANM [13]	β_2	R^2 (barn)	$B(E2)\uparrow e^2b^2$	Q_o (barn)	β_2	δ
76	164	88	548.0 9	1.894	0.1758	0.4314	0.9147	3.0323	0.1222	0.1101
	166	90	430.8 9	2.235	0.1894	0.4349	1.1541	3.4062	0.1361	0.1227
	168	92	341.2 2	2.549	0.2007	0.4384	1.4456	3.8122	0.1511	0.1362
	170	94	286.70 14	2.819	0.2094	0.4419	1.7069	4.1424	0.1629	0.1468
	172	96	227.77 9	3.053	0.2162	0.4454	2.1318	4.6294	0.1807	0.1628
	174	98	158.7 2	3.284	0.2225	0.4488	3.0362	5.5247	0.2140	0.1928
	176	100	135.1 4	3.514	0.2285	0.4522	3.5395	5.9651	0.2293	0.2066
	178	102	131.6 3	3.592	0.2292	0.4557	3.6063	6.0212	0.2297	0.2070
	180	104	132.3 3	3.450	0.2230	0.4591	3.5606	5.9829	0.2265	0.2041
	182	106	127.0 1	3.311	0.2169	0.4625	3.6820	6.0840	0.2287	0.2061
	184	108	119.80 9	3.129	0.2092	0.4658	3.8749	6.2414	0.2329	0.2099
	186	110	137.159 8	2.954	0.2019	0.4692	3.3607	5.8121	0.2153	0.1940
	188	112	155.021 11	2.778	0.1944	0.4726	2.9519	5.4476	0.2004	0.1806
	190	114	186.718 2	2.434	0.1807	0.4759	2.4336	4.9462	0.1807	0.1628
	192	116	205.79561 6	2.002	0.1627	0.4793	2.1926	4.6950	0.1703	0.1535
	194	118	218.509	1.603	0.1446	0.4826	2.0508	4.5406	0.1636	0.1474
196	120	300 20	1.248	0.1267	0.4859	1.4836	3.8619	0.1382	0.1245	

Table (3-19): Mass Number of Isotopes (A), Neutron Number (N), Gamma Energy of the First Excited State 2^+ (E_γ), Square Nuclear Average Radius (R^2), Reduced Electric Transition Probability $B(E2)\uparrow$ in unit of e^2b^2 , Intrinsic Quadrupole Moment (Q_o) in unit of barn, and Deformation Parameters (β_2, δ) for ^{78}Pt Isotopes.

(Z)	(A)	(N)	E_γ (keV) [50]	Theoretical Value		Present Work				
				$B(E2)\uparrow e^2b^2$ For SSANM [13]	β_2	R^2 (barn)	$B(E2)\uparrow e^2b^2$	Q_o (barn)	β_2	δ
78	168	90	582.0 20	1.752	0.1621	0.4384	0.8927	2.9957	0.1157	0.1043
	170	92	509 2	2.036	0.1734	0.4419	1.0127	3.1907	0.1223	0.1102
	172	94	457 2	2.283	0.1822	0.4454	1.1192	3.3543	0.1276	0.1149
	174	96	394 2	2.497	0.1891	0.4488	1.2882	3.5986	0.1358	0.1224
	176	98	263.9 10	2.711	0.1955	0.4522	1.9089	4.3803	0.1641	0.1478
	178	100	170.1 10	2.924	0.2015	0.4557	2.9389	5.4355	0.2020	0.1821
	180	102	152.23 24	2.997	0.2025	0.4591	3.2595	5.7243	0.2112	0.1903
	182	104	154.9 1	2.865	0.1966	0.4625	3.1798	5.6539	0.2071	0.1866
	184	106	162.97 8	2.736	0.1907	0.4650	3.0004	5.4921	0.1997	0.1799
	186	108	191.53 4	2.568	0.1834	0.4692	2.5346	5.0479	0.1822	0.1642
	188	110	265.63 5	2.406	0.1763	0.4726	1.8146	4.2711	0.1531	0.1379
	190	112	295.80 4	2.245	0.1691	0.4759	1.6181	4.0332	0.1435	0.1293
	192	114	316.50819 1	1.931	0.1557	0.4793	1.5017	3.8854	0.1373	0.1237
	194	116	328.435 10	1.541	0.1381	0.4826	1.4371	3.8010	0.1334	0.1202
	196	118	355.6841 20	1.187	0.1204	0.4859	1.3180	3.6401	0.1269	0.1143
	198	120	407.22 5	0.879	0.1029	0.4892	1.1435	3.3905	0.1174	0.1058
200	122	470.10 20	0.619	0.0858	0.4925	0.9839	3.1450	0.1082	0.0975	

Table (3-20): Mass Number of Isotopes (A), Neutron Number (N), Gamma Energy of the First Excited State 2^+ (E_γ), Square Nuclear Average Radius (R^2), Reduced Electric Transition Probability $B(E2)\uparrow$ in unit of e^2b^2 , Intrinsic Quadrupole Moment (Q_o) in unit of barn, and Deformation Parameters (β_2, δ) for $_{80}\text{Hg}$ Isotopes.

(Z)	(A)	(N)	E_γ (keV) [50]	Theoretical Value		Present Work				
				$B(E2)\uparrow e^2b^2$ For SSANM [13]	β_2	R^2 (barn)	$B(E2)\uparrow e^2b^2$	Q_o (barn)	β_2	δ
80	176	96	613.3 30	1.984	0.1631	0.4522	0.8639	2.9470	0.1076	0.0970
	178	98	558.3 10	2.178	0.1696	0.4557	0.9419	3.0772	0.1115	0.1005
	180	100	434.1 10	2.373	0.1757	0.4591	1.2024	3.4768	0.1251	0.1127
	182	102	351.8 3	2.440	0.1769	0.4625	1.4728	3.8479	0.1374	0.1238
	184	104	366.51 23	2.319	0.1712	0.4658	1.4034	3.7562	0.1332	0.1200
	186	106	405.33 14	2.201	0.1656	0.4692	1.2599	3.5589	0.1253	0.1129
	188	108	412.8 1	2.048	0.1586	0.4726	1.2283	3.5140	0.1228	0.1107
	190	110	416.4 2	1.902	0.1517	0.4759	1.2091	3.4865	0.1210	0.1090
	192	112	422.8 1	1.756	0.1448	0.4793	1.1825	3.4479	0.1188	0.1071
	194	114	428.0 2	1.475	0.1318	0.4826	1.1601	3.4151	0.1169	0.1053
	196	116	425.98 10	1.130	0.1146	0.4859	1.1577	3.4115	0.1159	0.1045
	198	118	411.80249 1	0.826	0.0973	0.4892	1.1895	3.4580	0.1167	0.1052
	200	120	367.944 1	0.568	0.0801	0.4925	1.3224	3.6461	0.1223	0.1102
	202	122	439.562 10	0.360	0.0634	0.4958	1.0996	3.3248	0.1108	0.0998
	204	124	436.552 8	0.200	0.0469	0.4990	1.0999	3.3253	0.1100	0.0992
206	126	1068.54 10	0.069	0.0274	0.5023	0.4465	2.1186	0.0697	0.0628	

Table (3-21): Mass Number of Isotopes (A), Neutron Number (N), Gamma Energy of the First Excited State 2^+ (E_γ), Square Nuclear Average Radius (R^2), Reduced Electric Transition Probability $B(E2)\uparrow$ in unit of e^2b^2 , Intrinsic Quadrupole Moment (Q_o) in unit of barn, and Deformation Parameters (β_2, δ) for $_{82}\text{Pb}$ Isotopes.

(Z)	(A)	(N)	E_γ (keV) [50]	Theoretical Value		Present Work				
				$B(E2)\uparrow e^2b^2$ For SSANM [13]	β_2	R^2 (barn)	$B(E2)\uparrow e^2b^2$	Q_o (barn)	β_2	δ
82	182	100	888.3 3	1.696	0.1439	0.4625	0.6128	2.4821	0.0865	0.0779
	184	102	701.5 5	1.754	0.1452	0.4658	0.7704	2.7829	0.0962	0.0867
	186	104	662.4 10	1.650	0.1398	0.4692	0.8100	2.8536	0.0980	0.0883
	188	106	723.9 2	1.549	0.1345	0.4726	0.7359	2.7199	0.0927	0.0836
	190	108	773.8 5	1.419	0.1279	0.4759	0.6836	2.6215	0.0887	0.0800
	192	110	835.6 3	1.295	0.1213	0.4793	0.6154	2.4873	0.0836	0.0753
	194	112	965 35 10	1.173	0.1146	0.4826	0.5404	2.3308	0.0778	0.0701
	196	114	1049.20 9	0.942	0.1020	0.4859	0.4938	2.2281	0.0739	0.0666
	198	116	1063.50 20	0.667	0.0853	0.4892	0.4839	2.2056	0.0726	0.0655
	200	118	1026.62 15	0.434	0.0683	0.4925	0.4979	2.2374	0.0732	0.0660
	202	120	960.66 4	0.251	0.0516	0.4958	0.5286	2.3052	0.0749	0.0675
	204	122	899.171 24	0.119	0.0353	0.4990	0.5611	2.3749	0.0767	0.0691
	206	124	803.10 5	0.036	0.0198	0.5023	0.6241	2.5048	0.0803	0.0724
	208	126	4085.4 3	Sph	----	0.5055	0.1219	1.1070	0.0353	0.0318
	210	128	799.7 1	0.134	0.0368	0.5088	0.6188	2.4941	0.0790	0.0712
	212	130	804.9 5	0.389	0.0622	0.5120	0.6109	2.4782	0.0780	0.0703
214	132	836 2	0.760	0.0864	0.5152	0.5845	2.4241	0.0758	0.0683	

Table (3-22): Mass Number of Isotopes (A), Neutron Number (N), Gamma Energy of the First Excited State 2^+ (E_γ), Square Nuclear Average Radius (R^2), Reduced Electric Transition Probability $B(E2)\uparrow$ in unit of e^2b^2 , Intrinsic Quadrupole Moment (Q_o) in unit of barn, and Deformation Parameters (β_2, δ) for ^{84}Po Isotopes.

(Z)	(A)	(N)	E_γ (keV) [50]	Theoretical Value		Present Work				
				$B(E2)\uparrow e^2b^2$ For SSANM [13]	β_2	R^2 (barn)	$B(E2)\uparrow e^2b^2$	Q_o (barn)	β_2	δ
84	192	108	262.0 20	2.959	0.1790	0.4793	2.1039	4.5990	0.1509	0.1360
	194	110	318.6 2	2.776	0.1722	0.4826	1.7182	4.1562	0.1355	0.1221
	196	112	463.12 9	2.594	0.1653	0.4859	1.1740	3.4355	0.1112	0.1002
	198	114	605.0 1	2.239	0.1525	0.4892	0.8926	2.9956	0.0963	0.0868
	200	116	665.90 10	1.795	0.1357	0.4925	0.8056	2.8458	0.0909	0.0819
	202	118	677.30 20	1.392	0.1187	0.4958	0.7868	2.8124	0.0892	0.0804
	204	120	684.342 10	1.039	0.1019	0.4990	0.7736	2.7887	0.0879	0.0792
	206	122	700.66 3	0.740	0.0854	0.5023	0.7507	2.7471	0.0860	0.0775
	208	124	686.528 20	0.493	0.0693	0.5055	0.7612	2.7663	0.0861	0.0776
	210	126	1181.40 2	0.260	0.0500	0.5088	0.4395	2.1021	0.0650	0.0586
	212	128	727.330 9	0.779	0.0860	0.5120	0.7094	2.6706	0.0820	0.0739
	214	130	609.316 7	1.311	0.1108	0.5152	0.8416	2.9086	0.0888	0.0800
	216	132	549.76 4	1.955	0.1345	0.5184	0.9269	3.0527	0.0926	0.0835
	218	134	511 2	2.402	0.1482	0.5216	0.9912	3.1566	0.0952	0.0858

Table (3-23): Mass Number of Isotopes (A), Neutron Number (N), Gamma Energy of the First Excited State 2^+ (E_γ), Square Nuclear Average Radius (R^2), Reduced Electric Transition Probability $B(E2)\uparrow$ in unit of e^2b^2 , Intrinsic Quadrupole Moment (Q_o) in unit of barn, and Deformation Parameters (β_2, δ) for ${}_{86}\text{Rn}$ Isotopes.

(Z)	(A)	(N)	E_γ (keV) [50]	Theoretical Value		Present Work				
				$B(E2)\uparrow e^2b^2$ For SSANM [13]	β_2	R^2 (barn)	$B(E2)\uparrow e^2b^2$	Q_o (barn)	β_2	δ
86	198	112	339.0 20	3.852	0.1954	0.4892	1.6698	4.0971	0.1287	0.1159
	200	114	432.9	3.409	0.1826	0.4925	1.2989	3.6135	0.1127	0.1016
	202	116	504.1	2.848	0.1658	0.4958	1.1080	3.3375	0.1034	0.0932
	204	118	542.9	2.326	0.1489	0.4990	1.0221	3.2055	0.0987	0.0889
	206	120	575.3	1.855	0.1321	0.5023	0.9583	3.1038	0.0949	0.0855
	208	122	635.8	1.440	0.1156	0.5055	0.8615	2.9430	0.0894	0.0806
	210	124	643.8	1.081	0.0995	0.5088	0.8454	2.9153	0.0880	0.0793
	212	126	1273.8	0.713	0.0803	0.5120	0.4246	2.0660	0.0620	0.0559
	214	128	694.7	1.496	0.1156	0.5152	0.7737	2.7889	0.0832	0.0749
	216	130	461.9	2.222	0.1401	0.5184	1.1564	3.4097	0.1010	0.0910
	218	132	342.22	3.057	0.1633	0.5216	1.6374	4.0572	0.1195	0.1077
	220	134	240.986	3.621	0.1766	0.5248	2.1896	4.6917	0.1373	0.1238
222	136	186.211	4.169	0.1884	0.5280	2.8166	5.3213	0.1548	0.1395	

Table (3-24): Mass Number of Isotopes (A), Neutron Number (N), Gamma Energy of the First Excited State 2^+ (E_γ), Square Nuclear Average Radius (R^2), Reduced Electric Transition Probability $B(E2)\uparrow$ in unit of e^2b^2 , Intrinsic Quadrupole Moment (Q_o) in unit of barn, and Deformation Parameters (β_2, δ) for ^{88}Ra Isotopes.

(Z)	(A)	(N)	E_γ (keV) [50]	Theoretical Value		Present Work				
				$B(E2)\uparrow e^2b^2$ For SSANM [13]	β_2	R^2 (barn)	$B(E2)\uparrow e^2b^2$	Q_o (barn)	β_2	δ
88	206	118	474.3 10	3.460	0.1763	0.5023	1.2170	3.4979	0.1045	0.0942
	208	120	520.2 10	2.871	0.1595	0.5055	1.1025	3.3292	0.0989	0.0891
	210	122	603.3 10	2.341	0.1432	0.5088	0.9446	3.0816	0.0909	0.0819
	212	124	629.3 5	1.869	0.1271	0.5120	0.8999	3.0078	0.0882	0.0795
	214	126	1382.4 10	1.365	0.1079	0.5152	0.4071	2.0230	0.0589	0.0531
	216	128	688.2 2	2.414	0.1427	0.5184	0.8127	2.8583	0.0828	0.0746
	218	130	389.1 2	3.334	0.1666	0.5216	1.4286	3.7897	0.1091	0.0983
	220	132	178.47 12	4.361	0.1894	0.5248	3.0957	5.5786	0.1596	0.1438
	222	134	111.12 2	5.042	0.2024	0.5280	4.9421	7.0486	0.2004	0.1806
	224	136	84.373 3	5.697	0.2139	0.5311	6.4700	8.0649	0.2280	0.2054
	226	138	67.67 1	6.375	0.2249	0.5343	8.0193	8.9788	0.2523	0.2273
	228	140	63.823 20	7.025	0.2340	0.5374	8.4529	9.2183	0.2575	0.2320
	230	142	57.4 1	7.628	0.2432	0.5406	9.3442	9.6922	0.2692	0.2426

Table (3-25): Mass Number of Isotopes (A), Neutron Number (N), Gamma Energy of the First Excited State 2^+ (E_γ), Square Nuclear Average Radius (R^2), Reduced Electric Transition Probability $B(E2)\uparrow$ in unit of e^2b^2 , Intrinsic Quadrupole Moment (Q_o) in unit of barn, and Deformation Parameters (β_2, δ) for ${}_{90}\text{Th}$ Isotopes.

(Z)	(A)	(N)	E_γ (keV) [50]	Theoretical Value		Present Work				
				$B(E2)\uparrow e^2b^2$ For SSANM [13]	β_2	R^2 (barn)	$B(E2)\uparrow e^2b^2$	Q_o (barn)	β_2	δ
90	216	126	1478.2	1.896	0.1236	0.5184	0.3958	1.9948	0.0565	0.0509
	218	128	689.66	3.128	0.1578	0.5216	0.8431	2.9114	0.0819	0.0738
	220	130	373.33	4.184	0.1814	0.5248	1.5481	3.9450	0.1103	0.0994
	222	132	183.310	5.346	0.2038	0.5280	3.1337	5.6128	0.1561	0.1406
	224	134	98.13	6.112	0.2166	0.5311	5.8205	7.6494	0.2114	0.1905
	226	136	72.204	6.844	0.2279	0.5343	7.8617	8.8901	0.2443	0.2201
	228	138	57.7594	7.599	0.2387	0.5374	9.7697	9.9104	0.2707	0.2439
	230	140	53.202	8.319	0.24483	0.5406	10.5454	10.2963	0.2796	0.2519
	232	142	49.3699	8.987	0.2566	0.5437	11.2983	10.6575	0.2877	0.2593
234	144	49.556	9.515	0.2625	0.5468	11.1928	10.6076	0.2848	0.2566	

Table (3-26): Mass Number of Isotopes (A), Neutron Number (N), Gamma Energy of the First Excited State 2^+ (E_γ), Square Nuclear Average Radius (R^2), Reduced Electric Transition Probability $B(E2)\uparrow$ in unit of e^2b^2 , Intrinsic Quadrupole Moment (Q_o) in unit of barn, and Deformation Parameters (β_2, δ) for ${}_{92}\text{U}$ Isotopes.

(Z)	(A)	(N)	E_γ (keV) [50]	Theoretical Value		Present Work				
				$B(E2)\uparrow e^2b^2$ For SSANM [13]	β_2	R^2 (barn)	$B(E2)\uparrow e^2b^2$	Q_o (barn)	β_2	δ
92	226	134	80.5 10	7.161	0.2280	0.5343	7.3680	8.6064	0.2313	0.2084
	228	136	59 10	7.966	0.2391	0.5374	9.9940	10.0235	0.2678	0.2413
	230	138	51.72 4	8.793	0.2498	0.5406	11.3346	10.6746	0.2836	0.2555
	232	140	47.522 7	9.580	0.2592	0.5437	12.2520	11.0982	0.2931	0.2641
	234	142	43.498 1	10.310	0.2674	0.5468	13.3230	11.5731	0.3039	0.2739
	236	144	45.242 3	10.880	0.2731	0.5499	12.7370	11.3157	0.2955	0.2663
	238	146	44.91 3	11.210	0.2756	0.5530	12.7591	11.3256	0.2941	0.2650
	240	148	45 1	11.490	0.2775	0.5561	12.6628	11.2827	0.2913	0.2625

Table (3-27): Mass Number of Isotopes (A), Neutron Number (N), Gamma Energy of the First Excited State 2^+ (E_γ), Square Nuclear Average Radius (R^2), Reduced Electric Transition Probability $B(E2)\uparrow$ in unit of e^2b^2 , Intrinsic Quadrupole Moment (Q_o) in unit of barn, and Deformation Parameters (β_2, δ) for ${}_{94}\text{Pu}$ Isotopes.

(Z)	(A)	(N)	E_γ (keV) [50]	Theoretical Value		Present Work				
				$B(E2)\uparrow e^2b^2$ For SSANM [13]	β_2	R^2 (barn)	$B(E2)\uparrow e^2b^2$	Q_o (barn)	β_2	δ
94	236	142	44.63 10	11.530	0.2752	0.5499	13.4791	11.6407	0.2975	0.2681
	238	144	44.08 3	12.150	0.2809	0.5530	13.5707	11.6802	0.2968	0.2675
	240	146	42.824 8	12.500	0.2833	0.5561	13.8910	11.8173	0.2986	0.2691
	242	148	44.54 2	12.800	0.2851	0.5592	13.2822	11.5554	0.2904	0.2617
	244	150	46 2	12.980	0.2855	0.5623	12.7902	11.3394	0.2834	0.2554
	246	152	44.2 4	13.130	0.2856	0.5654	13.2388	11.5554	0.2868	0.2617

Table (3-28): Mass Number of Isotopes (A), Neutron Number (N), Gamma Energy of the First Excited State 2^+ (E_γ), Square Nuclear Average Radius (R^2), Reduced Electric Transition Probability $B(E2)\uparrow$ in unit of e^2b^2 , Intrinsic Quadrupole Moment (Q_o) in unit of barn, and Deformation Parameters (β_2, δ) for ${}_{96}\text{Cm}$ Isotopes.

(Z)	(A)	(N)	E_γ (keV) [50]	Theoretical Value		Present Work				
				$B(E2)\uparrow e^2b^2$ For SSANM [13]	β_2	R^2 (barn)	$B(E2)\uparrow e^2b^2$	Q_o (barn)	β_2	δ
96	238	142	35 8	12.680	0.2810	0.5530	17.8264	13.3869	0.3331	0.3002
	240	144	38 5	13.340	0.2866	0.5561	16.3277	12.8119	0.3170	0.2857
	242	146	42.13 1	13.720	0.2890	0.5592	14.6458	12.1341	0.2986	0.2691
	244	148	42.965 10	14.030	0.2907	0.5623	14.2826	11.9827	0.2933	0.2643
	246	150	42.852 5	14.220	0.2910	0.5654	14.2426	11.9659	0.2913	0.2625
	248	152	43.38 3	14.390	0.2912	0.5684	13.9935	11.8608	0.2872	0.2588
	250	154	43 5	14.540	0.2911	0.5715	14.0417	11.8812	0.2861	0.2578

Table (3-29): Mass Number of Isotopes (A), Neutron Number (N), Gamma Energy of the First Excited State 2^+ (E_γ), Square Nuclear Average Radius (R^2), Reduced Electric Transition Probability $B(E2)\uparrow$ in unit of e^2b^2 , Intrinsic Quadrupole Moment (Q_o) in unit of barn, and Deformation Parameters (β_2, δ) for ${}_{98}\text{Cf}$ Isotopes.

(Z)	(A)	(N)	E_γ (keV) [50]	Theoretical Value		Present Work				
				$B(E2)\uparrow e^2b^2$ For SSANM [13]	β_2	R^2 (barn)	$B(E2)\uparrow e^2b^2$	Q_o (barn)	β_2	δ
98	244	146	40 2	14.970	0.2941	0.5623	15.9872	12.6776	0.3039	0.2739
	248	150	41.53 6	15.510	0.2961	0.5684	15.2322	12.3746	0.2935	0.2645
	250	152	42.722	15.680	0.2962	0.5715	14.7281	12.1681	0.2870	0.2587
	252	154	45.72 5	15.840	0.2961	0.5745	13.6894	11.7312	0.2753	0.2481

Table (3-30): Mass Number of Isotopes (A), Neutron Number (N), Gamma Energy of the First Excited State 2^+ (E_γ), Square Nuclear Average Radius (R^2), Reduced Electric Transition Probability $B(E2)\uparrow$ in unit of e^2b^2 , Intrinsic Quadrupole Moment (Q_o) in unit of barn, and Deformation Parameters (β_2, δ) for ${}_{100}\text{Fm}$ Isotopes.

(Z)	(A)	(N)	E_γ (keV) [50]	Theoretical Value		Present Work				
				$B(E2)\uparrow e^2b^2$ For SSANM [13]	β_2	R^2 (barn)	$B(E2)\uparrow e^2b^2$	Q_o (barn)	β_2	δ
100	248	148	44 8	16.610	0.3003	0.5684	14.9699	12.2676	0.2851	0.2569
	250	150	44 5	16.830	0.3007	0.5715	14.8900	12.2348	0.2828	0.2549
	252	152	46.6 12	17.010	0.3007	0.5745	13.9847	11.8571	0.2727	0.2457
	254	154	44.988 10	17.180	0.3006	0.5775	14.4097	12.0359	0.2753	0.2481
	256	156	48.1 10	17.160	0.2989	0.5806	13.4071	11.6096	0.2642	0.2381

Table (3-31): Mass number (A), Neutron Number (N), Root Mean Square Radii $\langle r^2 \rangle^{1/2}$, Major and minor axes (a, b) and the difference between them (ΔR) by three methods for ${}_{40}\text{Zr}$ Isotopes.

(Z)	(A)	(N)	Theoretical Value	Present Work					
			$\langle r^2 \rangle^{1/2}$ fm [51]	$\langle r^2 \rangle^{1/2}$ fm	a fm	b fm	ΔR_1 fm	ΔR_2 fm	ΔR_3 fm
40	102	62	4.5292	4.4503	2.0225	3.7510	1.6816	1.7284	1.9802
	104	64	-----	4.4792	2.0125	3.7810	1.7265	1.7685	2.0330

Table (3-32): Mass number (A), Neutron Number (N), Root Mean Square Radii $\langle r^2 \rangle^{1/2}$, Major and minor axes (a, b) and the difference between them (ΔR) by three methods for ${}_{42}\text{Mo}$ Isotopes.

(Z)	(A)	(N)	Theoretical Value	Present Work					
			$\langle r^2 \rangle^{1/2}$ fm [51]	$\langle r^2 \rangle^{1/2}$ fm	a fm	b fm	ΔR_1 fm	ΔR_2 fm	ΔR_3 fm
42	102	60	4.4914	4.4503	2.2445	3.4894	1.2029	1.2450	1.4165
	104	62	4.5249	4.4792	2.1326	3.6468	1.4747	1.5142	1.7365
	106	64	4.5490	4.5077	2.1126	3.6894	1.5416	1.5768	1.8154
	108	66	4.5602	4.5359	2.1725	3.6387	1.4358	1.4663	1.6908

Table (3-33): Mass number (A), Neutron Number (N), Root Mean Square Radii $\langle r^2 \rangle^{1/2}$, Major and minor axes (a, b) and the difference between them (ΔR) by three methods for ${}_{44}\text{Ru}$ Isotopes.

(Z)	(A)	(N)	Theoretical Value	Present Work					
			$\langle r^2 \rangle^{1/2}$ fm [51]	$\langle r^2 \rangle^{1/2}$ fm	a fm	b fm	ΔR_1 fm	ΔR_2 fm	ΔR_3 fm
44	102	58	4.4809	4.4503	2.3531	3.3432	0.9504	0.9902	1.1159
	104	60	4.5098	4.4792	2.3081	3.4265	1.0808	1.1184	1.2690
	106	62	-----	4.5077	2.2544	3.5176	1.2287	1.2632	1.4426
	108	64	-----	4.5359	2.2417	3.5537	1.2813	1.3120	1.5044
	110	66	-----	4.5637	2.2571	3.5538	1.2697	1.2967	1.4908
	112	68	-----	4.5912	2.2692	3.5577	1.2652	1.2886	1.4855

Table (3-34): Mass number (A), Neutron Number (N), Root Mean Square Radii $\langle r^2 \rangle^{1/2}$, Major and minor axes (a, b) and the difference between them (ΔR) by three methods for ${}_{46}\text{Pd}$ Isotopes.

(Z)	(A)	(N)	Theoretical Value	Present Work					
			$\langle r^2 \rangle^{1/2}$ fm [51]	$\langle r^2 \rangle^{1/2}$ fm	a fm	b fm	ΔR_1 fm	ΔR_2 fm	ΔR_3 fm
46	102	56	4.4827	4.4503	2.3832	3.3002	0.8782	0.9170	1.0311
	104	58	4.5078	4.4792	2.3978	3.3011	0.8674	0.9033	1.0184
	106	60	4.5138	4.5077	2.3974	3.3232	0.8925	0.9258	1.0479
	108	62	4.5563	4.5359	2.3804	3.3685	0.9573	0.9882	1.1240
	110	64	4.5782	4.5637	2.3645	3.4113	1.0189	1.0469	1.1963
	112	66	-----	4.5912	2.3644	3.4315	1.0422	1.0671	1.2237
	114	68	-----	4.6183	2.3687	3.4454	1.0549	1.0767	1.2386
	116	70	-----	4.6452	2.3883	3.4377	1.0303	1.0494	1.2097
	118	72	-----	4.6717	2.4238	3.4073	0.9664	0.9835	1.1346

Table (3-35): Mass number (A), Neutron Number (N), Root Mean Square Radii $\langle r^2 \rangle^{1/2}$, Major and minor axes (a, b) and the difference between them (ΔR) by three methods for ${}_{48}\text{Cd}$ Isotopes.

(Z)	(A)	(N)	Theoretical Value	Present Work					
			$\langle r^2 \rangle^{1/2}$ fm [51]	$\langle r^2 \rangle^{1/2}$ fm	a fm	b fm	ΔR_1 fm	ΔR_2 fm	ΔR_3 fm
48	102	54	4.4810	4.4503	2.4341	3.2184	0.7434	0.7799	0.8728
	104	56	4.5122	4.4792	2.4266	3.2587	0.7972	0.8321	0.9360
	106	58	4.5383	4.5077	2.4341	3.2694	0.8028	0.8353	0.9426
	108	60	4.5577	4.5359	2.4478	3.2704	0.7926	0.8226	0.9306
	110	62	4.5765	4.5637	2.4671	3.2627	0.7681	0.7955	0.8018
	112	64	4.5944	4.5912	2.4703	3.2788	0.7833	0.8085	0.9196
	114	66	4.6087	4.6183	2.4672	3.3042	0.8140	0.8370	0.9557
	116	68	4.6203	4.6452	2.4662	3.3259	0.8391	0.8597	0.9852
	118	70	4.6246	4.6717	2.4703	3.3397	0.8512	0.8694	0.9994
	120	72	4.6300	4.6980	2.4890	3.3316	0.8265	0.8426	0.9704
	122	74	-----	4.7850	2.5198	3.3047	0.7704	0.7850	0.9046
	124	76	-----	4.7496	2.5423	3.2896	0.7344	0.7473	0.8622
	126	78	-----	4.7750	2.5621	3.2782	0.7047	0.7161	0.8274

Table (3-36): Mass number (A), Neutron Number (N), Root Mean Square Radii $\langle r^2 \rangle^{1/2}$, Major and minor axes(a, b) and the difference between them (ΔR) by three methods for ${}_{50}\text{Sn}$ Isotopes.

(Z)	(A)	(N)	Theoretical Value	Present Work					
			$\langle r^2 \rangle^{1/2}$ fm [51]	$\langle r^2 \rangle^{1/2}$ fm	a fm	b fm	ΔR_1 fm	ΔR_2 fm	ΔR_3 fm
50	102	52		4.4503	2.5197	3.0908	0.5400	0.5711	0.6358
	104	54		4.4792	2.5151	3.1216	0.5761	0.6065	0.6784
	106	56		4.5077	2.5226	3.1323	0.5810	0.6097	0.6842
	108	58	4.5605	4.5359	2.5345	3.1355	0.2742	0.6010	0.6762
	110	60	4.5785	4.5637	2.5469	3.1377	0.5659	0.5907	0.6664
	112	62	4.5948	4.5912	2.5624	3.1343	0.5490	0.5719	0.6465
	114	64	4.6099	4.6183	2.5772	3.1318	0.5335	0.5546	0.6283
	116	66	4.6250	4.6452	2.5877	3.1358	0.5287	0.5481	0.6225
	118	68	4.6393	4.6717	2.5934	3.1476	0.5361	0.5541	0.6313
	120	70	4.6519	4.6980	2.5991	3.1589	0.5431	0.5598	0.6396
	122	72	4.6634	4.7239	2.6070	3.1665	0.5444	0.5596	0.6411
	124	74	4.6735	4.7496	2.6166	3.1709	0.5406	0.5543	0.6366
	126	76	4.6833	4.7750	2.6277	3.1727	0.5327	0.5450	0.6273
	128	78	4.6921	4.8002	2.6401	3.1719	0.5208	0.5318	0.6133
	130	80	4.7019	4.8250	2.6541	3.1681	0.5043	0.5140	0.5938
132	82	4.7093	4.8496	2.7459	3.0279	0.2744	0.2820	0.3231	
134	84		4.8740	2.6181	3.2651	0.6414	0.6470	0.7553	

Table (3-37): Mass number (A), Neutron Number (N), Root Mean Square Radii $\langle r^2 \rangle^{1/2}$, Major and minor axes(a,b) and the difference between them (ΔR) by three methods for ${}_{52}\text{Te}$ Isotopes.

(Z)	(A)	(N)	Theoretical Value	Present Work					
			$\langle r^2 \rangle^{1/2}$ fm [51]	$\langle r^2 \rangle^{1/2}$ fm	a fm	b fm	ΔR_1 fm	ΔR_2 fm	ΔR_3 fm
52	108	56		4.5359	2.4459	3.2733	0.7974	0.8274	0.9363
	110	58		4.5637	2.4671	3.2627	0.7681	0.7956	0.9019
	112	60		4.5912	2.4870	3.2536	0.7415	0.7666	0.8706
	114	62		4.6183	2.5036	3.2489	0.7225	0.7453	0.8483
	116	64	4.6847	4.6452	2.5097	3.2602	0.7297	0.7505	0.8568
	118	66	4.6956	4.6717	2.5051	3.2876	0.7638	0.7825	0.8968
	120	68	4.7038	4.6980	2.5053	3.3070	0.7852	0.8017	0.9219
	122	70	4.7095	4.7239	2.5183	3.3069	0.7741	0.7886	0.9089
	124	72	4.7183	4.7496	2.5398	3.2935	0.7408	0.7536	0.8698
	126	74	4.7266	4.7750	2.5650	3.2736	0.6971	0.7085	0.8185
	128	76	4.7346	4.8002	2.5900	3.2533	0.6531	0.6633	0.7668
	130	78	4.7423	4.8250	2.6151	3.2323	0.6082	0.6173	0.7141
	132	80	4.7500	4.8496	2.6414	3.2085	0.5590	0.5671	0.6563
	134	82	4.7569	4.8740	2.6773	3.1676	0.4829	0.4903	0.5670
	136	84	4.7815	4.8981	2.6056	3.3033	0.6947	0.6977	0.8157
138	86		4.9220	2.5714	3.3744	0.8045	0.8030	0.9446	

Table (3-38): Mass number (A), Neutron Number (N), Root Mean Square Radii $\langle r^2 \rangle^{1/2}$, Major and minor axes (a, b) and the difference between them (ΔR) by three methods for ^{56}Ba Isotopes.

(Z)	(A)	(N)	Theoretical Value	Present Work					
			$\langle r^2 \rangle^{1/2}$ fm [51]	$\langle r^2 \rangle^{1/2}$ fm	a fm	b fm	ΔR_1 fm	ΔR_2 fm	ΔR_3 fm
56	118	62		4.6717	2.2623	3.6224	1.3490	1.3603	1.5838
	120	64	4.8092	4.6980	2.2609	3.6423	1.3741	1.3814	1.6134
	122	66	4.8153	4.7239	2.2970	3.6149	1.3129	1.3179	1.5415
	124	68	4.8185	4.7496	2.3544	3.5583	1.1995	1.2039	1.4084
	126	70	4.8221	4.7750	2.3946	3.5223	1.1244	1.1278	1.3202
	128	72	4.8255	4.8002	2.4311	3.4900	1.0564	1.0588	1.2404
	130	74	4.8283	4.8250	2.4895	3.4249	0.9322	0.9354	1.0945
	132	76	4.8303	4.8496	2.5459	3.3593	0.8093	0.8133	0.9503
	134	78	4.8322	4.8740	2.5950	3.3018	0.7023	0.7068	0.8246
	136	80	4.8334	4.8981	2.6422	3.2447	0.5977	0.6026	0.7018
	138	82	4.8378	4.9220	2.7054	3.1578	0.4469	0.4524	0.5247
	140	84	4.8684	4.9457	2.6251	3.3086	0.6834	0.6835	0.8024
	142	86	4.8953	4.9691	2.5590	3.4276	0.8762	0.8686	1.0288
	144	88	4.9236	4.9924	2.4524	3.5963	1.1660	1.1439	1.3690
	146	90	4.9479	5.0154	2.4415	3.6269	1.2122	1.1854	1.4233
148	92	4.9731	5.0382	2.3898	3.7107	1.3579	1.3209	1.5943	

Table (3-39): Mass number (A), Neutron Number (N), Root Mean Square Radii $\langle r^2 \rangle^{1/2}$, Major and minor axes (a, b) and the difference between them (ΔR) by three methods for ^{58}Ce Isotopes.

(Z)	(A)	(N)	Theoretical Value	Present Work					
			$\langle r^2 \rangle^{1/2}$ fm [51]	$\langle r^2 \rangle^{1/2}$ fm	a fm	b fm	ΔR_1 fm	ΔR_2 fm	ΔR_3 fm
58	124	66	-----	4.7496	2.2129	3.7355	1.5262	1.5226	1.7920
	126	68	-----	4.7750	2.2858	3.6640	1.3818	1.3782	1.6223
	128	70	-----	4.8002	2.3567	3.5907	1.2367	1.2340	1.4521
	130	72	-----	4.8250	2.4196	3.5237	1.1058	1.1041	1.2983
	132	74	-----	4.8496	2.4840	3.4508	0.9669	0.9668	1.1352
	134	76	-----	4.8740	2.5366	3.3914	0.8539	0.8548	1.0025
	136	78	4.8739	4.8981	2.5931	3.3231	0.7277	0.7300	0.8544
	138	80	4.8737	4.9220	2.6477	3.2541	0.6030	0.6063	0.7080
	140	82	4.8771	4.9457	2.7226	3.1470	0.4198	0.4245	0.4929
	142	84	4.9063	4.9691	2.6427	3.2981	0.6561	0.6554	0.7704
	144	86	4.9303	4.9924	2.5860	3.4040	0.8257	0.8181	0.9695
	146	88	4.9590	5.0154	2.5203	3.5175	1.0146	0.9972	1.1912
	148	90	4.9893	5.0382	2.4201	3.6711	1.2840	1.2510	1.5076
	150	92	-----	5.0608	2.2845	3.8557	1.6257	1.5712	1.8088
	152	94	-----	5.0831	2.2354	3.9271	1.7567	1.6917	1.9626

Table (3-40): Mass number (A), Neutron Number (N), Root Mean Square Radii $\langle r^2 \rangle^{1/2}$, Major and minor axes (a, b) and the difference between them (ΔR) by three methods for ${}_{60}\text{Nd}$ Isotopes.

(Z)	(A)	(N)	Theoretical Value	Present Work					
			$\langle r^2 \rangle^{1/2}$ fm [51]	$\langle r^2 \rangle^{1/2}$ fm	a fm	b fm	ΔR_1 fm	ΔR_2 fm	ΔR_3 fm
60	128	68		4.8002	2.2257	3.7541	1.5402	1.5285	1.8083
	130	70		4.8250	2.2953	3.6863	1.4020	1.3910	1.6461
	132	72	4.9174	4.8496	2.3909	3.5799	1.1964	1.1891	1.4047
	134	74	4.9128	4.8740	2.4763	3.4794	1.0067	1.0031	1.1820
	136	76	4.9111	4.8981	2.5325	3.4152	0.8847	0.8828	1.0388
	138	78	4.9123	4.9220	2.5951	3.3379	0.7426	0.7428	0.8719
	140	80	4.9101	4.9457	2.6552	3.2601	0.6030	0.6050	0.7080
	142	82	4.9123	4.9691	2.7302	3.1524	0.4186	0.4223	0.4914
	144	84	4.9421	4.9924	2.6621	3.2846	0.6237	0.6225	0.7323
	146	86	4.9696	5.0154	2.6162	3.3746	0.7657	0.7585	0.8990
	148	88	4.9999	5.0382	2.5605	3.4754	0.9306	0.9149	1.0926
	150	90	5.0400	5.0608	2.3786	3.7401	1.4039	1.3616	1.6483
	152	92		5.0831	2.1871	3.9811	1.8647	1.7941	2.1894
	154	94		5.1053	2.1928	3.9887	1.8707	1.7960	2.1965
156	96		5.1274	2.1843	4.0118	1.9080	1.6274	2.2402	

Table (3-41): Mass number (A), Neutron Number (N), Root Mean Square Radii $\langle r^2 \rangle^{1/2}$, Major and minor axes (a, b) and the difference between them (ΔR) by three methods for ${}_{62}\text{Sm}$ Isotopes.

(Z)	(A)	(N)	Theoretical Value	Present Work					
			$\langle r^2 \rangle^{1/2}$ fm [51]	$\langle r^2 \rangle^{1/2}$ fm	a fm	b fm	ΔR_1 fm	ΔR_2 fm	ΔR_3 fm
62	130	68		4.8250	2.2103	3.7887	1.5955	1.5783	1.8733
	132	70		4.8496	2.2512	3.7567	1.5241	1.5055	1.7895
	134	72		4.8740	2.3340	3.6709	1.3527	1.3369	1.5883
	136	74		4.8981	2.4586	3.5215	1.0711	1.0629	1.2576
	138	76	4.9599	4.9220	2.5308	3.4352	0.9093	0.9045	1.0676
	140	78	4.9565	4.9457	2.6082	3.3352	0.7281	0.7270	0.8549
	142	80	4.9518	4.9691	2.6638	3.2640	0.5996	0.6002	0.7040
	144	82	4.9524	4.9924	2.7425	3.1494	0.4040	0.4069	0.4744
	146	84	4.9808	5.0154	2.6793	3.2741	0.5967	0.5948	0.7006
	148	86	5.0042	5.0382	2.6522	3.3351	0.6891	0.6830	0.8090
	150	88	5.0387	5.0608	2.5885	3.4501	0.8767	0.8616	1.0294
	152	90	5.0819	5.0831	2.3718	3.7636	1.4389	1.3917	1.6894
	154	92	5.1053	5.1053	2.2516	3.9226	1.7386	1.6710	2.0413
	156	94		5.1274	2.2365	3.9539	1.7914	1.7174	2.1034
	158	96		5.1492	2.2348	3.9695	1.8136	1.7347	2.1294
160	98		5.1708	2.2373	3.9803	1.8263	1.7431	2.1442	

Table (3-42): Mass number (A), Neutron Number (N), Root Mean Square Radii $\langle r^2 \rangle^{1/2}$, Major and minor axes (a, b) and the difference between them (ΔR) by three methods for ${}_{64}\text{Gd}$ Isotopes.

(Z)	(A)	(N)	Theoretical Value	Present Work					
			$\langle r^2 \rangle^{1/2}$ fm [51]	$\langle r^2 \rangle^{1/2}$ fm	a fm	b fm	ΔR_1 fm	ΔR_2 fm	ΔR_3 fm
64	138	74		4.8250	2.4391	3.5653	1.1394	1.1262	1.3378
	140	76		4.8496	2.5323	3.4502	0.9253	0.9179	1.0864
	142	78		4.8740	2.6142	3.3433	0.7320	0.7291	0.8594
	144	80		4.8981	2.6695	3.2726	0.6039	0.6031	0.7091
	146	82	4.9801	4.9220	2.7627	3.1324	0.3673	0.3698	0.4313
	148	84	5.0080	4.9457	2.6936	3.2680	0.5771	0.5745	0.6776
	150	86	5.0342	4.9691	2.6796	3.3081	0.6342	0.6286	0.7446
	152	88	5.0774	4.9924	2.6037	3.4435	0.8558	0.8398	1.0048
	154	90	5.1223	5.0154	2.3879	3.7580	1.4189	1.3701	1.6660
	156	92	5.1420	5.0382	2.2962	3.8848	1.6546	1.5885	1.9426
	158	94	5.1569	5.0608	2.2692	3.9303	1.7354	1.6612	2.0375
	160	96	5.1734	5.0831	2.2625	3.9517	1.7688	1.6892	2.0768
	162	98		5.1053	2.2541	3.9748	1.8061	1.7207	2.1206

Table (3-43): Mass number (A), Neutron Number (N), Root Mean Square Radii $\langle r^2 \rangle^{1/2}$, Major and minor axes (a, b) and the difference between them (ΔR) by three methods for ${}_{66}\text{Dy}$ Isotopes.

(Z)	(A)	(N)	Theoretical Value	Present Work					
			$\langle r^2 \rangle^{1/2}$ fm [51]	$\langle r^2 \rangle^{1/2}$ fm	a fm	b fm	ΔR_1 fm	ΔR_2 fm	ΔR_3 fm
66	142	76		4.9691	2.5363	3.4613	0.9349	0.9250	1.0976
	144	78		4.9924	2.6178	3.3550	0.7419	0.7371	0.8711
	146	80	5.0438	5.0154	2.6691	3.2906	0.6242	0.6215	0.7328
	148	82	5.0455	5.0382	2.7598	3.1557	0.3947	0.3959	0.4634
	150	84	5.0706	5.0608	2.7049	3.2666	0.5652	0.5617	0.6636
	152	86	5.0950	5.0831	2.6840	3.3178	0.6409	0.6337	0.7525
	154	88	5.1241	5.1053	2.6089	3.4516	0.8606	0.8426	1.0104
	156	90	5.1622	5.1274	2.4323	3.7155	1.3293	1.2832	1.5607
	158	92	5.1815	5.1492	2.3461	3.8389	1.5559	1.4928	1.8268
	160	94	5.1951	5.1708	2.3151	3.8903	1.6472	1.5752	1.9339
	162	96	5.2074	5.1923	2.3026	3.9189	1.6945	1.6163	1.9895
	164	98	5.2218	5.2135	2.2812	3.9573	1.7619	1.6761	2.0687
	166	100		5.2346	2.3108	3.9361	1.7109	1.6253	2.0088

Table (3-44): Mass number (A), Neutron Number (N), Root Mean Square Radii $\langle r^2 \rangle^{1/2}$, Major and minor axes (a, b) and the difference between them (ΔR) by three methods for ${}_{68}\text{Er}$ Isotopes.

(Z)	(A)	(N)	Theoretical Value	Present Work					
			$\langle r^2 \rangle^{1/2}$ fm [51]	$\langle r^2 \rangle^{1/2}$ fm	a fm	b fm	ΔR_1 fm	ΔR_2 fm	ΔR_3 fm
68	144	76		4.9924	2.5550	3.4505	0.9062	0.8955	1.0640
	148	80		5.0382	2.6720	3.3033	0.6357	0.6313	0.7463
	150	82	5.0548	5.0608	2.7635	3.1670	0.4032	0.4034	0.4734
	152	84	5.0843	5.0831	2.7142	3.2683	0.5585	0.5540	0.6558
	154	86	5.1129	5.1053	2.6820	3.3377	0.6652	0.6557	0.7810
	156	88	5.1429	5.1274	2.6234	3.4456	0.8408	0.8222	0.9872
	158	90	5.1761	5.1492	2.5246	3.6053	1.1163	1.0807	1.3107
	160	92	5.2045	5.1708	2.4314	3.7458	1.3681	1.3144	1.6111
	162	94	5.2246	5.1923	2.3819	3.8228	1.5065	1.4409	1.7689
	164	96	5.2389	5.2135	2.3592	3.8647	1.5789	1.5054	1.8538
	166	98	5.2516	5.2346	2.3291	3.9145	1.6680	1.5854	1.9584
	168	100	5.2644	5.2556	2.3388	3.9163	1.6627	1.5775	1.9523
	170	102	5.2789	5.2764	2.3464	3.9205	1.6624	1.5742	1.9518
172	104		5.2970	2.3520	3.9270	1.6664	1.5750	1.9565	

Table (3-45): Mass number (A), Neutron Number (N), Root Mean Square Radii $\langle r^2 \rangle^{1/2}$, Major and minor axes (a, b) and the difference between them (ΔR) by three methods for ${}_{70}\text{Yb}$ Isotopes.

(Z)	(A)	(N)	Theoretical Value	Present Work					
			$\langle r^2 \rangle^{1/2}$ fm [51]	$\langle r^2 \rangle^{1/2}$ fm	a fm	b fm	ΔR_1 fm	ΔR_2 fm	ΔR_3 fm
70	152	82	5.0423	5.0831	2.7693	3.1745	0.4058	0.4051	0.4778
	154	84	5.0875	5.1053	2.7244	3.2683	0.5493	0.5439	0.6468
	156	86	5.1219	5.1274	2.6856	3.3483	0.6738	0.6627	0.7935
	158	88	5.1498	5.1492	2.6391	3.4375	0.8176	0.7985	0.8628
	160	90	5.1781	5.1708	2.5829	3.5372	0.9842	0.9543	1.1589
	162	92	5.2054	5.1923	2.5146	3.6490	1.1782	1.1344	1.3874
	164	94	5.2307	5.2135	2.4497	3.7505	1.3590	1.3008	1.6004
	166	96	5.2525	5.2346	2.4077	3.8183	1.4799	1.4106	1.7426
	168	98	5.2702	5.2556	2.3711	3.8773	1.5859	1.5062	1.8675
	170	100	5.2853	5.2764	2.3702	3.8918	1.6055	1.5215	1.8906
	172	102	5.2995	5.2970	2.3598	3.9176	1.6479	1.5578	1.9405
	174	104	5.3108	5.3174	2.3622	3.9277	1.6593	1.5655	1.9540
	176	106	5.3215	5.3377	2.3985	3.8965	1.5890	1.4980	1.8711
178	108		5.3579	2.4177	3.8858	1.5594	1.4681	1.8363	

Table (3-46): Mass number (A), Neutron Number (N), Root Mean Square Radii $\langle r^2 \rangle^{1/2}$, Major and minor axes (a,b) and the difference between them (ΔR) by three methods for ${}_{72}\text{Hf}$ Isotopes.

(Z)	(A)	(N)	Theoretical Value	Present Work					
			$\langle r^2 \rangle^{1/2}$ fm [51]	$\langle r^2 \rangle^{1/2}$ fm	a fm	b fm	ΔR_1 fm	ΔR_2 fm	ΔR_3 fm
72	154	82		5.1053	2.7764	3.1796	0.4047	0.4032	0.4751
	156	84		5.1274	2.7371	3.2640	0.5328	0.5269	0.6255
	158	86		5.1492	2.6795	3.3744	0.7090	0.6950	0.8324
	160	88		5.1708	2.6609	3.4196	0.7774	0.7587	0.9128
	162	90		5.1923	2.6212	3.4957	0.9015	0.8746	1.0584
	164	92		5.2135	2.5756	3.5777	1.0390	1.0021	1.2199
	166	94		5.2346	2.5242	3.6646	1.1893	1.1404	1.3964
	168	96		5.2556	2.4740	3.7465	1.3339	1.2726	1.5662
	170	98	5.2898	5.2764	2.4270	3.8211	1.4679	1.3941	1.7234
	172	100	5.3065	5.2970	2.4216	3.8415	1.4985	1.4199	1.7594
	174	102	5.3201	5.3174	2.4193	3.8576	1.5212	1.4382	1.7861
	176	104	5.3286	5.3377	2.4219	3.8675	1.5320	1.4456	1.7988
	178	106	5.3371	5.3579	2.4497	3.8454	1.4806	1.3958	1.7384
	180	108	5.3470	5.3779	2.4614	3.8435	1.4685	1.3822	1.7241
	182	110	5.3516	5.3977	2.4858	3.8249	1.4240	1.3391	1.5838
184	112		5.4174	2.5220	3.7902	1.3490	1.2682	1.5838	

Table (3-47): Mass number (A), Neutron Number (N), Root Mean Square Radii $\langle r^2 \rangle^{1/2}$, Major and minor axes (a, b) and the difference between them (ΔR) by three methods for ${}_{74}\text{W}$ Isotopes.

(Z)	(A)	(N)	Theoretical Value	Present Work					
			$\langle r^2 \rangle^{1/2}$ fm [51]	$\langle r^2 \rangle^{1/2}$ fm	a fm	b fm	ΔR_1 fm	ΔR_2 fm	ΔR_3 fm
74	162	88		5.1923	2.6898	3.3899	0.7172	0.7001	0.8421
	164	90		5.2135	2.6551	3.4596	0.8289	0.8045	0.9732
	166	92		5.2346	2.6187	3.5296	0.9438	0.9109	1.1081
	168	94		5.2556	2.5842	3.5947	1.0522	1.0105	1.2354
	170	96		5.2764	2.5429	3.6673	1.1767	1.1245	1.3816
	172	98		5.2970	2.4944	3.7470	1.3174	1.2526	1.5468
	174	100		5.3174	2.4824	3.7766	1.3650	1.2942	1.6027
	176	102		5.3377	2.4837	3.7883	1.3788	1.3046	1.6189
	178	104		5.3579	2.4869	3.7974	1.3878	1.3105	1.6294
	180	106	5.3491	5.3779	2.4911	3.8050	1.3940	1.3139	1.6368
	182	108	5.3559	5.3977	2.4924	3.8163	1.4075	1.3239	1.6525
	184	110	5.3658	5.4174	2.5311	3.7780	1.3257	1.2469	1.5565
	186	112	5.3743	5.4370	2.5650	3.7452	1.2549	1.1802	1.4734
	188	114		5.4564	2.6104	3.6950	1.1524	1.0846	1.3531
	190	116		5.4757	2.6899	3.5927	0.9557	0.9028	1.1221

Table (3-48): Mass number (A), Neutron Number (N), Root Mean Square Radii $\langle r^2 \rangle^{1/2}$, Major and minor axes (a,b) and the difference between them (ΔR) by three methods for ${}_{76}\text{Os}$ Isotopes.

(Z)	(A)	(N)	Theoretical Value	Present Work					
			$\langle r^2 \rangle^{1/2}$ fm [51]	$\langle r^2 \rangle^{1/2}$ fm	a fm	b fm	ΔR_1 fm	ΔR_2 fm	ΔR_3 fm
76	164	88	-----	5.2135	2.7228	3.3526	0.6448	0.6298	0.7571
	166	90	-----	5.2346	2.7014	3.4027	0.7214	0.7013	0.8470
	168	92	-----	5.2556	2.6774	3.4555	0.8041	0.7781	0.9442
	170	94	-----	5.2764	2.6594	3.4982	0.8704	0.8388	1.0219
	172	96	-----	5.2970	2.6290	3.5583	0.9689	0.9293	1.1376
	174	98	-----	5.3174	2.5659	3.6632	1.1518	1.0973	1.3524
	176	100	-----	5.3377	2.5388	3.7145	1.2389	1.1757	1.4546
	178	102	-----	5.3579	2.5427	3.7227	1.2459	1.1800	1.4628
	180	104	-----	5.3779	2.5541	3.7206	1.2333	1.1665	1.4481
	182	106	5.3491	5.3977	2.5543	3.7336	1.2496	1.1793	1.4671
	184	108	5.3823	5.4174	2.5500	3.7526	1.2772	1.2026	1.4996
	186	110	5.3909	5.4370	2.5918	3.7081	1.1851	1.1164	1.3914
	188	112	5.3993	5.4564	2.6276	3.6705	1.1068	1.0429	1.2995
	190	114	5.4062	5.4757	2.6730	3.6177	1.0014	0.9447	1.1758
	192	116	5.4126	5.4948	2.6989	3.5924	0.9472	0.8935	1.1122
194	118	-----	5.5138	2.7173	3.5779	0.9129	0.8606	1.0719	
196	120	-----	5.5327	2.7732	3.5047	0.7738	0.7315	0.9086	

Table (3-49): Mass number (A), Neutron Number (N), Root Mean Square Radii $\langle r^2 \rangle^{1/2}$, Major and minor axes (a,b) and the difference between them (ΔR) by three methods for ${}_{78}\text{Pt}$ Isotopes.

(Z)	(A)	(N)	Theoretical Value	Present Work					
			$\langle r^2 \rangle^{1/2}$ fm [51]	$\langle r^2 \rangle^{1/2}$ fm	a fm	b fm	ΔR_1 fm	ΔR_2 fm	ΔR_3 fm
78	168	90	-----	5.2556	2.7426	3.3459	0.6157	0.5998	0.7229
	170	92	-----	5.2764	2.7389	3.3732	0.6532	0.6342	0.7669
	172	94	-----	5.2970	2.7341	3.3962	0.6840	0.6622	0.8031
	174	96	-----	5.3174	2.7233	3.4285	0.7310	0.7052	0.8583
	176	98	-----	5.3377	2.6726	3.5218	0.8864	0.8492	1.0408
	178	100	5.3728	5.3579	2.6004	3.6421	1.0958	1.0417	1.2866
	180	102	5.3891	5.3779	2.5862	3.6759	1.1498	1.0896	1.3500
	182	104	5.3969	5.3977	2.5996	3.6705	1.1315	1.0709	1.3285
	184	106	5.4015	5.4174	2.6197	3.6553	1.0951	1.0356	1.2857
	186	108	5.4037	5.4370	2.6604	3.6096	1.0029	0.9492	1.1775
	188	110	5.4053	5.4564	2.7242	3.5269	0.8455	0.8027	0.9928
	190	112	5.4108	5.4757	2.7481	3.5034	0.7956	0.7553	0.9342
	192	114	5.4169	5.4948	2.7653	3.4900	0.7638	0.7246	0.8968
	194	116	5.4236	5.5138	2.7779	3.4836	0.7446	0.7057	0.8743
	196	118	5.4307	5.5327	2.7956	3.4688	0.7107	0.6732	0.8344
198	120	5.4383	5.5515	2.8191	3.4442	0.6597	0.6251	0.7746	
200	122	-----	5.5701	2.8420	3.4200	0.6099	0.5780	0.7161	

Table (3-50): Mass number (A), Neutron Number (N), Root Mean Square Radii $\langle r^2 \rangle^{1/2}$, Major and minor axes (a,b) and the difference between them (ΔR) by three methods for ${}_{80}\text{Hg}$ Isotopes.

(Z)	(A)	(N)	Theoretical Value	Present Work					
			$\langle r^2 \rangle^{1/2}$ fm [51]	$\langle r^2 \rangle^{1/2}$ fm	a fm	b fm	ΔR_1 fm	ΔR_2 fm	ΔR_3 fm
80	176	96	-----	5.3377	2.7832	3.3461	0.5815	0.5630	0.6827
	178	98	-----	5.3579	2.7809	3.3649	0.6049	0.5841	0.7102
	180	100	-----	5.3779	2.7598	3.4142	0.6809	0.6545	0.7994
	182	102	5.3833	5.3977	2.7406	3.4593	0.7508	0.7186	0.8815
	184	104	5.3949	5.4174	2.7540	3.4522	0.7302	0.6982	0.8574
	186	106	5.4017	5.4370	2.7745	3.4335	0.6894	0.6590	0.8094
	188	108	5.4085	5.4564	2.7843	3.4318	0.6783	0.6475	0.7964
	190	110	5.4158	5.4757	2.7928	3.4321	0.6706	0.6393	0.7873
	192	112	5.4232	5.4948	2.8019	3.4311	0.6609	0.6292	0.7759
	194	114	5.4309	5.5138	2.8106	3.4308	0.6523	0.6202	0.7659
	196	116	5.4385	5.5327	2.8172	3.4337	0.6494	0.6165	0.7625
	198	118	5.4463	5.5515	2.8204	3.4421	0.6560	0.6217	0.7703
	200	120	5.4551	5.5701	2.8142	3.4657	0.6894	0.6515	0.8094
	202	122	5.4648	5.5886	2.8416	3.4341	0.6266	0.5925	0.7357
	204	124	5.4744	5.6070	2.8477	3.4374	0.6246	0.5898	0.7334
206	126	5.4837	5.6252	2.9310	3.3083	0.3966	0.3773	0.4657	

Table (3-51): Mass number (A), Neutron Number (N), Root Mean Square Radii $\langle r^2 \rangle^{1/2}$, Major and minor axes (a,b) and the difference between them (ΔR) by three methods for ${}_{82}\text{Pb}$ Isotopes.

(Z)	(A)	(N)	Theoretical Value	Present Work					
			$\langle r^2 \rangle^{1/2}$ fm [51]	$\langle r^2 \rangle^{1/2}$ fm	a fm	b fm	ΔR_1 fm	ΔR_2 fm	ΔR_3 fm
82	182	100	5.3788	5.3977	2.8393	3.2963	0.4725	0.4570	0.5547
	184	102	5.3930	5.4174	2.8258	3.3342	0.5278	0.5085	0.6197
	186	104	5.4027	5.4370	2.8275	3.3459	0.5393	0.5184	0.6332
	188	106	5.4139	5.4564	2.8427	3.3347	0.5122	0.4920	0.6014
	190	108	5.4222	5.4757	2.8553	3.3275	0.4919	0.4722	0.5776
	192	110	5.4300	5.4948	2.8702	3.3163	0.4651	0.4461	0.5461
	194	112	5.4372	5.5138	2.8863	3.3027	0.4343	0.4165	0.5100
	196	114	5.4444	5.5327	2.8987	3.2952	0.4138	0.3965	0.4858
	198	116	5.4524	5.5515	2.9060	3.2966	0.4082	0.3906	0.4793
	200	118	5.4911	5.5701	2.9098	3.3040	0.4127	0.3942	0.4846
	202	120	5.4705	5.5886	2.9113	3.3153	0.4238	0.4039	0.4976
	204	122	5.4803	5.6070	2.9127	3.3267	0.4352	0.4139	0.5110
	206	124	5.4902	5.6252	2.9104	3.3445	0.4575	0.4341	0.5372
	208	126	5.5012	5.6434	3.0012	3.1942	0.2016	0.1931	0.2366
	210	128	5.5208	5.6614	2.9224	3.3506	0.4527	0.4282	0.5315
	212	130	5.5396	5.6793	2.9289	3.3525	0.4483	0.4236	0.5264
	214	132	5.5577	5.6971	2.9368	3.3503	0.4372	0.4126	0.5133

Table (3-52): Mass number (A), Neutron Number (N), Root Mean Square Radii $\langle r^2 \rangle^{1/2}$, Major and minor axes (a, b) and the difference between them (ΔR) by three methods for ${}_{84}\text{Po}$ Isotopes.

(Z)	(A)	(N)	Theoretical Value	Present Work					
			$\langle r^2 \rangle^{1/2}$ fm [51]	$\langle r^2 \rangle^{1/2}$ fm	a fm	b fm	ΔR_1 fm	ΔR_2 fm	ΔR_3 fm
84	192	108	5.5220	5.4948	2.7381	3.5326	0.8395	0.7945	0.9857
	194	110	5.5167	5.5138	2.7738	3.4901	0.7561	0.7163	0.8877
	196	112	5.5136	5.5327	2.8265	3.4184	0.6228	0.5919	0.7313
	198	114	5.5146	5.5515	2.8604	3.3755	0.5412	0.5151	0.6355
	200	116	5.5199	5.5701	2.8757	3.3632	0.5125	0.4874	0.6017
	202	118	5.5281	5.5886	2.8837	3.3632	0.5048	0.4795	0.5926
	204	120	5.5378	5.6070	2.8910	3.3643	0.4989	0.4733	0.5857
	206	122	5.5480	5.6252	2.8994	3.3635	0.4898	0.4641	0.5751
	208	124	5.5584	5.6434	2.9040	3.3691	0.4917	0.4651	0.5773
	210	126	5.5704	5.6614	2.9494	3.3029	0.3724	0.3535	0.4373
	212	128	-----	5.6793	2.9211	3.3662	0.4717	0.4452	0.5538
	214	130	-----	5.6971	2.9124	3.3943	0.5121	0.4819	0.6013
	216	132	5.6359	5.7148	2.9094	3.4124	0.5358	0.5029	0.6291
	218	134	5.6558	5.7324	2.9089	3.4262	0.5523	0.5174	0.6485

Table (3-53): Mass number (A), Neutron Number (N), Root Mean Square Radii $\langle r^2 \rangle^{1/2}$, Major and minor axes (a, b) and the difference between them (ΔR) by three methods for ${}_{86}\text{Rn}$ Isotopes.

(Z)	(A)	(N)	Theoretical Value	Present Work					
			$\langle r^2 \rangle^{1/2}$ fm [51]	$\langle r^2 \rangle^{1/2}$ fm	a fm	b fm	ΔR_1 fm	ΔR_2 fm	ΔR_3 fm
86	198	112	-----	5.5515	2.7968	3.4804	0.7231	0.6836	0.8489
	200	114	-----	5.5701	2.8331	3.4348	0.6356	0.6018	0.7462
	202	116	5.5521	5.5886	2.8560	3.4101	0.5851	0.5541	0.6870
	204	118	5.5568	5.6070	2.8700	3.4001	0.5601	0.5301	0.6576
	206	120	5.5640	5.6252	2.8820	3.3932	0.5406	0.5112	0.6347
	208	122	5.5725	5.6434	2.8974	3.3804	0.5109	0.4830	0.5999
	210	124	5.5813	5.6614	2.9048	3.3811	0.5045	0.4763	0.5923
	212	126	5.5915	5.6793	2.9598	3.2978	0.3564	0.3380	0.4185
	214	128	-----	5.6971	2.9234	3.3753	0.4796	0.4518	0.5631
	216	130	-----	5.7148	2.8928	3.4405	0.5845	0.5477	0.6863
	218	132	5.6540	5.7324	2.8605	3.5068	0.6934	0.6463	0.8141
	220	134	5.6731	5.7499	2.8287	3.5701	0.7994	0.7414	0.9386
	222	136	5.6915	5.7673	2.7971	3.6316	0.9039	0.8344	1.0613

Table (3-54): Mass number (A), Neutron Number (N), Root Mean Square Radii $\langle r^2 \rangle^{1/2}$, Major and minor axes (a,b) and the difference between them (ΔR) by three methods for $_{88}\text{Ra}$ Isotopes.

(Z)	(A)	(N)	Theoretical I Value	Present Work					
			$\langle r^2 \rangle^{1/2}$ fm [51]	$\langle r^2 \rangle^{1/2}$ fm	a fm	b fm	ΔR_1 fm	ΔR_2 fm	ΔR_3 fm
88	206	118	-----	5.6252	2.8632	3.4250	0.5954	0.5619	0.6990
	208	120	5.5850	5.6434	2.8789	3.4118	0.5648	0.5328	0.6632
	210	122	5.5917	5.6614	2.8991	3.3908	0.5212	0.4917	0.6119
	212	124	5.5991	5.6793	2.9090	3.3870	0.5071	0.4779	0.5953
	214	126	5.6079	5.6971	2.9703	3.2925	0.3400	0.3222	0.3992
	216	128	-----	5.7148	2.9287	3.3792	0.4789	0.4505	0.5622
	218	130	-----	5.7324	2.8813	3.4725	0.6330	0.5912	0.7432
	220	132	5.6683	5.7499	2.7831	3.6412	0.9289	0.8581	1.0907
	222	134	5.6874	5.7673	2.7014	3.7738	1.1702	1.0724	1.3739
	224	136	5.7046	5.7845	2.6458	3.8629	1.3349	1.2171	1.5673
	226	138	5.7211	5.8017	2.5958	3.9410	1.4817	1.3452	1.7397
	228	140	5.7370	5.8188	2.5879	3.9622	1.5168	1.3742	1.7809
	230	142	5.7551	5.8357	2.5653	4.0022	1.5901	1.4369	1.8670

Table (3-55): Mass number (A), Neutron Number (N), Root Mean Square Radii $\langle r^2 \rangle^{1/2}$, Major and minor axes (a,b) and the difference between them (ΔR) by three methods for $_{90}\text{Th}$ Isotopes.

(Z)	(A)	(N)	Theoretical I Value	Present Work					
			$\langle r^2 \rangle^{1/2}$ fm [51]	$\langle r^2 \rangle^{1/2}$ fm	a fm	b fm	ΔR_1 fm	ΔR_2 fm	ΔR_3 fm
90	216	126	-----	5.7148	2.9797	3.2890	0.3268	0.3093	0.3837
	218	128	-----	5.7324	2.9349	3.3816	0.4755	0.4467	0.5582
	220	130	-----	5.7499	2.8832	3.4820	0.6423	0.5988	0.7541
	222	132	-----	5.7673	2.7946	3.6355	0.9111	0.8409	1.0697
	224	134	-----	5.7845	2.6818	3.8130	1.2380	1.1312	1.4535
	226	136	-----	5.8017	2.6138	3.9172	1.4345	1.3035	1.6843
	228	138	5.7488	5.8188	2.5581	4.0008	1.5945	1.4426	1.8721
	230	140	5.7670	5.8357	2.5414	4.0325	1.6517	1.4910	1.9393
	232	142	5.7848	5.8526	2.5263	4.0619	1.7047	1.5356	2.0016
	234	144	-----	5.8694	2.5368	4.0591	1.6919	1.5222	1.9865

Table (3-56): Mass number (A), Neutron Number (N), Root Mean Square Radii $\langle r^2 \rangle^{1/2}$, Major and minor axes (a, b) and the difference between them (ΔR) by three methods for ${}_{92}\text{U}$ Isotopes.

(Z)	(A)	(N)	Theoretical Value	Present Work					
			$\langle r^2 \rangle^{1/2}$ fm [51]	$\langle r^2 \rangle^{1/2}$ fm	a fm	b fm	ΔR_1 fm	ΔR_2 fm	ΔR_3 fm
92	226	134	-----	5.8017	2.6424	3.8787	1.3585	1.2363	1.5951
	228	136	-----	5.8188	2.5646	3.9924	1.5776	1.4278	1.8523
	230	138	-----	5.8357	2.5323	4.0440	1.6752	1.5117	1.9669
	232	140	-----	5.8526	2.5138	4.0774	1.7366	1.5636	2.0390
	234	142	5.8291	5.8694	2.4920	4.1142	1.8058	1.6222	2.1202
	236	144	5.8431	5.8860	2.5154	4.0958	1.7606	1.5804	2.0672
	238	146	5.8571	5.9026	2.5222	4.0975	1.7572	1.5753	2.0632
	240	148	-----	5.9191	2.5322	4.0953	1.7457	1.5631	2.0496

Table (3-57): Mass number (A), Neutron Number (N), Root Mean Square Radii $\langle r^2 \rangle^{1/2}$, Major and minor axes (a, b) and the difference between them (ΔR) by three methods for ${}_{94}\text{Pu}$ Isotopes.

(Z)	(A)	(N)	Theoretical Value	Present Work					
			$\langle r^2 \rangle^{1/2}$ fm [51]	$\langle r^2 \rangle^{1/2}$ fm	a fm	b fm	ΔR_1 fm	ΔR_2 fm	ΔR_3 fm
94	236	142	-----	5.8860	2.5107	4.1016	1.7727	1.5909	2.0813
	238	144	5.8535	5.0519	2.5158	4.1055	1.7737	1.5897	2.0825
	240	146	5.8701	5.9191	2.5150	4.1164	1.7895	1.6014	2.1011
	242	148	5.8823	5.9355	2.5378	4.0983	1.7450	1.5605	2.0488
	244	150	5.8948	5.9518	2.5577	4.0836	1.7077	1.5259	2.0050
	246	152	-----	5.9355	2.5533	4.0990	1.7326	1.5457	2.0343

Table (3-58): Mass number (A), Neutron Number (N), Root Mean Square Radii $\langle r^2 \rangle^{1/2}$, Major and minor axes (a,b) and the difference between them (ΔR) by three methods for ${}_{96}\text{Cm}$ Isotopes.

(Z)	(A)	(N)	Theoretical Value	Present Work					
			$\langle r^2 \rangle^{1/2}$ fm [51]	$\langle r^2 \rangle^{1/2}$ fm	a fm	b fm	ΔR_1 fm	ΔR_2 fm	ΔR_3 fm
96	238	142	-----	5.9026	2.4290	4.2086	1.9905	1.7796	2.3371
	240	144	-----	5.9191	2.4713	4.1690	1.8997	1.6977	2.2304
	242	146	5.8285	5.9355	2.5186	4.1220	1.7942	1.6034	2.1066
	244	148	5.8429	5.9518	2.5346	4.1122	1.7670	1.5776	2.0746
	246	150	5.8562	5.9680	2.5428	4.1120	1.7597	1.5692	2.0661
	248	152	5.8687	5.9841	2.5559	4.1056	1.7395	1.5497	2.0424
	250	154	-----	6.0002	2.5618	4.1080	1.7379	1.5463	2.0405

Table (3-59): Mass number (A), Neutron Number (N), Root Mean Square Radii $\langle r^2 \rangle^{1/2}$, Major and minor axes (a,b) and the difference between them (ΔR) by three method for ${}_{98}\text{Cf}$ Isotopes.

(Z)	(A)	(N)	Theoretical Value	Present Work					
			$\langle r^2 \rangle^{1/2}$ fm [51]	$\langle r^2 \rangle^{1/2}$ fm	a fm	b fm	ΔR_1 fm	ΔR_2 fm	ΔR_3 fm
98	244	146	----	5.9518	2.5094	4.1430	1.8313	1.6336	2.1501
	248	150	----	5.9841	2.5410	4.1240	1.7779	1.5830	2.0874
	250	152	----	6.0002	2.5596	4.1107	1.7435	1.5512	2.0471
	252	154	----	6.0161	2.5905	4.0816	1.6765	1.4911	1.9683

Table (3-60): Mass number(A), Neutron Number(N), Root Mean Square Radii $\langle r^2 \rangle^{1/2}$, Major and minor axes (a, b) and the difference between them (ΔR) by three method for ${}_{100}\text{Fm}$ Isotopes.

(Z)	(A)	(N)	Theoretical Value	Present Work					
			$\langle r^2 \rangle^{1/2}$ fm [51]	$\langle r^2 \rangle^{1/2}$ fm	a fm	b fm	ΔR_1 fm	ΔR_2 fm	ΔR_3 fm
100	248	148	-----	5.9841	2.5606	4.0996	1.7272	1.5390	2.0280
	250	150	-----	6.0002	2.5694	4.0984	1.7180	1.5290	2.0171
	252	152	5.8285	6.0161	2.5966	4.0729	1.6605	1.4773	1.9497
	254	154	5.8429	6.0320	2.5938	4.0871	1.6812	1.4933	1.9739
	256	156	-----	6.0478	2.6230	4.0594	1.6174	1.4363	1.8990

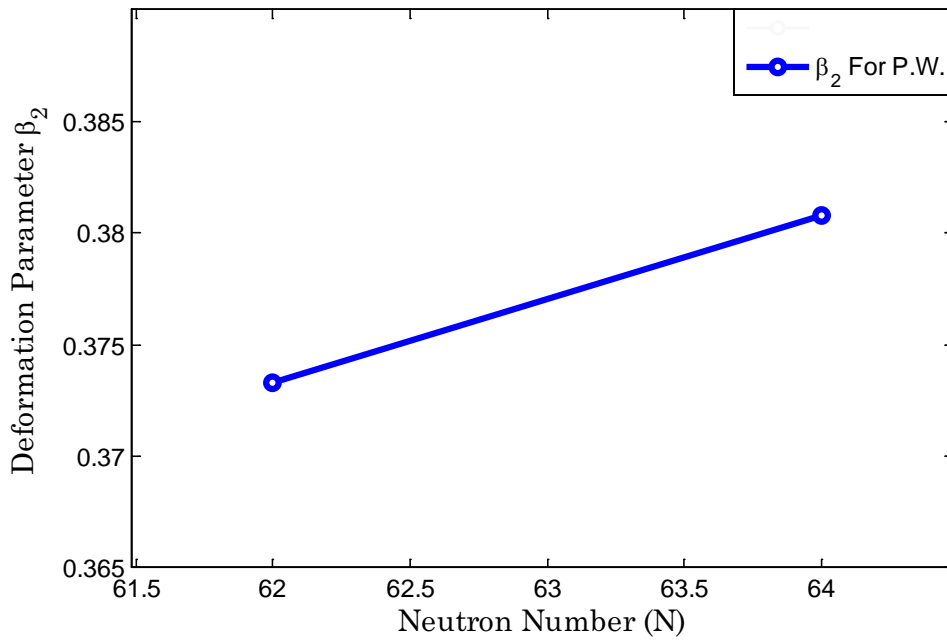


Figure (3-1): Represents the relationship of Deformation Parameter (β_2) value of the Present Work as a function of neutron Number for the ($_{40}\text{Zr}$) Isotopes.

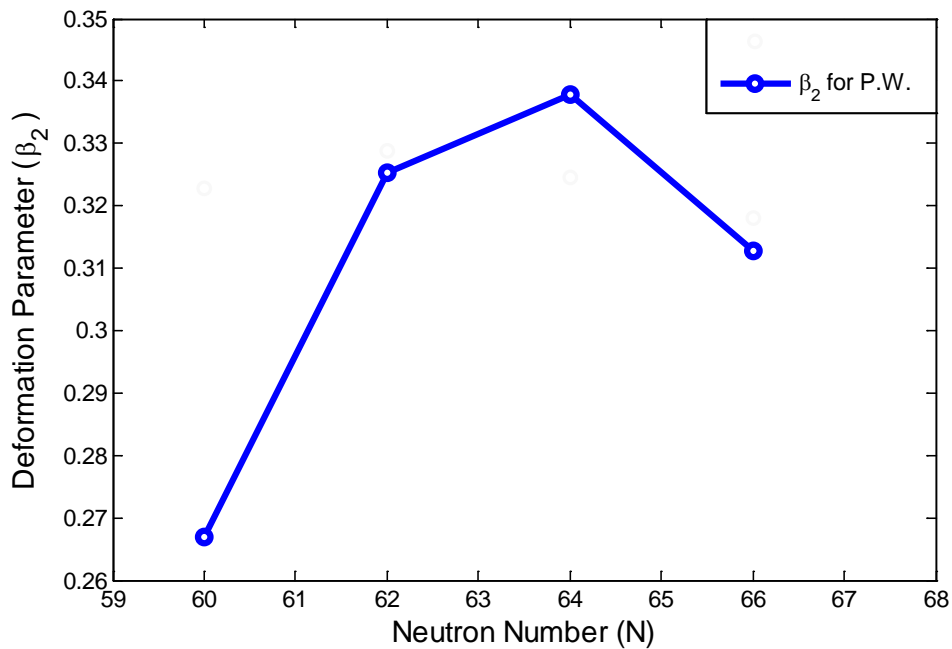


Figure (3-2): Represents the relationship of Deformation Parameter (β_2) value of the Present Work as a function of neutron Number for the ($_{42}\text{Mo}$) Isotopes.

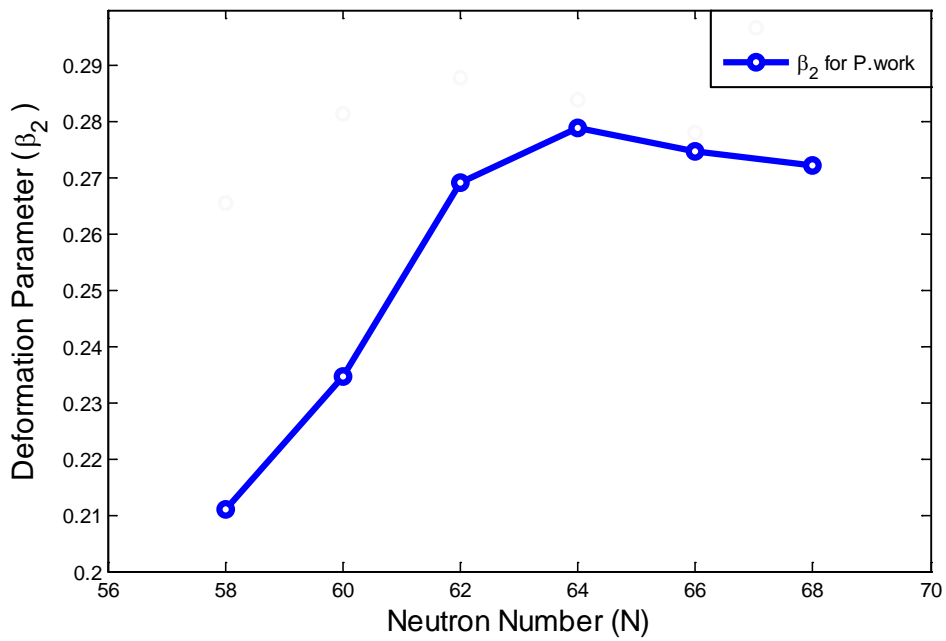


Figure (3-3): Represents the relationship of Deformation Parameter (β_2 value of the Present Work as a function of neutron Number for the (^{44}Ru) Isotopes.

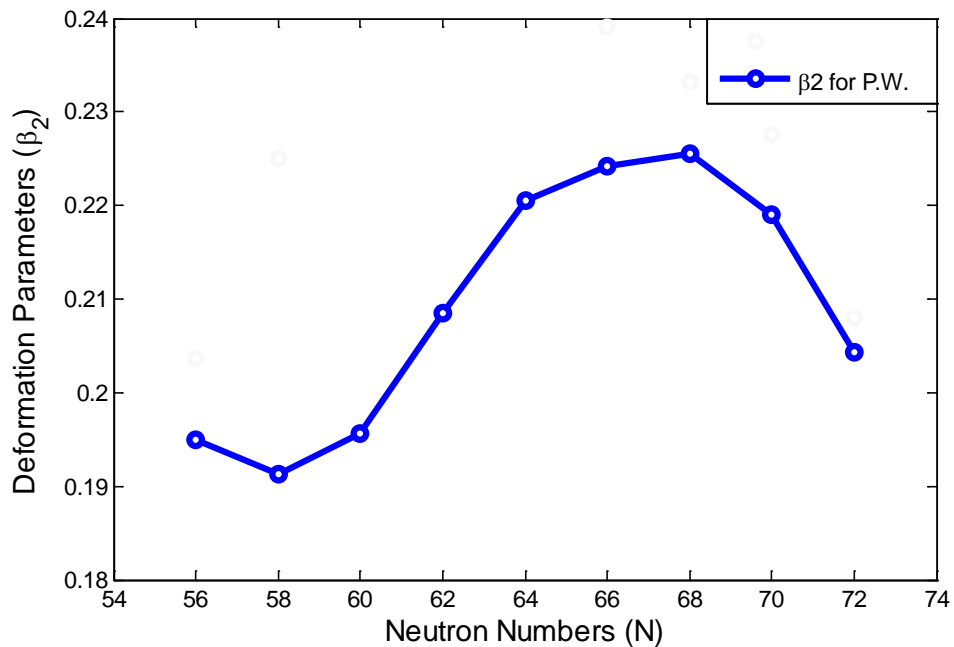


Figure (3-4): Represents the relationship of Deformation Parameter (β_2) value of the Present Work as a function of neutron Number for the (^{46}Pd) Isotopes.

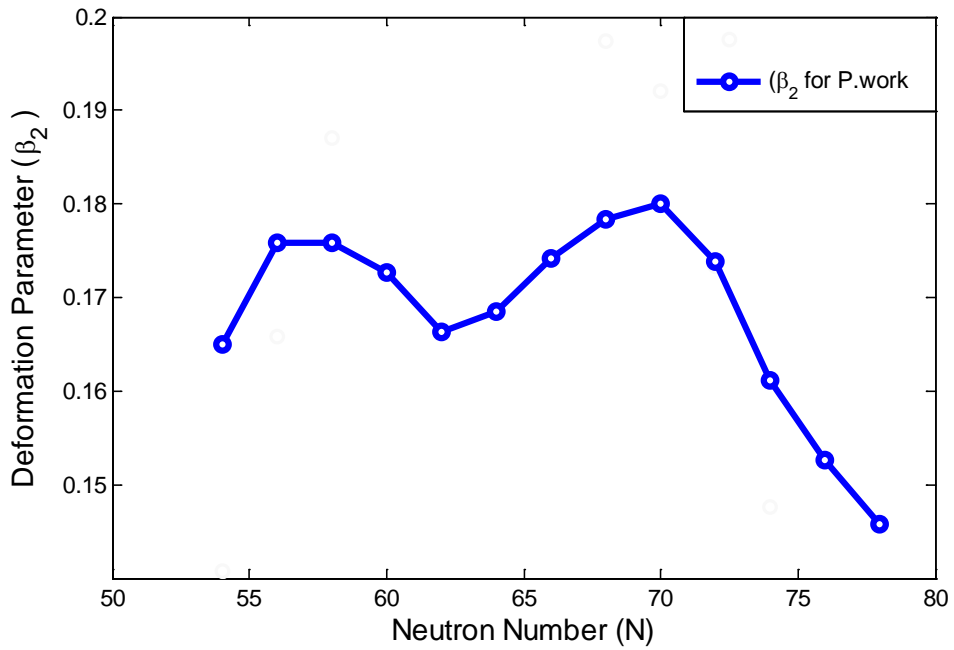


Figure (3-5): Represents the relationship of Deformation Parameter (β_2) value of the Present Work as a function of neutron Number for the (^{48}Cd) Isotopes.

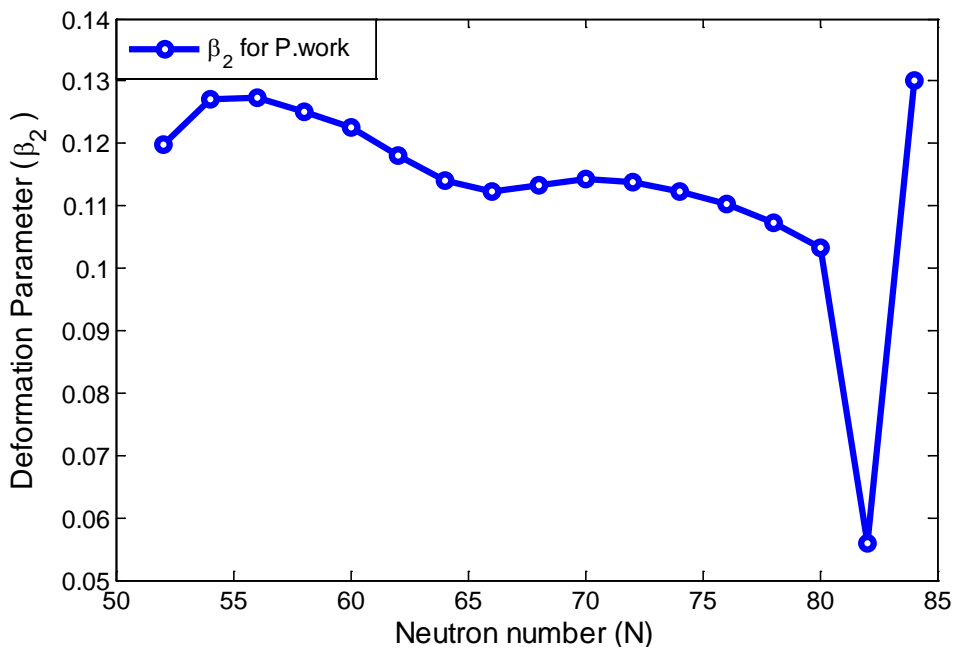


Figure (3-6): Represents the relationship of Deformation Parameter (β_2) value of the Present Work as a function of neutron Number for the (^{50}Sn) Isotopes.

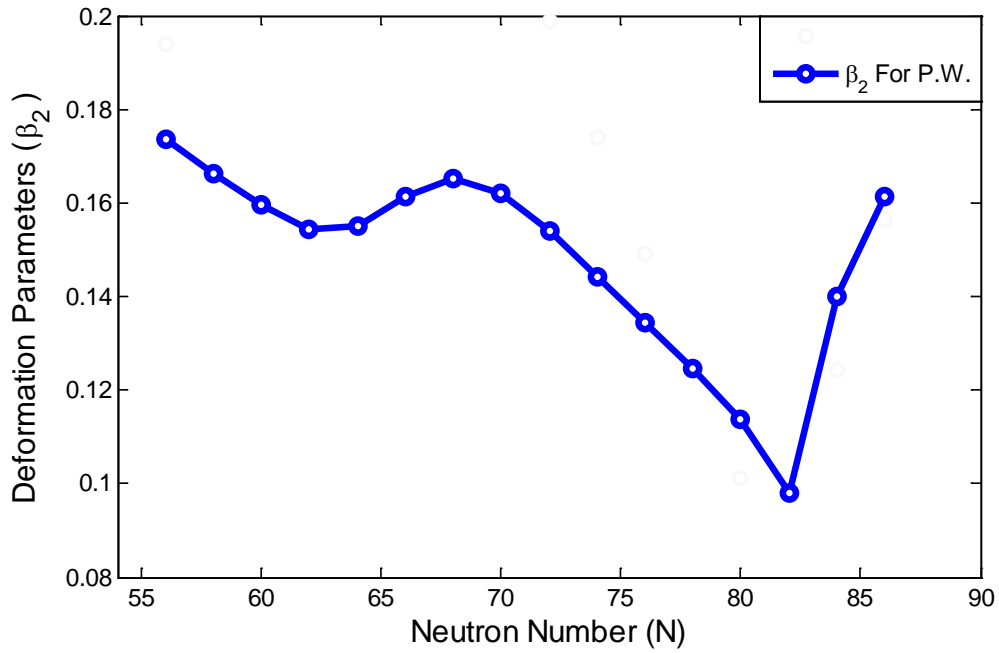


Figure (3-7): Represents the relationship of Deformation Parameter (β_2) value of the Present Work as a function of neutron Number for the (^{52}Te) Isotopes.

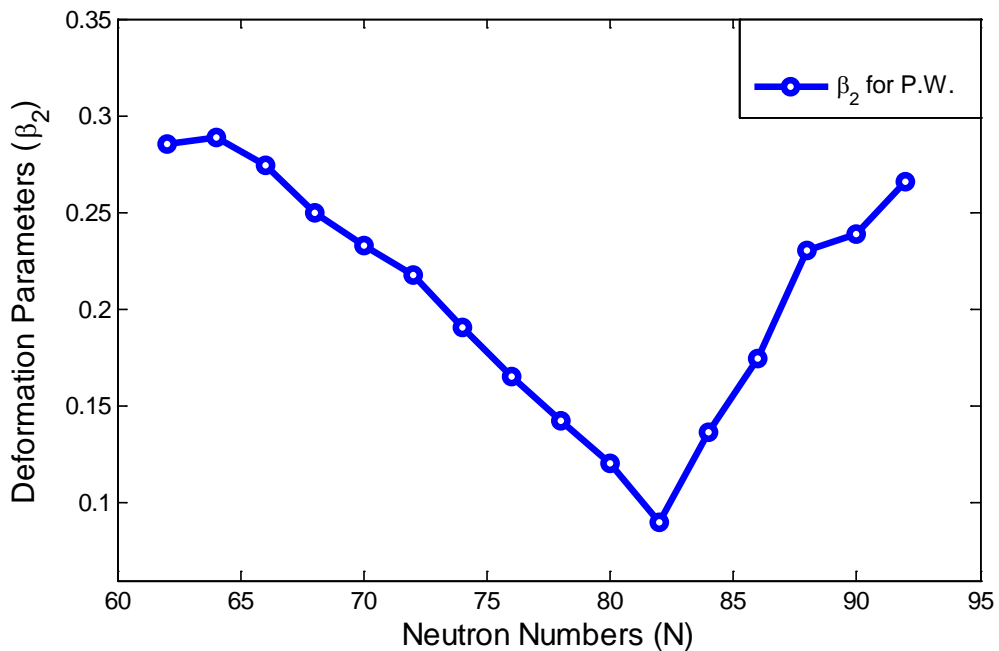


Figure (3-8): Represents the relationship of Deformation Parameter (β_2) value of the Present Work as a function of neutron Number for the (^{56}Ba) Isotopes.

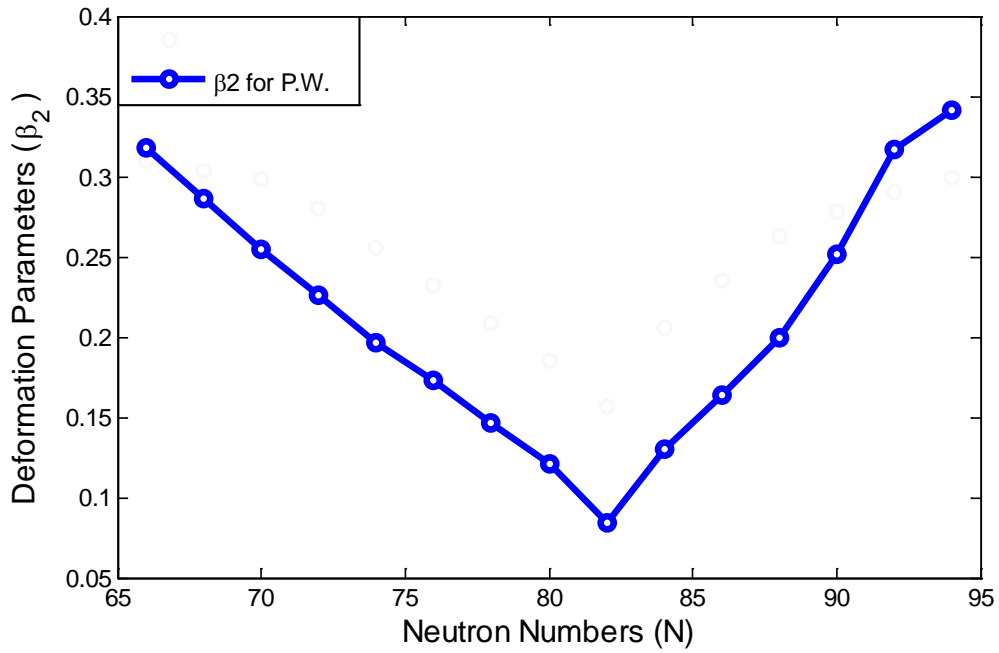


Figure (3-9): Represents the relationship of Deformation Parameter (β_2) value of the Present Work as a function of neutron Number for the (^{58}Ce) Isotopes.

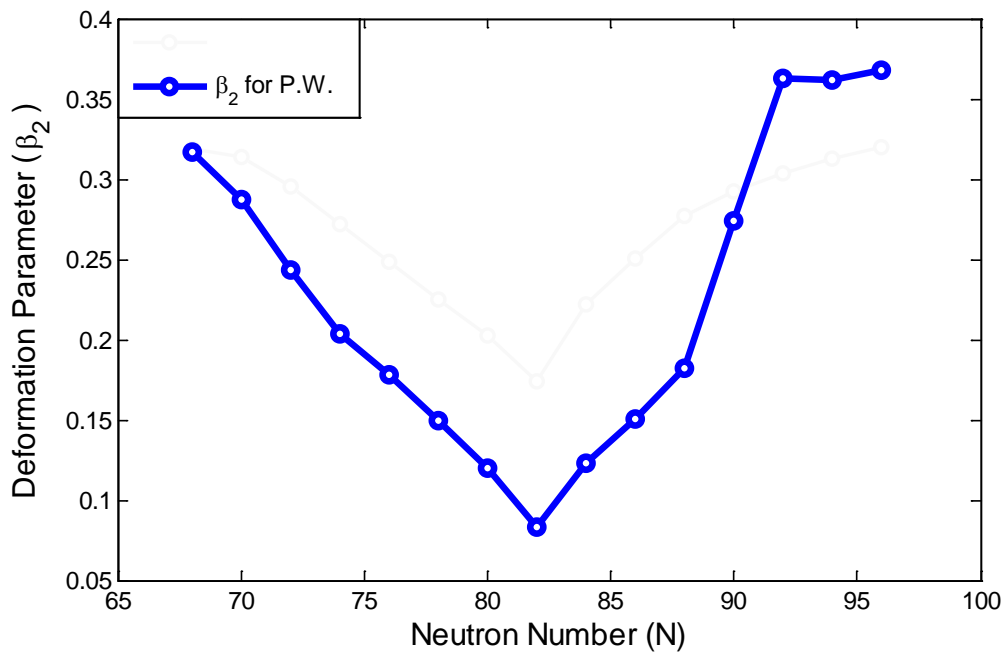


Figure (3-10): Represents the relationship of Deformation Parameter (β_2) value of the Present Work as a function of neutron Number for the (^{60}Nd) Isotopes.

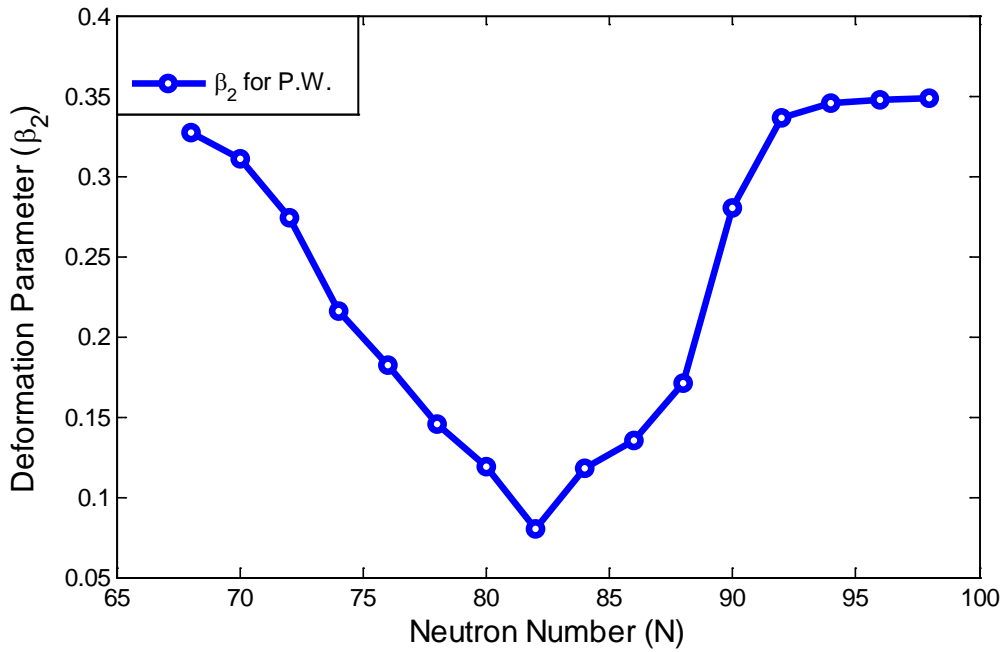


Figure (3-11): Represents the relationship of Deformation Parameter (β_2) value of the Present Work as a function of neutron Number for the (^{62}Sm) Isotopes.

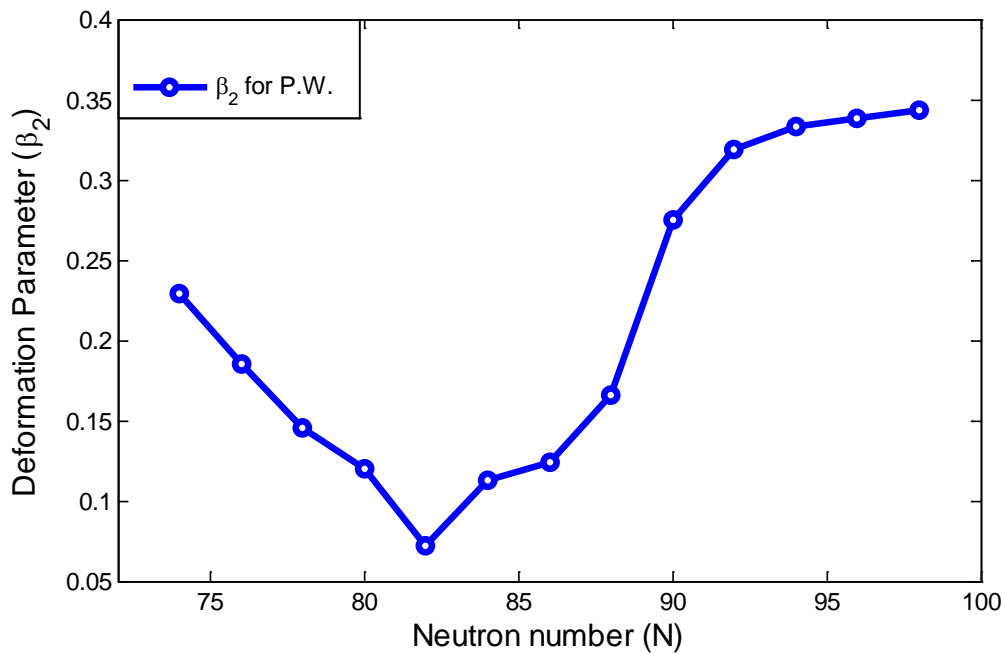


Figure (3-12): Represents the relationship of Deformation Parameter (β_2) value of the Present Work as a function of neutron Number for the (^{64}Gd) Isotopes.

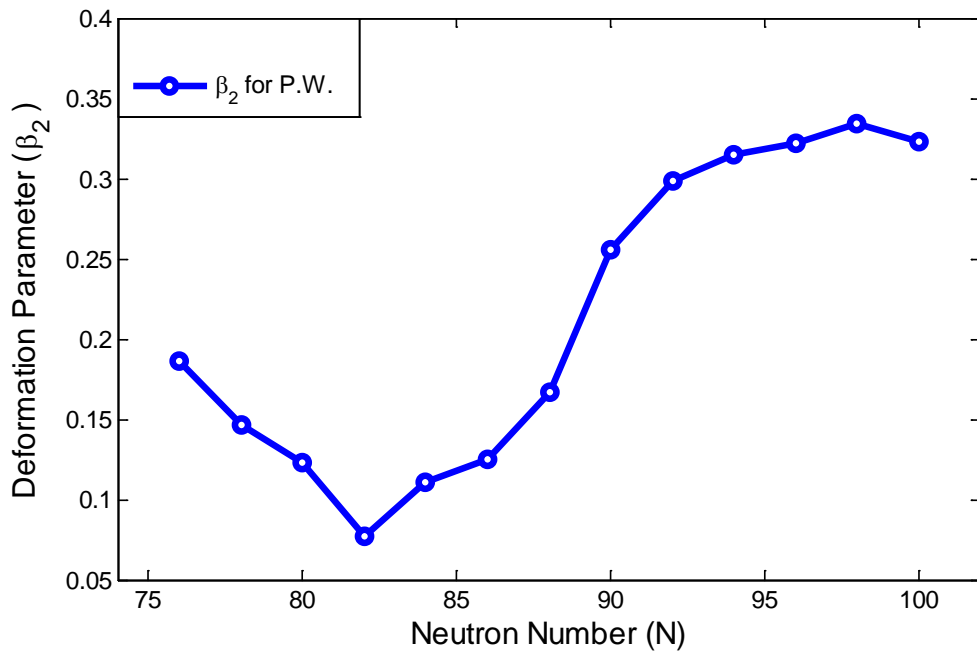


Figure (3-13): Represents the relationship of Deformation Parameter (β_2) value of the Present Work as a function of neutron Number for the (^{66}Dy) Isotopes.

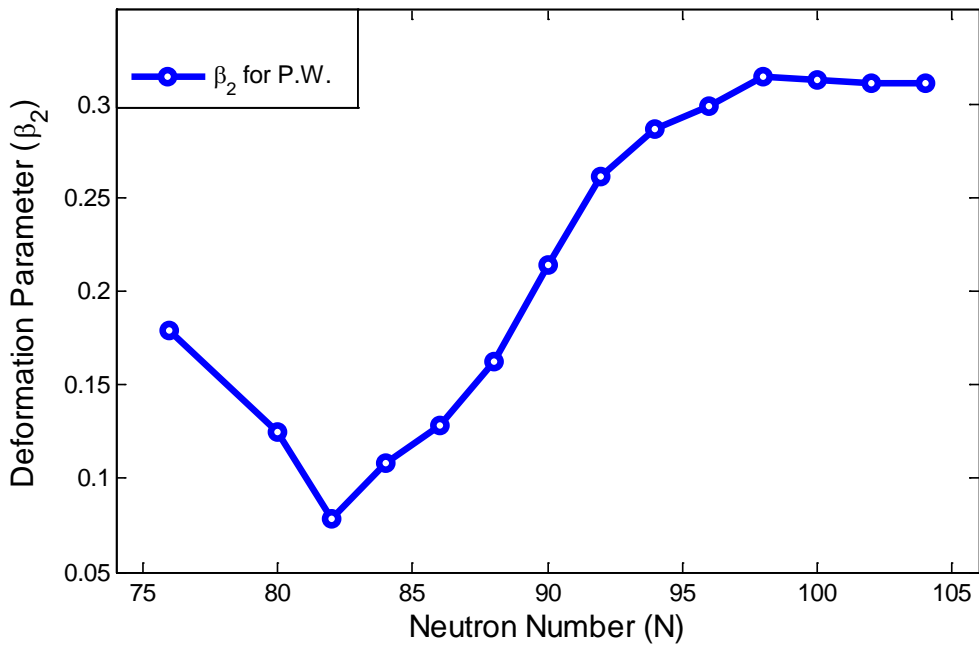


Figure (3-14): Represents the relationship of Deformation Parameter (β_2) value of the Present Work as a function of neutron Number for the (^{68}Er) Isotopes.

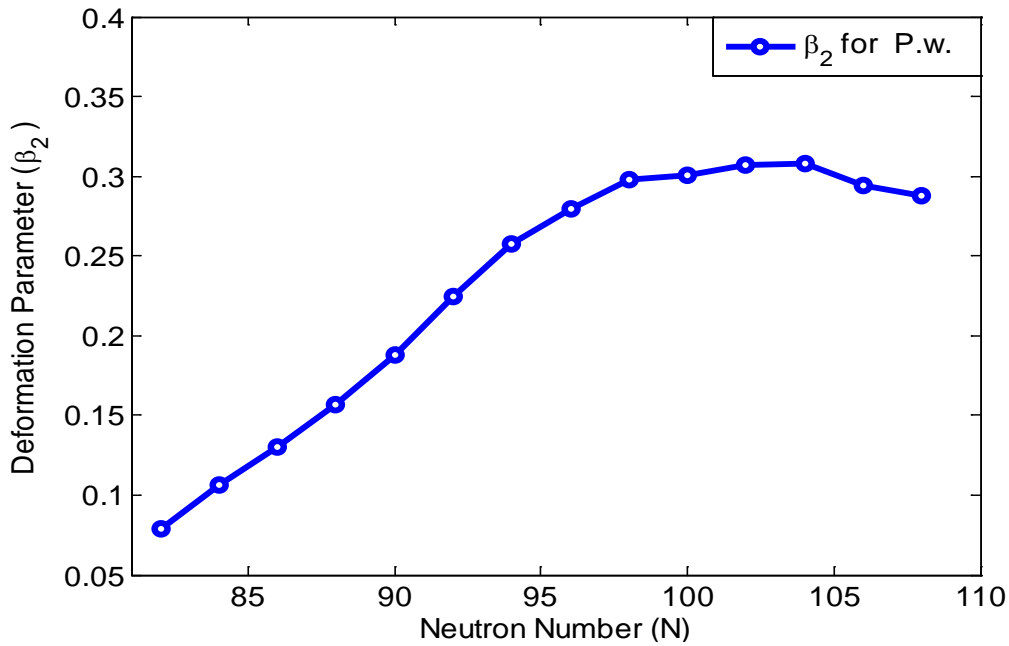


Figure (3-15): Represents the relationship of Deformation Parameter (β_2) value of the Present Work as a function of neutron Number for the (^{70}Yb) Isotopes.

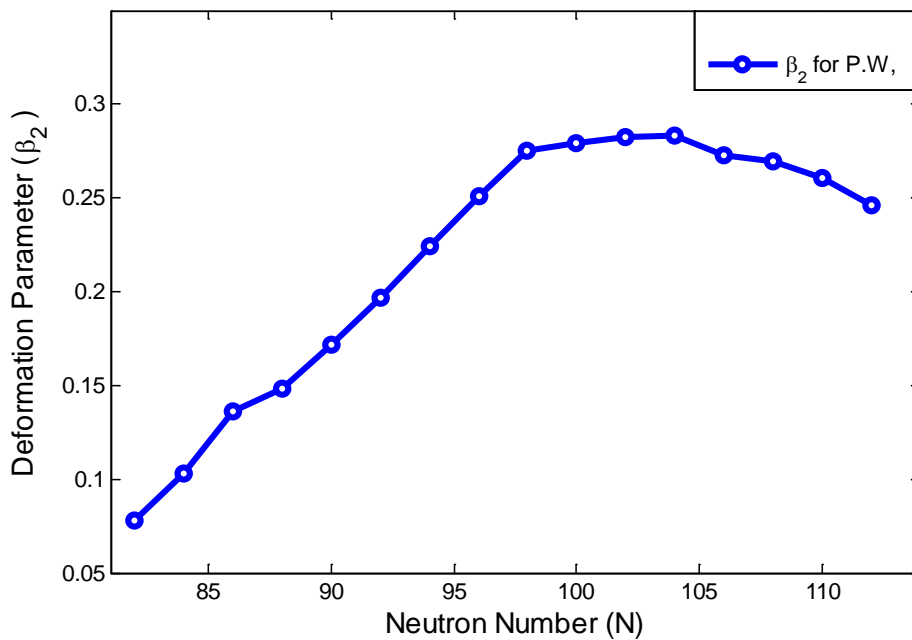


Figure (3-16): Represents the relationship of Deformation Parameter (β_2) value of the Present Work as a function of neutron Number for the (^{72}Hf) Isotopes.

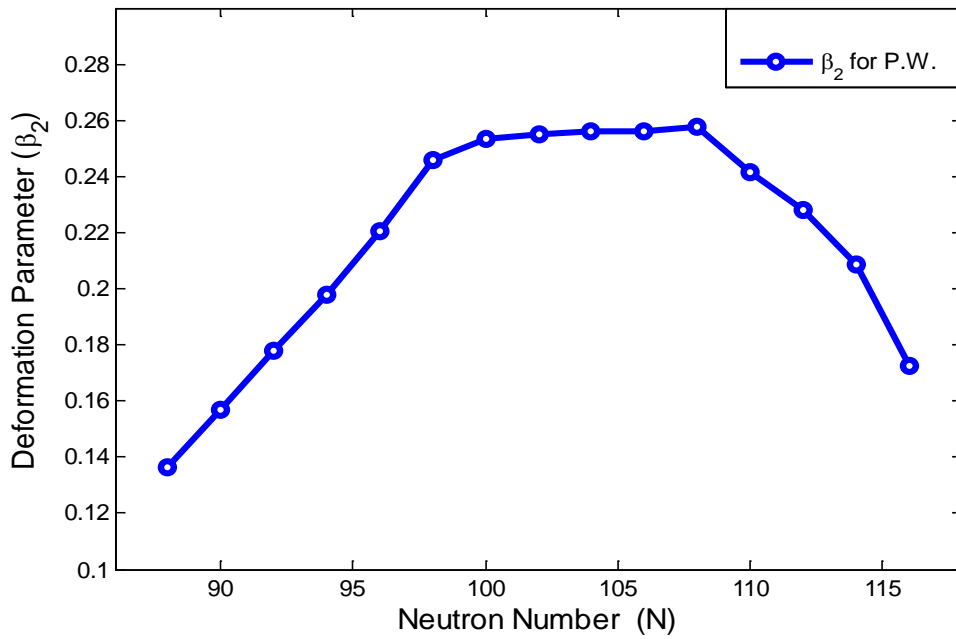


Figure (3-17): Represents the relationship of Deformation Parameter (β_2) value of the Present Work as a function of neutron Number for the (^{74}W) Isotopes.

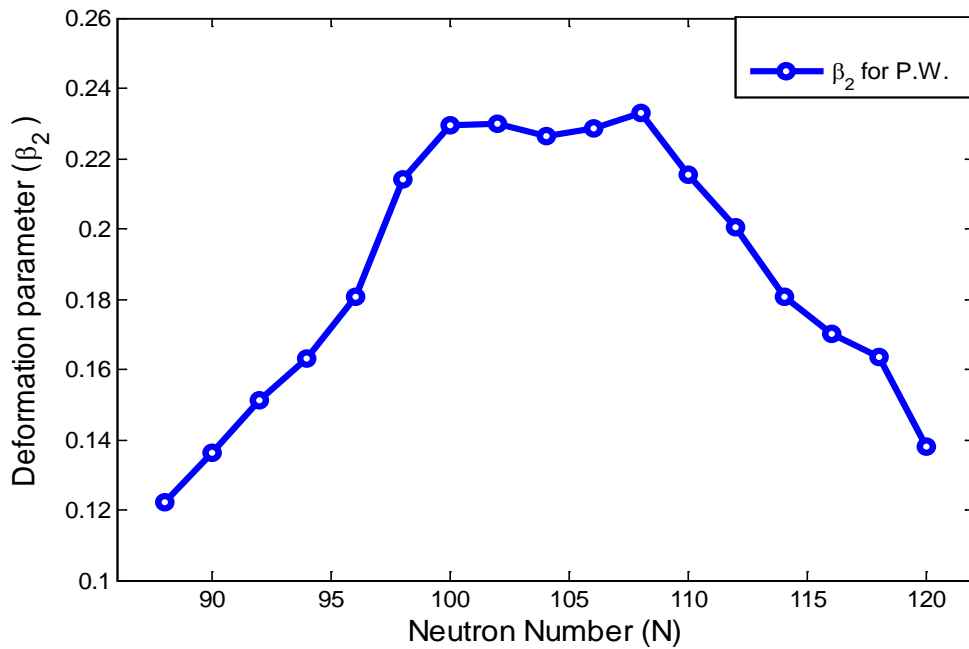


Figure (3-18): Represents the relationship of Deformation Parameter (β_2) value of the Present Work as a function of neutron Number for the (^{76}Os) Isotopes.

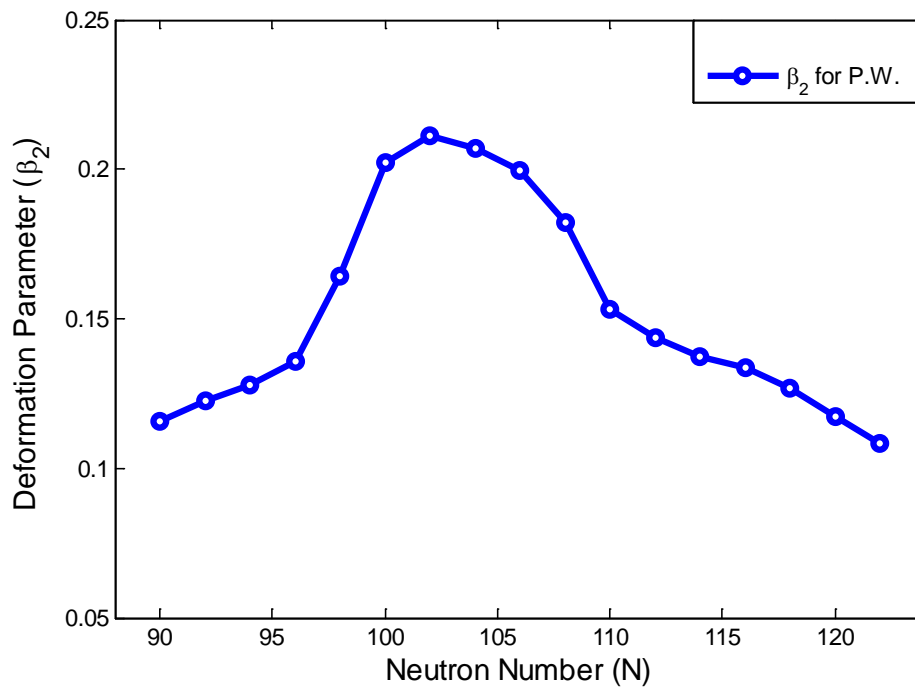


Figure (3-19): Represents the relationship of Deformation Parameter (β_2) value of the Present Work as a function of neutron Number for the ($_{78}\text{Pt}$) Isotopes.

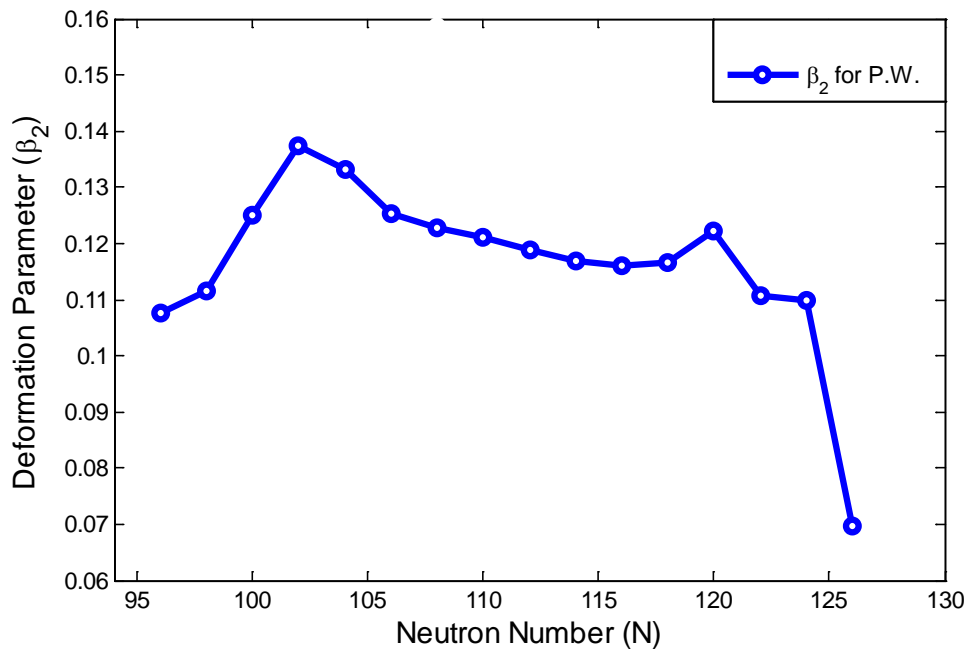


Figure (3-20): Represents the relationship of Deformation Parameter (β_2) value of the Present Work as a function of neutron Number for the ($_{80}\text{Hg}$) Isotopes.

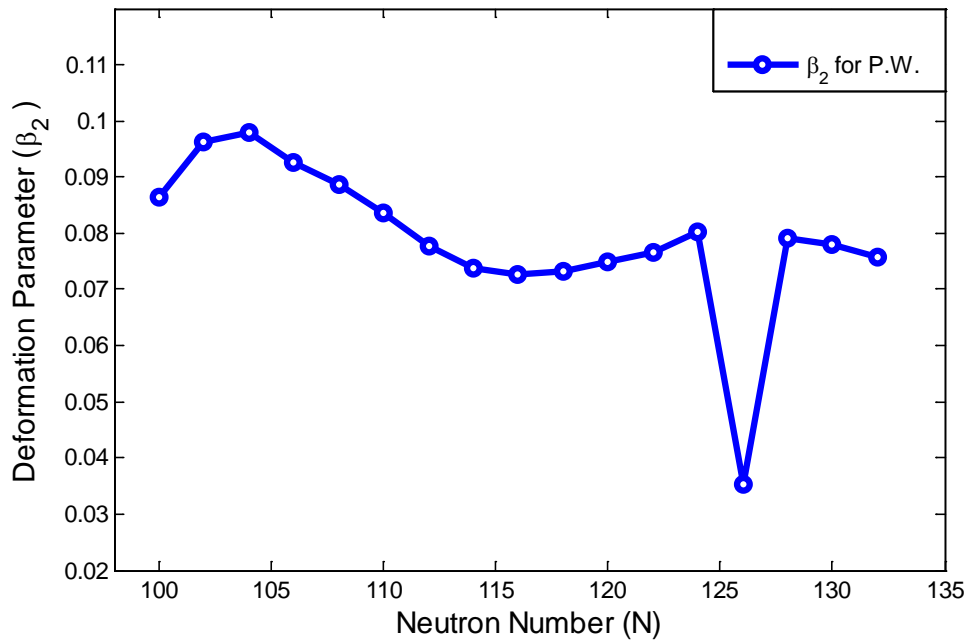


Figure (3-21): Represents the relationship of Deformation Parameter (β_2) value of the Present Work as a function of neutron Number for the (^{82}Pb) Isotopes.

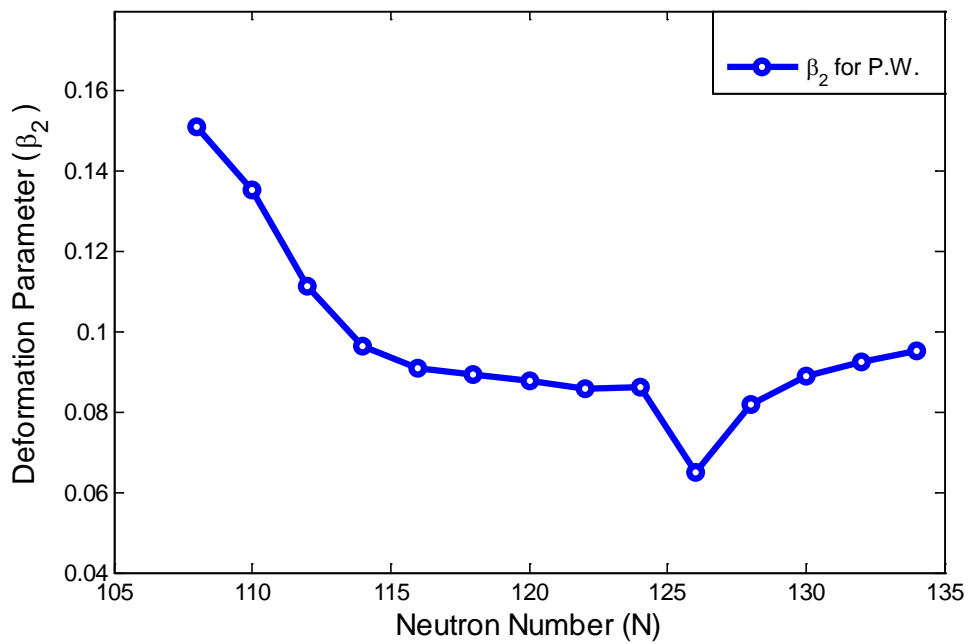


Figure (3-22): Represents the relationship of Deformation Parameter (β_2) value of the Present Work as a function of neutron Number for the (^{84}Po) Isotopes.

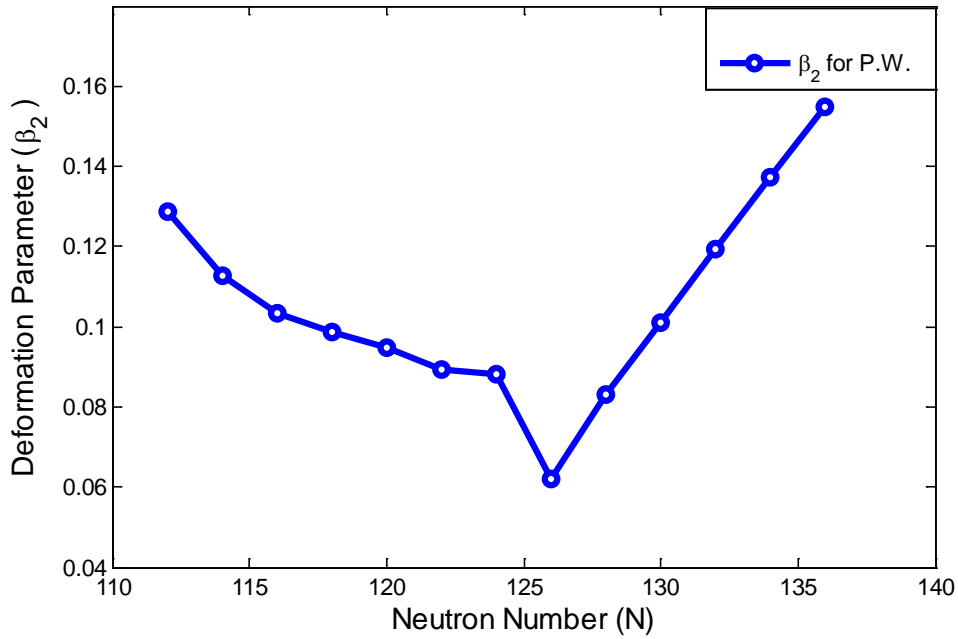


Figure (3-23): Represents the relationship of Deformation Parameter (β_2) value of the Present Work as a function of neutron Number for the $(_{86}\text{Rn})$ Isotopes.

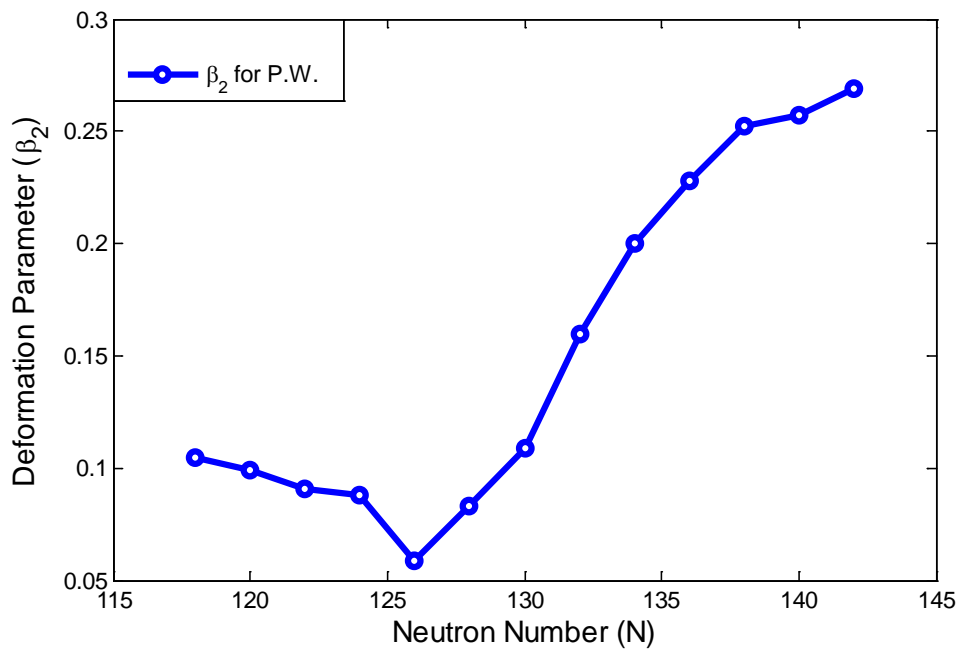


Figure (3-24): Represents the relationship of Deformation Parameter (β_2) value of the Present Work as a function of neutron Number for the $(_{88}\text{Ra})$ Isotopes.

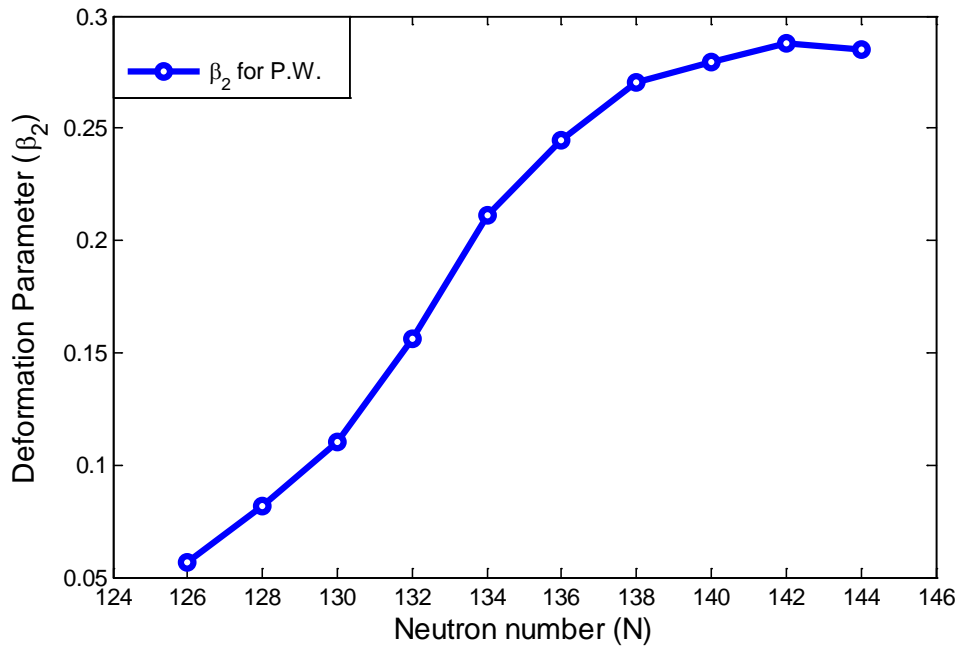


Figure (3-25): Represents the relationship of Deformation Parameter (β_2) value of the Present Work as a function of neutron Number for the ($_{90}\text{Th}$) Isotopes.

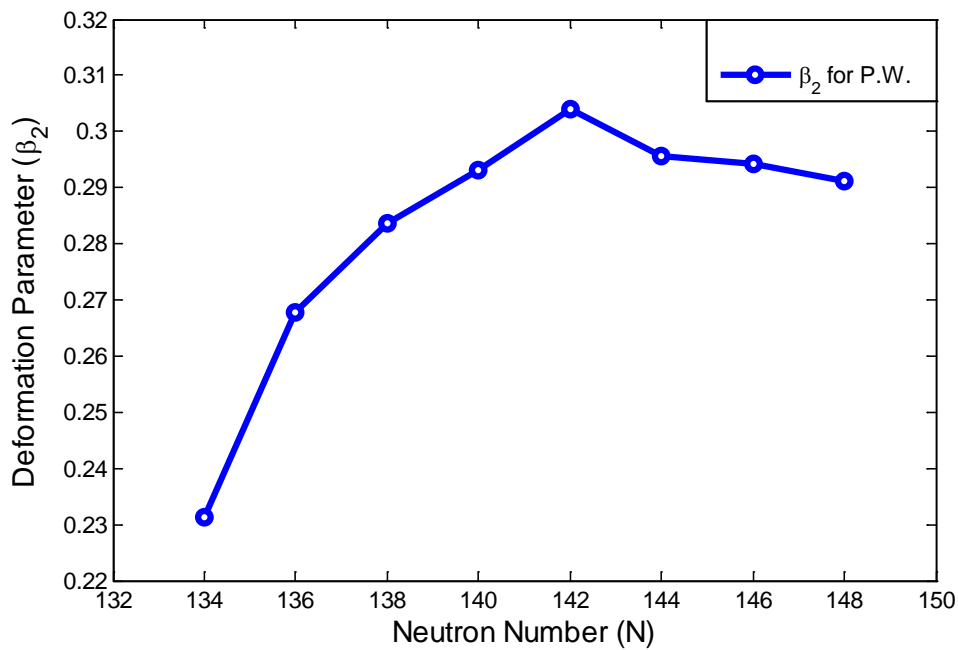


Figure (3-26): Represents the relationship of Deformation Parameter (β_2) value of the Present Work as a function of neutron Number for the ($_{92}\text{U}$) Isotopes.

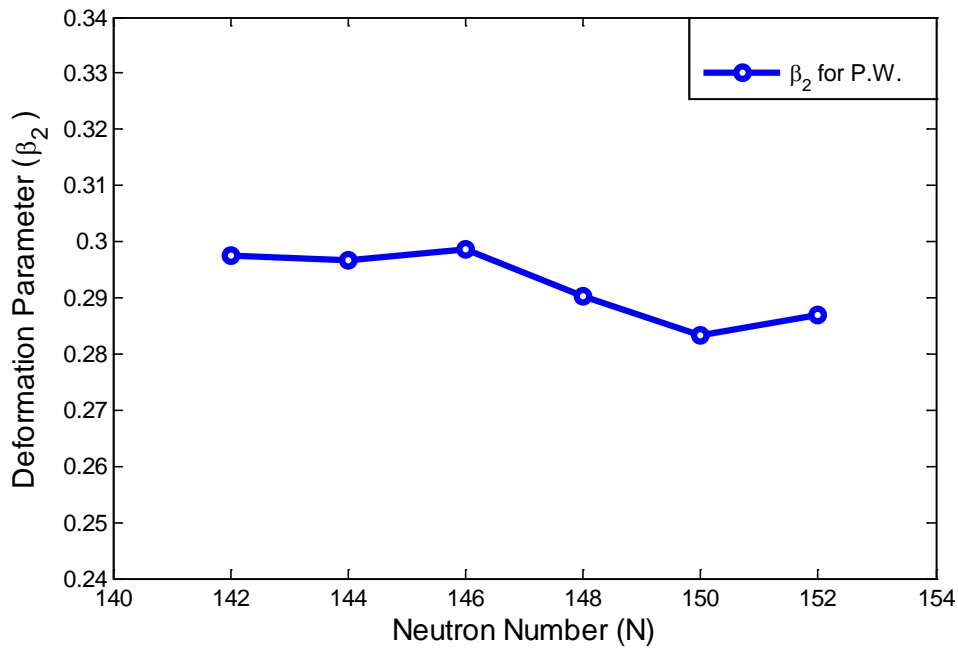


Figure (3-27): Represents the relationship of Deformation Parameter (β_2) value of the Present Work as a function of neutron Number for the ($_{94}\text{Pu}$) Isotopes.

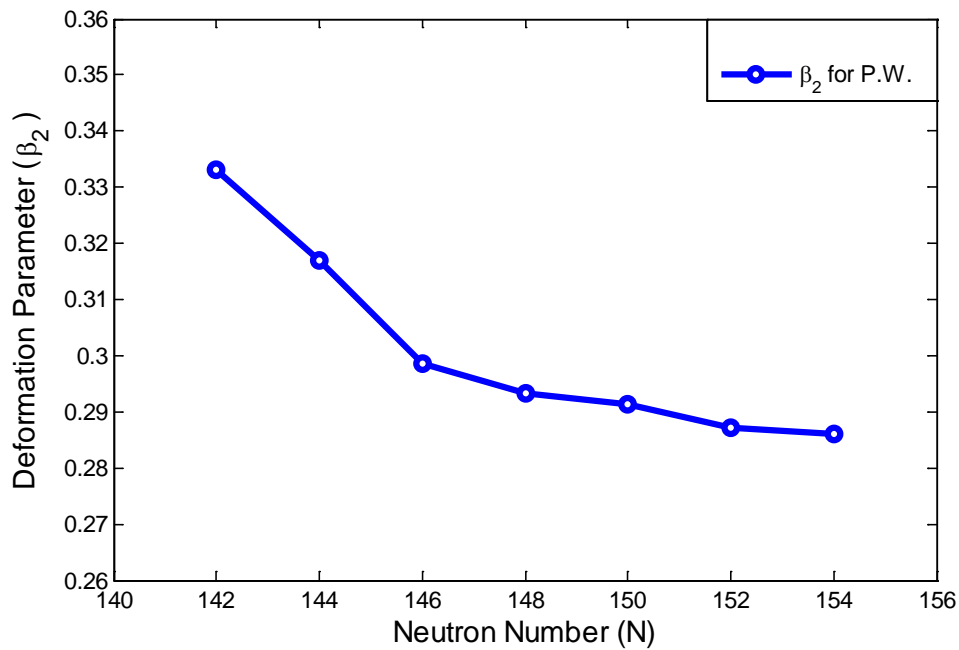


Figure (3-28): Represents the relationship of Deformation Parameter (β_2) value of the Present Work as a function of neutron Number for the ($_{96}\text{Cm}$) Isotopes.

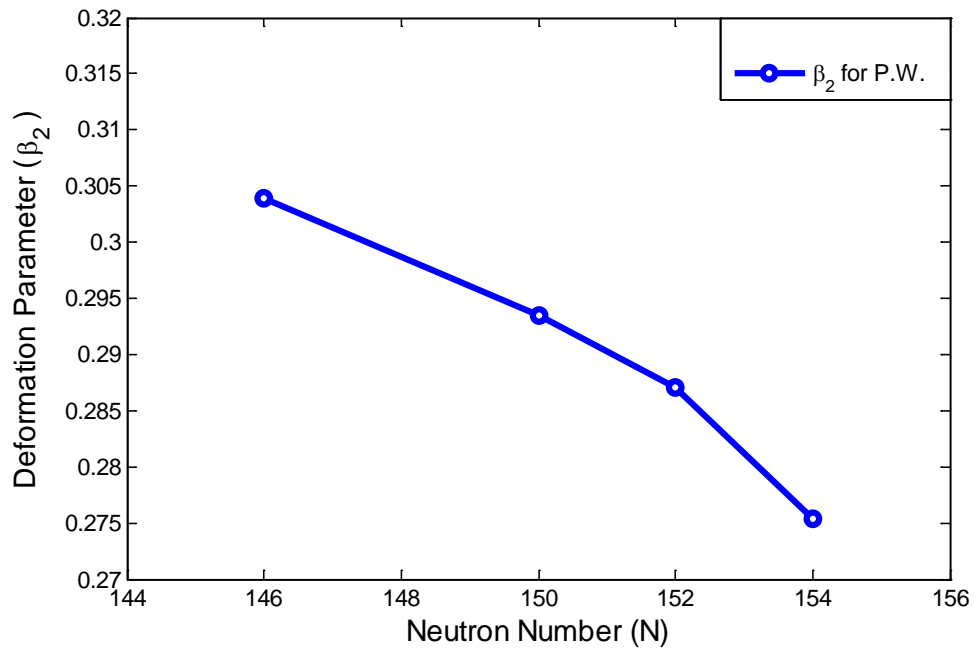


Figure (3-29): Represents the relationship of Deformation Parameter (β_2) value of the Present Work as a function of neutron Number for the ($_{98}\text{Cf}$) Isotopes.

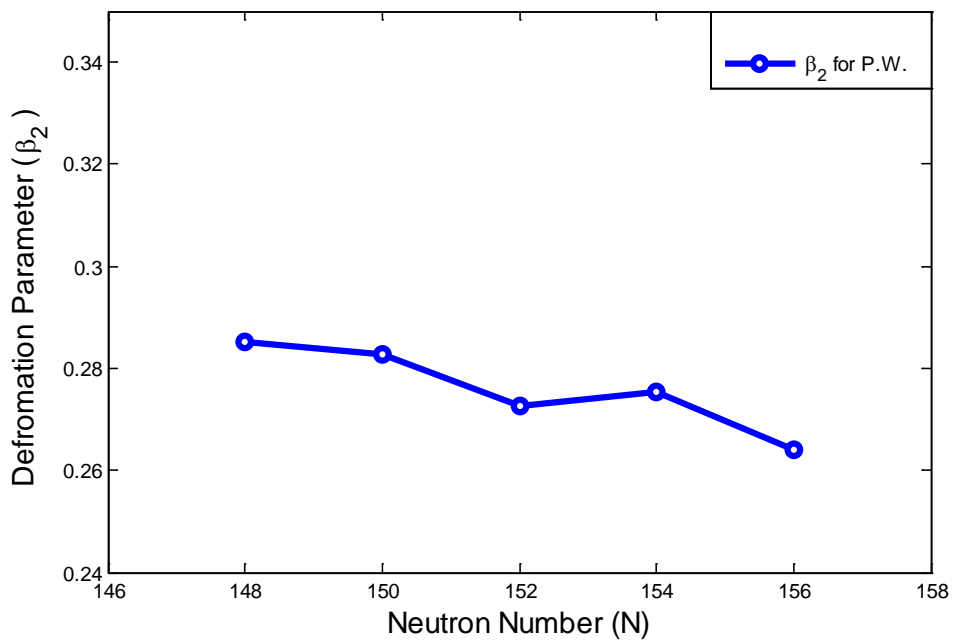


Figure (3-30): Represents the relationship of Deformation Parameter (β_2) value of the Present Work as a function of neutron Number for the ($_{100}\text{Fm}$) Isotopes.

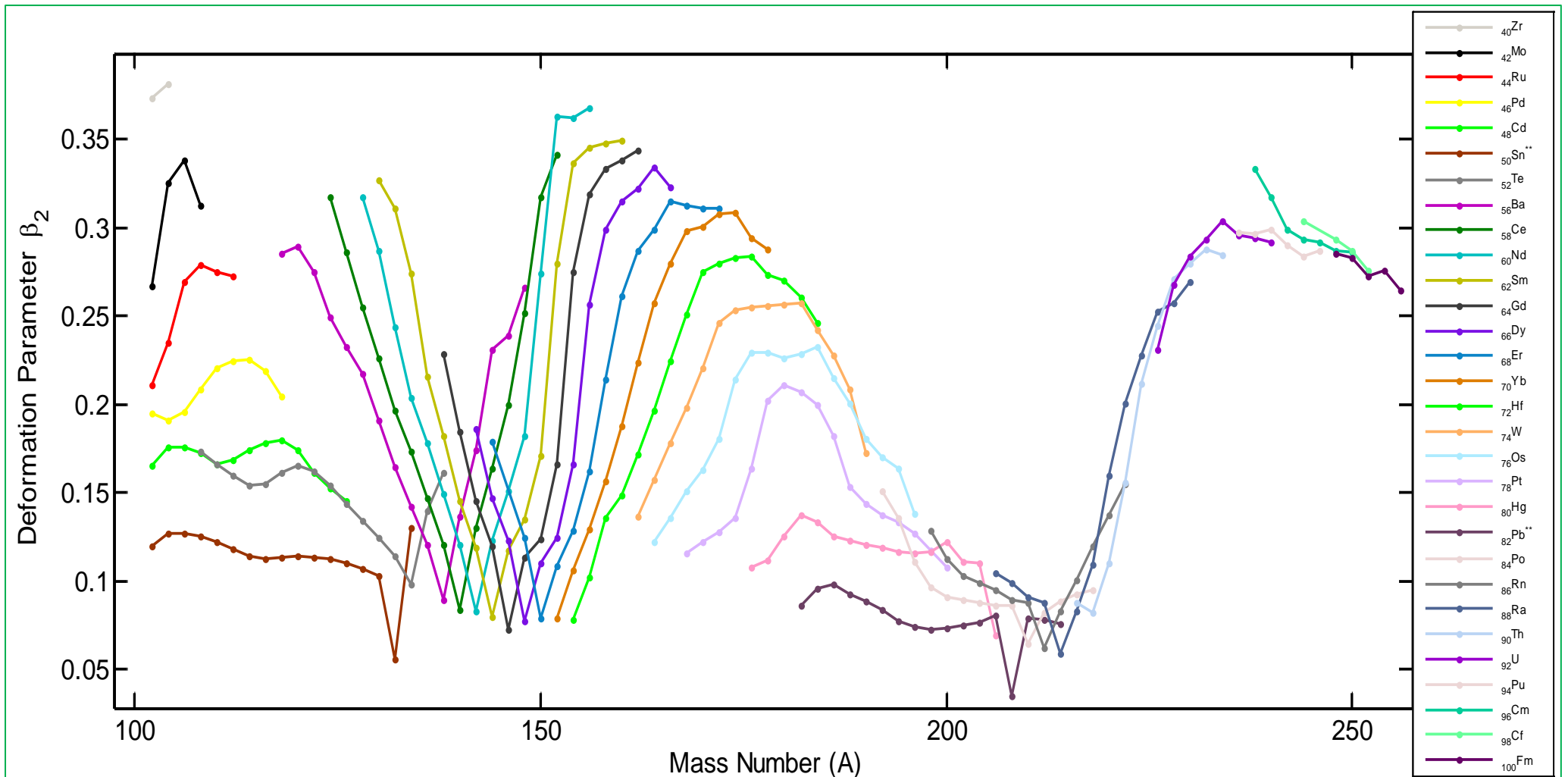


Figure (3-31): the relationship of deformation parameters β_2 for (30) elements as a function of mass numbers A

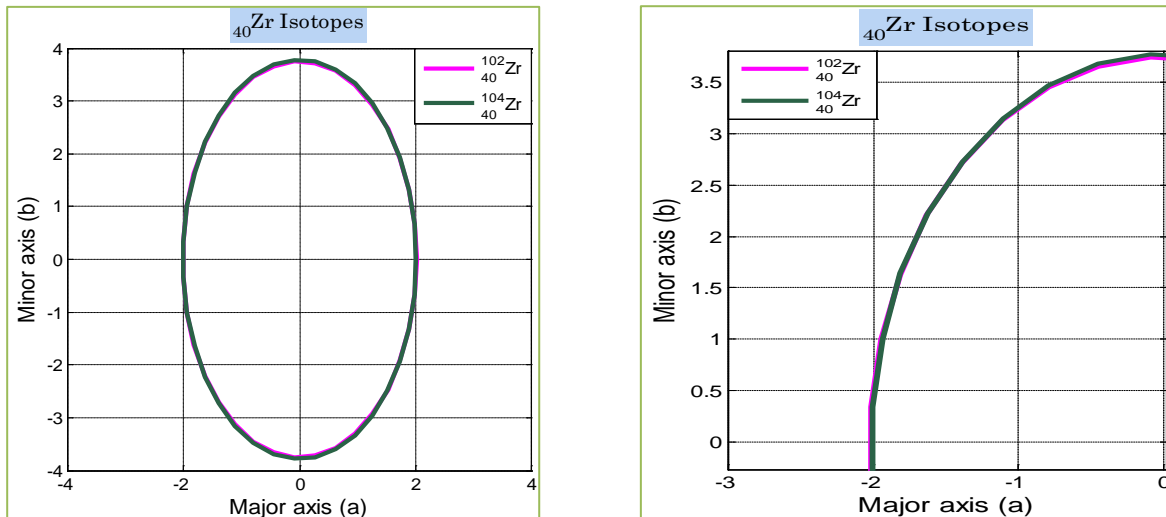


Figure (3-32): Shapes of axially symmetric quadrupole deformation for ${}_{40}\text{Zr}$ isotopes from major a and minor b axes.

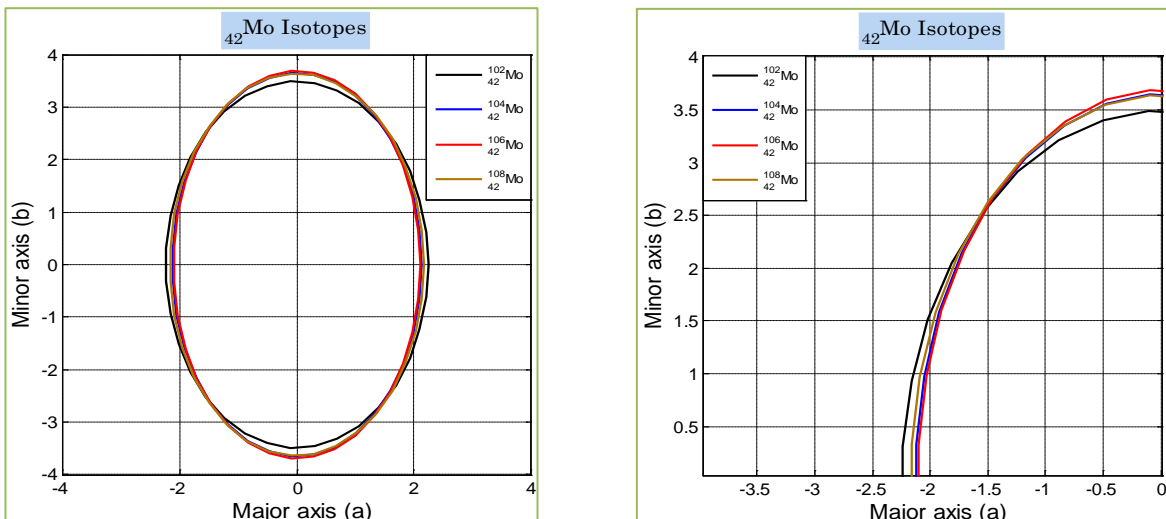


Figure (3-33): Shapes of axially symmetric quadrupole deformation for ${}_{42}\text{Mo}$ isotopes from major a and minor b axes.

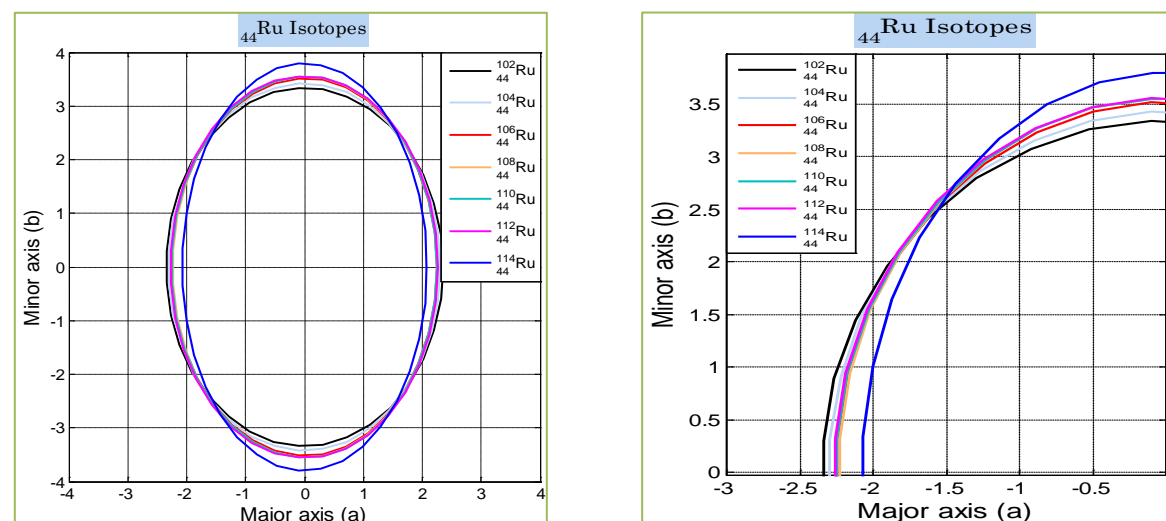


Figure (3-34): Shapes of axially symmetric quadrupole deformation for ${}_{44}\text{Ru}$ isotopes from major a and minor b axes.

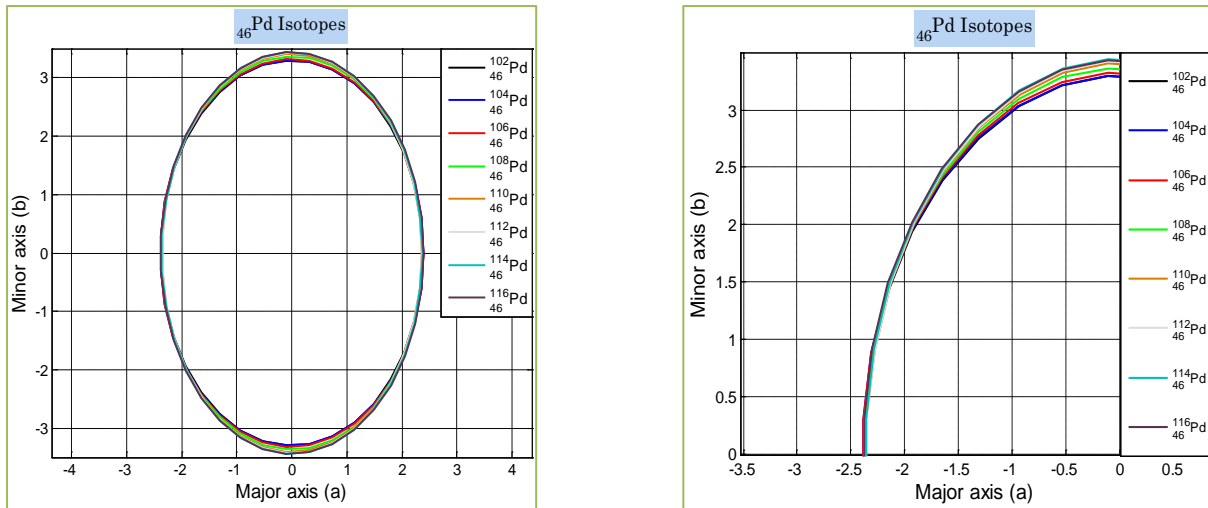


Figure (3-35): Shapes of axially symmetric quadrupole deformation for ${}_{46}\text{Pd}$ isotopes from major a and minor b axes.

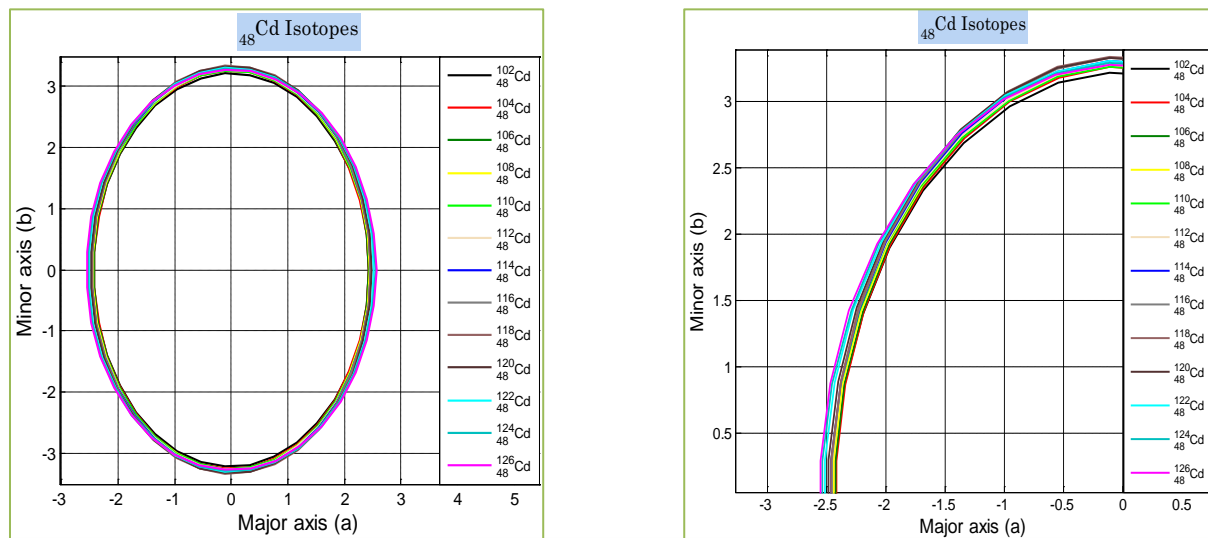


Figure (3-36): Shapes of axially symmetric quadrupole deformation for ${}_{48}\text{Cd}$ isotopes from major a and minor b axes.

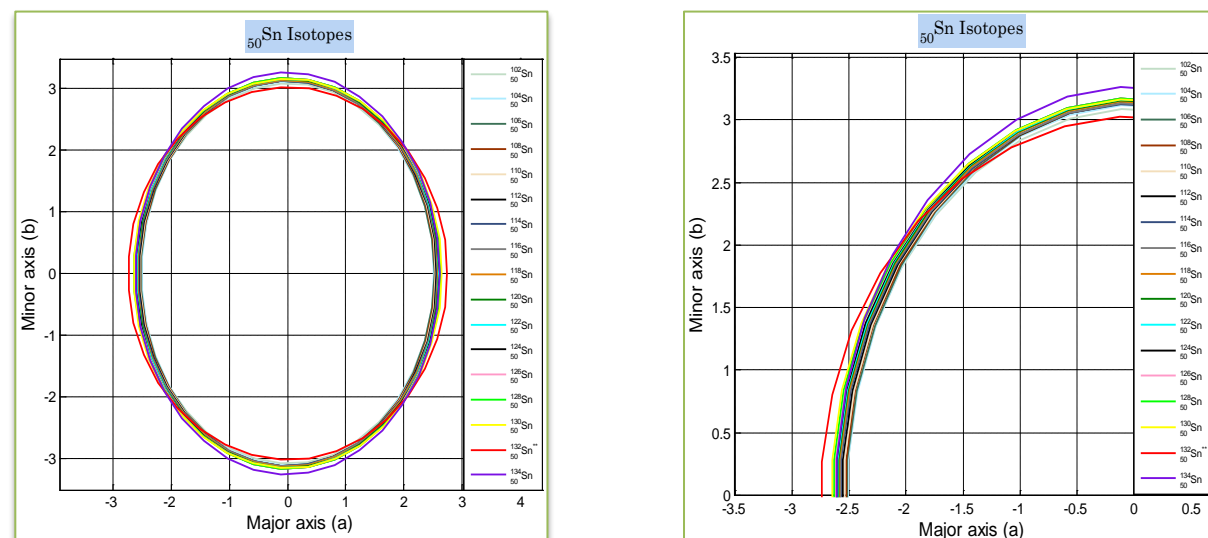


Figure (3-37): Shapes of axially symmetric quadrupole deformation for ${}_{50}\text{Sn}$ isotopes from major a and minor b axes.

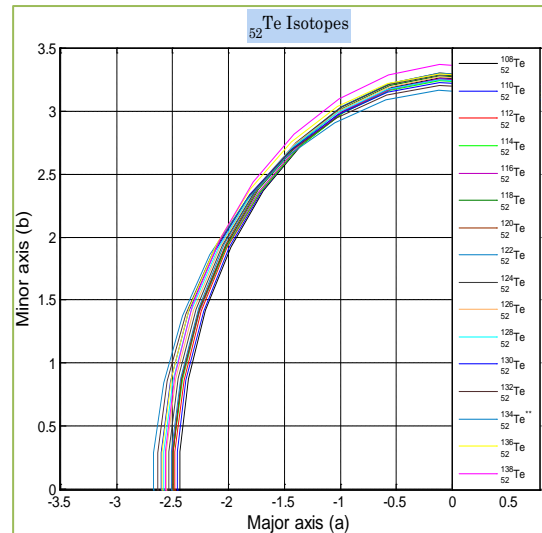
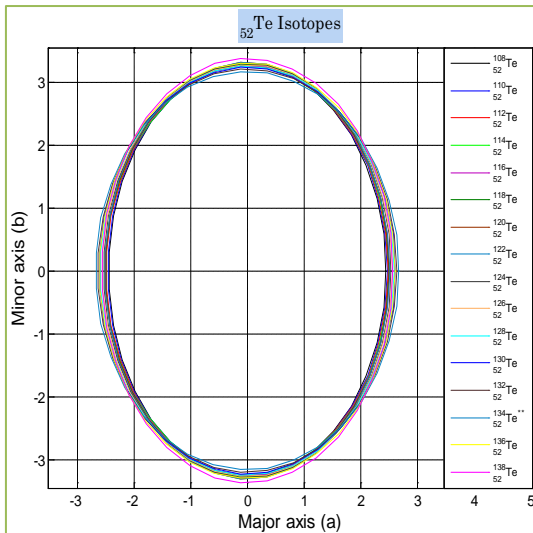


Figure (3-38): Shapes of axially symmetric quadrupole deformation for $_{52}\text{Te}$ isotopes isotope from major a and minor b axes.

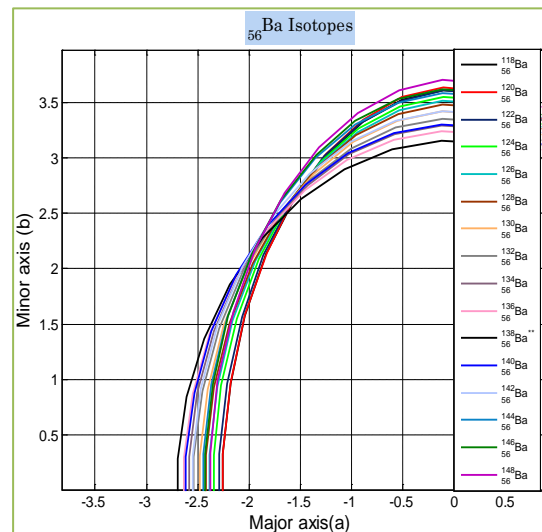
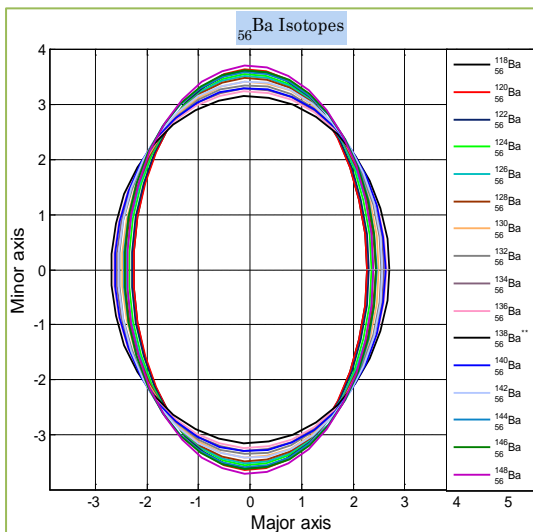


Figure (3-39): Shapes of axially symmetric quadrupole deformation for $_{56}\text{Ba}$ isotopes from major a and minor b axes.

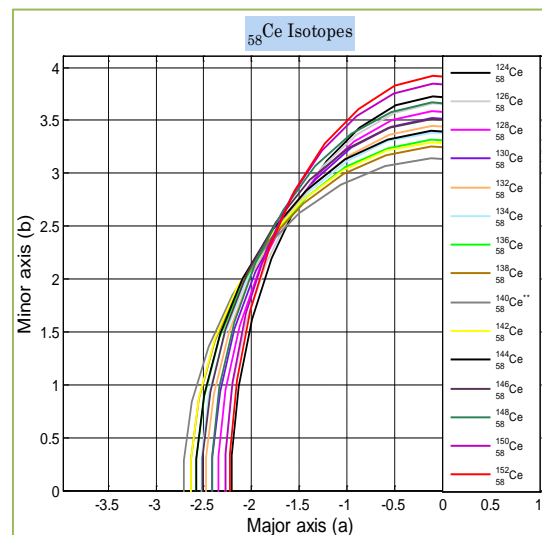
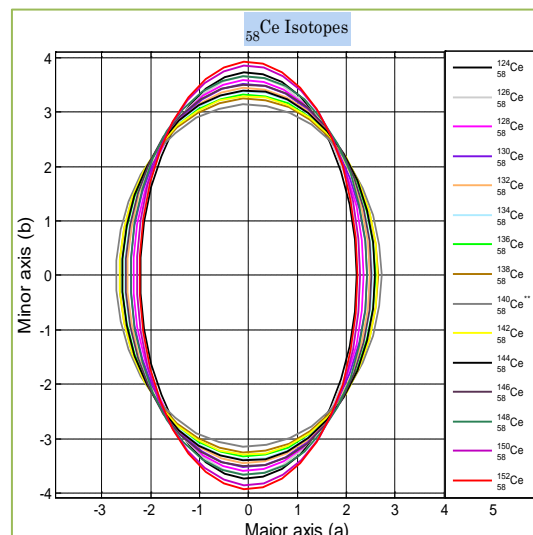


Figure (3-40): Shapes of axially symmetric quadrupole deformation for $_{58}\text{Ce}$ isotopes from major a and minor b axes.

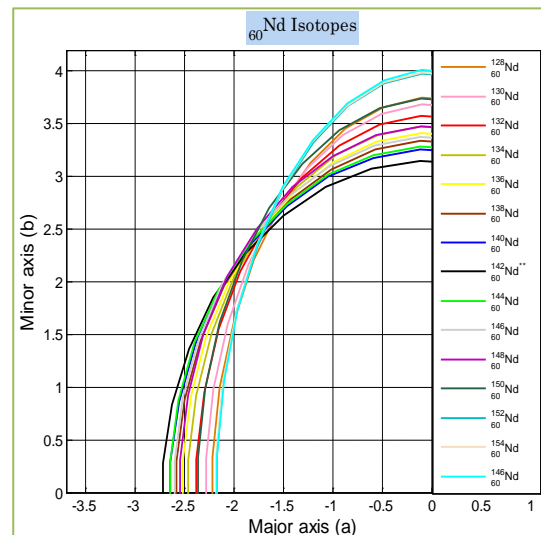
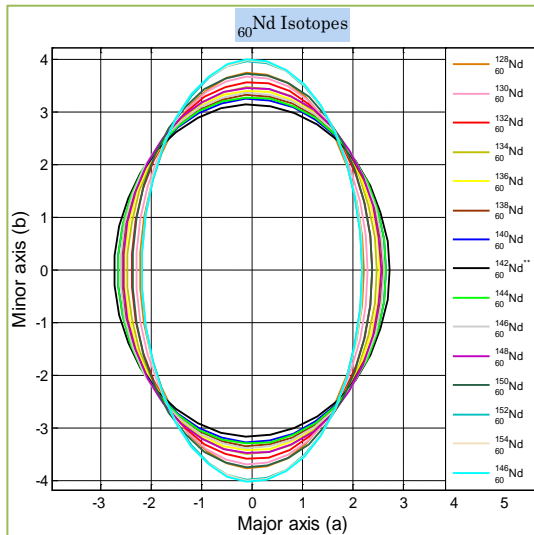


Figure (3-41): Shapes of axially symmetric quadrupole deformation for ${}_{60}\text{Nd}$ isotopes from major a and minor b axes.

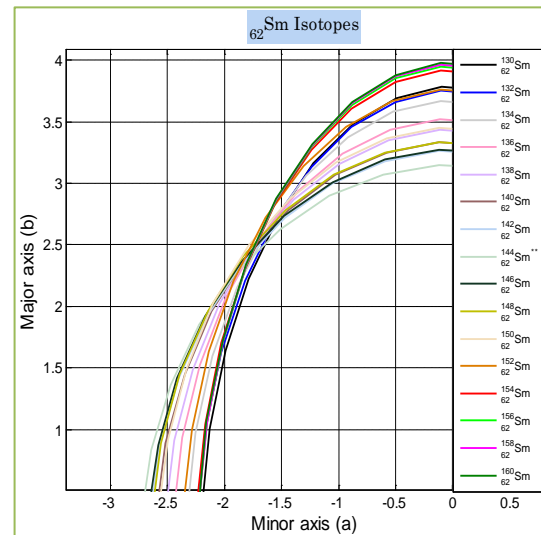
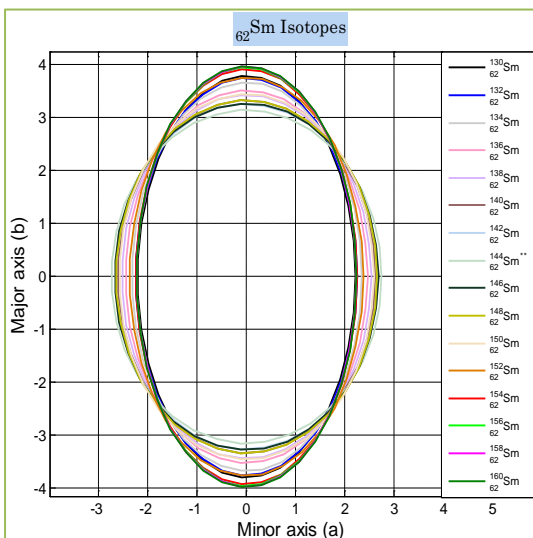


Figure (3-42): Shapes of axially symmetric quadrupole deformation for ${}_{62}\text{Sm}$ isotopes from major a and minor b axes.

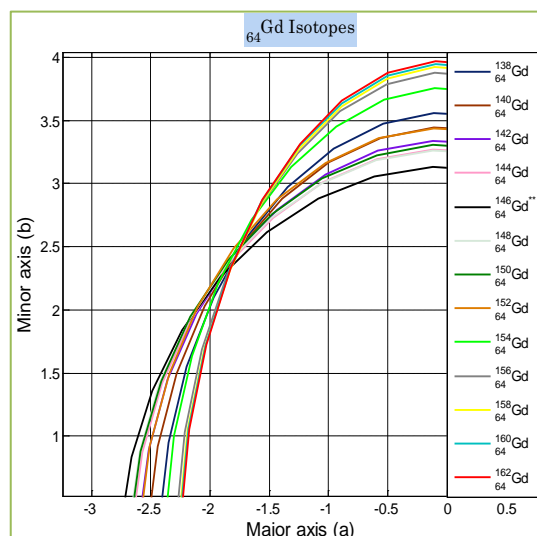
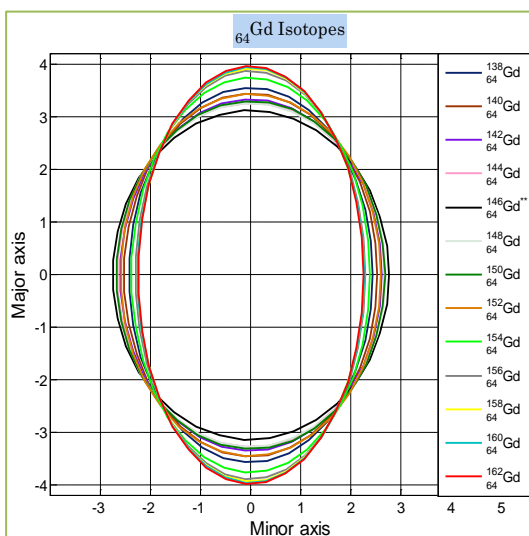


Figure (3-43): Shapes of axially symmetric quadrupole deformation for ${}_{64}\text{Gd}$ isotopes from major a and minor b axes.

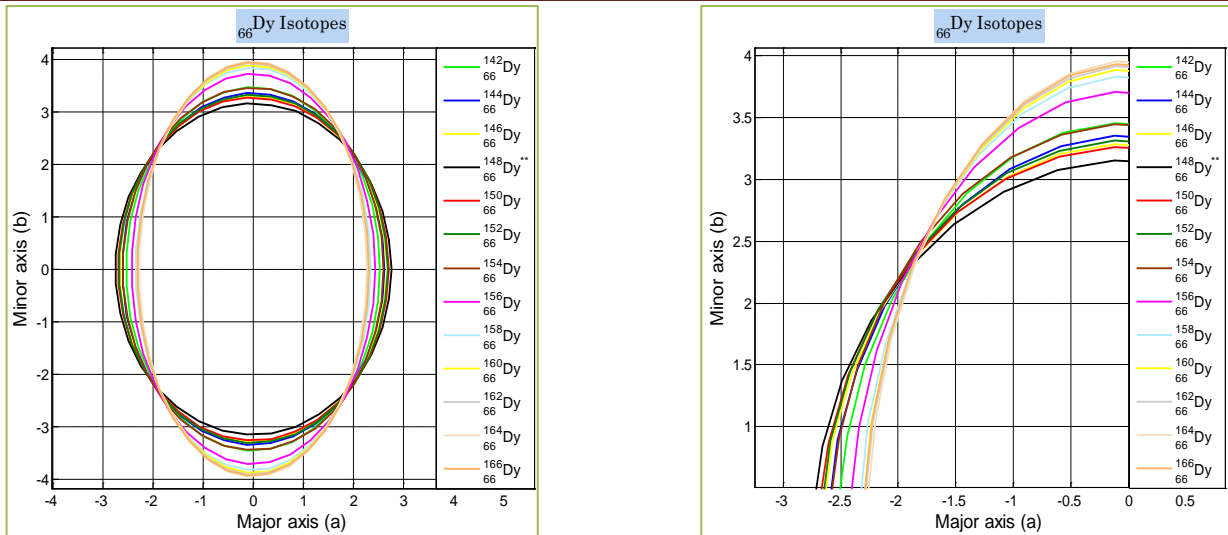


Figure (3-44): Shapes of axially symmetric quadrupole deformation for ^{66}Dy isotopes from major a and minor b axes.

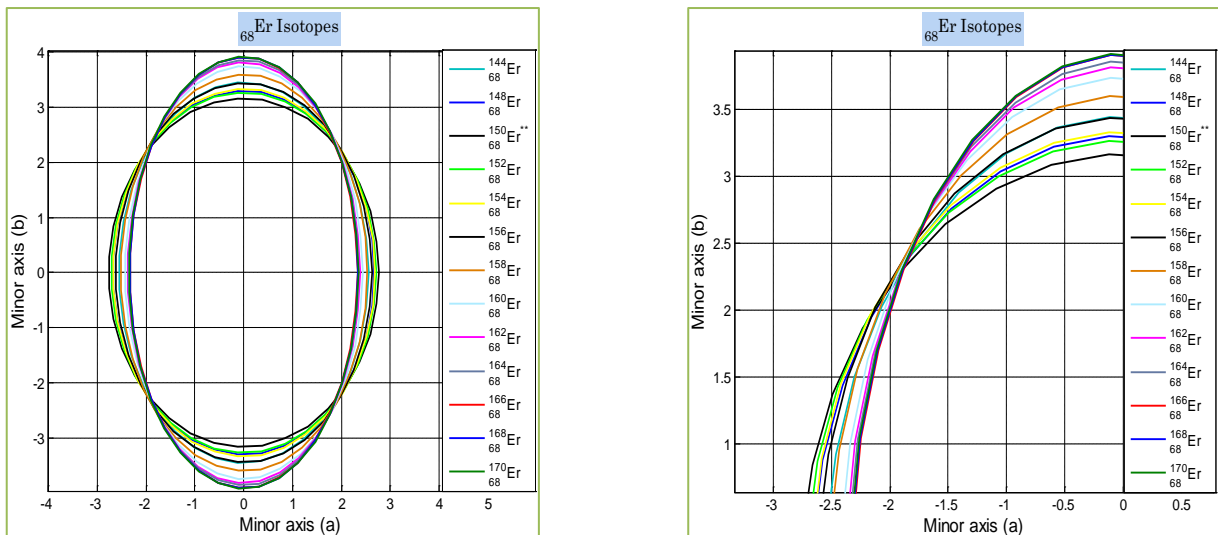


Figure (3-45): Shapes of axially symmetric quadrupole deformation for ^{68}Er isotopes from major a and minor b axes.

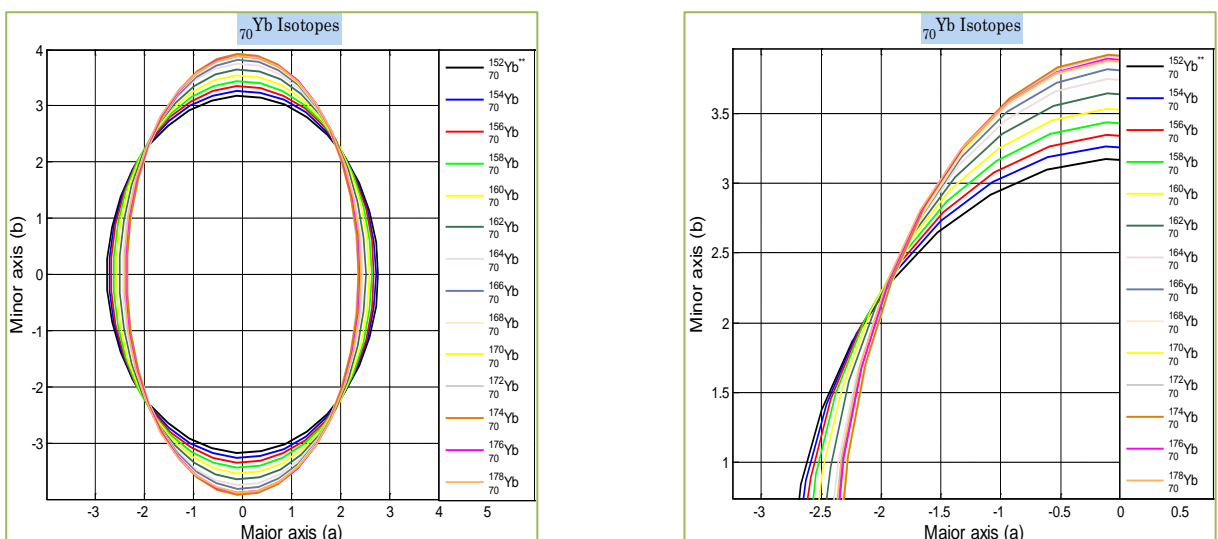


Figure (3-46): Shapes of axially symmetric quadrupole deformation for ^{70}Yb isotopes from major a and minor b axes.

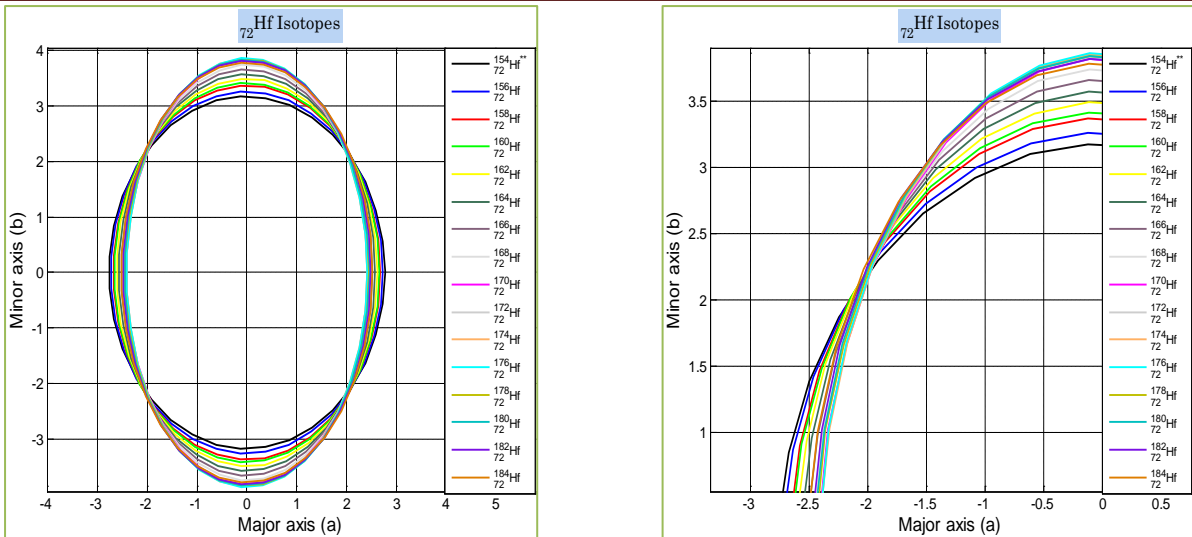


Figure (3-47): Shapes of axially symmetric quadrupole deformation for ${}_{72}\text{Hf}$ isotopes from major a and minor b axes.

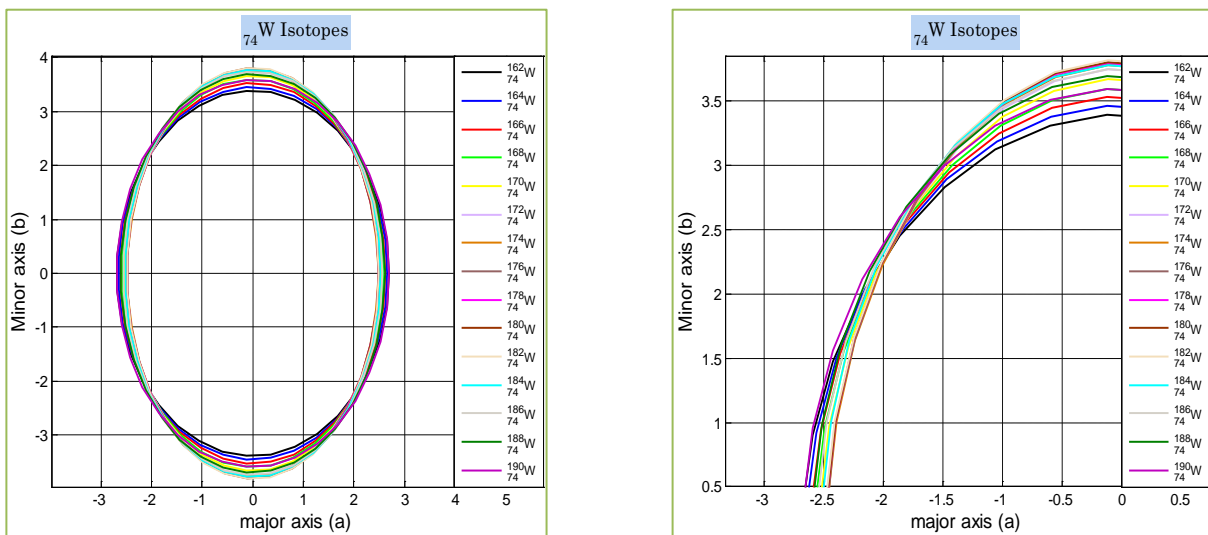


Figure (3-48): Shapes of axially symmetric quadrupole deformation for ${}_{74}\text{W}$ isotopes from major a and minor b axes.

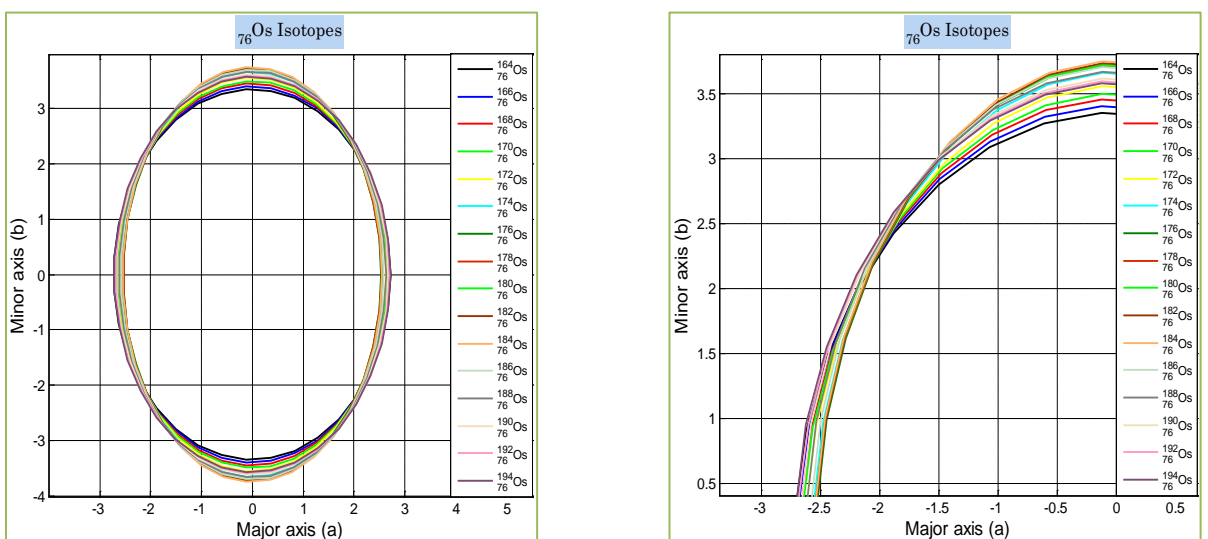


Figure (3-49): Shapes of axially symmetric quadrupole deformation for ${}_{76}\text{Os}$ isotopes from major a and minor b axes.

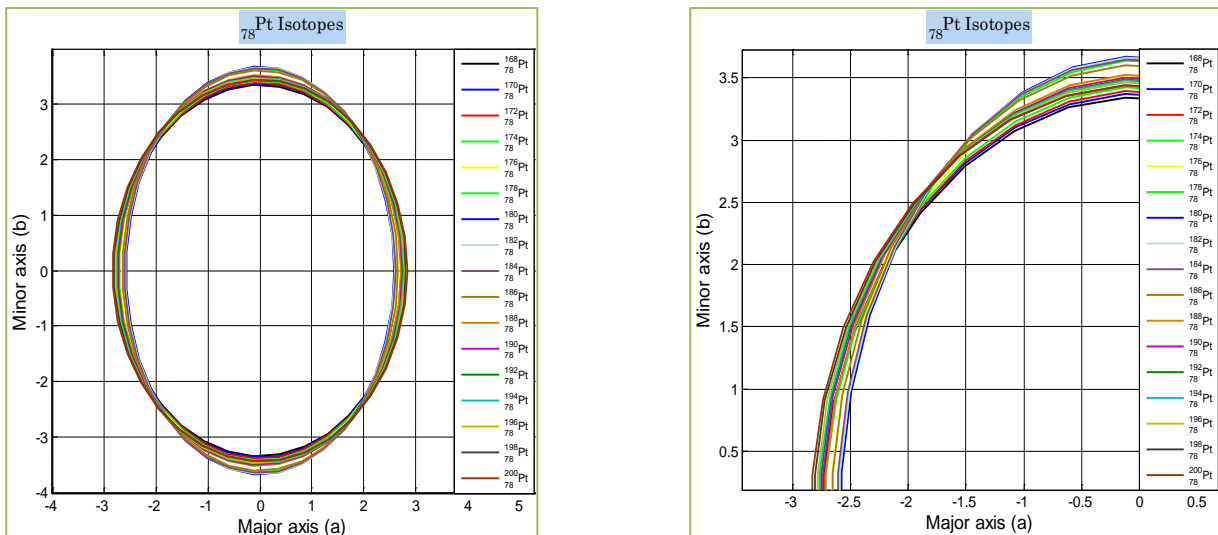


Figure (3-50): Shapes of axially symmetric quadrupole deformation for $_{78}\text{Pt}$ isotopes from major a and minor b axes.

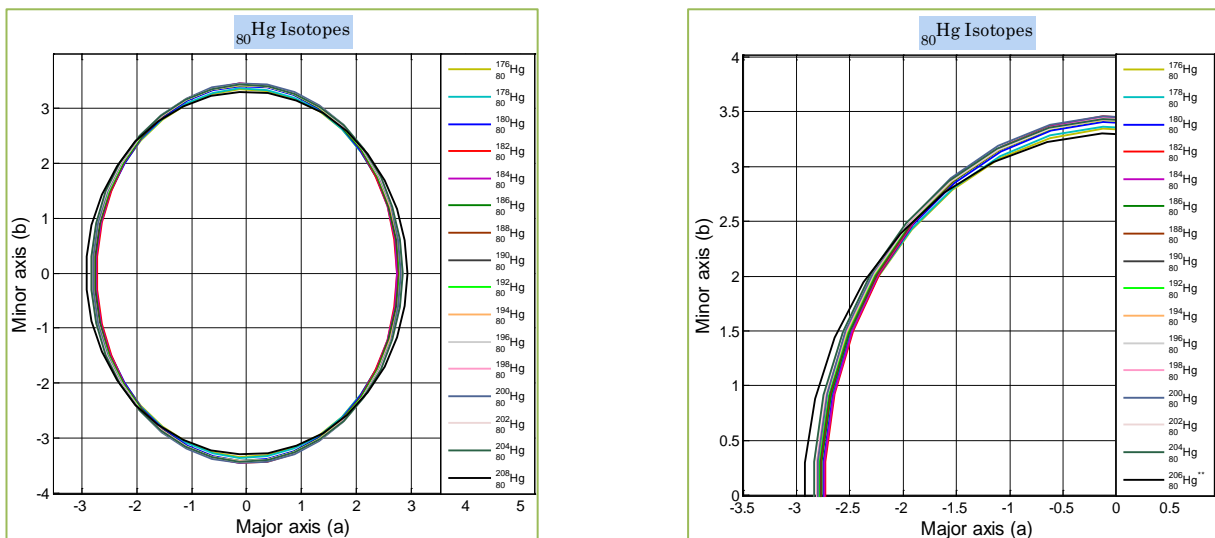


Figure (3-51): Shapes of axially symmetric quadrupole deformation for $_{80}\text{Hg}$ isotopes from major a and minor b axes.

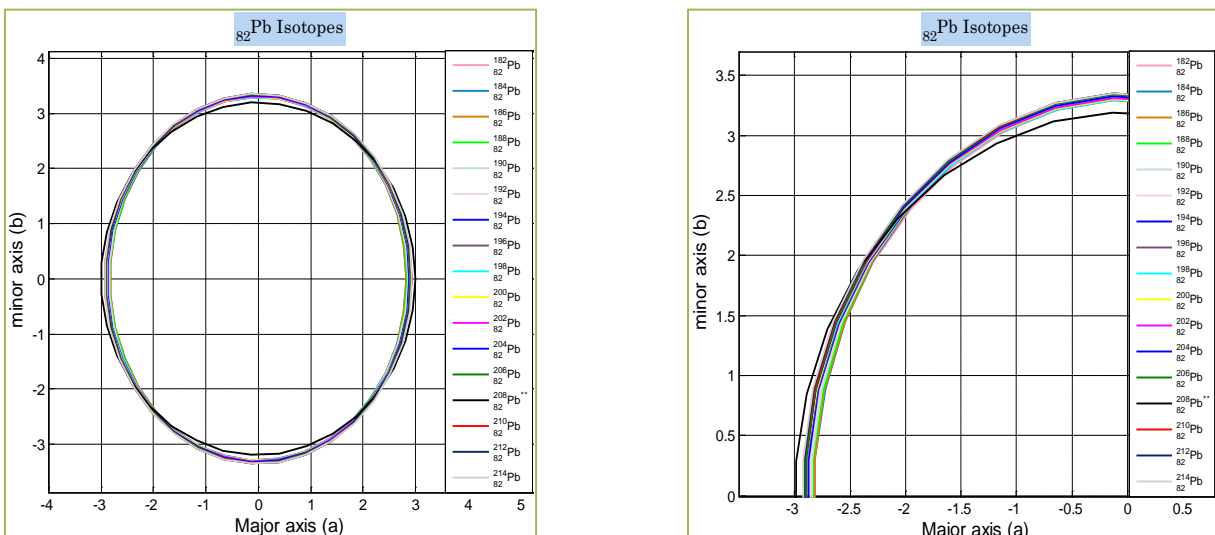


Figure (3-52): Shapes of axially symmetric quadrupole deformation for $_{82}\text{Pb}$ isotopes from major a and minor b axes.

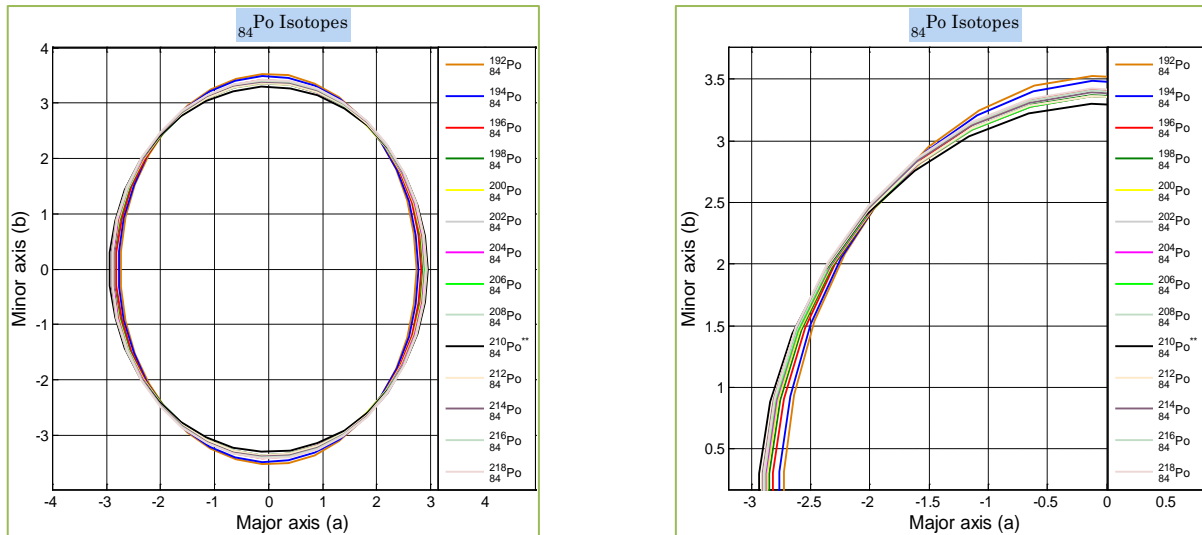


Figure (3-53): Shapes of axially symmetric quadrupole deformation for ^{84}Po isotopes from major a and minor b axes.

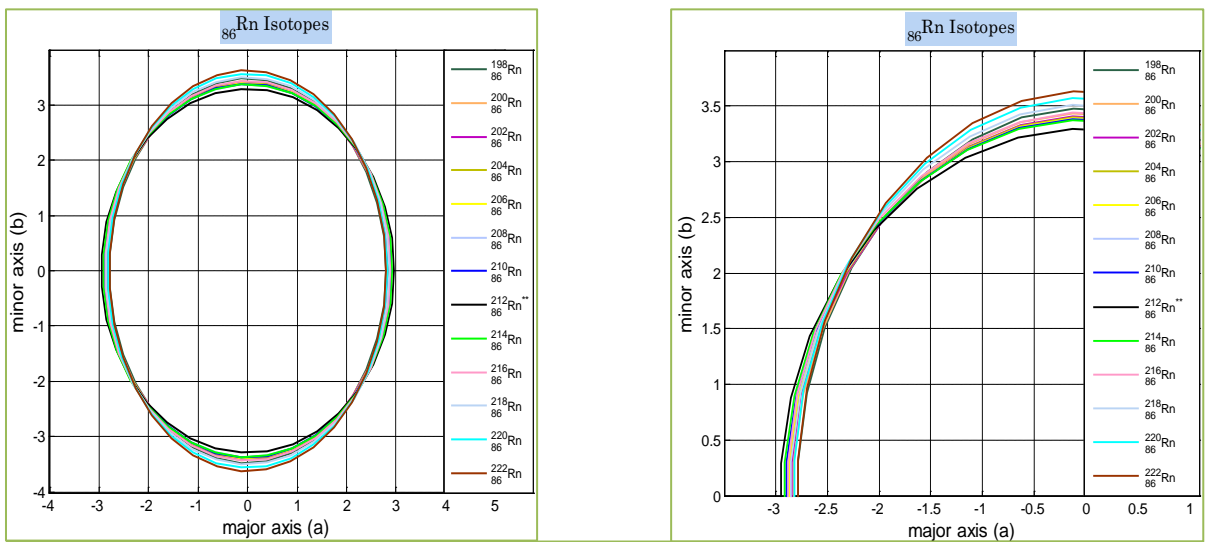


Figure (3-54): Shapes of axially symmetric quadrupole deformation for ^{86}Rn isotopes from major a and minor b axes.

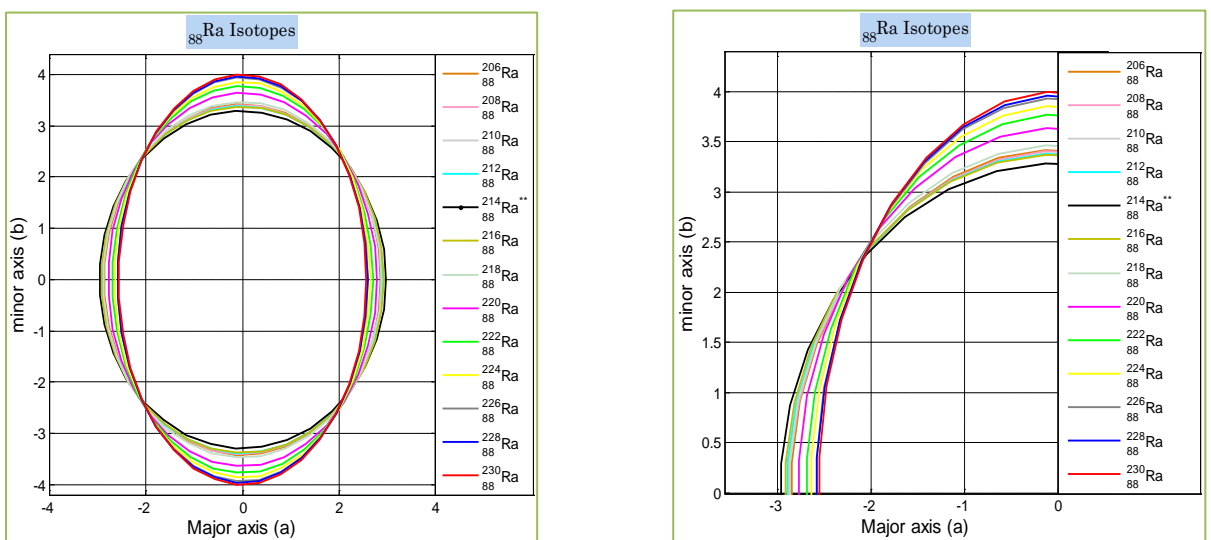


Figure (3-55): Shapes of axially symmetric quadrupole deformation for ^{88}Ra isotopes from major a and minor b axes.

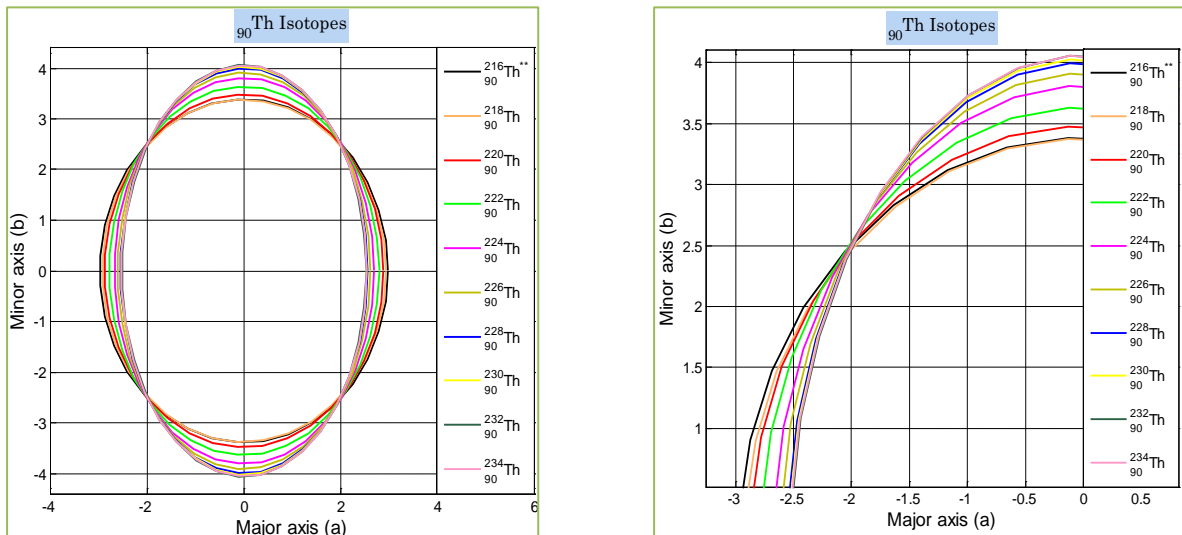


Figure (3-56): Shapes of axially symmetric quadrupole deformation for ${}_{90}\text{Th}$ isotopes from major a and minor b axes.

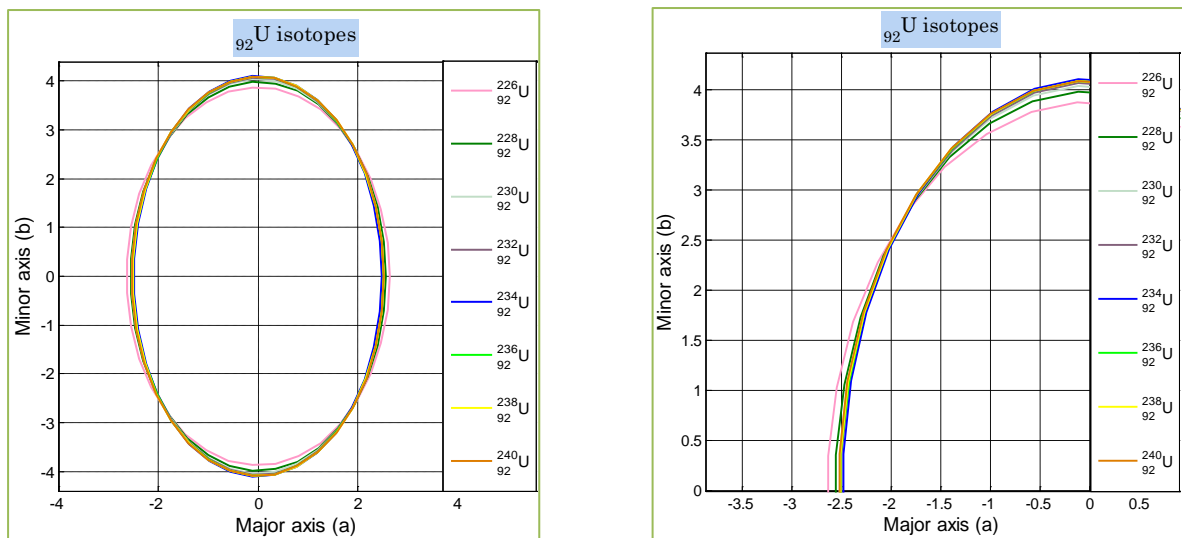


Figure (3-57): Shapes of axially symmetric quadrupole deformation for ${}_{92}\text{U}$ isotopes from major a and minor b axes.

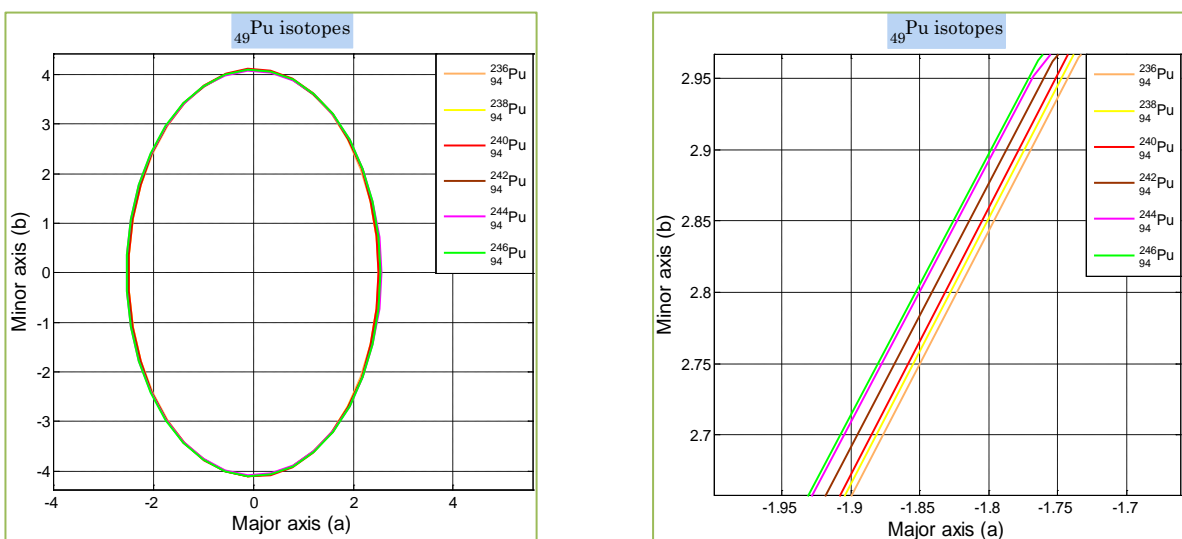


Figure (3-58): Shapes of axially symmetric quadrupole deformation for ${}_{94}\text{Pu}$ isotopes from major a and minor b axes.

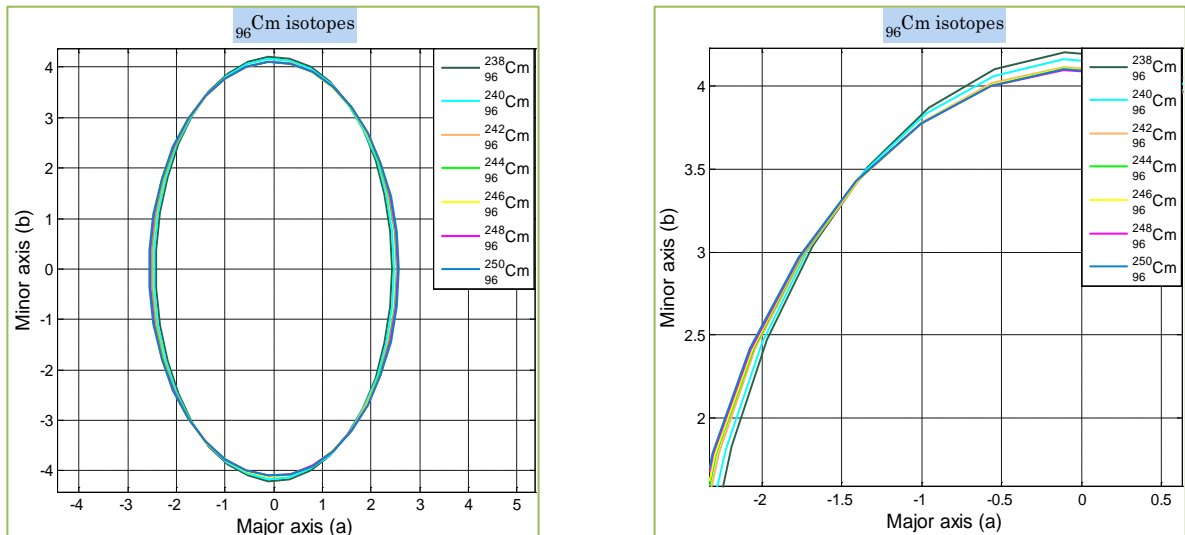


Figure (3-59): Shapes of axially symmetric quadrupole deformation for ${}_{96}\text{Cm}$ isotopes from major a and minor b axes.

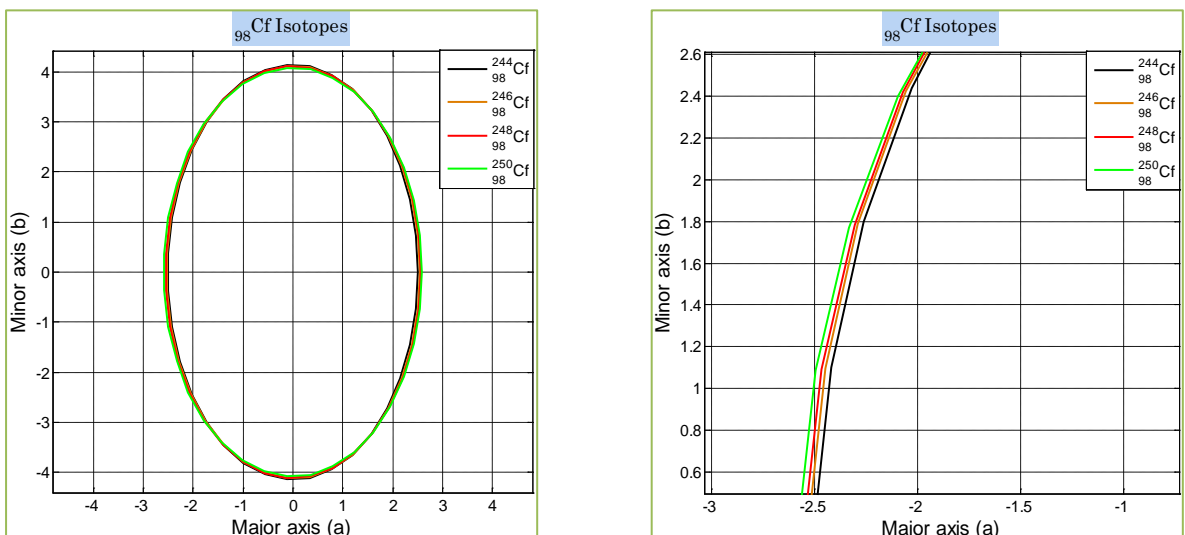


Figure (3-60): Shapes of axially symmetric quadrupole deformation for ${}_{98}\text{Cf}$ isotopes from major a and minor b axes.

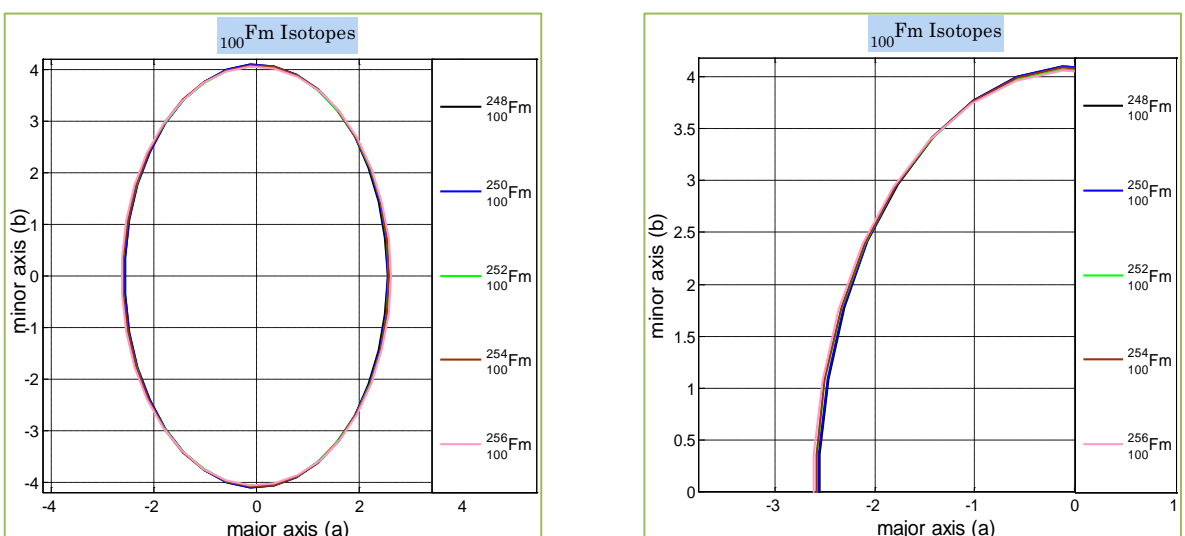
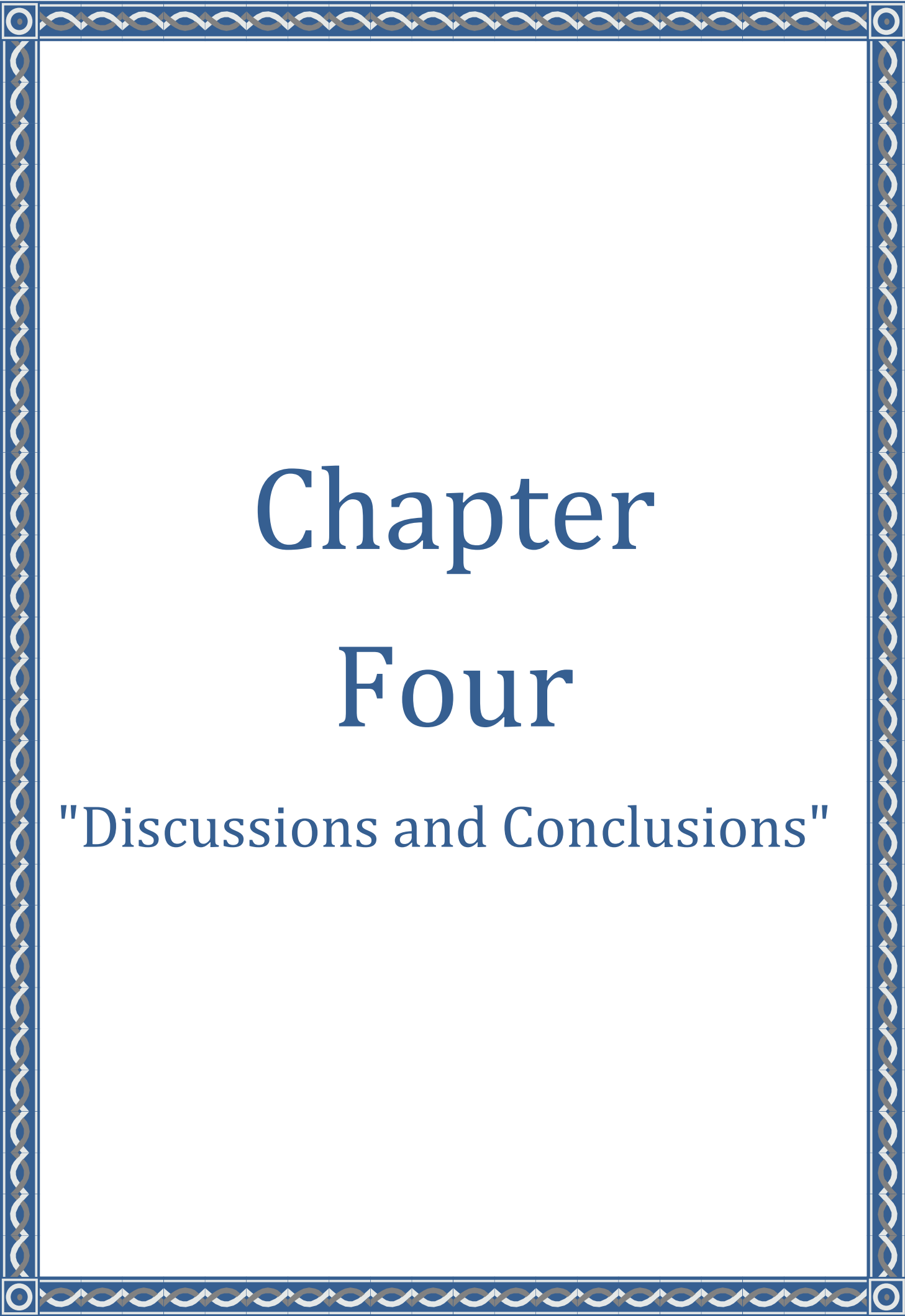


Figure (3-61): Shapes of axially symmetric quadrupole deformation for ${}_{100}\text{Fm}$ isotopes from major a and minor b axes.



Chapter Four

"Discussions and Conclusions"

4-1 Introduction:

The present study focuses on the studying of even- even nuclei forms for elements with mass numbers greater than 100, which included the study of deformation parameters β_2 and δ derived from the $B(E2) \uparrow$ and Q_0 values, respectively. The diversity of nuclei forms for selected elements and their differences were observed by drawing two-dimensional shapes of single element isotopes, in addition to drawing three-dimensional shapes (axially symmetric) to distinguish between them by using semi-major and semi minor (a, b) axes.

It is also found in these nuclei (which most of them show a collective behavior), the energy of the first excited state (2^+) begins to decrease as a sort of smoothly when the mass number A increases except for regions near closed shells where the energy values of first excited states are relatively high and the nuclei are more stable and more spherical, as suggested by Ref. [34].

Far away from closed shells, the nucleons outside the core polarize the whole or partial vibrations of the core to one direction and permanent deformation of the nucleus can be acquired. When adding more nucleons outside the closed shell, the polarization effect grows, and the notice quadrupole moments can be illustrated, as suggested by Ref. [43].

From observation the values of the intrinsic electric quadrupole moments (Q_0) of selected elements, tables from (3-1) to(3-30), we found that these values vary according to their mass numbers which mean of non-spherical charge distribution, and when approaching to the magic numbers of protons and/or neutrons (50,82,126), these values become less than those for the other isotopes of the same element, in other words the values of deformation parameter δ become as low as possible and therefore the nucleus of this isotope is more stable and the charges are spherically distributed compared to other isotopes for the same element. On the other hand, we also found when the mass numbers are less than 150 ($A < 150$), these values seem to be less than those with mass number between 150 and 190 ($150 < A < 190$), this is belonged to collective behavior (vibrational

and rotational) of nucleons which is the single particle model cannot explain the large observed quadrupole moments.

Also for the comparison purpose, the reduced electric transition $B(E2) \uparrow$ values of the present work and the predicted values of SSANM show a little variation between these results, because our present work is based on using of the Global Best Fit (GBF) equation when compared with the SSANM values of Ref. [13]. This simple difference is reflected in the values of the deformation parameters β_2 derived from $B(E2) \uparrow$ values, as shown in the tables from (3-1) to (3-30).

Also From observable values of the root mean square charge radii $\langle r^2 \rangle^{1/2}$, table (3-31) to (3-60), we found that these values increased as the mass number A increases. For comparison purposes, it was found that the calculated values of present work $\langle r^2 \rangle^{1/2}$ correspond well to the experimental values of $\langle r^2 \rangle^{1/2}$ in Ref. [51].

Also, the values of (ΔR) (the difference between the semi-major and semi-minor axes (a, b)) were calculated using three different methods, tables (3-32) to (3-60), and it was found that these results were fairly close.

What has been mentioned above can be explained in detail in the following:

4-1-1 Zirconium isotopes $^{102-104}_{40}\text{Zr}$

From table (3-1), we observe that the values of the deformation parameters β_2 are (0.3733) for $^{102}_{40}\text{Zr}$ and (0.3808) for $^{104}_{40}\text{Zr}$, These values are considered very high when compared with the values of the other deformation parameters, and this is due to several factors: the energies of the first excites 2^+ for these two isotopes ($E_\gamma=151.77, 140.3$ keV) respectively, are small if compared with those of magic numbers. The numbers of nucleons in the sub-shell out of closed shell are far from the magic numbers ($Z = 40, N = 62,64$) which means the gaps between the shells are low spaces, this will lead to increase the transition of nucleons between these states which in turn increased the values of the reduced electric transition. Also the high values of electric quadrupole moments are due to

the non-spherical charge distribution. All these factors encourage the nucleus to be unstable and in ellipsoidal and permanently highly deformed shapes especially for $^{104}_{40}\text{Zr}$ as shown in the figures (3-32) and Appendix (A-1). Also figure (3-1) illustrates the relationship between deformation parameters as a function of the neutron numbers.

4-1-2 Molybdenum isotopes $^{102-108}_{42}\text{Mo}$:

From table (3-2) we observe that the maximum value of deformation Parameter is ($\beta_2 = 0.3378$) corresponds to the value of the first excited energy 2^+ ($E_\gamma = 171.548$ keV) for $^{106}_{42}\text{Mo}$, and the minimum value of deformation ($\beta_2 = 0.2670$ keV) corresponds to the value of the first excited energy 2^+ ($E_\gamma = 296.597$ keV) for $^{102}_{42}\text{Mo}$. The other deformation values of other isotopes vary between these two values. This is due to the fact that the lower of first excited state energy 2^+ , the greater the reduced transition probability $B(E2) \uparrow$. Thus, the value of deformation β_2 increases. As well as the values of the deformation parameters δ of the same isotopes, figure (3-2) explains this behavior. Also from table (3-2) we note that increasing number of nucleons outside the closed shell leads to increase polarization effect and thus increasing the electric quadrupole moments Q_0 which result from the non-spherical charge distribution and then increase the deformation ratio of the nucleus as shown in the figure (3-33).

4-1-3 Ruthenium Isotopes $^{102-114}_{44}\text{Ru}$:

Table (3-3) shows that the values of the first excited state energy 2^+ will decrease gradually with the increase of mass numbers A , (the gaps between the ground and first excited states will be decreased with increase of A) so that the $B(E2) \uparrow$ will increase and values of deformation parameters β_2 seem to be increased too. This is evident from the fact that the lowest deformation value is belongs to $^{102}_{44}\text{Ru}$ and equals to ($\beta_2 = 0.2110$) with ($E_\gamma = 475.079$ keV) while the highest deformation value is belongs to $^{110}_{44}\text{Ru}$ and equals ($\beta_2 = 0.2748$) with ($E_\gamma = 240.71$ keV). This behavior is clearly in the figure (3-3) which represents

the relationship between the deformation parameters as a function of neutron numbers

This belongs to the fact that nucleus with few nucleon outside closed shall or sub-shall closures at 6, 40, 58 and elsewhere will be sub-stable and treated in terms of a model based on vibration about spherical equilibrium shape. In other word some nuclei are not a good approximation to assume spherical symmetry and that these nuclei must be considered to have non-spherical mass distribution as suggested by Ref. [52]. Shapes of these nuclei are shown in figures (3-34) and appendix (A-3).

4-1-4 Palladium isotopes $^{102-118}_{46}\text{Pd}$:

Table (3-4) shows that the minimum value of ($\beta_2 = 0.1913$) corresponds to the ($E_\gamma = 555.81$ keV) for $^{104}_{46}\text{Pd}$. This is due to the fact that the atomic number is ($Z = 46$) less than (4) nucleons from magic number 50 (Semi-magic) while the number of neutrons ($N = 58$) is more than the magic number with (8); therefore this isotope is more stable than others and thus less deformed. As the number of neutrons increases, the energies of the first excited states 2^+ will decrease (decreasing the gaps between the levels) and the reduced electric transition $B(E2) \uparrow$ will increase and the ratio of deformation to its maximum values ($\beta_2 = 0.2256$) with ($E_\gamma = 332.50$) for $^{114}_{46}\text{Pd}$ isotope. After that, when the number of nucleons increases and close to the magic number (82), the deformation parameters values will decrease as illustrated in figure (3-3)

In general the nucleus of these isotopes has deformed shapes as shown in the figures (3-35) and Appendix (A-4), and the collective motion in this case is a vibration about the spherical shape and no rotational motion is found.

4-1-5 Cadmium isotopes $^{102-126}_{48}\text{Cd}$

Table (3-5) explains that the values of the first excited state energy 2^+ will decrease gradually with the increase of mass numbers A , (the gaps between the ground and first excited states will be decrease with increase of A) so that the $B(E2) \uparrow$ will increase and values of deformation parameters β_2 seem to be

increased too. This is evident from deformation value ($\beta_2 = 0.1650$) belonged to $^{102}_{48}\text{Cd}$ corresponding to ($E_\gamma = 776.55$) while the highest deformation value belonged to $^{118}_{44}\text{Cd}$ and equals to ($\beta_2 = 0.1800$) with ($E_\gamma = 487.77$). After that, since the atomic number is constant ($Z = 48$) and close to magic number (50), any increase of the neutron numbers outside close shells offset by an increase in the energy values of E_γ and number of neutrons close to the magic number (82). Thus the values of deformation parameters will decrease by increasing the number of neutrons to reach to its minimum values ($\beta_2 = 0.1458$) for $^{126}_{48}\text{Cd}$ with ($E_\gamma = 652$ keV). This behavior is clear in figure (3-5) which represents the relationship between the deformation parameters as a function of neutron numbers.

These results confirm the fact that when the number of nucleons is closer to the magic numbers, the nuclei will be more stable and close to spherical shape and the motion of the nucleons in the sub-shell is a vibration about spherical shape. Shapes of these nuclei are shown in figures (3-36) and Appendix (A-5).

4-1-6 Tin isotopes $^{102-134}_{50}\text{Sn}$:

Clearly from table (3-6), that the lowest value of the deformation parameter is for the $^{132}_{50}\text{Sn}$ equals to ($\beta_2 = 0.0559$) and the largest distortion value for $^{134}_{50}\text{Sn}$ is ($\beta_2 = 0.1300$). The remaining values of β_2 are ranging between these two values. This is due to the fact that the $^{182}_{50}\text{Sn}$ is one of the isotopes with the double magic numbers ($Z = 50, N = 82$), and therefore this isotope is more stable than the other isotopes. Furthermore, the energy level of the first excited state 2^+ of the isotope $^{182}_{50}\text{Sn}$ is very high ($E_\gamma = 4041.1$ keV), (the gap is large between the ground and the first excited states, thus the hardness of transfer nucleons between these two states), compared with the energy levels of the same states for other isotopes. This means that the nucleus of $^{132}_{50}\text{Sn}$ isotope has closed shell, spherically symmetric, and it is especially stable.

More nucleons are added outside the closed shell in the $^{134}_{50}\text{Sn}$ isotope and the energy level of the first excited state 2^+ is ($E_\gamma = 725$ keV). All these factors are encouraging the small deformation of this nuclide.

These are confirmed in Figure (3-5), which shows the relationship between deformation parameters β_2 as a function of neutrons numbers N . It is clear that the distortion of nuclides decreases as neutron numbers close to the magic number of (82). Then the value of β_2 begins to increase thereafter as the N increased.

Generally speaking, all the isotopes of $_{50}\text{Sn}$ show a small deviation from the spherical shape, with the exception of the isotope $^{132}_{50}\text{Sn}$ as shown in the figures (3-37) and appendix (A-6).

4-1-7 Tellurium isotopes $^{108-138}_{52}\text{Te}$

Table (3-7) shows that the maximum value of deformation is ($\beta_2 = 0.1737$) corresponds to the first excited State energy 2^+ ($E_\gamma = 625.4$ keV) for $^{108}_{52}\text{Te}$ isotope and when increasing number of nucleons, β_2 will be decreased until reaching to the $^{134}_{52}\text{Te}$, where the distortion parameter value is equal to ($\beta_2 = 0.0979$) which represents minimum value that corresponds to the first excited state energy 2^+ ($E_\gamma = 1279.04$ keV), also the atomic number is ($Z = 52$) while neutron number equals to the magic number ($N = 82$), these factors made the nucleus of this isotope the most stable compared to the other isotopes of Tellurium and more spherical than others. These results are shown in figure (3-6).

We confirmed these results from same table when we found that the intrinsic electric quadrupole moments values (deviation from the spherical shape) started with a high value for $^{108}_{52}\text{Te}$ isotope and then will decrease with increased number of nucleon until reaching the minimum value of Q_0 (magic number $N = 82$) for $^{134}_{52}\text{Te}$ isotope. Figure (3-38) and appendix (A-7) show the shapes of the $_{52}\text{Te}$ isotopes which tend to be spherical

4-1-8 Barium isotopes $^{118-148}_{56}\text{Ba}$

Table (3-8) shows that the highest value of deformation parameter equals to ($\beta_2 = 0.2889$) that corresponds to the energy level ($E_\gamma = 183$ keV) for $^{120}_{56}\text{Ba}$.

After that, the values of the reduced electric transition $B(E2) \uparrow$ will decrease when the neutrons number increases and approach from the magic number ($N = 82$), and thus the values of the deformation parameters derived from it will also decrease until reaching to the lowest value ($\beta_2 = 0.0897$) that corresponds to energy level ($E_\gamma = 2126$ keV) for $^{138}_{56}\text{Ba}$ which is nearly spherical nucleus. Then, the increase in the number of neutrons will correspond by decreasing in the values of the first excited states energy and this will lead to an increase in the deformation parameters values from the lowest one. This is shown in figure (3-8) which gives the relationship between the deformation parameter β_2 as a function of the neutron numbers N . Also figures (3-39) and appendix (A-8) showed that these nuclei are vibrating around spherical shapes.

4-1-9 Cerium isotopes $^{124-152}_{58}\text{Ce}$

Table (3-9) shows us that with $Z = 58$ and $N = 66$ the β_2 value derived from the reduced transition probability $B(E2) \uparrow$ will be ($\beta_2 = 0.3174$) corresponds to the energy level ($E_\gamma = 142$ keV) for $^{124}_{58}\text{Ce}$, This values will decrease gradually when the neutrons number approach from magic number ($N = 82$) until reaching to the minimum value ($\beta_2 = 0.0839$) that corresponding to energy level ($E_\gamma = 1596.227$ keV) for $^{142}_{58}\text{Ce}$. After that, the increase in the number of neutrons leads to an Increase in β_2 values to be on its maximum values ($\beta_2 = 0.3414$) corresponds to the energy level ($E_\gamma = 82$ keV) for $^{152}_{58}\text{Ce}$. These are the normal cases of rotation levels. Where the shells of these nuclei are half busy, and many states of single particles are strongly present, overlapping, and plot such that the nuclei get prolonged shapes. Figures (3-40) and Appendix (A-9) explain these shapes.

4-1-10 Neodymium isotopes $^{128-156}_{60}\text{Nd}$.

From table (3-10), when $Z = 60$ and $N = 68$ the β_2 value derived from $B(E2) \uparrow$ will be ($\beta_2 = 0.3170$) corresponds to the energy level ($E_\gamma = 133.66$ keV) for $^{128}_{60}\text{Nd}$ isotope, this values will decrease gradually when the neutron number close from the magic number, and when N equals to 82 the

deformation parameter β_2 will reaching to the minimum value ($\beta_2 = 0.0832$) with the energy level ($E_\gamma = 1575.83$ keV) for $^{142}_{60}\text{Nd}$ isotope. More increasing in the neutrons number will lead to an Increase in β_2 values. It was observed that there was a significant increase in the deformation parameter values when the mass number $A \geq 150$, and the energy levels become less than values of other isotopes to reach to the highest value ($\beta_2 = 0.3676$) at the energy level ($E_\gamma = 66.9$) for $^{156}_{60}\text{Nd}$. These are the typical examples of rotational levels which are no more vibrations about spherical shapes as shown in the figures (3-41) and Appendix (A-10).

4-1-11 Samarium isotopes $^{130-160}_{62}\text{Sm}$

From table (3-11), when $Z = 62$ and $N = 68$ the β_2 value derived from $B(E2) \uparrow$ became ($\beta_2 = 0.3267$) with the energy level ($E_\gamma = 122$ keV) for $^{130}_{62}\text{Sm}$ isotope, and then β_2 will decrease gradually when the neutron number is close to the magic number ($N = 82$) to became ($\beta_2 = 0.0799$) with energy level ($E_\gamma = 1660.2$ KeV) for $^{144}_{62}\text{Sm}$ isotope. In the region of mass number ($150 \leq A \leq 160$), we notice that the energy of the first excited state decreases significantly to be from ($E_\gamma = 333.863$ keV) to ($E_\gamma = 70.6$ keV), and as a result the values of deformation parameter β_2 will increase with the increase of $B(E2) \uparrow$. From other side these results were confirmed from the values of electric quadrupole moments Q_0 that show significant increasing in the same region and the nuclei get elongated and become permanently deformed.

This is clear evidence about transforming the collective motion of nucleons from vibrational about spherical shape to a rotational motion. This is also clear from figure (3-11) which represents the relationship between the deformation parameter β_2 as a function of the neutron numbers (N), where there is almost constant plateau in the region of ($90 \leq N \leq 98$). This is evident from figures (3-42) and appendix (A-11) which represent the shapes of axially symmetric quadrupole deformation.

4-1-12 Gadolinium isotopes $^{138-162}_{64}\text{Gd}$

From table (3-12), when $Z = 64$ and $N = 74$ the β_2 value derived from $B(E2) \uparrow$ became ($\beta_2 = 0.2287$) with the energy level ($E_\gamma = 220.19$ keV) for $^{138}_{64}\text{Gd}$ isotope, and then β_2 will decrease gradually when the neutron number close to the magic number ($N = 82$) to became ($\beta_2 = 0.0723$) with energy level ($E_\gamma = 1971.97$ keV) for $^{146}_{64}\text{Gd}$ isotope. Then β_2 will rise again when number of neutrons increase. In the region of ($90 \leq N \leq 98$), we notice that the energy of the first excited state decreases significantly from ($E_\gamma = 123.0714$ keV) to ($E_\gamma = 71$ keV), and as a result the deformation parameter values β_2 will increase with the decrease of E_γ to be at its maximum value ($\beta_2 = 0.3436$) at ($E_\gamma = 71$ keV) for $^{162}_{64}\text{Gd}$ isotope. From other side these results were confirmed from the values of electric quadrupole moments, which show significant increasing in the same region and the nuclei get elongated and become permanently deformed.

In figure (3-12) which represents the relationship between the deformation parameter β_2 as a function of the neutron numbers N , there is almost constant plateau in the region of ($90 \leq N \leq 98$) which explains the collective rotational motion of deformed nuclei.

4-1-13 Dysprosium Isotopes $^{142-166}_{66}\text{Dy}$

From table (3-13) when $Z = 66$ and $N = 76$ the β_2 value derived from $B(E2) \uparrow$ became ($\beta_2 = 0.1858$) with the energy level ($E_\gamma = 315.9$ keV) for $^{142}_{66}\text{Dy}$ isotope, and then β_2 will decrease gradually when the neutron number is close to the magic number ($N = 82$) to become ($\beta_2 = 0.0774$) with energy level ($E_\gamma = 1677.3$ keV) for $^{148}_{66}\text{Dy}$ isotope. Then β_2 will rise again when number of neutrons is increased. When the mass numbers ($A \geq 150$), we notice that the energy of the first excited state decreasing significantly, and as a result the deformation parameter values β_2 will increases, until reaching to ($156 \leq A \leq 166$) then β_2 will take approximately equal values as shown in

Figure (3-13). On the other hand it indicates that these nuclei have electric quadrupole moments that can only be due to non-spherical distribution of nuclear charge. These results are evidence about collective rotational motion.

4-1-14 Erbium isotopes $^{144-172}_{68}\text{Er}$

From table (3-14), when $Z = 68$ and $N = 76$ the β_2 value derived from $B(E2) \uparrow$ became ($\beta_2 = 0.1793$) with the energy level ($E_\gamma = 330$ keV) for $^{144}_{68}\text{Er}$ isotope, and then β_2 will decrease gradually with the increase of N , and when neutron number is equal to the magic number ($N = 82$), Then the value of β_2 will be at its minimum value ($\beta_2 = 0.0787$) with energy level ($E_\gamma = 1578.87$ keV) for $^{150}_{68}\text{Er}$, which means that nucleus of this isotope is more stable than others. After that the values of deformation parameters β_2 will increase significantly by increasing the number of neutrons for isotopes N (taking into account that the number of protons is constant $Z = 68$) until the values of deformation are approximately equal in the confined area between ($94 \leq N \leq 104$) and this is evident by figure (3-14) that represents the relationship between deformation values β_2 as a function of the neutrons number N .

These are the normal cases of rotation levels. Where the shells of these nuclei are half busy, and many states of single particles are strongly present, overlapping, and plot such that the nuclei get prolonged shapes. Figures (3-45) and (A-14) show these prolonged shapes.

4-1-15 Ytterbium isotopes $^{152-178}_{70}\text{Yb}$

From observable table (3-15), we find that it starts with $^{152}_{70}\text{Yb}$, where the number of neutrons represents a magic number ($N = 82$) and the number of protons ($Z = 70$), The energy of the first excited state 2^+ ($E_\gamma = 1531.4$ keV) (the gap is large between the ground and the first excited states, thus the hardness of transfer nucleons between these two states), So that the reduced electric transmission probability $B(E2) \uparrow$ is low and therefore the deformation parameter will be at its minimum value ($\beta_2 = 0.0789$), this will lead that this isotope is more stable, almost spherical and the most tightly bound shape.

From the same table, values of β_2 will increase with the increase of N until reach to the confined area between ($92 \leq N \leq 108$), deformation values are approximately equal and ranging from ($\beta_2 = 0.2241$) with ($E_\gamma = 166.85$ keV) for $^{162}_{70}\text{Yb}$ to ($\beta_2 = 0.2875$) with ($E_\gamma = 84$ keV) for $^{178}_{70}\text{Yb}$.

The maximum value of ($\beta_2 = 0.3083$) for $^{162}_{70}\text{Yb}$, this is due to the minimum value of energy ($E_\gamma = 76$ keV) which in turn leads to maximum value of $B(E2) \uparrow$ and then the highest value of deformation. This seems to be clear in the figure (3-15), which shows the relationship between β_2 as a function of the neutrons number N . As a result, these nuclei will be less stable, non-spherical shape and will be more elongated.

On the other hand from observable same table we find the deformation values δ derived from Q_0 , become as low as possible because it started with magic number ($N = 82$) and the values of the intrinsic electric quadrupole moment become on its minimum value. When adding more nucleons in the shell or sub shell outside close shell this will lead to restrict the vibrations of wholly or partially to one direction (polarization the core), and the nucleus can get a permanent deformation

4-1-16 Hafnium isotopes $^{154-184}_{72}\text{Hf}$

Table (3-16) shows that the deformation parameter β_2 value derived from $B(E2) \uparrow$ for $^{154}_{72}\text{Hf}$ isotope with $Z = 72$, $N = 82$ (magic number) and first excited state 2^+ ($E_\gamma = 1513$ keV), will be at its minimum value ($\beta_2 = 0.0783$), which means that the nucleus of this isotope is more stable than others and almost spherical shape. Then we notice that the values of the first excited state E_γ decrease gradually with increase of N , so values of $B(E2) \uparrow$ will increase and therefore β_2 will rise again until reaching to its maximum value ($\beta_2 = 0.2835$) corresponding to ($E_\gamma = 88.351$ keV) for $^{176}_{72}\text{Hf}$. This behavior is clearly in the figure (3-16) which represents relation between β_2 and N . This is due to adding more nucleons to fill the unfilled shell outside the closed shell, which in turn leads

to elongate the nucleus gradually until reaching the ellipsoidal shape and the collective motion of the outer nucleons which will appear in the form of rotational modes excitation as suggested in ref. [35].

On the other hand the values of Q_0 from the same table show that adding more nucleons in the shell or sub shell outside close shell this will lead to restrict the vibrations of wholly or partially to one direction (polarization the core), and the nucleus can get a permanent deformation. Figures (3-47) and Appendix (A-16) show the nucleus shapes of these isotopes.

4-1-17 Tungsten isotopes $^{162-190}_{74}\text{W}$

Table (3-17) shows that the lowest value of the deformation Parameter β_2 is for $^{162}_{74}\text{W}$ nuclide ($\beta_2 = 0.1365$) is corresponding to the energy of the first excited state 2^+ ($E_\gamma = 450.2$ keV), and this energy is considered high compared to the same energy levels for the other Tungsten isotopes (this means that the gap between the ground state and the first excited state is large, and hence the difficulty of transfer of nucleons between these two states compared to other isotopes, which are the gaps between those states are small). Thus, the value of the reduced transition probability will be small and therefore the value of the β_2 derived from it is small. After that, the energy values of the first excited states will decrease gradually with increase of nucleons numbers, thereby increasing the reduced transition probability and resulting in increase of deformation parameters β_2 until reaching to the maximum value ($\beta_2 = 0.2576$) corresponding to the energy ($E_\gamma = 100.1060$ keV) for $^{182}_{74}\text{W}$. Then the values of the deformation parameters begin to decrease as the number of nucleon increases. This is evident in Figure (3-17), which represents the relationship between deformation parameters as a function of the number of neutrons.

From the same table, large value of intrinsic quadrupole moments Q_0 can be observed, this belonged to the collective behavior (vibrational and rotational) of nucleons out of closed shell. Figures (3-48) and Appendix (A-17) show the shapes

of axially symmetric quadrupole deformation for ${}_{74}\text{W}$ isotopes from major a and minor b axes.

4-1-18 Osmium isotopes ${}^{164-196}_{76}\text{Os}$

It's clearly from table (3-18), that the lowest value of the deformation parameter β_2 is for ${}^{164}_{76}\text{Os}$ nuclide ($\beta_2 = 0.1222$) is corresponding to the energy of the first excited state 2^+ ($E_\gamma = 548$ keV), thus, the value of the reduced transition probability will be small, as the value of the β_2 derivative is also small. After that, the energy values of the first excited states will decrease gradually with increased number of nucleons (the gap between the ground state and the first excited state will be small), and therefore the ease of nucleon transition between these two states, resulting in increased values of reduced transition probability and thus increasing the values of deformation parameters β_2 until reaching to the its maximum value ($\beta_2 = 0.2329$) for ${}^{184}_{76}\text{Os}$ isotope corresponding to the energy ($E_\gamma = 119.80$ keV). Then the values of the deformation parameters begin to decrease as numbers of nucleons increase. This behavior of deformation is clear in Figure (3-18), which represents the relationship between β_2 and N .

From the same table, there will be more nucleons outside the closed shell, then the polarization effect grows, and large value of intrinsic quadrupole moments Q_0 can be observed. Figures (3-49) and appendix (A-18) show the shapes of axially symmetric quadrupole deformation for ${}_{76}\text{Os}$ isotopes from major a and minor b axes.

4-1-19 Platinum isotopes ${}^{168-200}_{78}\text{Pt}$

Table (3-19) shows the lowest value of the deformation parameter β_2 is for ${}^{200}_{78}\text{Pt}$ nuclide ($\beta_2 = 0.1082$) is corresponding to the energy of the first excited state ($E_\gamma = 470.10$ keV), since number of neutrons ($N = 122$) and ($Z = 78$) are close to the magic number (82), so that this nucleus will be more stable and tend to be in spherical shape. While the maximum value of β_2 is for ${}^{180}_{78}\text{Pt}$ nuclide and equals to ($\beta_2 = 0.2112$) is corresponding to the energy of the first excited state ($E_\gamma = 152.23$ keV), other values of β_2 are ranging between these two values. This

is obvious in figure (3-19), which represents the relationship between deformation parameters as a function of the number of neutrons. Also figure (3-50) shows the shapes of axially symmetric quadrupole deformation for $_{78}\text{Pt}$ isotopes from major a and minor b axes.

4-1-20 Mercury isotopes $^{176-206}_{80}\text{Hg}$

Table (3-20) shows that the highest value of the deformation parameter is ($\beta_2 = 0.1374$) corresponding to the energy value of the first excited state ($E_\gamma = 351.8$ keV) for $^{182}_{80}\text{Hg}$ isotope. In general, when increasing the number of nucleon, the energy values of 2^+ will gradually increase (the gap between the ground 0^+ and the first excited 2^+ states will be increased). Therefore, the reduced electric transition probability decreased, and the values of the deformation parameters are also decreased until they reach $^{206}_{80}\text{Hg}$ where ($\beta_2 = 0.0697$) is at the lowest value corresponding to the ($E_\gamma = 1068.54$ keV) which is considered very high compared to other isotopes, where the number of neutrons ($N = 126$) represents a magic number. On this basis, this nuclide is more stable and more spherical than others as shown in figure (A-20).

In general, these isotopes are stable and spherical and the collective motion of the nucleons in the sub-shell is vibration about spherical shape, this is obvious from figure (3-51) which represents shapes of axially symmetric quadrupole deformation for $_{80}\text{Hg}$ isotopes from major a and minor b axes.

From the same table, we observe that the values of intrinsic quadrupole moments Q_0 are small compared to the elements which have large values of deformation; this confirmed what was mentioned about that these isotopes are more stable than other isotopes of the elements that preceded them.

4-1-21 lead isotopes $^{182-214}_{82}\text{Pb}$

It is clearly from table (3-21), that the atomic number is $Z = 82$ which represents a magic number, and the Neutrons number ranges from $N = 100$ to $N = 132$, and also note that the energies of the first excited states are considered large compared to the previous isotopes, which means that the gaps between the

ground states and the first excited states are large (the difficulty of transfer of nucleons between these two states). Therefore, reduced electrical transition probabilities values of these isotopes are small and the deformation parameters values derived from them are small too and almost equal, as shown in figure (3-21), except for the $^{208}_{82}\text{Pb}$ nuclide (double magic numbers), where $(\beta_2 = 0.0353)$ corresponding to the $(E_\gamma = 4085.4 \text{ keV})$ which is considered very high energy. Based on the above this nuclide is one of the most stable isotopes and has a spherical shape (closed shell).

In general, lead element isotopes are more stable and have spherical shapes if compared with the other isotopes as illustrated in figures (3-52) and appendix (A-21).

From the same table, we observe that the values of intrinsic quadrupole moments Q_0 are small compared to the elements which have large values of deformation; this confirmed what was mentioned about that these isotopes are more stable than other isotopes of the elements that preceded them. The results of some lead isotopes were matched very well with the results in the Ref. [30].

4-1-22 Polonium isotopes $^{192-218}_{84}\text{Po}$

From Table (3-22), it is clear that the highest value of the deformation parameter belongs to the $^{192}_{84}\text{Po}$ isotope and equals to $(\beta_2 = 0.1509)$ corresponding to the first excited state energy $(E_\gamma = 262 \text{ keV})$. By increasing the number of neutrons and approaching the magic number (126), we notice a gradual increase in the energy values of the first excited states E_γ , and thus decrease the values of the reduced electric transition which in turn decrease β_2 until reaching its minimum value at the $^{210}_{84}\text{Po}$ isotope where number of neutrons $N = 126$ (magic number) so that $(\beta_2 = 0.0650)$ corresponding to $(E_\gamma = 1181.40 \text{ keV})$. After that any increase of valence nucleons in the sub-shell outside closed shell will lead to increase in the deformation parameter values. This behavior is illustrated by Figure (2-22), which represents the relationship between the deformation parameter β_2 as a function of the Neutrons number N .

From the same table, as for the intrinsic quadrupole moments Q_0 values, it is observed that when the values of the deformation parameters are significant, the values of the corresponding Q_0 are also large and when the values of deformation are low, the shape of the nucleus tends to be spherical shape, the values of Q_0 are also small.

Generally, when the values of the deformation parameters are low, the overall shape of the nuclei tends to the spherical and collective motion of nucleon appears in the vibrational mode about spherical shape as shown in the figures (3-53) and appendix (A-22).

4-1-23 Radon isotopes $^{198-222}_{86}\text{Rn}$

Table (3-23) shows us that the values of the deformation parameters start with $^{198}_{86}\text{Rn}$ isotope where ($\beta_2 = 0.1287$) is corresponding to the first excited state energy ($E_\gamma = 339$ keV). Next, increasing number of nucleons in outer shells makes them close to the magic number ($N = 126$), corresponding to gradual increase in the value of E_γ from the value of the first isotope, this will lead to decrease of $B(E2) \uparrow$ values, which in turn decrease the β_2 values to reach to its minimum value at $^{212}_{86}\text{Rn}$ isotope where ($\beta_2 = 0.0620$) is corresponding to ($E_\gamma = 1273.8$). Thus, this isotope is considered stable and spherical than other Radon isotopes, After that any increasing in the number of neutrons will be offset by a decreasing in the energy level and therefore the values of $B(E2) \uparrow$ will increase, which in turn results in the increase the β_2 values, this behavior is illustrated in figure (3-23). When increasing the number of neutrons outside the closed shell, this will increase the polarization effect and therefore the nucleus will be more elongated and especially for isotopes with mass number ($A > 220$) as shown in figure (3-54).

4-1-24 Radium isotopes $^{206-230}_{88}\text{Ra}$

From table (3-24), we observe that the values of the deformation parameters start with $^{206}_{88}\text{Ra}$ isotope where ($\beta_2 = 0.1045$) is corresponding to the first excited state energy ($E_\gamma = 474.3$ keV). Next, increasing the number of nucleons in the

outer shells makes them close to the magic number ($N = 126$), corresponding to gradual increase in the value of E_γ from the value of the first isotope, this will lead to decrease $B(E2)$ values, which in turn decreases the β_2 values until reaching to its minimum value at ${}^{214}_{88}\text{Ra}$ isotope where ($\beta_2 = 0.0589$) is corresponding to ($E_\gamma = 1382.4$ keV). Thus, the nucleus of this isotope is considered more stable and spherical than other ${}_{88}\text{Ra}$ isotopes, this behavior is illustrated in the figure (3-24) which represents the relationship between β_2 and N .

After that, any increase in the number of neutrons is corresponding by a gradually decrease in energies value of the first excited states (this means that the gaps between the ground and first excited states will be decreased gradually and therefore the ease of transition of neutrons between these two states), on this basis, the values of the electric transition will be large and therefore the values of the distortion parameters in turn will be significant, therefore the nucleus will be more elongated and permanently deformed especially for isotopes with mass number ($A > 220$) as shown in figures (3-55) and appendix (A-24).

4-1-25 Thorium isotopes ${}^{216-234}_{90}\text{Th}$

Table (3-25) shows that the nucleus of the (thorium-216) is stable, less deformed and almost spherical because it contains the neutrons magic number ($N = 126$), In addition, the energy of the first excited state equals to ($E_\gamma = 1478$ keV) which is considered large energy compared with others. On this basis, the reduced electric transition values are small and this in turn makes the values of the deformation parameter ($\beta_2 = 0.0565$) as low as possible, figure (3-53) illustrates nuclei shapes of ${}_{90}\text{Th}$.

Next, when number of neutrons in the shells out of closed shell is increased, it is noticed that there is a gradual increasing in the values of reduced electric transition $B(E2) \uparrow$, which in turn leads an increase of deformation parameters values. This means that nuclei shapes will take ellipsoidal shapes and no more spherical shape will be (increased of deformed nuclei). This process occurs with a significant decrease in the energy values of the first excited state, the gap between

the ground state and the first excited state is small, thus, the ease transition of nucleons between these two states. This behavior is illustrated in figure (3-25).

4-1-26 Uranium isotopes $^{226-240}_{92}\text{U}$

It is clear from Table (3-26) that the minimum value of the deformation parameter is ($\beta_2 = 0.2313$), corresponding to the energy of the first excited state ($E_\gamma = 80.5$ keV) for (U-226), and the highest value of the deformation parameter is ($\beta_2 = 0.3039$) corresponding to the energy of the first excited state ($E_\gamma = 43.498$ KeV) for (U-234). Other values are ranging between these values. It's also noted that these values of β_2 are considered large values if compared to the other isotopes with mass number less than 150 ($A < 150$), which means large deformed shapes as shown in figures (3-57) and (A-26), corresponds small values of the first excited state energies (the gaps between shells are low spaces), also number of nucleons in the sub-shell outside closed shell are filled with many nucleons and the collective motion of these nucleons will be rotational motion. On the other hand, the values of the intrinsic electric Quadrupole moments Q_0 are significant.

4-1-27 Plutonium Isotopes $^{236-246}_{94}\text{Pu}$

From Table (3-27), we observe that the energy values of the first excited state are ranging between ($42.824 \leq E_\gamma \leq 46$) in unit of keV, where these energy values are very few if compared to the energies values of nuclei with magic numbers. Therefore, the gaps between the ground and the first excited states are very low, which means that the probability transition of nucleons between these two states are very high, this is evident from the high values of $B(E2) \uparrow$. On this basis, the values of the deformation parameters derived from $B(E2) \uparrow$ will be high, since the highest deformation value ($\beta_2 = 0.2986$) is corresponding to the energy of the first excited state ($E_\gamma = 42.824$ keV) for $^{240}_{94}\text{Pu}$ while the lowest deformation value ($\beta_2 = 2834$) is corresponding to the energy of the first excited state ($E_\gamma = 46$ keV) for $^{244}_{94}\text{Pu}$. On the other hand, the values of the intrinsic electric Quadrupole moments Q_0 are also significant which means non-spherical

charge distribution. All these factors will encourage the nucleus to be in permanently deformed shape as shown in figures (3-58) and appendix (A-27); in addition to the collective motion of nucleons will be rotational motion.

2-1-28 Curium Isotopes $^{238-250}_{96}\text{Cm}$

Table (3-28) shows that the isotope of $^{238}_{96}\text{Cm}$ has the largest value of the distortion parameter and equals to ($\beta_2 = 0.3331$), corresponding to the energy of the first excited state ($E_\gamma = 35$ keV). After that when increasing number of nucleons, there will be a slight increase in the values of the first excited state energy even though these values are small. This will make the values of reduced electrical transition decreased slightly. Therefore, the values of the deformation parameters decreased too, this behavior is illustrated in figure (3-28).

Despite this reduction in deformation parameters values, they remain large compared to the deformation values of the other element as shown in figures (3-59) and appendix (A-28).

On the other hand, the values of the intrinsic electric quadrupole moments are large if compared to the other values of the other elements. This indicates the large distortion values of the isotopes of this element.

4-1-29 Californium isotopes $^{244-252}_{98}\text{Cf}$

Table (3-29) shows that there are four isotopes chosen from this element, the highest value of the deformation parameter belongs to $^{244}_{98}\text{Cf}$ and equals to ($\beta_2 = 0.3039$), corresponding to the first excited state energy ($E_\gamma = 40$ keV) and the lowest value of the deformation parameter belongs to $^{252}_{98}\text{Cf}$ equals ($\beta_2 = 0.2753$) to correspond to the energy of the first excited state ($E_\gamma = 45.72$ keV).

Also we note that the number of nucleons ($Z = 98$ and $244 \leq N \leq 252$) that fill the shells outside closed shell are large, the energy values of the first excited state of the selected Californium isotopes are considered very small if compared with the energy of the closed shell (the distances between the ground state and the first excited state are small so that the transition of the nucleons

between these two states is very easy). Therefore, the values of the reduced electrical transition will be large; In addition to that, the values of intrinsic electric Quadrupole moments are large too. All these factors work to make the deformation parameters are large, which in turn make the nuclei of these isotopes permanently deformed and elliptical shapes as shown in Figures (3-60) and appendix (A-29). In addition, the collective motion of nucleons in the external orbits is rotational motion.

4-1-30 Fermium isotopes $^{248-256}_{100}\text{Fm}$

Table (3-30) shows that the values of ($Z = 100$ and $248 \leq N \leq 256$). Also, the energies values of the first excited states 2^+ , although they are very low values compared to the energies of the magical numbers (the distances between the ground state and the first excited state are small so that the nucleons transition between these two states are very easy), but they gradually increase by increasing the number of nucleons. This means that the values of the reduced electric transition $B(E2) \uparrow$ are very high and gradually decrease by increasing the energy values of the first excited states, this in turn makes the value of the deformation parameter for $^{248}_{100}\text{Fm}$ isotope ($\beta_2 = 0.2851$) represents the highest value corresponding to the energy of the first excited state ($E_\gamma = 44$ keV) while the lowest value ($\beta_2 = 0.2642$) belongs to the $^{256}_{100}\text{Fm}$ isotope corresponds to the energy of the first excited state ($E_\gamma = 48.1$ keV). This behavior is illustrated in figure (3-30). In general; the values of the deformation parameters (β_2, δ) derived from [$B(E2) \uparrow, Q_0$] respectively are significant relative to the deformation values of the elements with a mass number less than 150 ($A < 150$). As a result, the nuclei of these isotopes are deformed, the collective motion of nucleons is a rotational motion, in addition to the fact that the forms of these nuclei are elliptical as shown in Fig.(3-61) and appendix (A-30).

4-2 Conclusions:

From the results (and the figures of 2D and 3D Shapes of the nuclei we conclude the following:

- 4-2-1 When the number of nucleons represents magic numbers, the nucleus will be stable and spherical shape, especially when both of proton and neutron represent a magic number (double magic), then nucleus is more stable, non-deformed and more spherical than nuclei of other isotopes such as $^{132}_{50}\text{Sn}_{82}$ and $^{208}_{82}\text{Pb}_{126}$ isotopes.
- 4-2-2 The energy of the first excited state (2^+) begins to decrease sort of smoothly when the mass number A increases except for regions near closed shells where the energy values of first excited states are relatively high and the nuclei are more stable and more spherical.
- 4-2-3 When the numbers of nucleons come closer to the magic numbers, the forms of the nuclei tend to be spherical and the Collective motion of nucleons out of closed shell is a vibrational motion around the spherical shape.
- 4-2-4 Far from magic numbers, the motion of the nucleons out of closed shell will be rotational motion and the nucleus will be more distorted especially in the region ($150 \leq A \leq 190$) and ($A \geq 220$).
- 4-2-5 The prolate shape is the dominant form of all deformed nuclei except for $^{132}_{50}\text{Sn}_{82}$ and $^{208}_{82}\text{Pb}_{126}$ nuclide where these two are non-deformed and spherical.

4-3 Suggestions and Future Works

- Study the shapes and properties of the deformed nuclei which have mass number less than 100 ($A \leq 100$).
- Study the shapes of even-odd, odd-even, and odd-odd nuclides.
- Study the distortion parameters for same or another excited states for example $8^+ \rightarrow 6^+$, $6^+ \rightarrow 4^+$ and $4^+ \rightarrow 2^+$.

References

References

- [1]. Goergen A. , (2008), "The hidden shapes of atomic nuclei", Institute of Research into the Fundamental Laws of the Universe. (<http://irfu.cea.fr>)
- [2]. Lucas R., (2001), "Nuclear shapes " Europhysics News, Volume 32, Number 1, January-February. (<http://www.europhysicsnews.org>)
- [3]. Vretenar D., (2016)," Nuclear shape phase transitions", EPJ Web of Conferences, 0400 DOI: 10.1051/epjconf/201611 0400, P(2).
- [4]. Basdevant J. L., Rich J. and Spiro M. p. (2005), "Fundamentals in Nuclear Physics, from Nuclear Structure to Cosmology", Springer. Science+Business Media, Inc, P(9-12-74-81) .
- [5]. Povh B., Rith K., Scholz Ch., and Zetsche F., (2008), "Particles and Nuclei, An Introduction to the Physical Concepts", Springer-Verlag Berlin Heidelberg, P(14-21-254).
- [6]. مصطفى عبد المهدي المجالي، (2005)، "الوقاية الإشعاعية المبادي والتطبيقات".
- [7]. Beiser A., (2003), "Concepts of Modern Physics", Sixth Edition, The McGraw-Hill Companies, Inc, P(392).
- [8]. Philip R. G.,(2016)," Introduction to Nuclear and Subnuclear Physics" student handout version, Dipartimento di Scienza e Alta Tecnologia Università degli Studi dell' Insubria in Como via Valleggio 11, 22100 Como (CO), Italy, P(38).
- [9]. Norman D. Cook, (2010), "Models of the Atomic Nucleus", Second Edition, DOI 10.1007/978-3-642-14737-1, Springer-Verlag Berlin Heidelberg, P(60-73).
- [10]. Kenneth J. Shultis and Richard E. Faw (2002), "Fundamentals in nuclear Science and engineering", Marcel Dekker, Inc., New York, Ch (3.2.6).
- [11]. Iwasaki H., Motobayashi T. and others, (2000), "Quadrupole deformation of ^{12}Be studied by proton inelastic scattering", Physics Letters B 481-7–13.
- [12]. Benhamouda N., M.R. Oudih, N.H. Allal and Fella, (2001), "Electric quadrupole moments of even-even Sm neutron-rich nuclei", Elsevier, Nuclear Physics A690, 219c-222c.

References

- [13]. Raman S. , (2001), "Transition Probability from the Ground State to the First- Excited State of Even –Even Nuclide" Atomic Data and Nuclear Data Tables 78, 1–128, doi:10.1006/adnd.2001.0858.
- [14]. Bizzeti P. G. and A. M. Bizzeti-Sona, (2004), "Description of nuclear octupole and quadrupole deformation close to the axial symmetry and phase transitions in the octupole mode", Physical Review C 70, 064319.
- [15]. Chmel S., S. Frauendorf, and H. Hubel, (2007), "Deformation parameters and transition probabilities for shears bands in Pb isotopes", Physical Review C 75, 044309.
- [16]. Boboshin I., B. Ishkhanov, S. Komarov, V. Orlin, N. Peskov, and V. Varlamov, (2007), "Investigation of Quadrupole Deformation of Nucleus and its Surface Dynamic Vibrations" International Conference on Nuclear Data for Science and Technology. DOI: 10.1051/ndata:07103 P.65-68.
- [17]. Al-Sayed A. (2009), "The effect of nuclear deformation on level statistics", Journal of Statistical Mechanics, IOP Publishing Ltd and SISSA, doi:10.1088/1742-5468/2009/02/P02062.
- [18]. Hamamoto I. and B. R. Mottelson, (2009), "Further examination of prolate - shape dominance in nuclear deformation", Physical Review C 79, 034317.
- [19]. Barbero C., G. Jorge Hirsch, E. Alejandro Mariano, (2012), "Deformation and shell effects in nuclear mass formulas", Elsevier, Nuclear Physics A 874 81–97.
- [20]. Mohammadi S., (2012), "Quadrupole Moment Calculation of Deformed Nuclei", Journal of Physics: Conference Series 381 012129. doi:10.1088/1742-6596/381/1/012129.
- [21]. Smith A. G., J. L. Durell, W. R. Phillips, and W. Urban, (2012), "Lifetime measurements and nuclear deformation in the $A \approx 100$ region", Physical Review C 86, 014321.
- [22]. Azad Kareem M., (2014), "The Reduced Transition Probabilities, Quadrupole Moments and Moment of Inertia of Some Even- Even Nuclei", Zanco Journal of Pure and Applied Sciences, Vol.26, No.1.

References

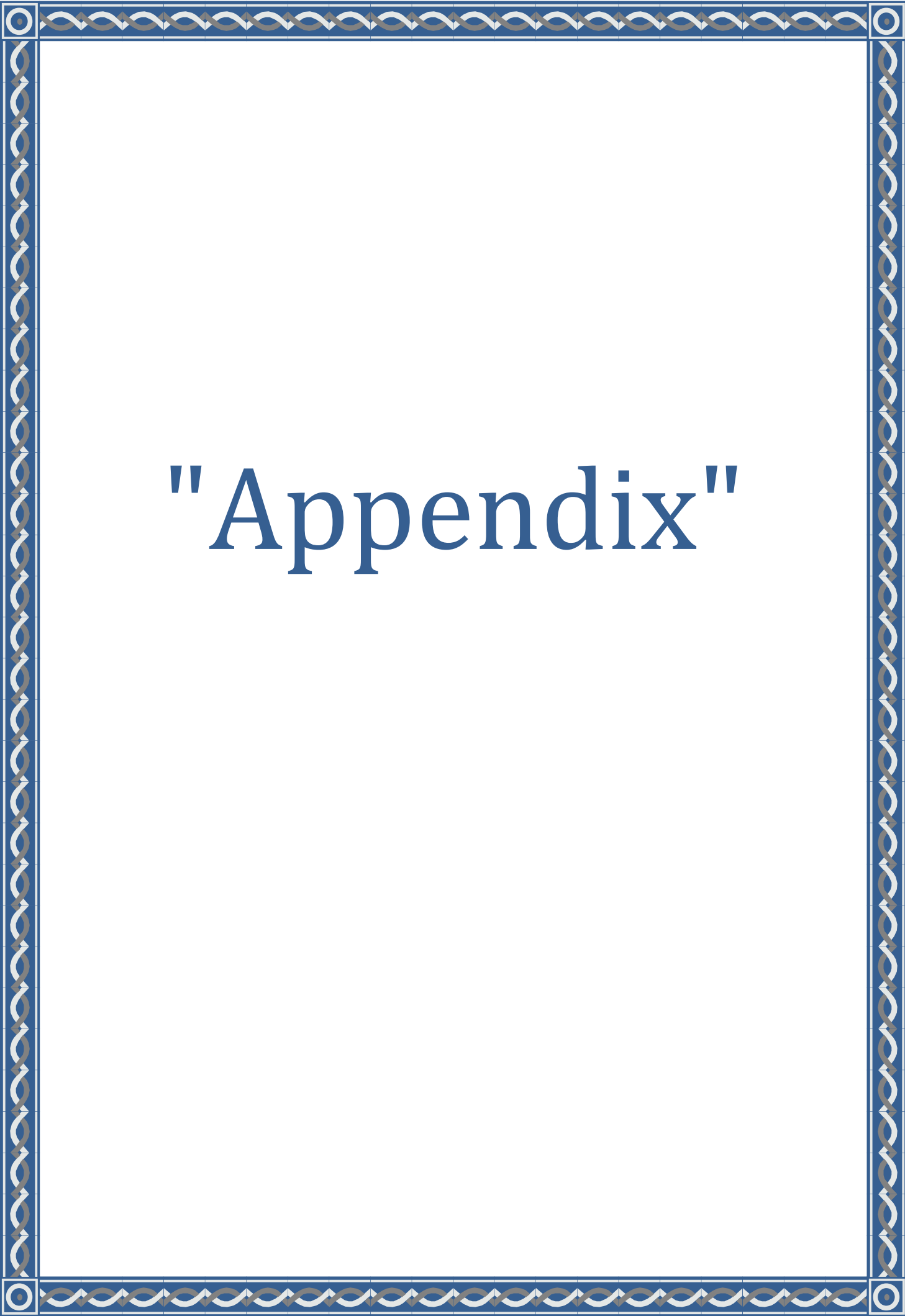
- [23]. Pritychenko B., M. Birch, M. Horoi, and B. Singh, (2014), "B(E2) Evaluation for $0_1^+ \rightarrow 2_1^+$ Transitions in Even-Even Nuclei", Elsevier, Nuclear Data Sheets 120, 112–114.
- [24]. Gado K. A., (2014), "Quadupole Moments Calculation of Deformed Even-Even $^{156-170}\text{Er}$ Isotopes", Global Journals Inc. (USA). Volume 14 Issue 1 Version 1.0
- [25]. Haberichter M., P. H. C. Lau, and N. S. Manton, (2015), "Electromagnetic Transition Strengths for Light Nuclei in the Skyrme model", Kent Academic Repository. Phys. Rev. C 93, 034304
- [26]. Möllera P., A. J. Sierka, T. Ichikawab and H. Sagawac, (2015), "Nuclear ground-state masses and deformations: FRDM (2012)", Atomic Data and Nuclear Data Tables.
- [27]. Ertuğral F., E. Guliyev and A. Kuliev,(2015) "Quadrupole Moments and Deformation Parameters of the $^{166-180}\text{Hf}$, $^{180-186}\text{W}$ and $^{152-168}\text{Sm}$ Isotopes", DOI: 10.12693/APhysPolA.128.B-254, Article in Acta Physica Polonica Series a.
- [28]. Saad R. Hadi (2015), " Study of Excited Structure for Even-Even Nuclides of $Z = 50, 48, 46$ in The First Excited State", M.Sc. Thesis, Physics Department, College of Education for Pure Science / Ibn Al-Haitham, Baghdad University.
- [29]. Pritychenko B., M. Birch, B. Singh, and M. Horoi (2016), "Tables of E2 Transition Probabilities from the first 2_1^+ States in Even-Even Nuclei", Atomic Data and Nuclear Data Tables Volume 107, Pages 1-139
- [30]. Jani Hassan H. (2016), " Study The Deformation for The Even- Even Nuclei (Ca, Kr, Xe and Pb)", M.Sc. Thesis, Physics Department, College of Education for Pure Science / Ibn Al-Haitham, Baghdad University.
- [31]. Wong S.M.Samuel, (2004), "Introductory Nuclear Physics", Second Edition, WILEY-VCH Verlag GmbH and Co. KGaA, Weinheim, P (12-224-225).
- [32]. Bohr A. and Mottelson B. R., (1998) "Nuclear structure, Vol.II, Nuclear Deformations", by World Scientific Publishing Co. Pte. Ltd.

References

- [33]. Al-Sayed A. and A. Y. Abul-Magd, (2006), " Level statistics of deformed even-even nuclei", The American Physical Society DOI:10.1103/ PhysRev C. 74.037301.
- [34]. Kenneth S. Krane , (1988), "Introductory Nuclear Physics", by Joun Willey and Sons, Inc, P(49-139-142).
- [35]. Roy R. R. and Nigam B.P., (1967), "Nuclear Physics Theory and Experiment", By John Wiley and Sons, INC. P(274-275).
- [36]. Greiner W. J. A.Maruhn, (1996),"Nuclear Models", Springer- Verlag Berlin Heidelberg, P(108).
- [37]. Marinova K., (2015),"Nuclear Charge Radii Systematics", Journal of Physical and Chemical Reference Data 44, 031214; doi: 10.1063/1.4921236.
- [38]. Angeli I., Yu. P. Gangrsky, K. P. Marinova, and I. N. Boboshin, (2009)," *N* and *Z* dependence of nuclear charge radii", Journal of Physics G: Nuclear and Particle Physics, doi:10.1088/0954-3899/36/8/085102.
- [39]. Papuga J., (2015), "Structure of potassium isotopes studied with collinear laser spectroscopy" Dissertation presented in partial fulfillment of the requirements for the degree of Doctor in Science, KU Leuven – Faculty of Science.
- [40]. Neugart R. and G. Neyens, (2006)," Nuclear Moments", Lect. Notes Phys.700, 135–189, Springer-Verlag Berlin Heidelberg.
- [41]. Neyens G.,(2003),"Nuclear magnetic and quadrupole moments for nuclear structure research on exotic nuclei" Rep. Prog. Phys. 66 (2003) 633–689 IOP Publishing Ltd. Printed in the UK.
- [42]. Buchmann A. J., E. M. Henley, (2001), "Intrinsic quadrupole moment of the nucleon", Phys.Rev. C63 015202.
- [43]. Henley M. E. and A. Garcia, (2007), "Subatomic Physics (3rd Edition)", World Scientific Publishing Co. Pte. Ltd, P(544).
- [44]. Ridha A. Abdulwahab, (2009), "Deformation parameters and nuclear radius of Zirconium (Zr) isotopes using the Deformed Shell Model", Wasit Journal for Science & Medicine, P(115 - 125).

References

- [45]. Testov D. A., A. A. Aleksandrov, and others , (2008), "A Technique for Measuring the Quadrupole Deformation Parameter of Transuranium Nuclei", ISSN 0020-4412, Instruments and Experimental Techniques, Vol. 51, No. 5, pp. 661–664. Pleiades Publishing, Ltd.
- [46]. Ertugrala F., E. Guliyev, and A.A. Kuliev, (2015), " Quadrupole Moments and Deformation Parameters of the $^{166-180}\text{Hf}$, $^{180-186}\text{W}$ and $^{152-168}\text{Sm}$ Isotopes", DOI: 10.12693/APhysPolA.128.B-254, ACTA PHYSICA POLONICA A.
- [47]. Margraf J., R.D. Heil, U. Kneissl, and U. Maier, (1993), "Deformation dependence of low lying $M1$ strengths in even isotopes", Physical Review C Physical Review C, Volume 47, Number 4.
- [48]. Raman S., (2002), "A Tale of Two Compilations: Quadrupole Deformations and Internal Conversion Coefficients", Journal of Nuclear Science and Technology, Supplement 2, p. 450-454 (August).
- [49]. Akkoyun S., T. Bayram, and S.O. Kara, (2015), "A study on estimation of electric quadrupole transition probability in nuclei", Journal of Nuclear Sciences, Vol. 2, No. 1, Jan., 7-10.
- [50]. Fireston R.B. and V.S. Shirly; " Table of Isotopes eighth edition ", New York. (99).
- [51]. Angeli I. a, K.P. Marinova (2013)," Table of experimental nuclear ground state charge radii: An update", Atomic Data and nuclear Data Table 99(2013) 69-95.
- [52]. Martin B. R., (2006), "Nuclear and Particle Physics, An Introduction", John Wiley & Sons Ltd, England.



"Appendix"

Appendix

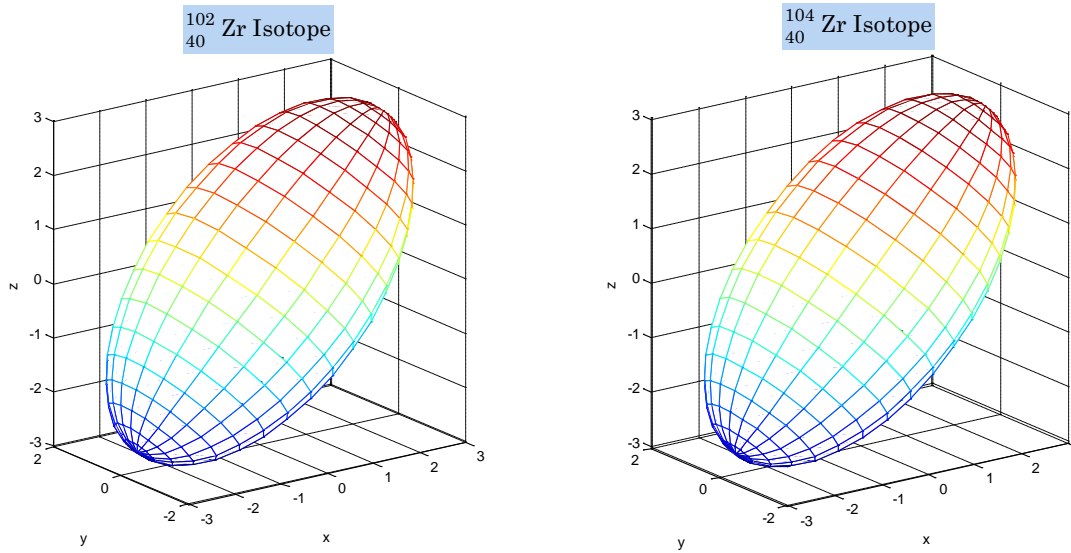


Figure (A-1): axially-symmetric quadrupole deformations, the prolate shape of Nucleus with($x = y < z$) (where z is the minor axis (b) (symmetric axis) and (x,y) are major axes (a) for Zr isotopes.

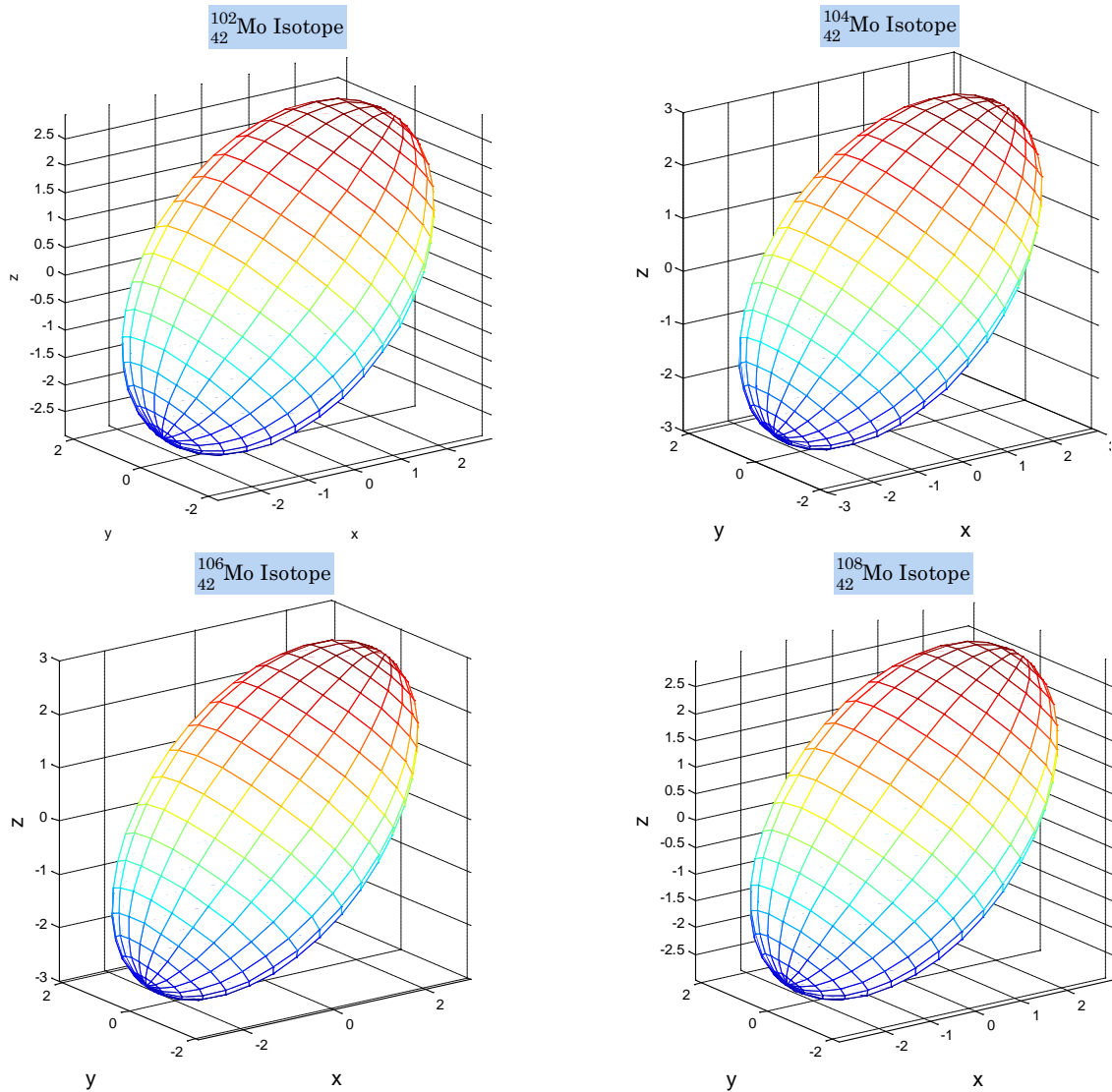


Figure (A-2): axially-symmetric quadrupole deformations, the prolate shape of Nucleus with($x = y < z$) (where z is the minor axis (b) (symmetric axis) and (x,y) are major axes (a) for Mo isotopes.

Appendix

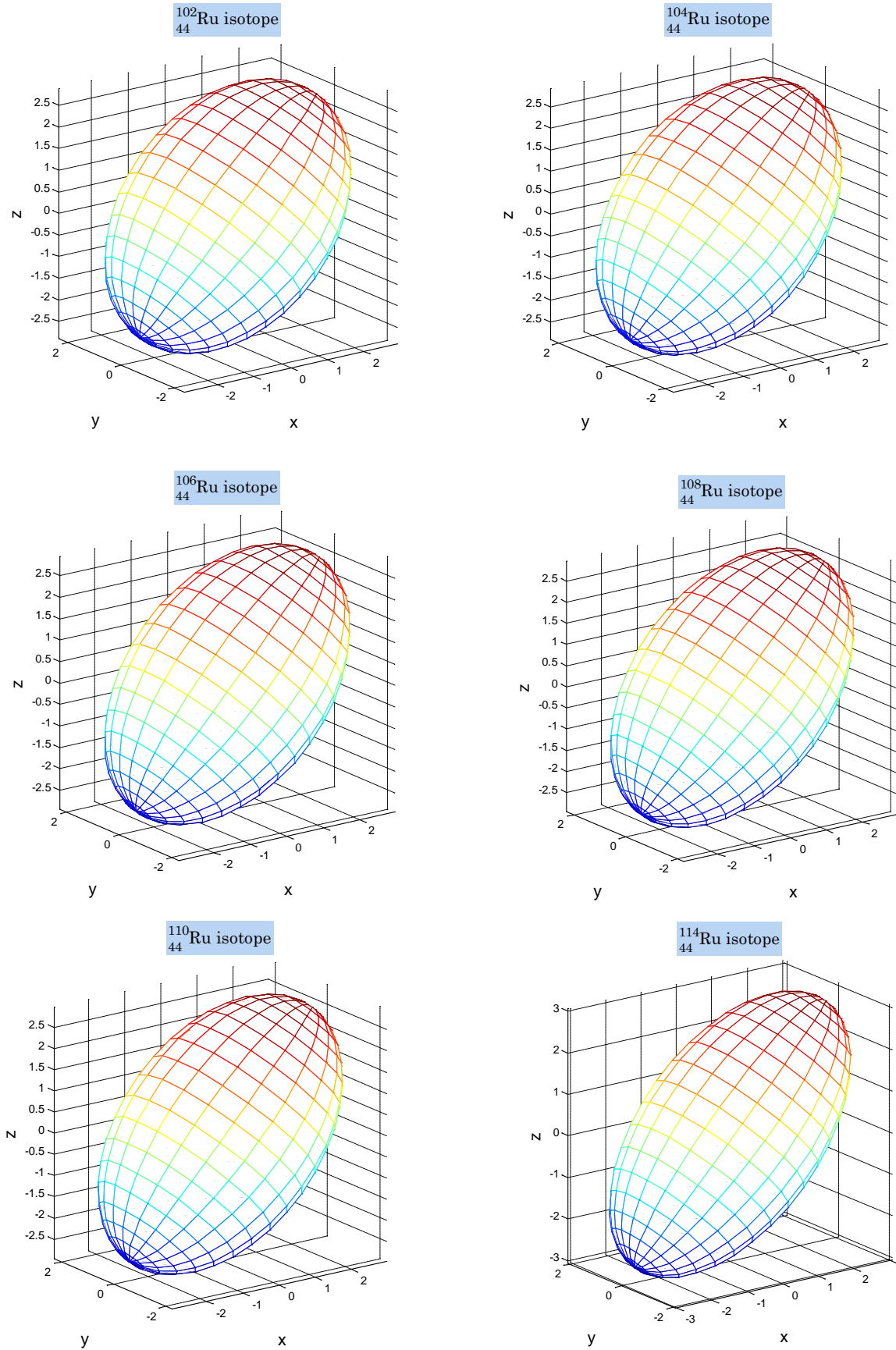


Figure (A-3): axially-symmetric quadrupole deformations, the prolate shape of Nucleus with $(x = y < z)$ (where z is the minor axis (b) (symmetric axis) and (x,y) are major axes (a) for Ru isotopes

Appendix

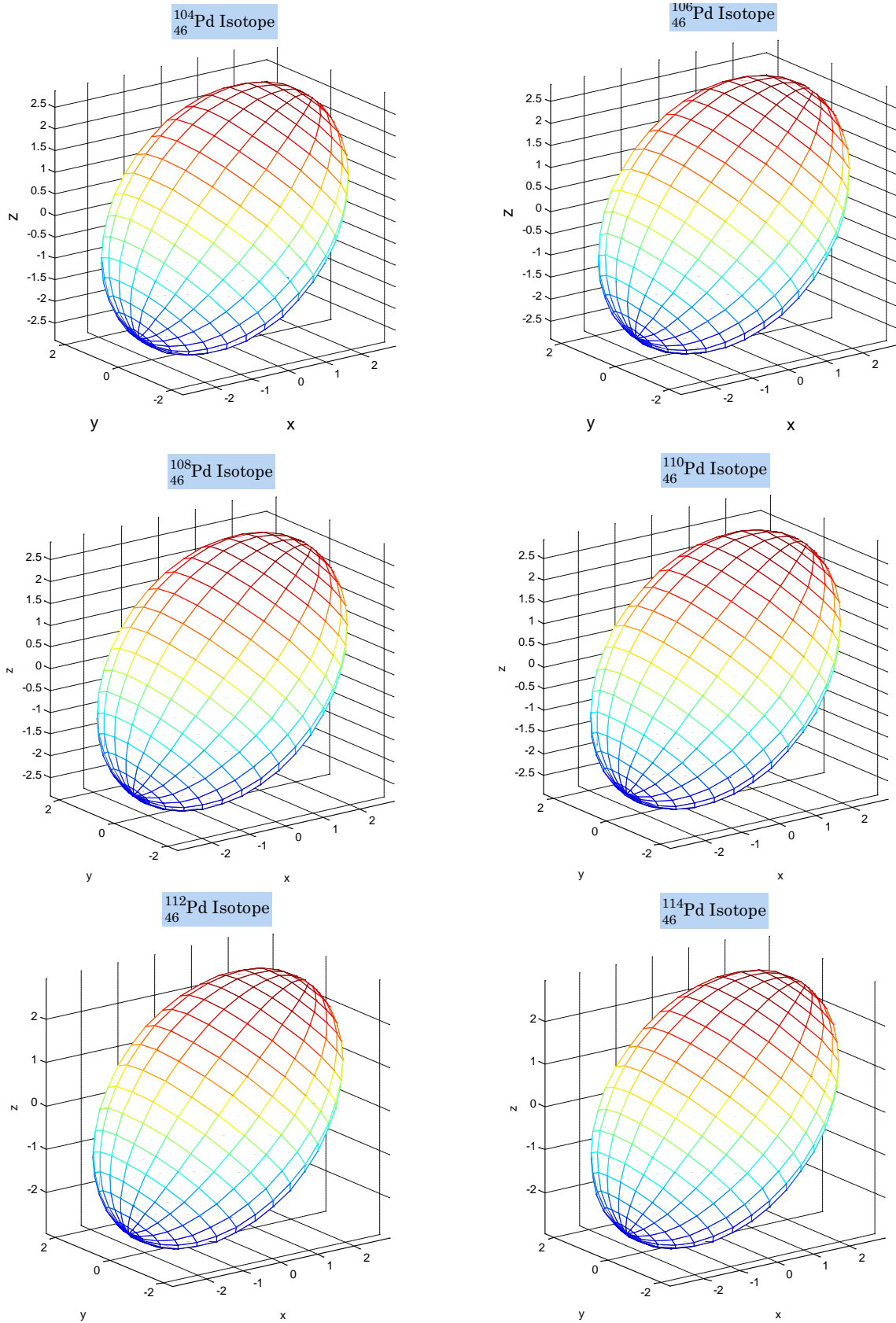


Figure (A-4): axially-symmetric quadrupole deformations, the prolate shape of Nucleus with $(x = y < z)$ (where z is the minor axis (b) (symmetric axis) and (x,y) are major axes (a) for Pd isotopes.

Appendix

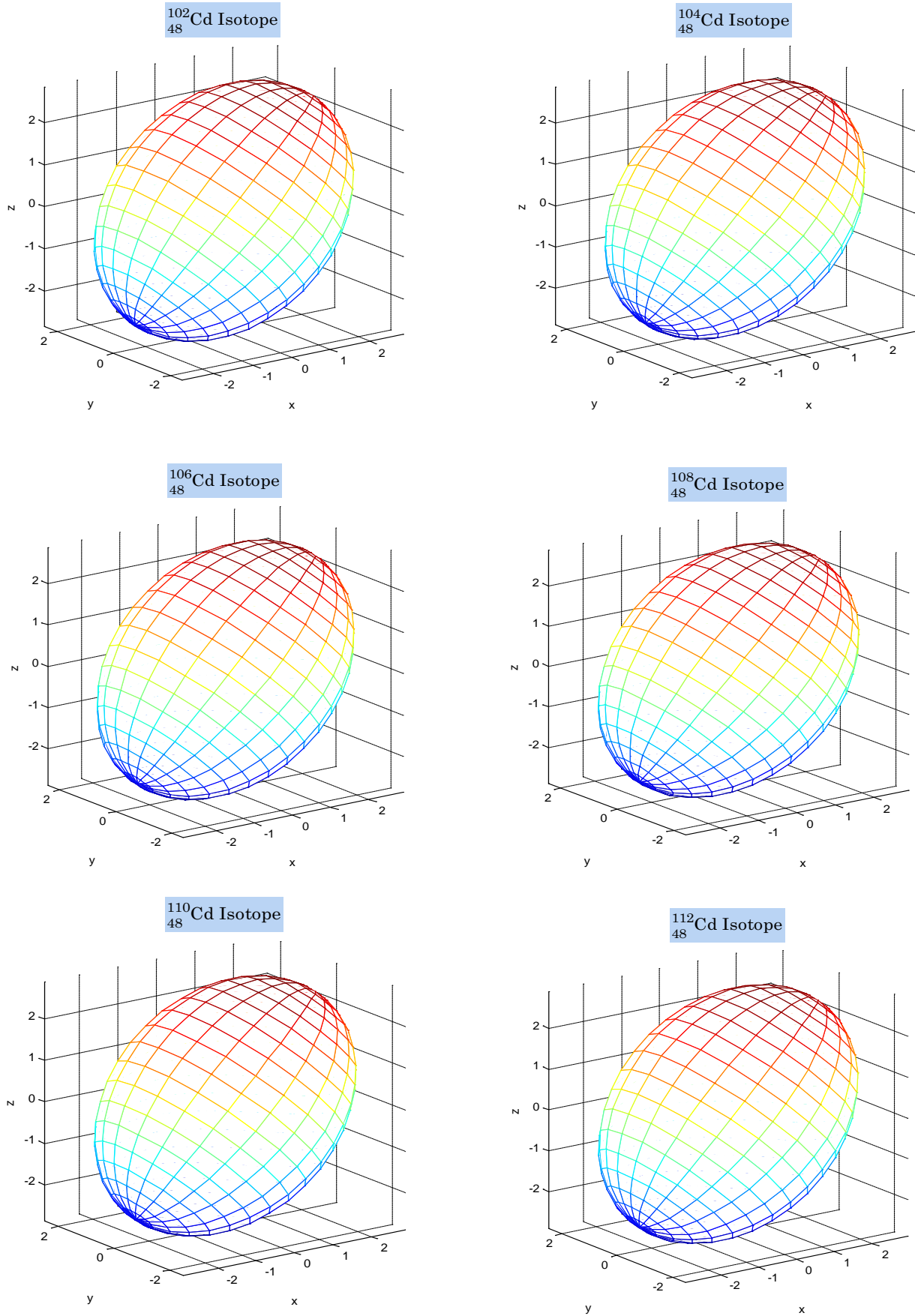


Figure (A-5): axially-symmetric quadrupole deformations, the prolate shape of Nucleus with $(x = y < z)$ (where z is the minor axis (b) (symmetric axis) and (x,y) are major axes (a) for Cd isotopes. **(to be continued)**

Appendix

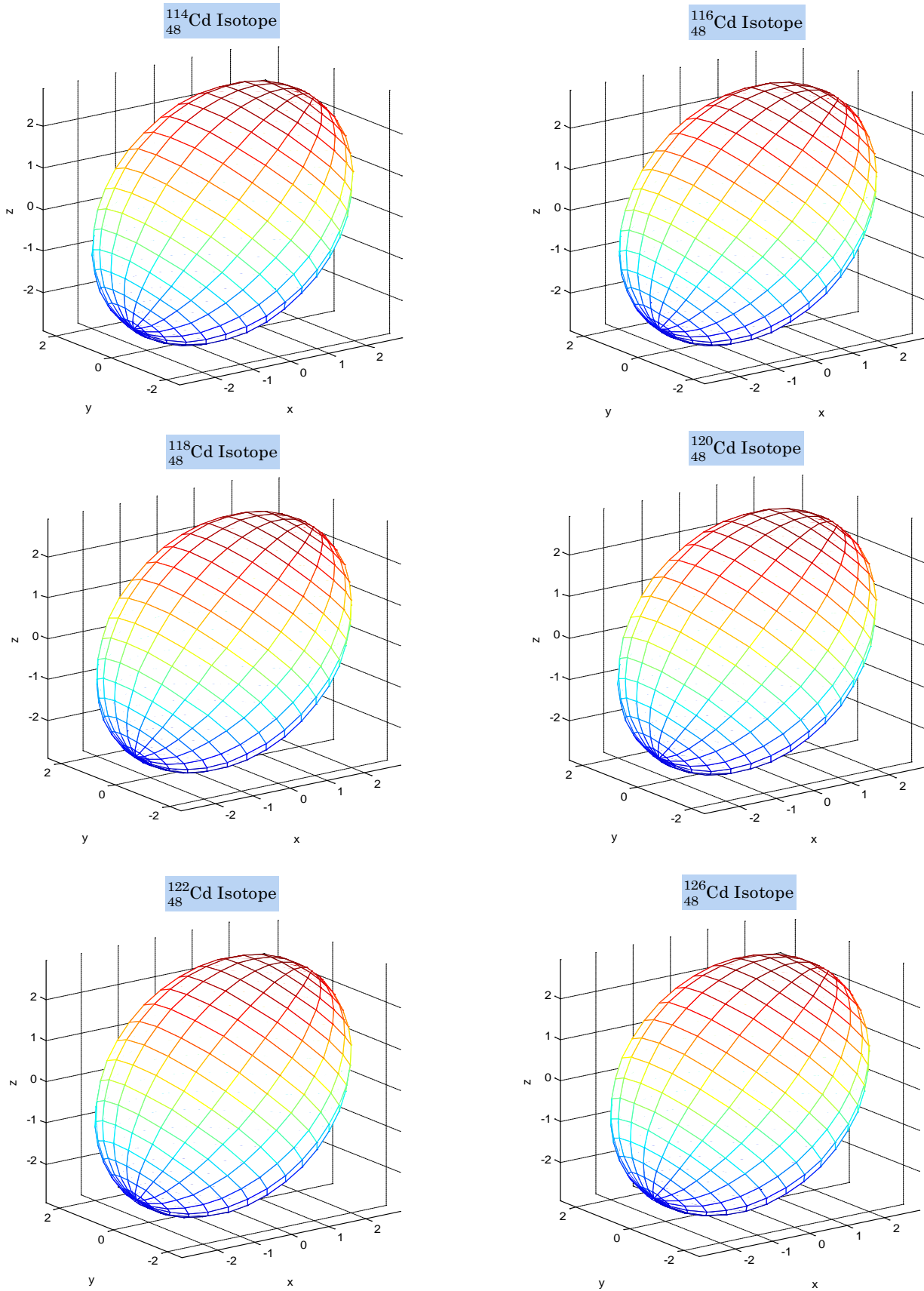


Figure (A-5): axially-symmetric quadrupole deformations, the prolate shape of Nucleus with $(x = y < z)$ (where z is the minor axis (b) (symmetric axis) and (x,y) are major axes (a) for Cd isotopes.

Appendix

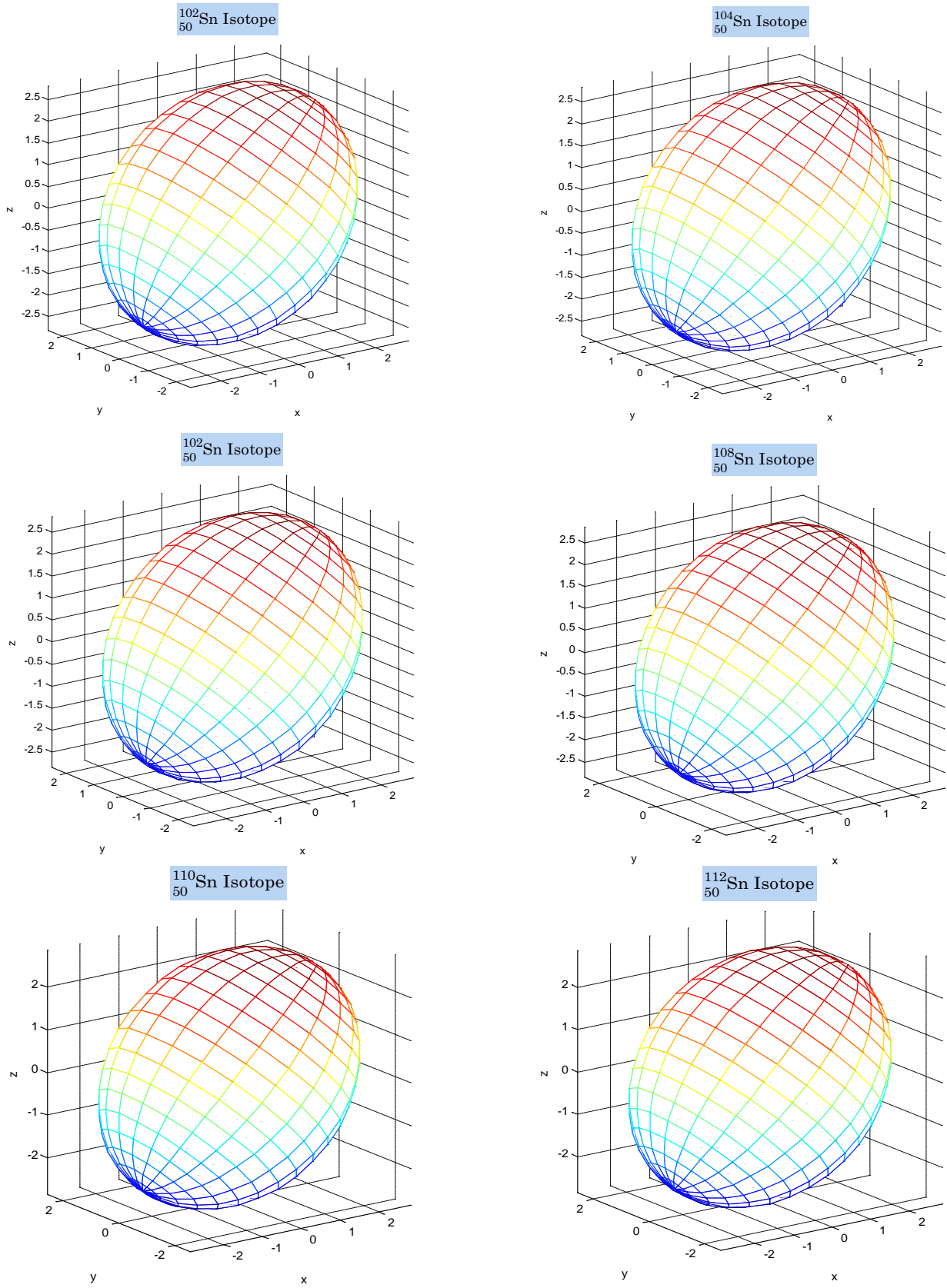


Figure (A-6): axially-symmetric quadrupole deformations, the prolate shape of Nucleus with $(x = y < z)$ (where z is the minor axis (b) (symmetric axis) and (x,y) are major axes (a) for Sn isotopes. **(to be continued)**

Appendix

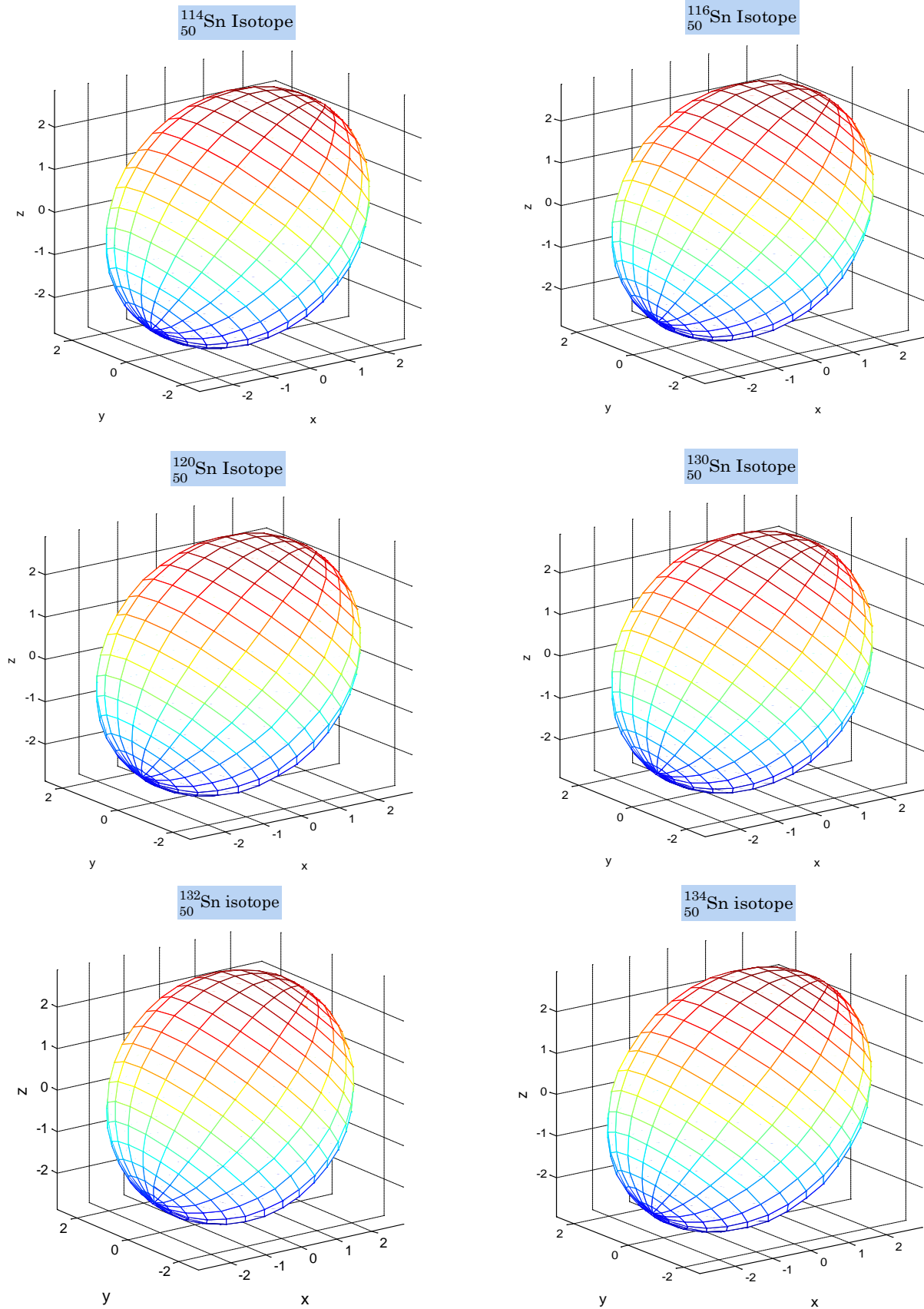


Figure (A-6): axially-symmetric quadrupole deformations, the prolate shape of Nucleus with $(x = y < z)$ (where z is the minor axis (b) (symmetric axis) and (x,y) are major axes (a) for Sn isotopes.

Appendix

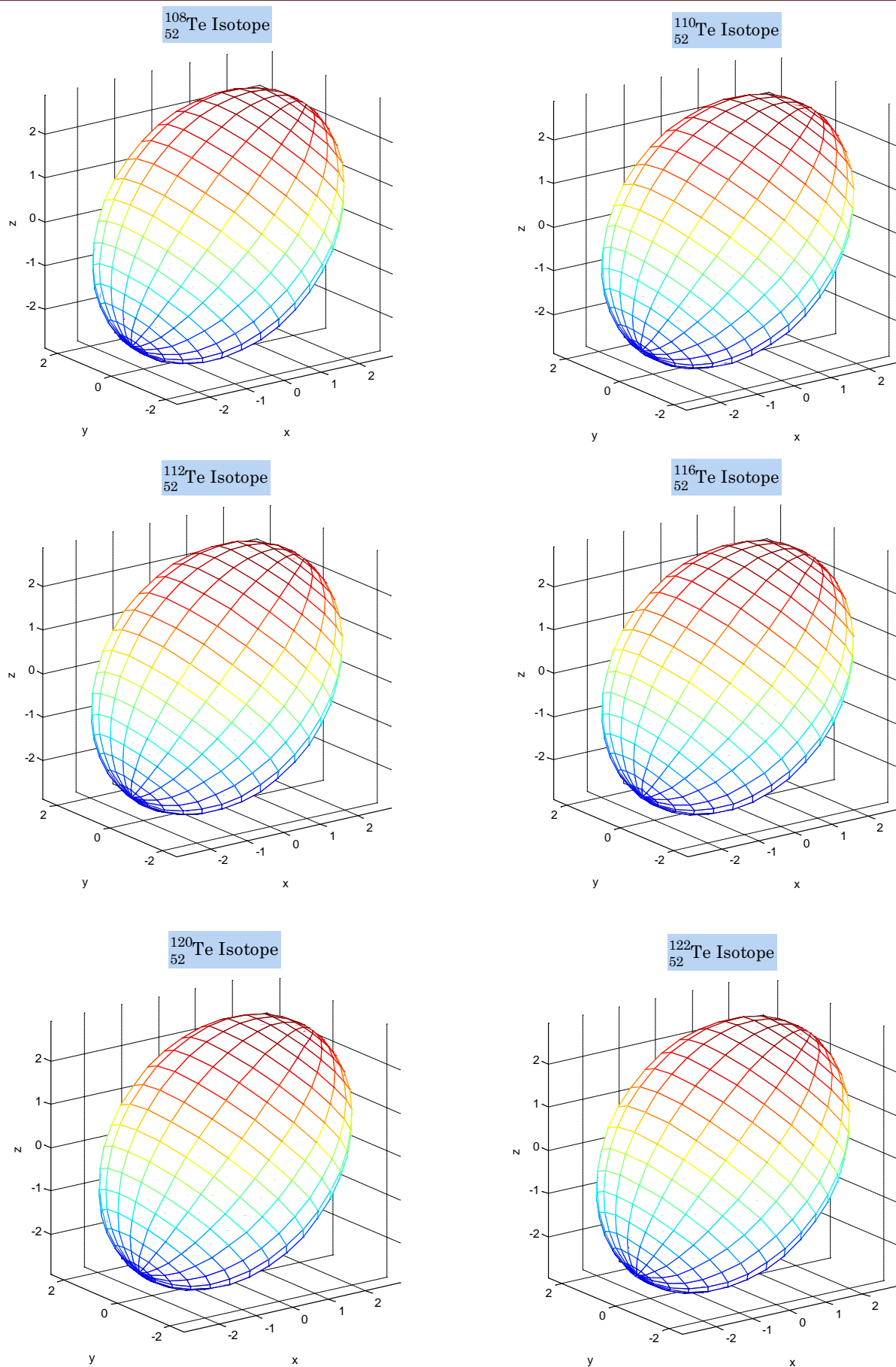


Figure (A-7): axially-symmetric quadrupole deformations, the prolate shape of Nucleus with $(x = y < z)$ (where z is the minor axis (b) (symmetric axis) and (x,y) are major axes (a) for Te isotopes. **(to be continued)**

Appendix

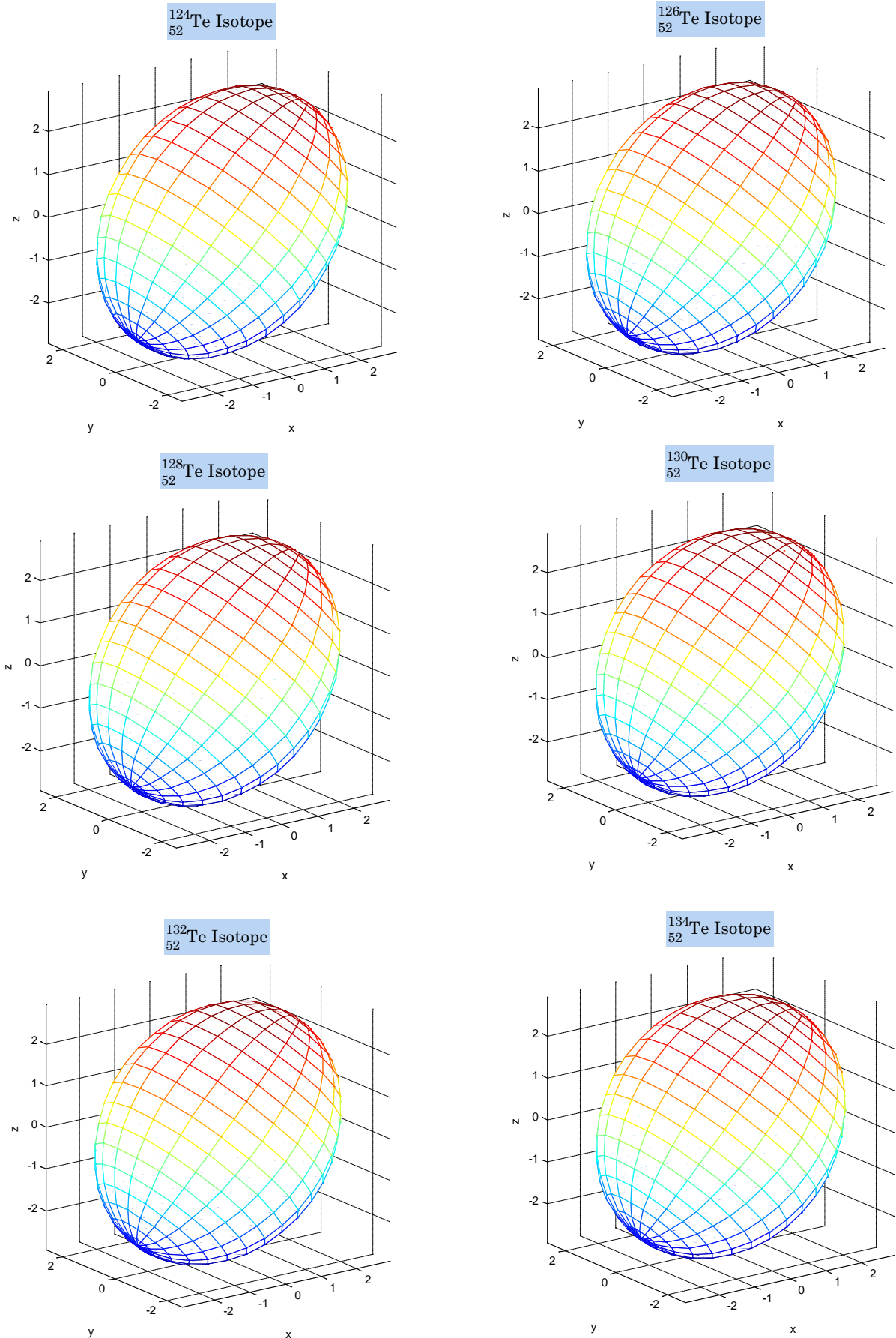


Figure (A-7): axially-symmetric quadrupole deformations, the prolate shape of Nucleus with $(x = y < z)$ (where z is the minor axis (b) (symmetric axis) and (x,y) are major axes (a) for Te isotopes.

Appendix

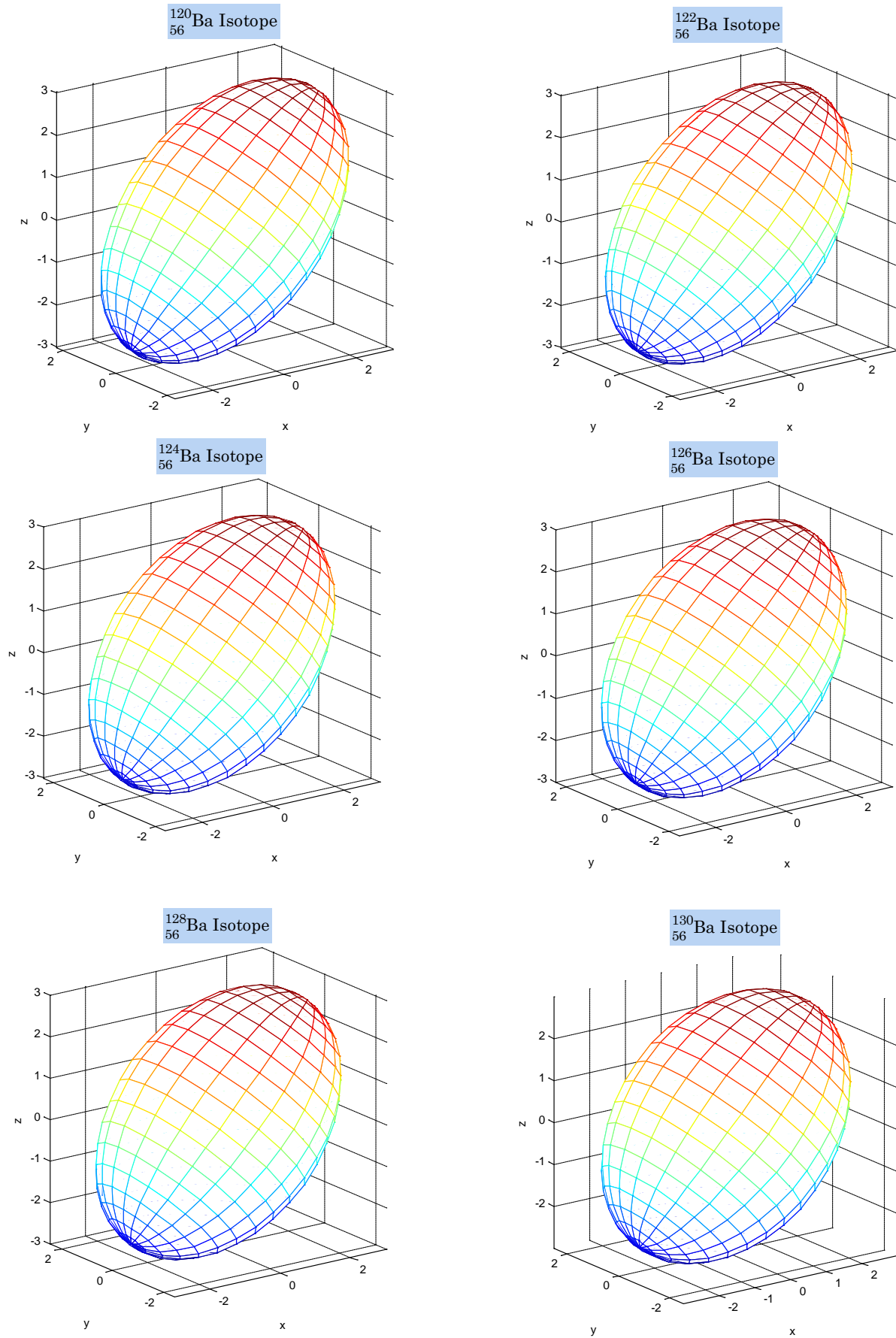


Figure (A-8): axially-symmetric quadrupole deformations, the prolate shape of Nucleus with $(x = y < z)$ (where z is the minor axis (b) (symmetric axis) and (x,y) are major axes (a) for Ba isotopes. **(to be continued)**

Appendix

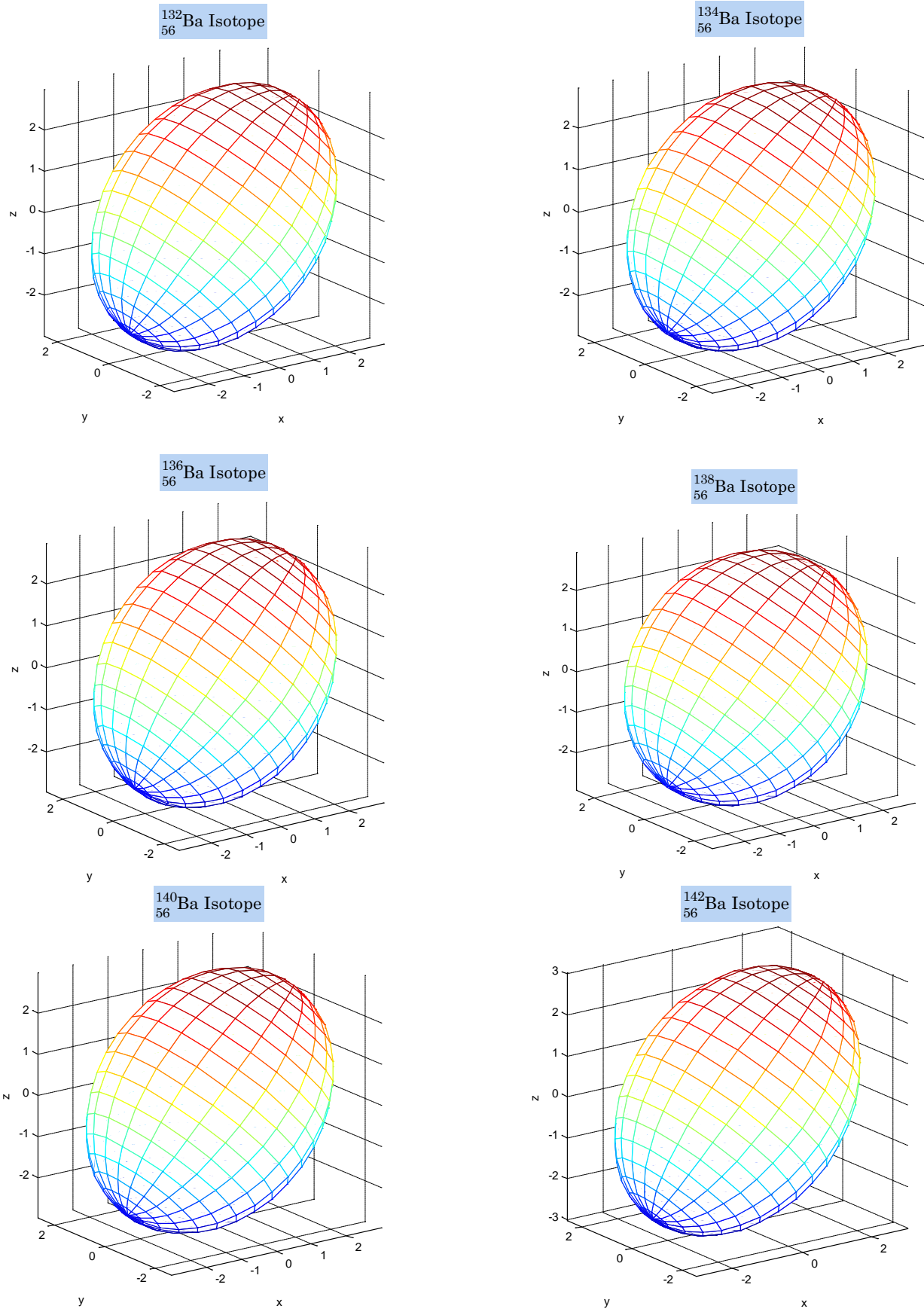


Figure (A-8): axially-symmetric quadrupole deformations, the prolate shape of Nucleus with $(x = y < z)$ (where z is the minor axis (b) (symmetric axis) and (x,y) are major axes (a) for Ba isotopes.

Appendix

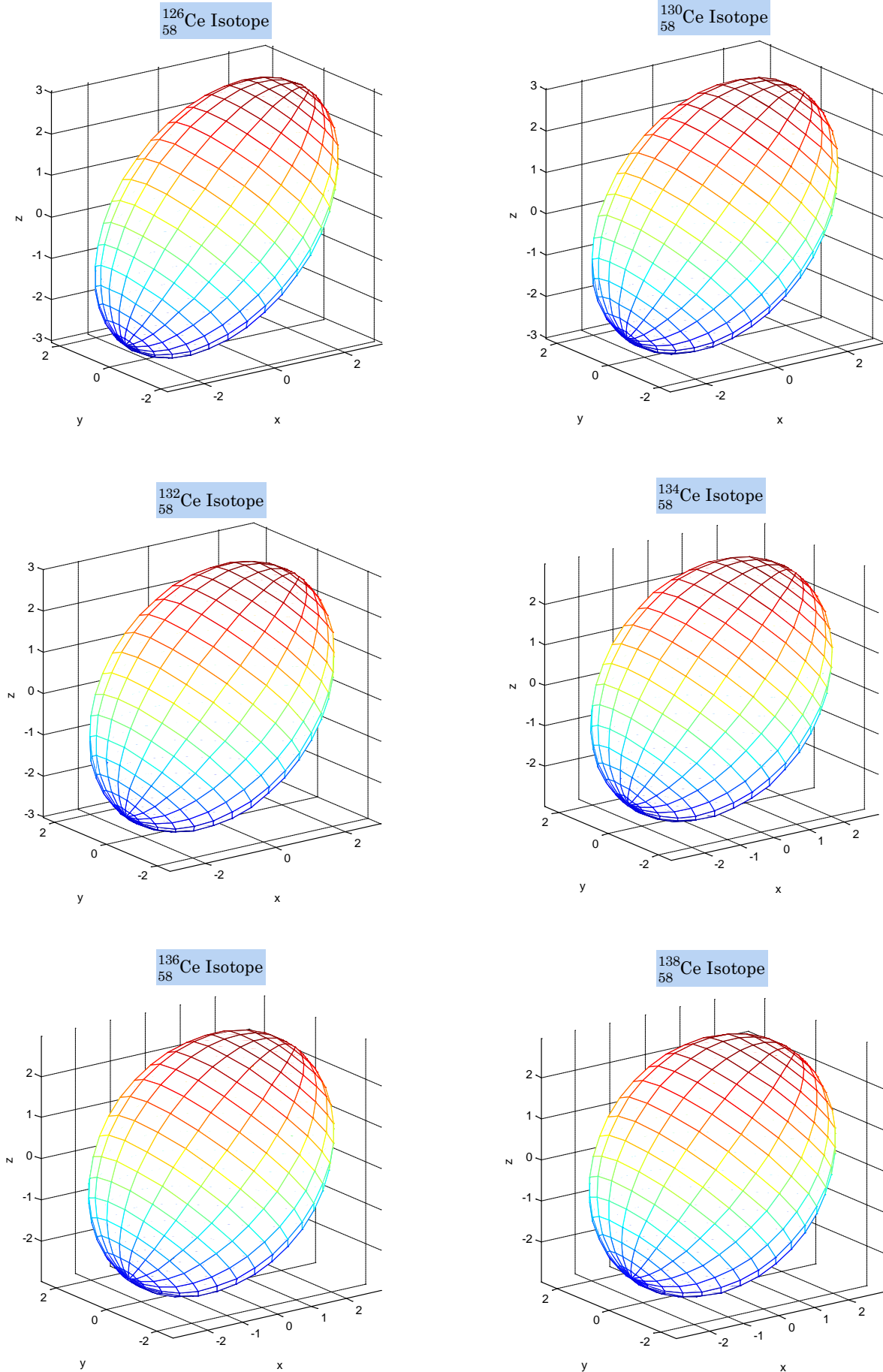


Figure (A-9): axially-symmetric quadrupole deformations, the prolate shape of Nucleus with $(x = y < z)$ (where z is the minor axis (b) (symmetric axis) and (x,y) are major axes (a) for Ce isotopes.

(to be continued)

Appendix

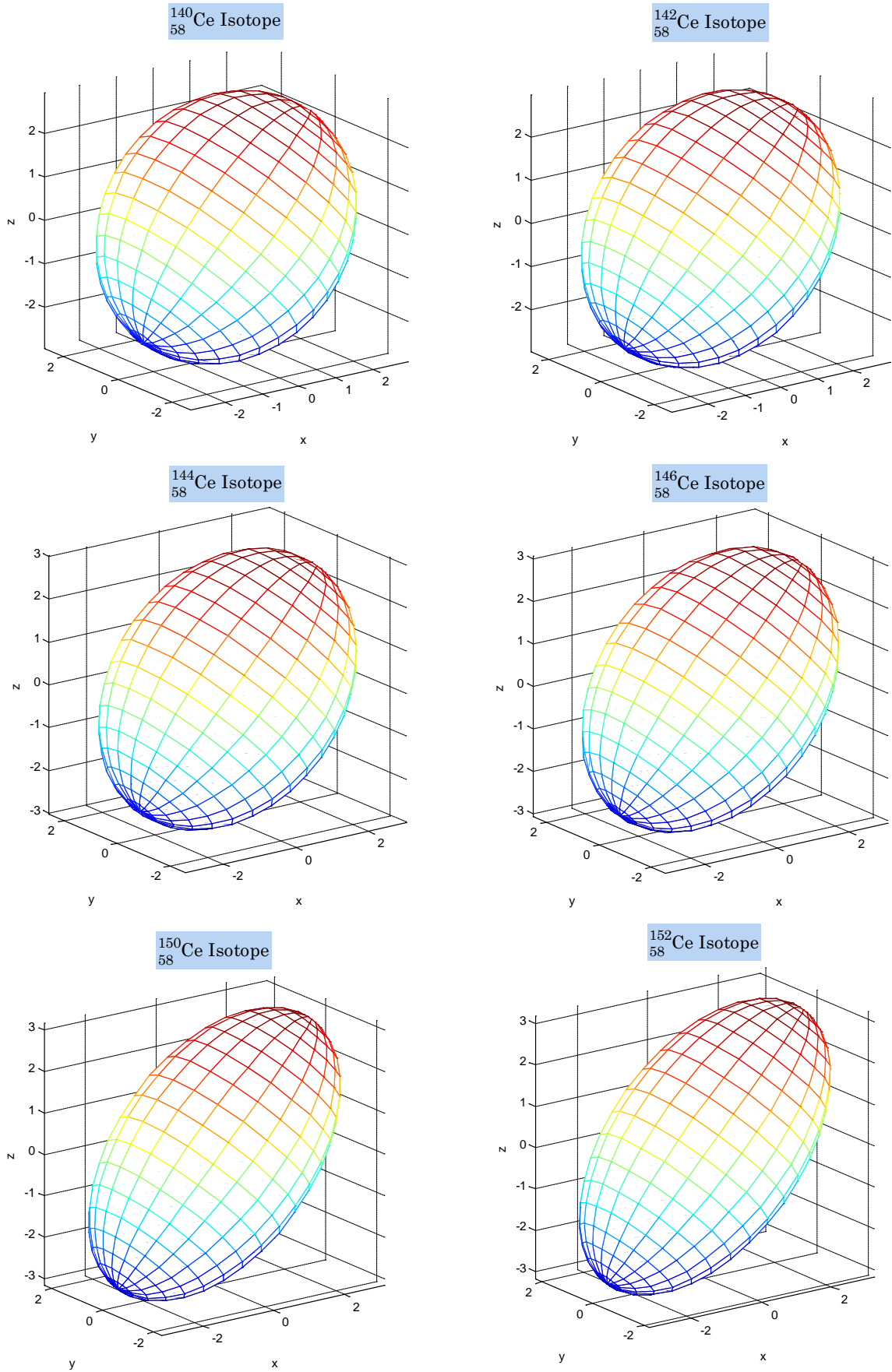


Figure (A-9): axially-symmetric quadrupole deformations, the prolate shape of Nucleus with $(x = y < z)$ (where z is the minor axis (b) (symmetric axis) and (x,y) are major axes (a) for Ce isotopes.

Appendix

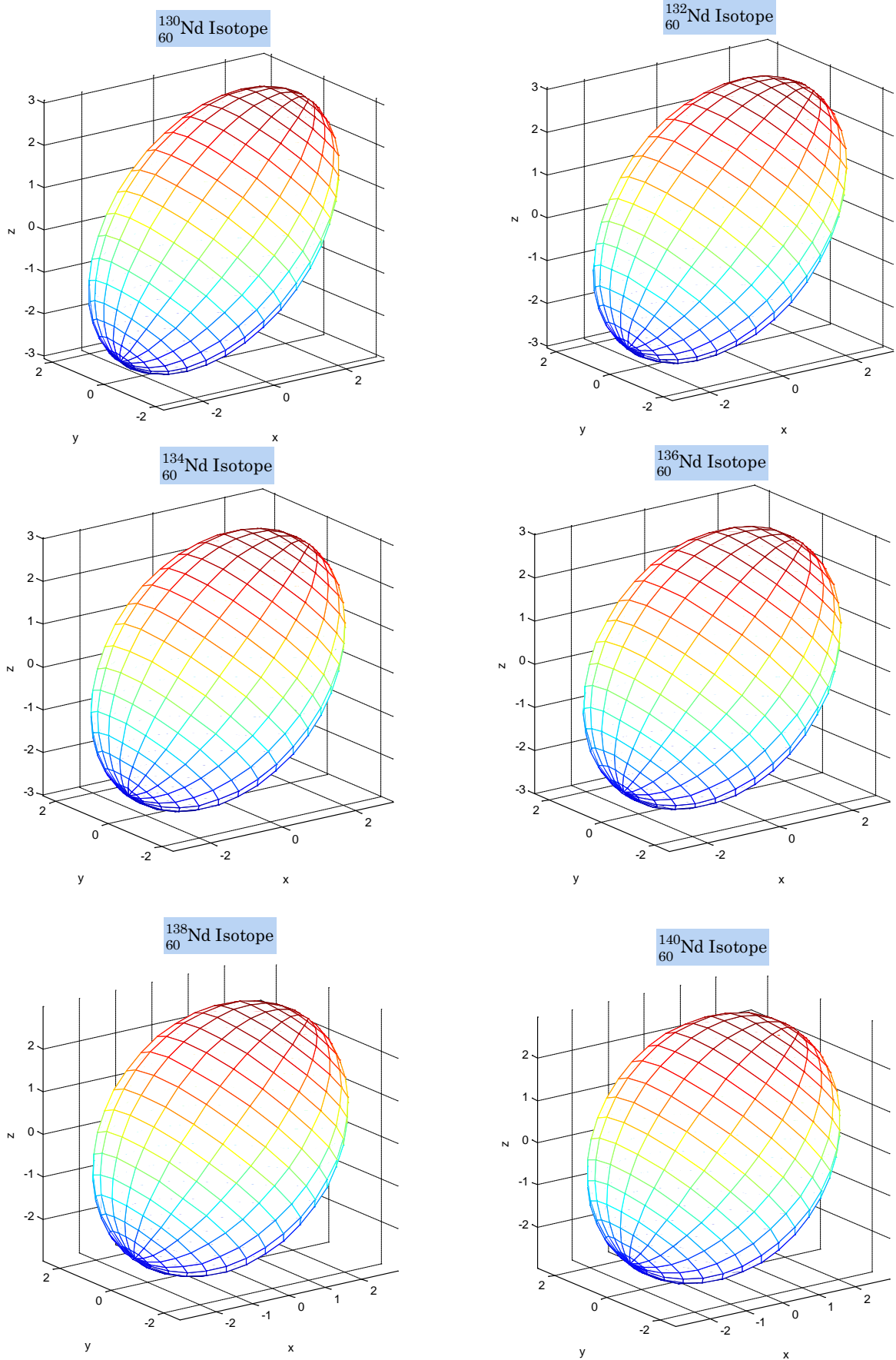


Figure (A-10): axially-symmetric quadrupole deformations, the prolate shape of Nucleus with $(x = y < z)$ (where z is the minor axis (b) (symmetric axis) and (x,y) are major axes (a) for Nd isotopes. **(to be continued)**

Appendix

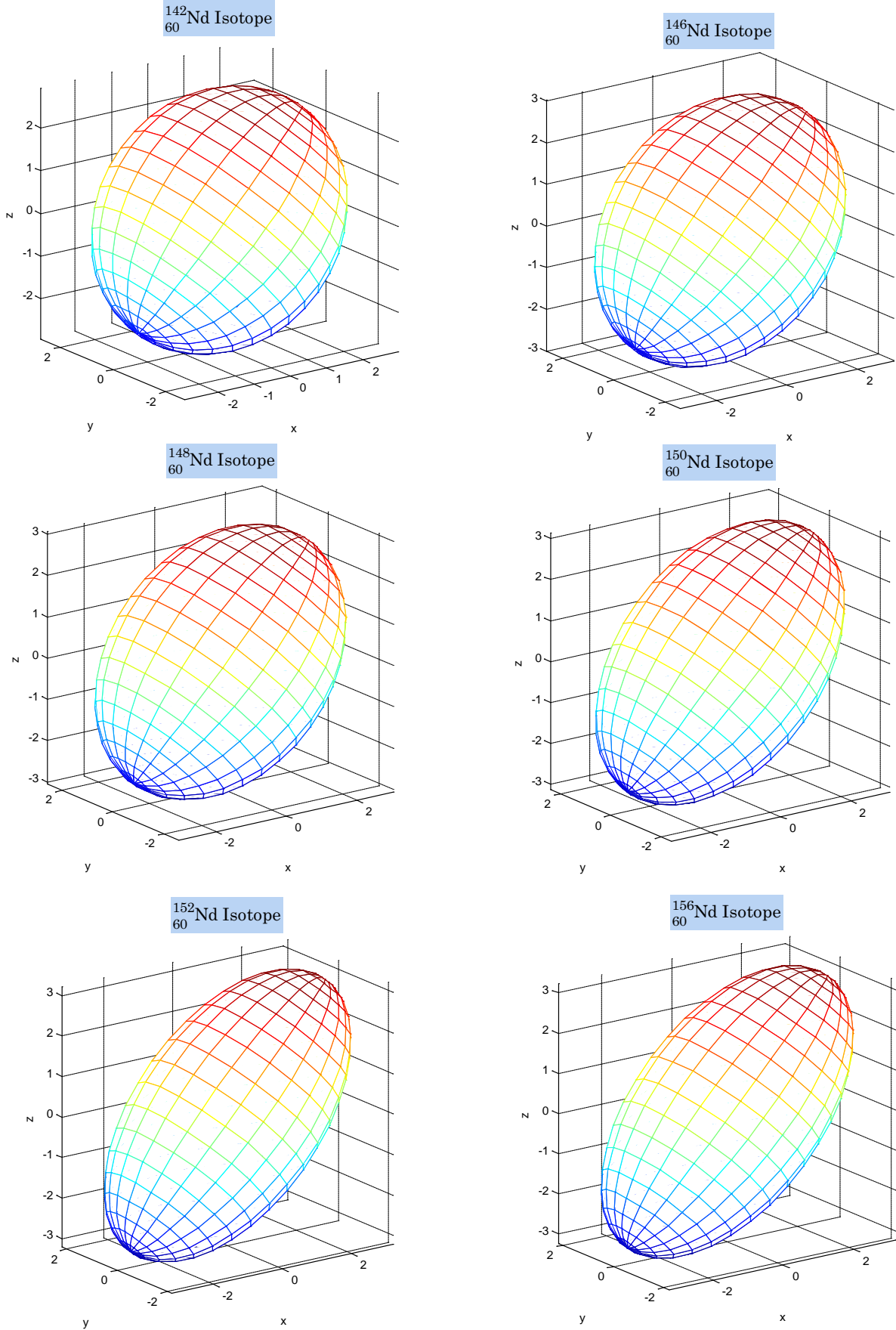


Figure (A-10): axially-symmetric quadrupole deformations, the prolate shape of Nucleus with $(x = y < z)$ (where z is the minor axis (b) (symmetric axis) and (x,y) are major axes (a) for Nd isotopes.

Appendix

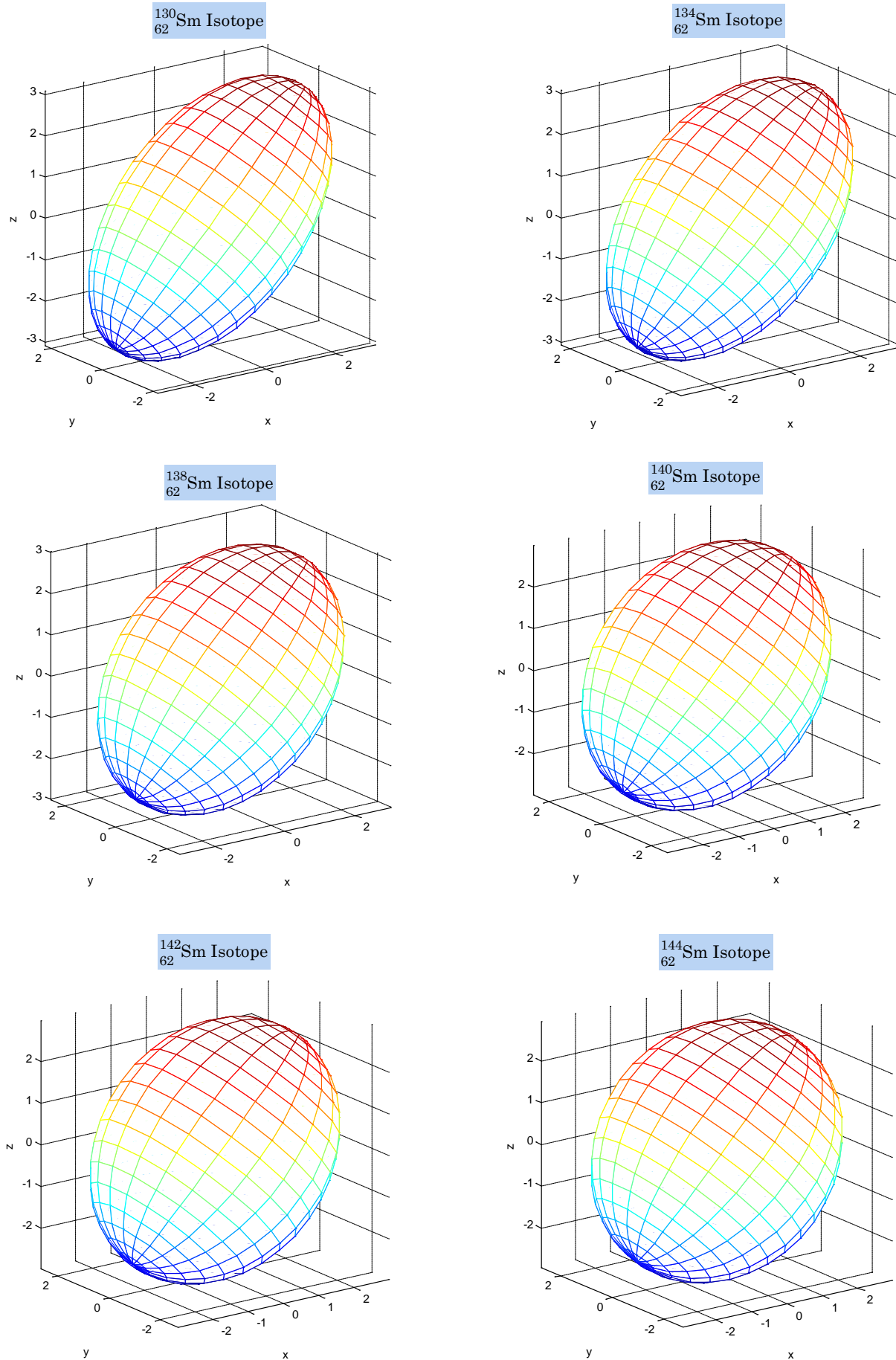


Figure (A-11): axially-symmetric quadrupole deformations, the prolate shape of Nucleus with $(x = y < z)$ (where z is the minor axis (b) (symmetric axis) and (x,y) are major axes (a) for Sm isotopes.

(to be continued)

Appendix

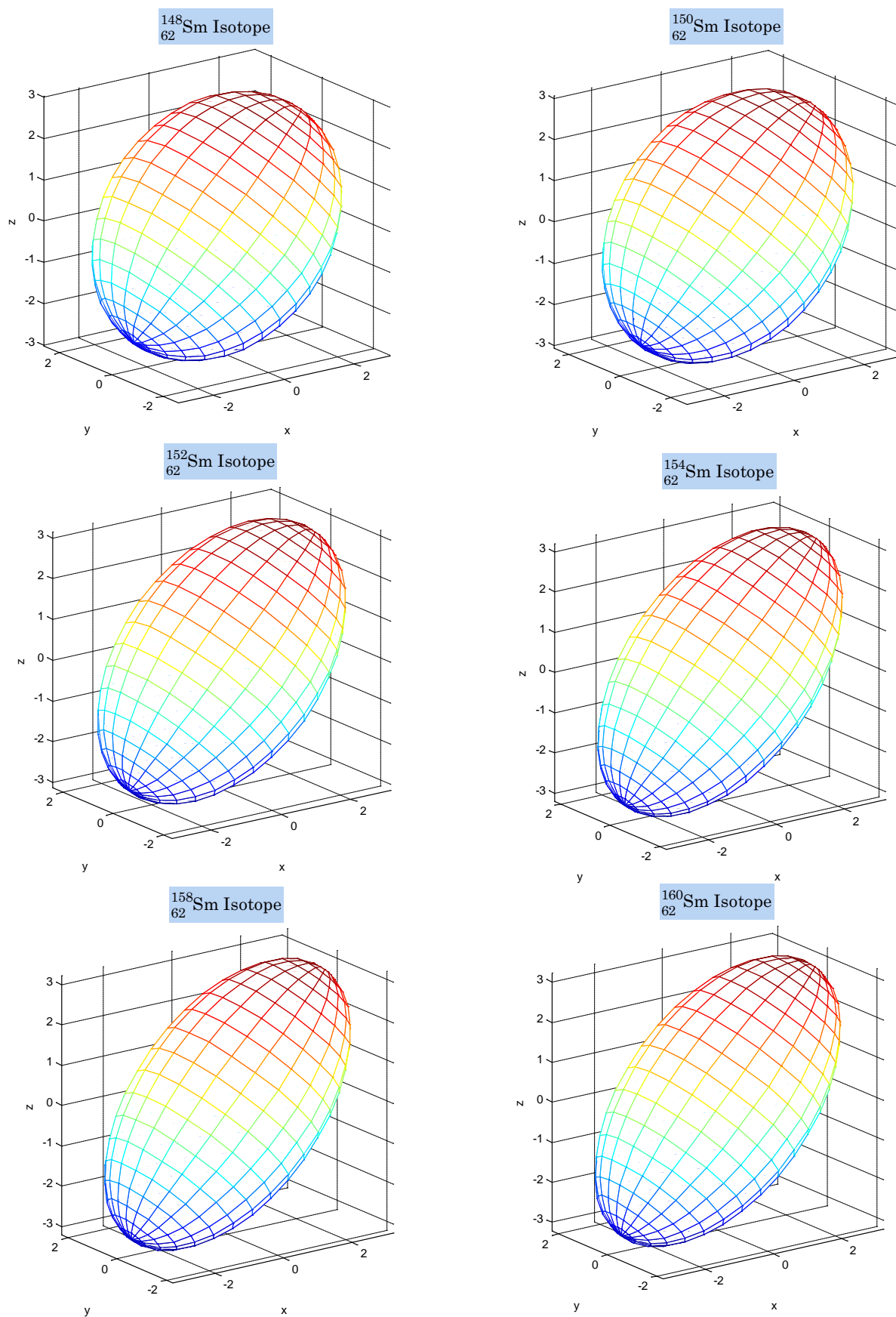


Figure (A-11): axially-symmetric quadrupole deformations, the prolate shape of Nucleus with ($x = y < z$) (where z is the minor axis (b) (symmetric axis) and (x,y) are major axes (a) for Sm isotopes.

Appendix

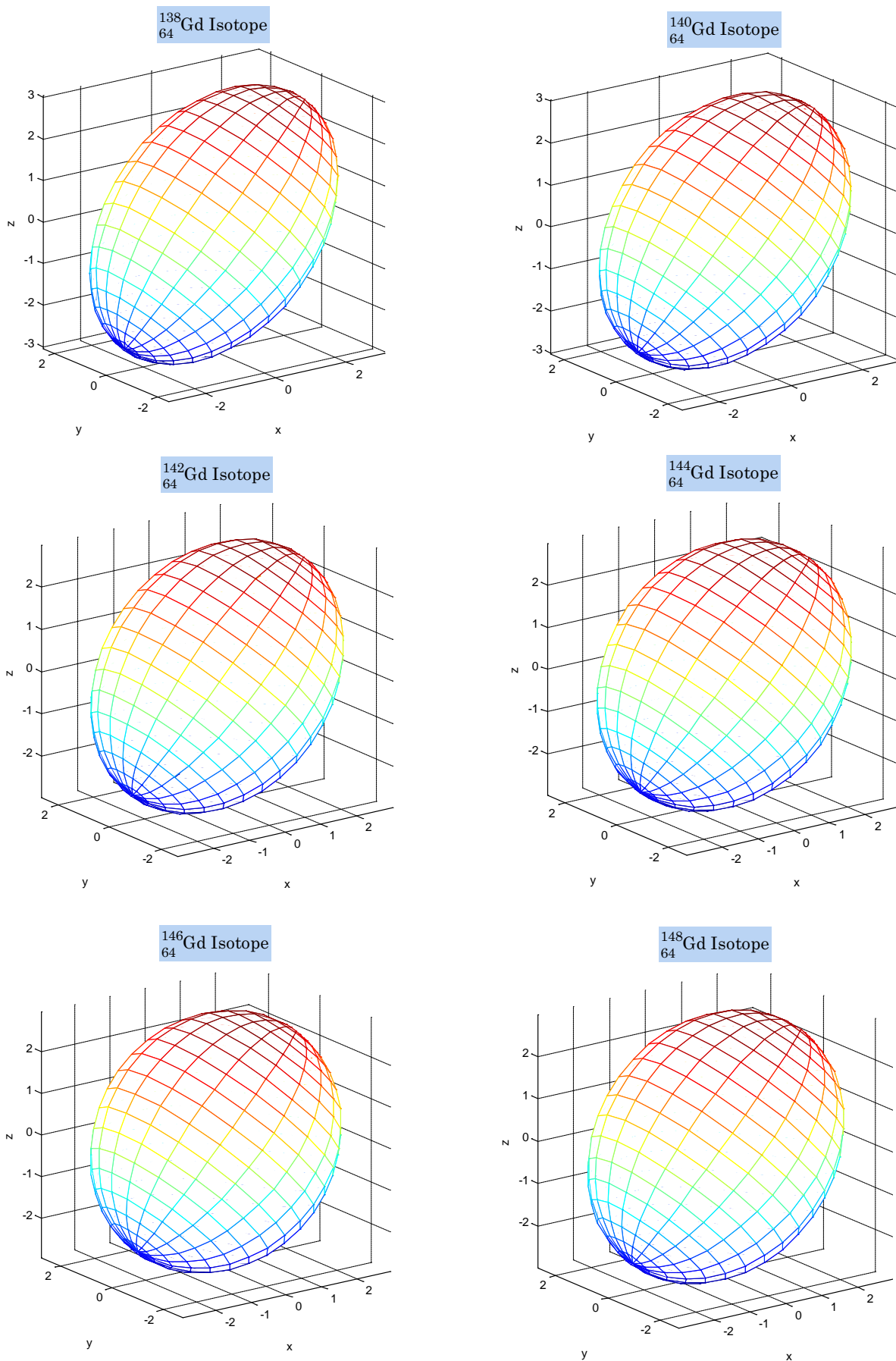


Figure (A-12): axially-symmetric quadrupole deformations, the prolate shape of Nucleus with $(x = y < z)$ (where z is the minor axis (b) (symmetric axis) and (x, y) are major axes (a) for Gd isotopes. **(to be continued)**

Appendix

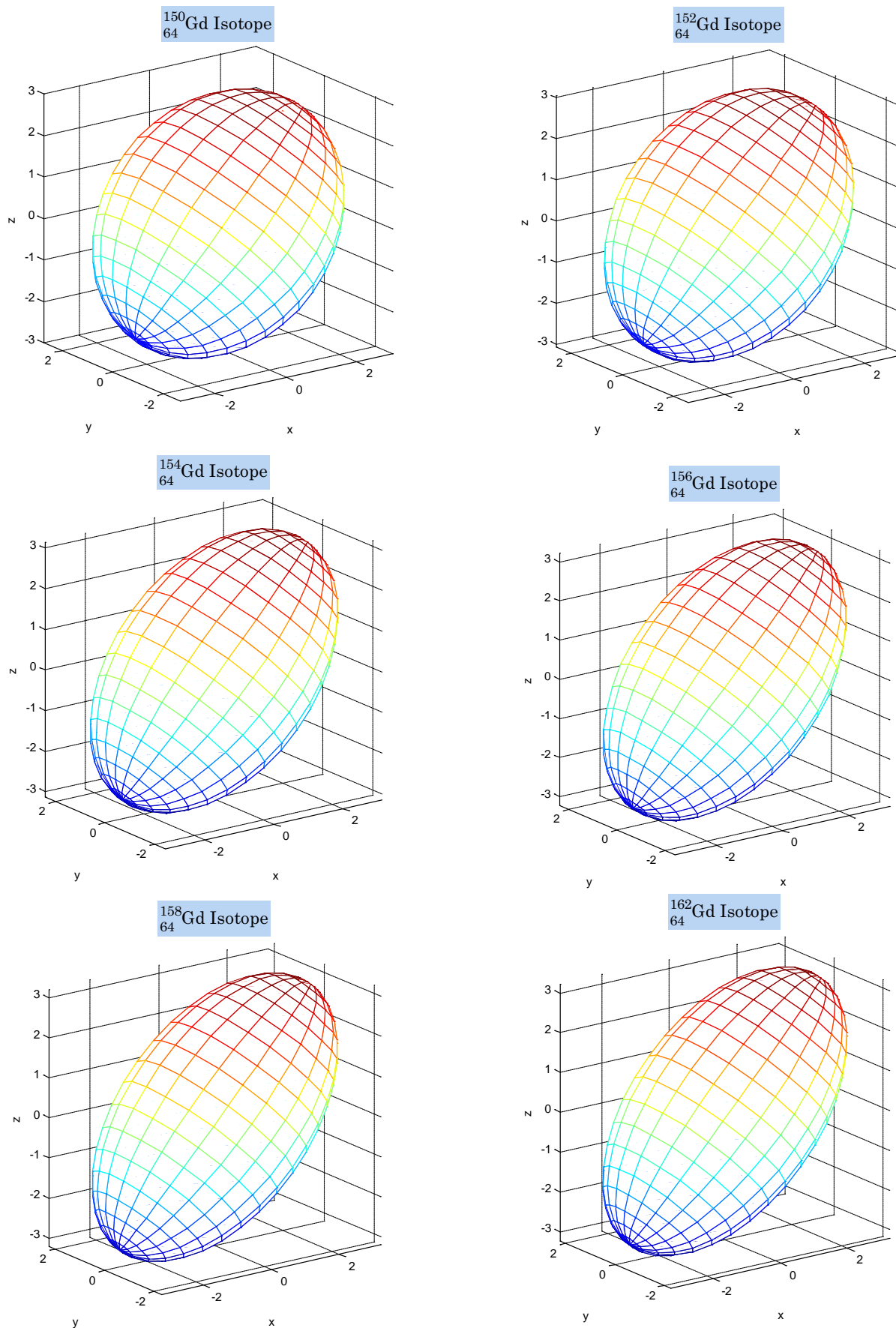


Figure (A-12): axially-symmetric quadrupole deformations, the prolate shape of Nucleus with ($x = y < z$) (where z is the minor axis (b) (symmetric axis) and (x,y) are major axes (a) for Gd isotopes.

Appendix

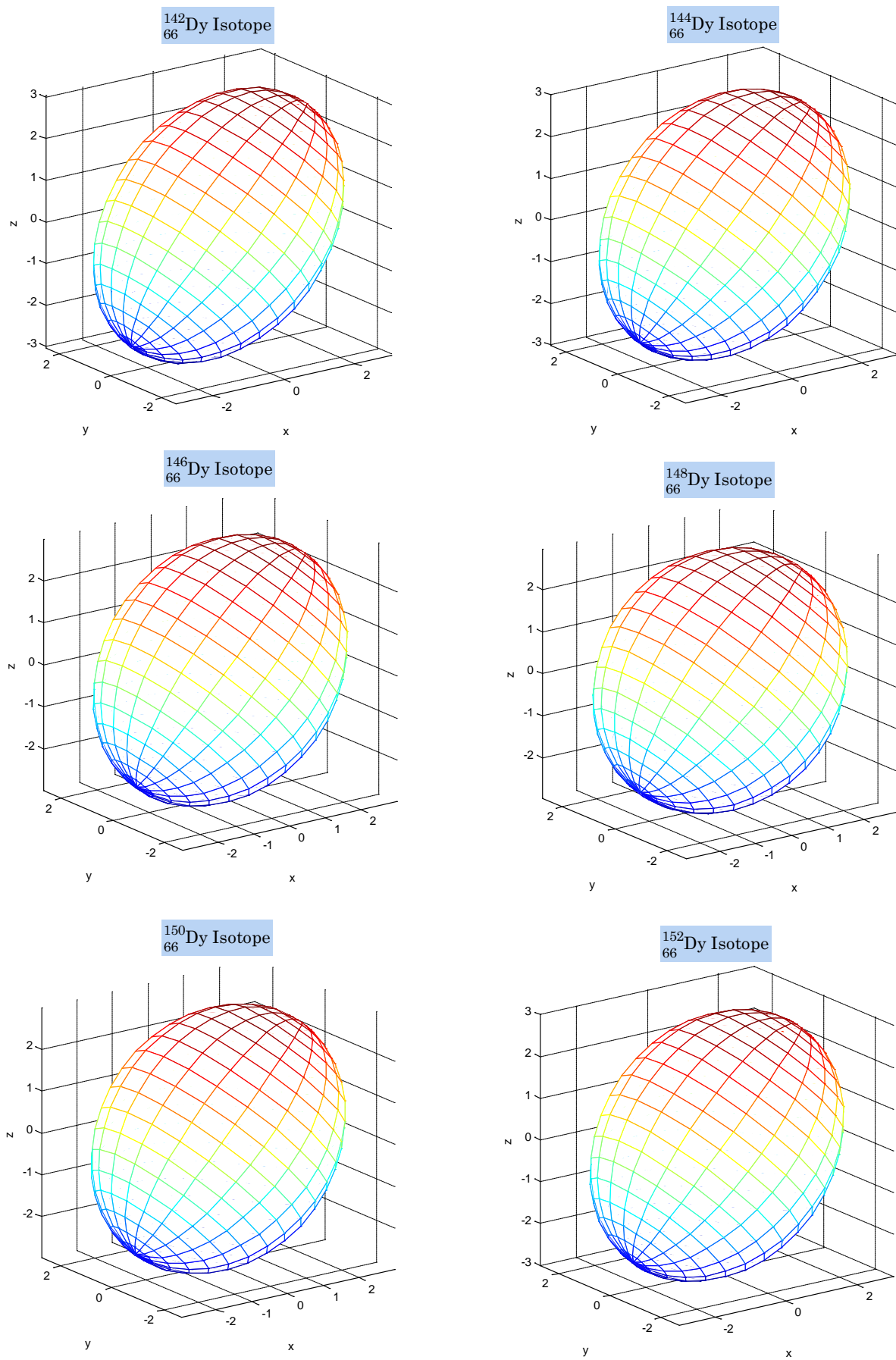


Figure (A-13): axially-symmetric quadrupole deformations, the prolate shape of Nucleus with $(x = y < z)$ (where z is the minor axis (b) (symmetric axis) and (x,y) are major axes (a) for Dy isotopes. **(to be continued)**

Appendix

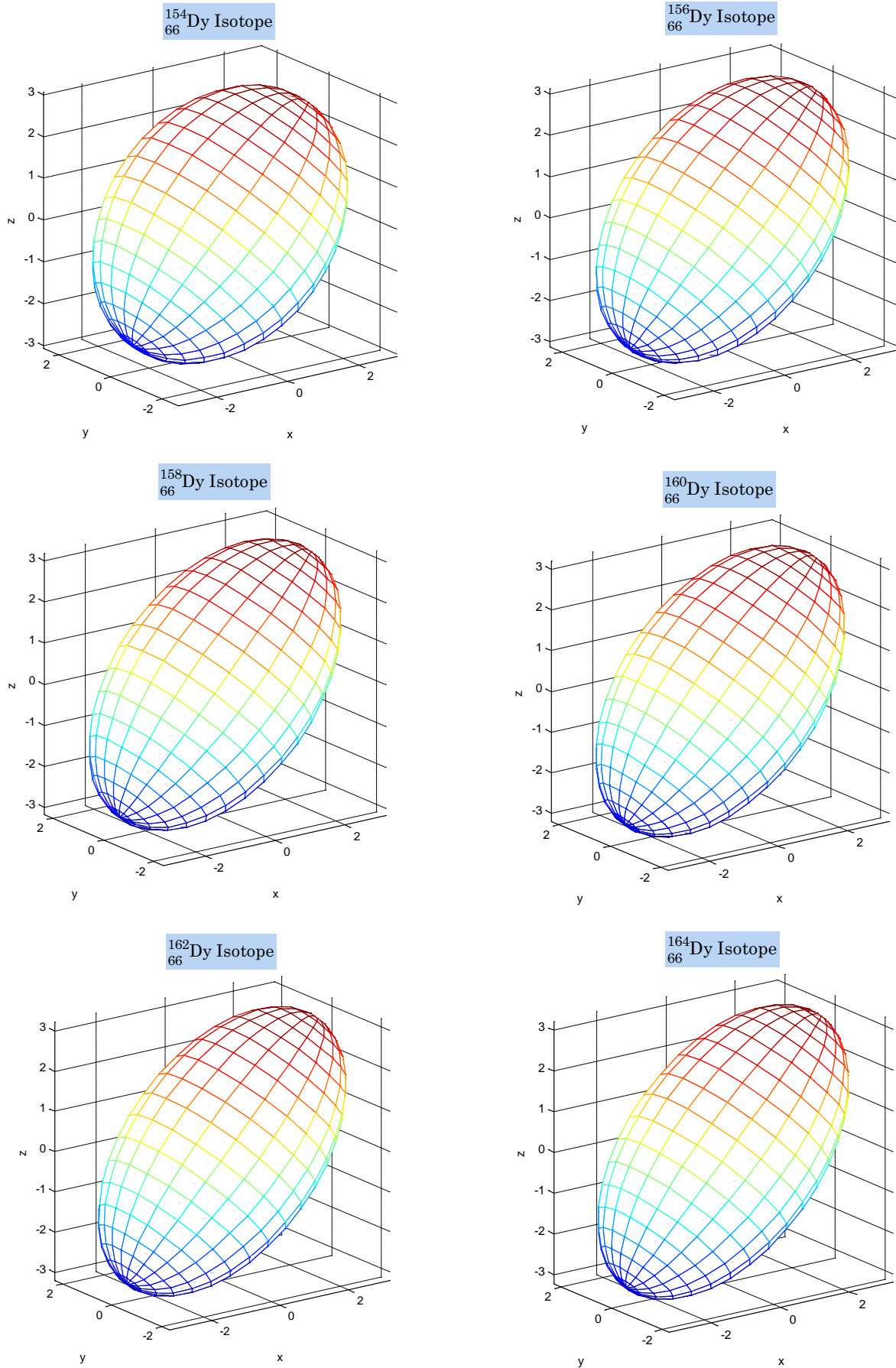


Figure (A-13): axially-symmetric quadrupole deformations, the prolate shape of Nucleus with $(x = y < z)$ (where z is the minor axis (b) (symmetric axis) and (x,y) are major axes (a) for Dy isotopes.

Appendix

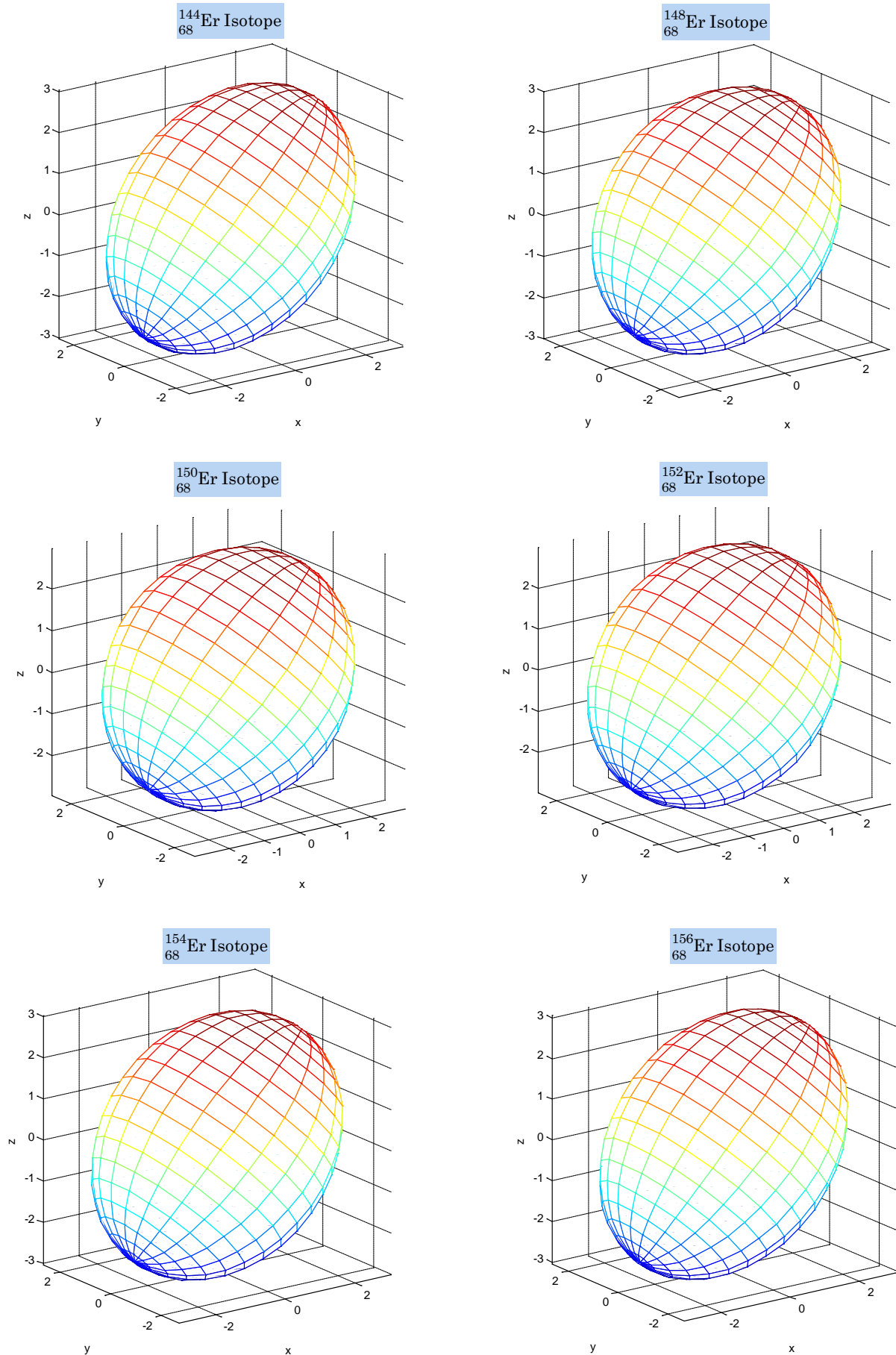


Figure (A-14): axially-symmetric quadrupole deformations, the prolate shape of Nucleus with $(x = y < z)$ (where z is the minor axis (b) (symmetric axis) and (x,y) are major axes (a) for Er isotopes. **(to be continued)**

Appendix

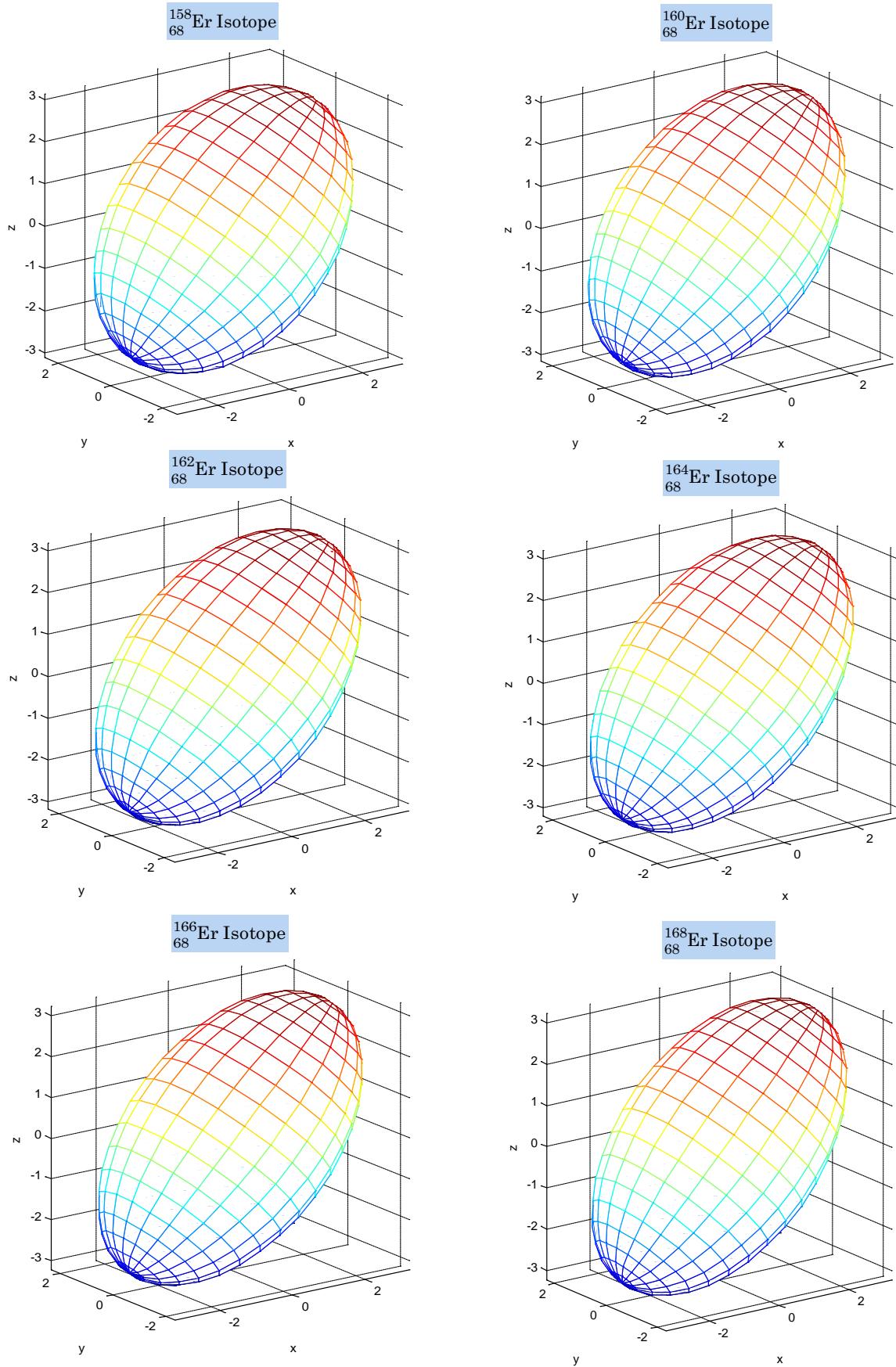


Figure (A-14): axially-symmetric quadrupole deformations, the prolate shape of Nucleus with $(x = y < z)$ (where z is the minor axis (b) (symmetric axis) and (x,y) are major axes (a) for Er isotopes.

Appendix

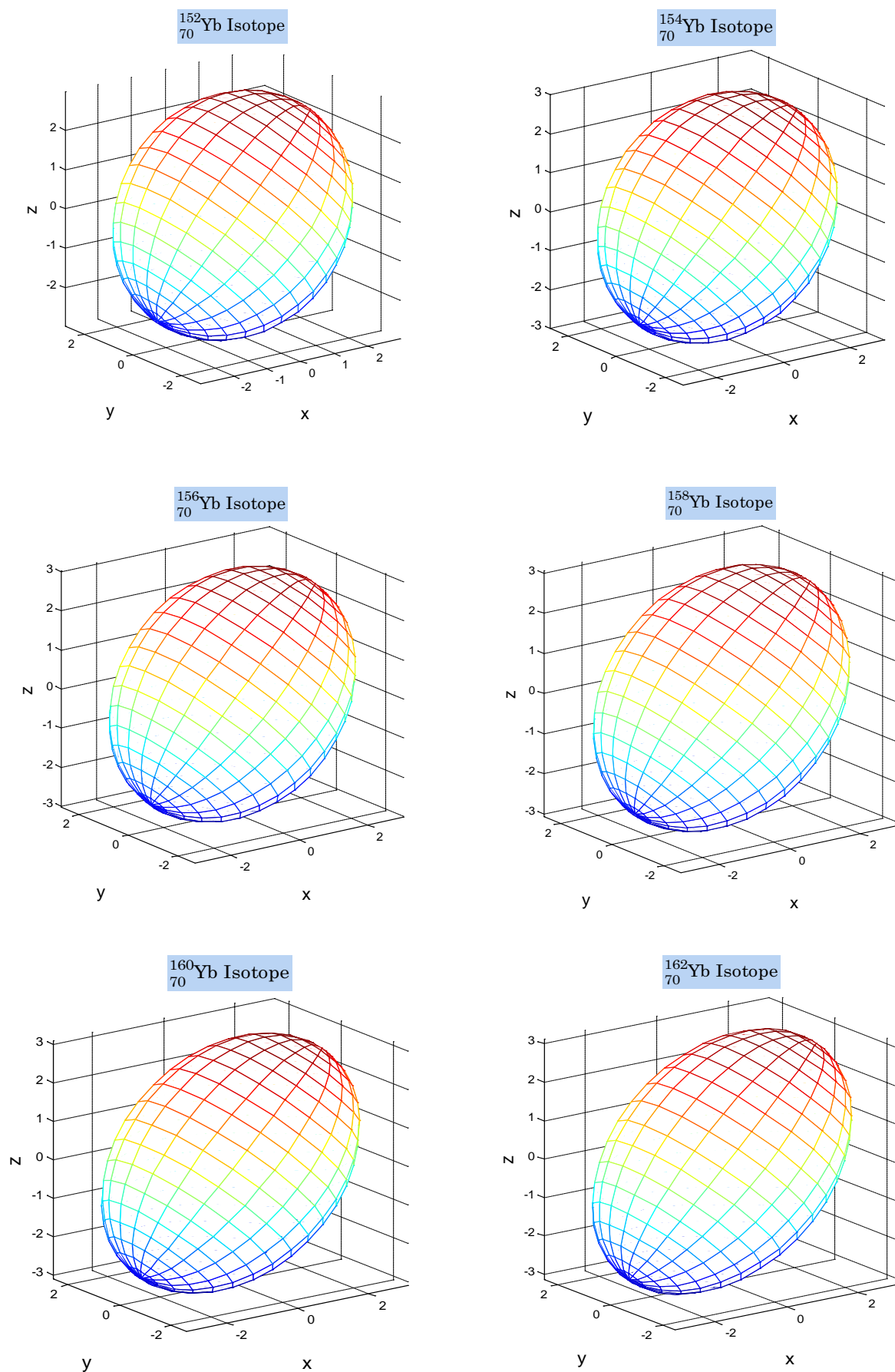


Figure (A-15): axially-symmetric quadrupole deformations, the prolate shape of Nucleus with $(x = y < z)$ (where z is the minor axis (b) (symmetric axis) and (x,y) are major axes (a) for Yb isotopes. **(to be continued)**

Appendix

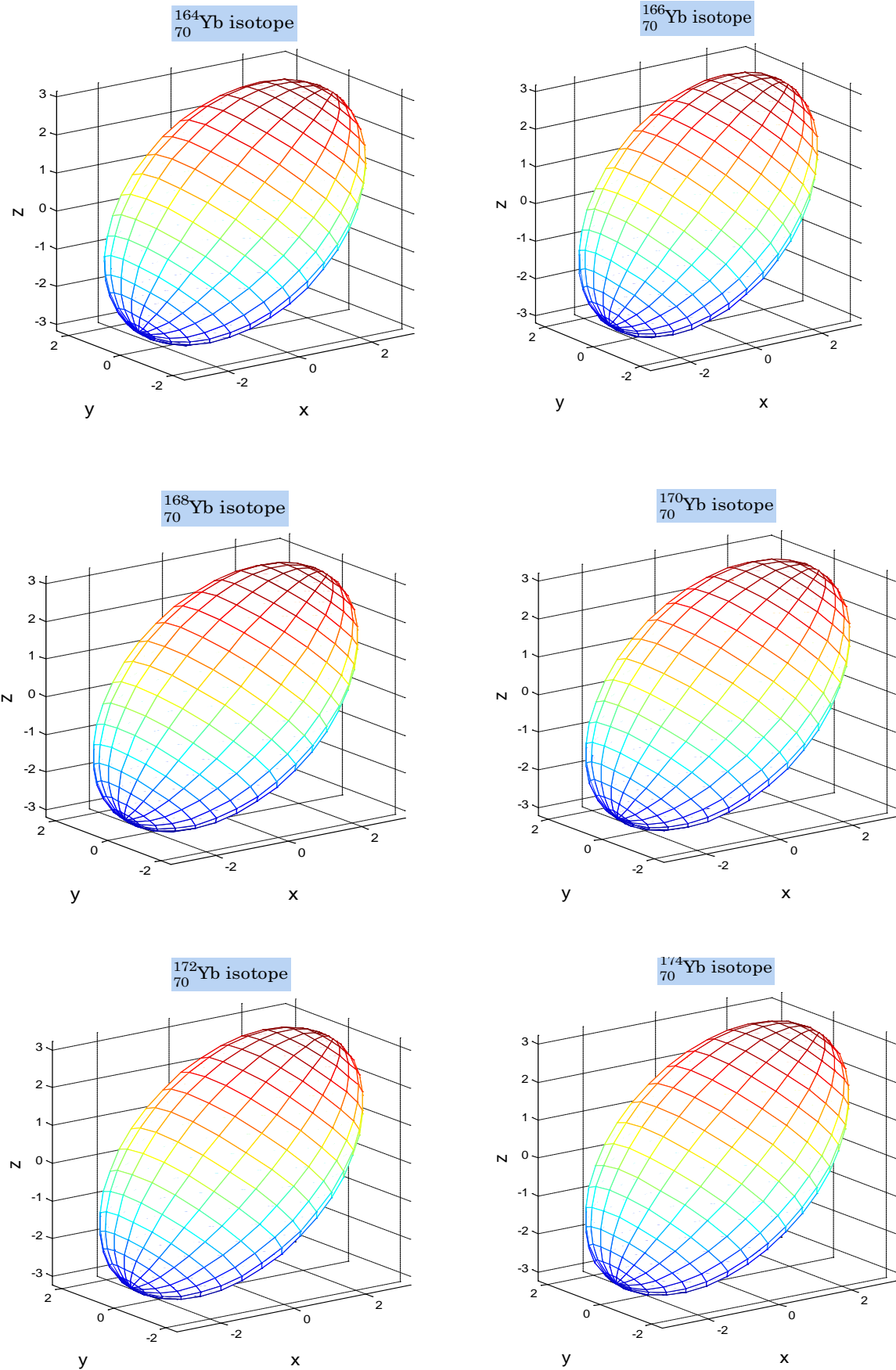


Figure (A-15): axially-symmetric quadrupole deformations, the prolate shape of Nucleus with $(x = y < z)$ (where z is the minor axis (b) (symmetric axis) and (x,y) are major axes (a) for Yb isotopes.

Appendix

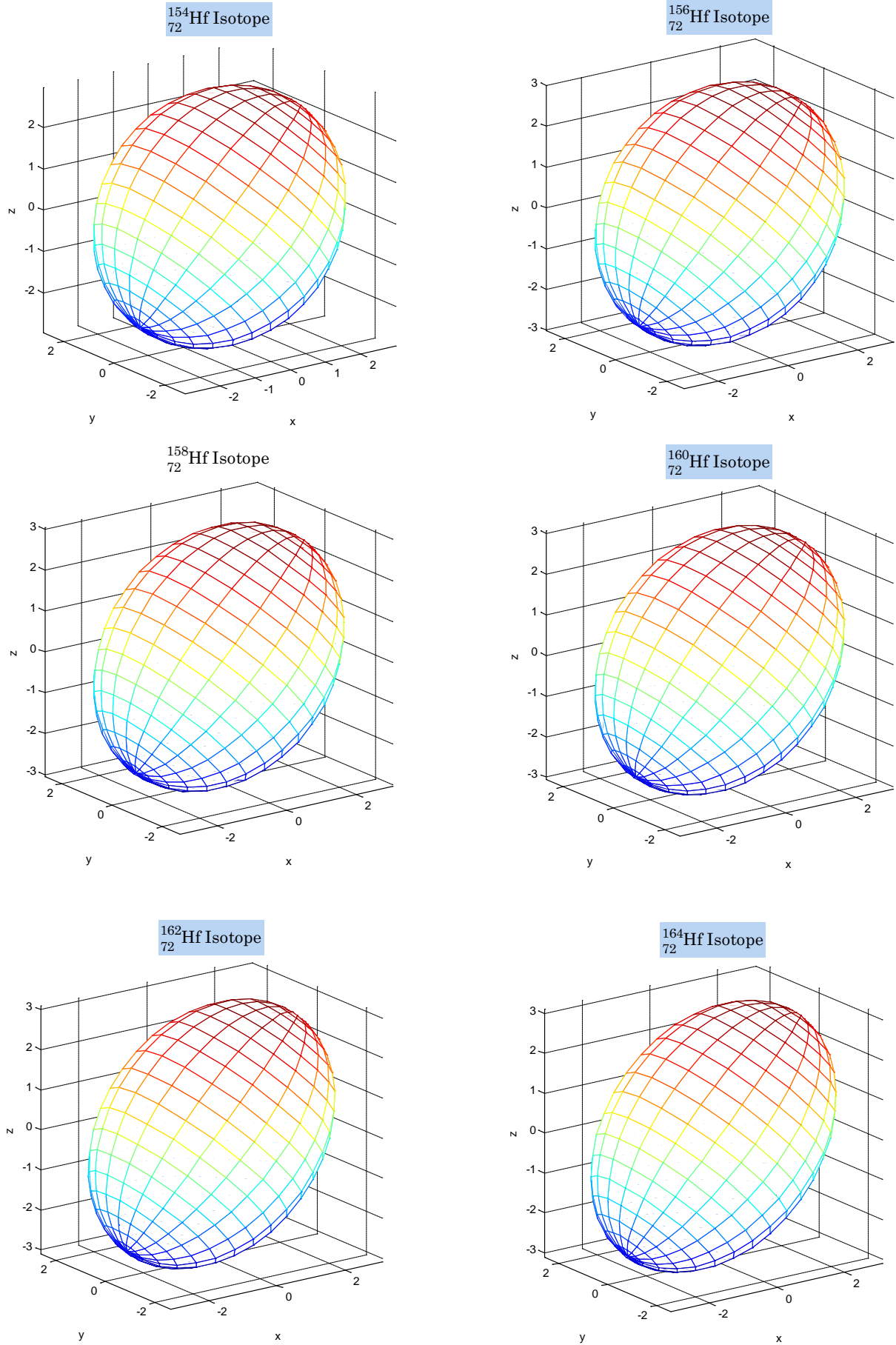


Figure (A-16): axially-symmetric quadrupole deformations, the prolate shape of Nucleus with $(x = y < z)$ (where z is the minor axis (b) (symmetric axis) and (x,y) are major axes (a) for Hf isotopes. **(to be continued)**

Appendix

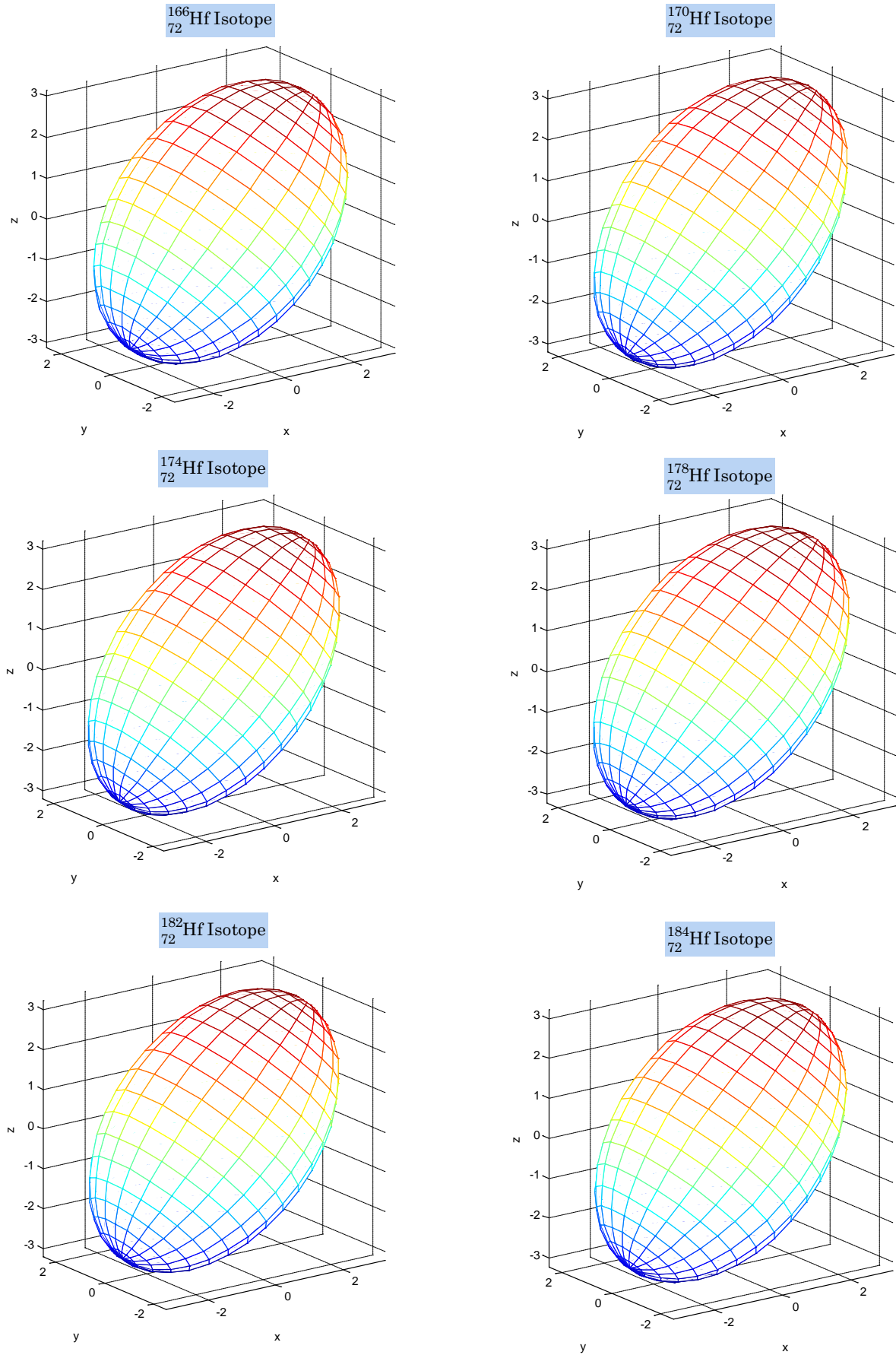


Figure (A-16): axially-symmetric quadrupole deformations, the prolate shape of Nucleus with $(x = y < z)$ (where z is the minor axis (b) (symmetric axis) and (x,y) are major axes (a) for hf isotopes.

Appendix

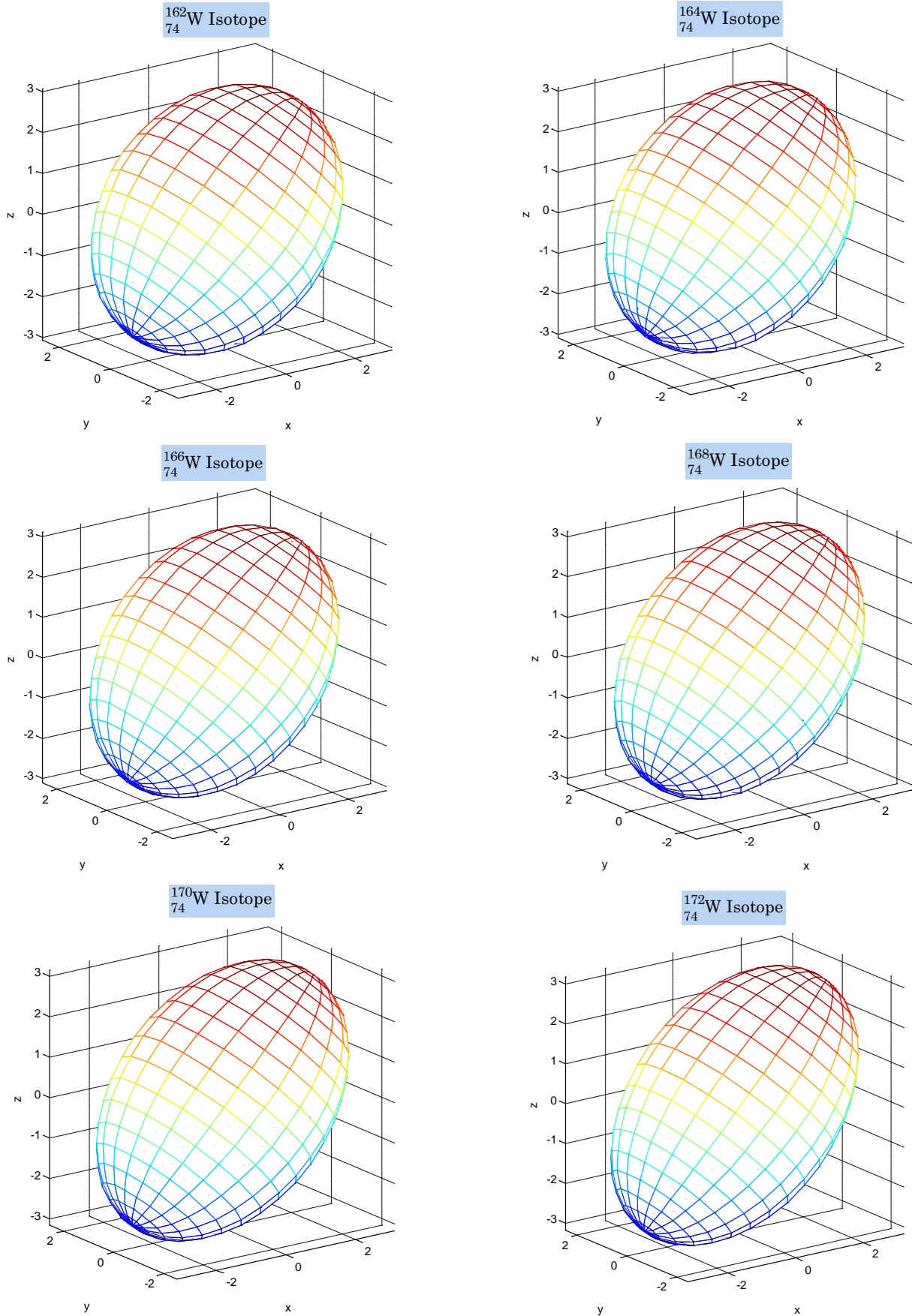


Figure (A-17): axially-symmetric quadrupole deformations, the prolate shape of Nucleus with $(x = y < z)$ (where z is the minor axis (b) (symmetric axis) and (x,y) are major axes (a) for W isotopes.

(to be continued)

Appendix

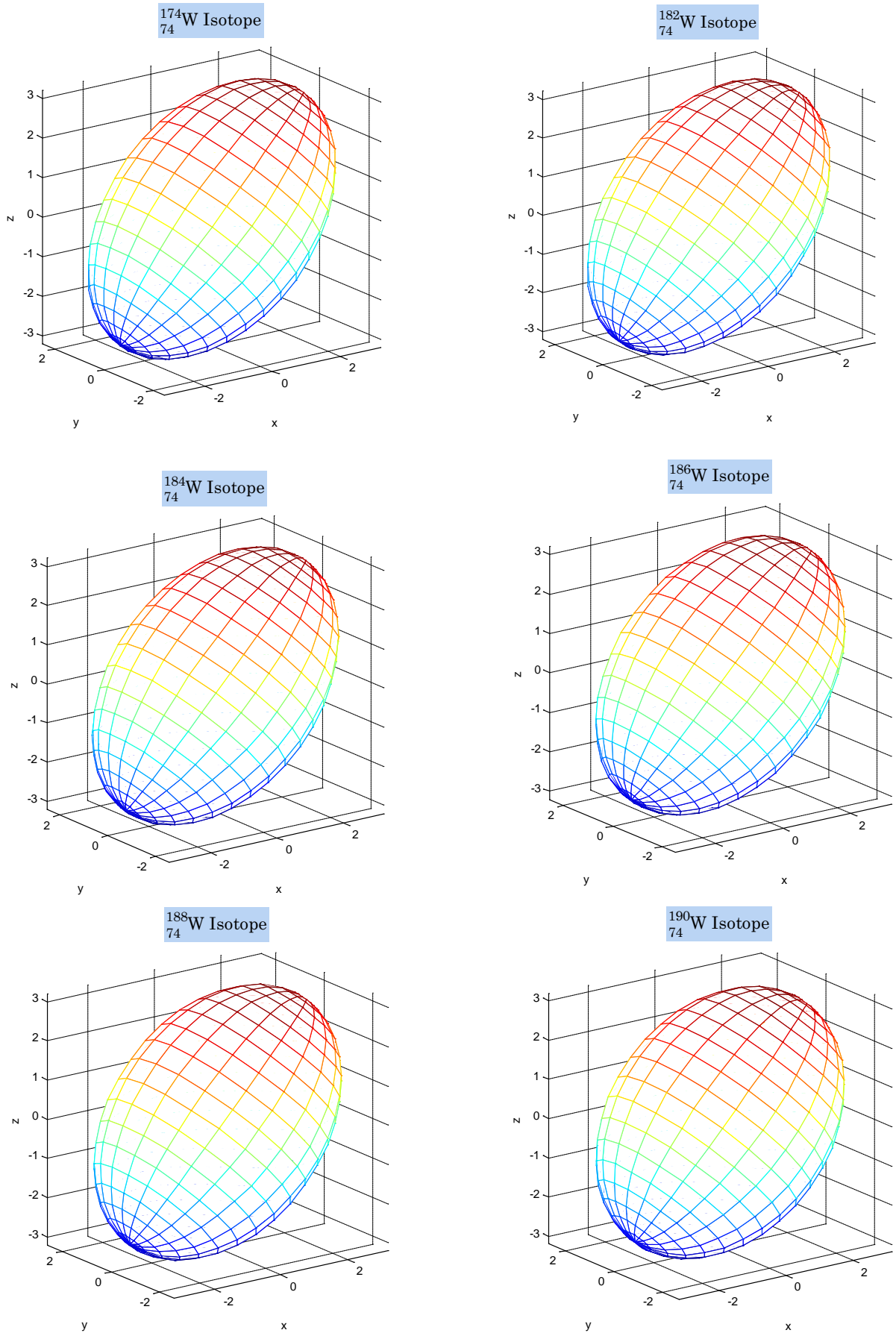


Figure (A-17): axially-symmetric quadrupole deformations, the prolate shape of Nucleus with $(x = y < z)$ (where z is the minor axis (b) (symmetric axis) and (x,y) are major axes (a) for W isotopes.

Appendix

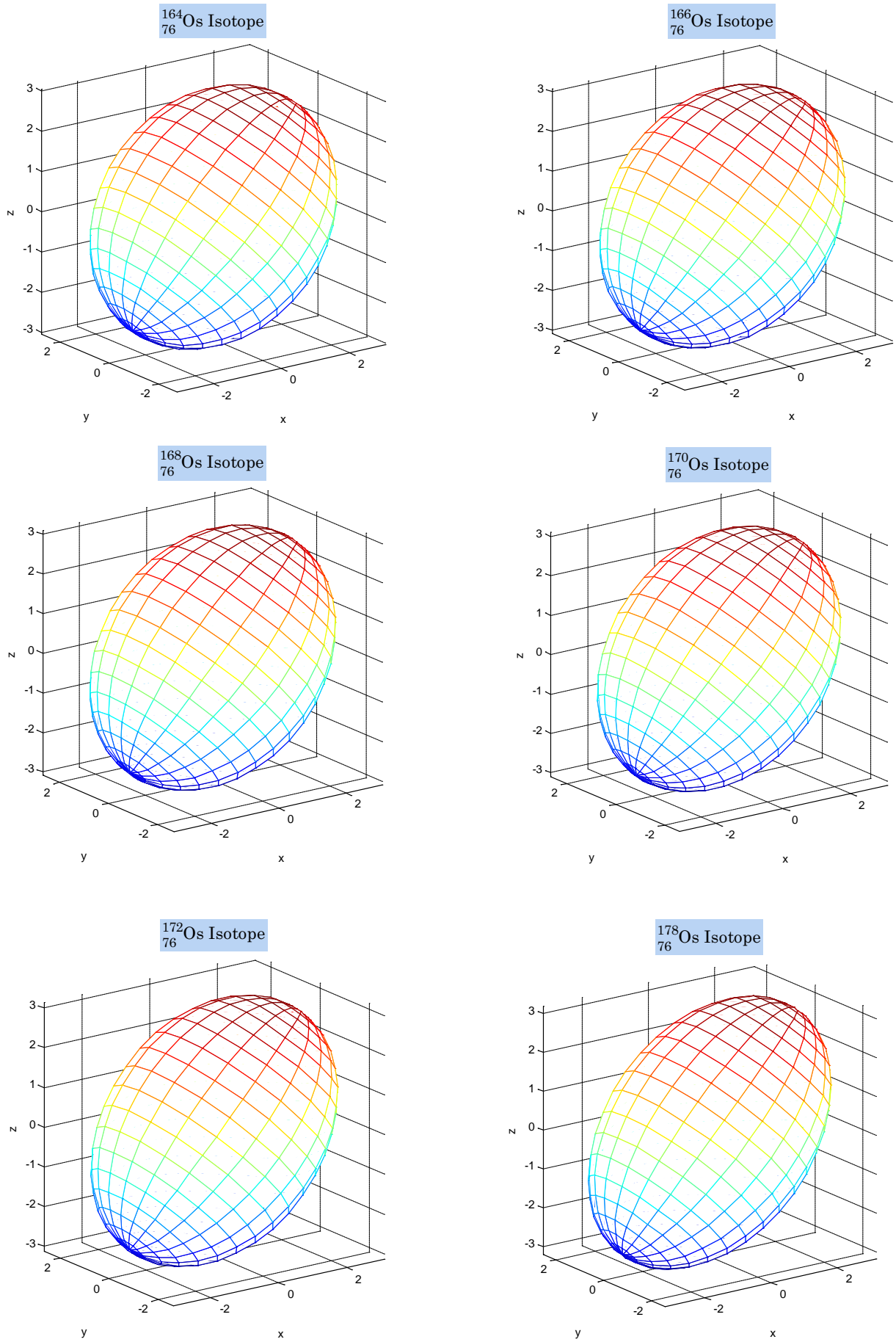


Figure (A-18): axially-symmetric quadrupole deformations, the prolate shape of Nucleus with $(x = y < z)$ (where z is the minor axis (b) (symmetric axis) and (x,y) are major axes (a) for Os isotopes.

Appendix

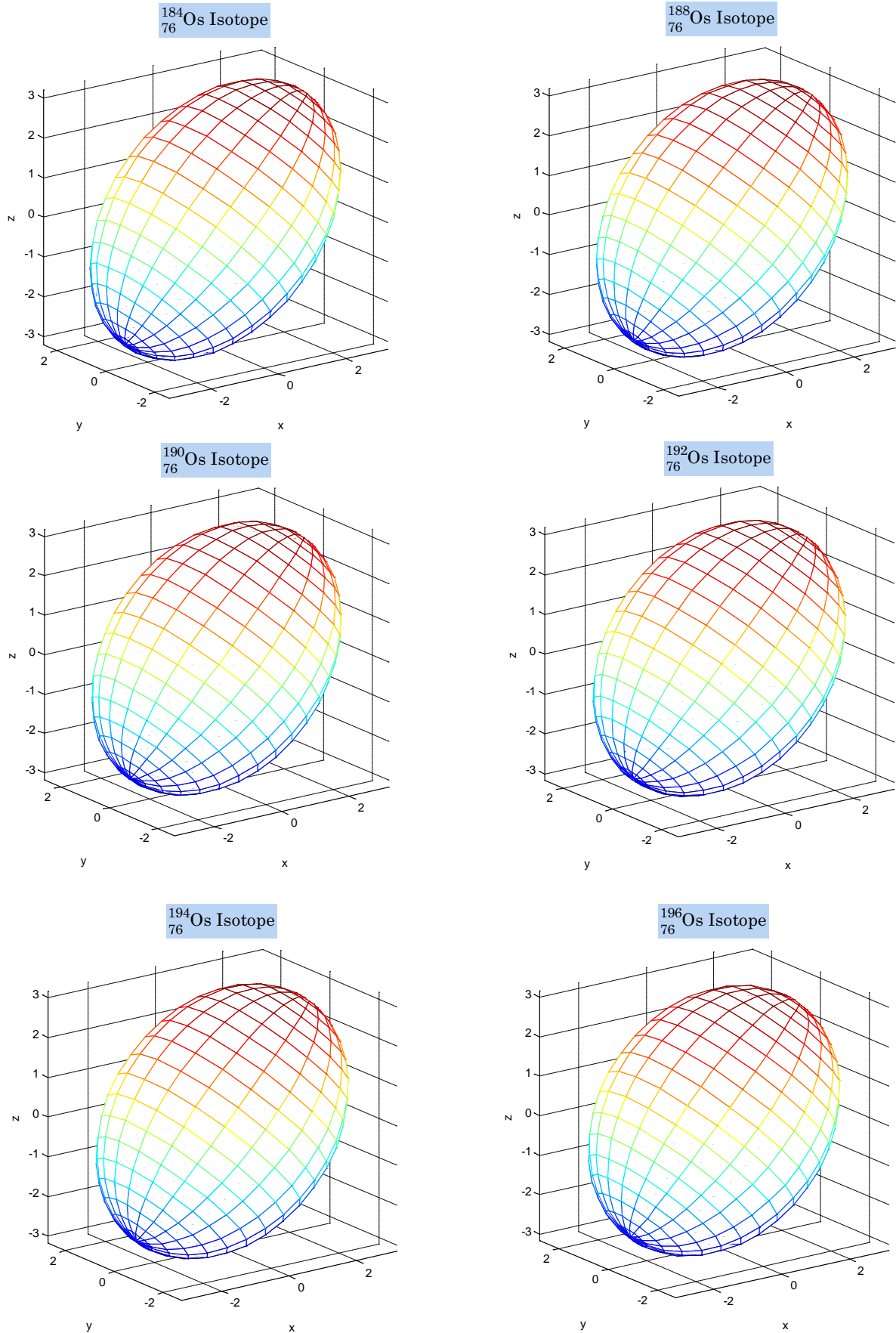


Figure (A-18): axially-symmetric quadrupole deformations, the prolate shape of Nucleus with $(x = y < z)$ (where z is the minor axis (b) (symmetric axis) and (x,y) are major axes (a) for Os isotopes.

Appendix

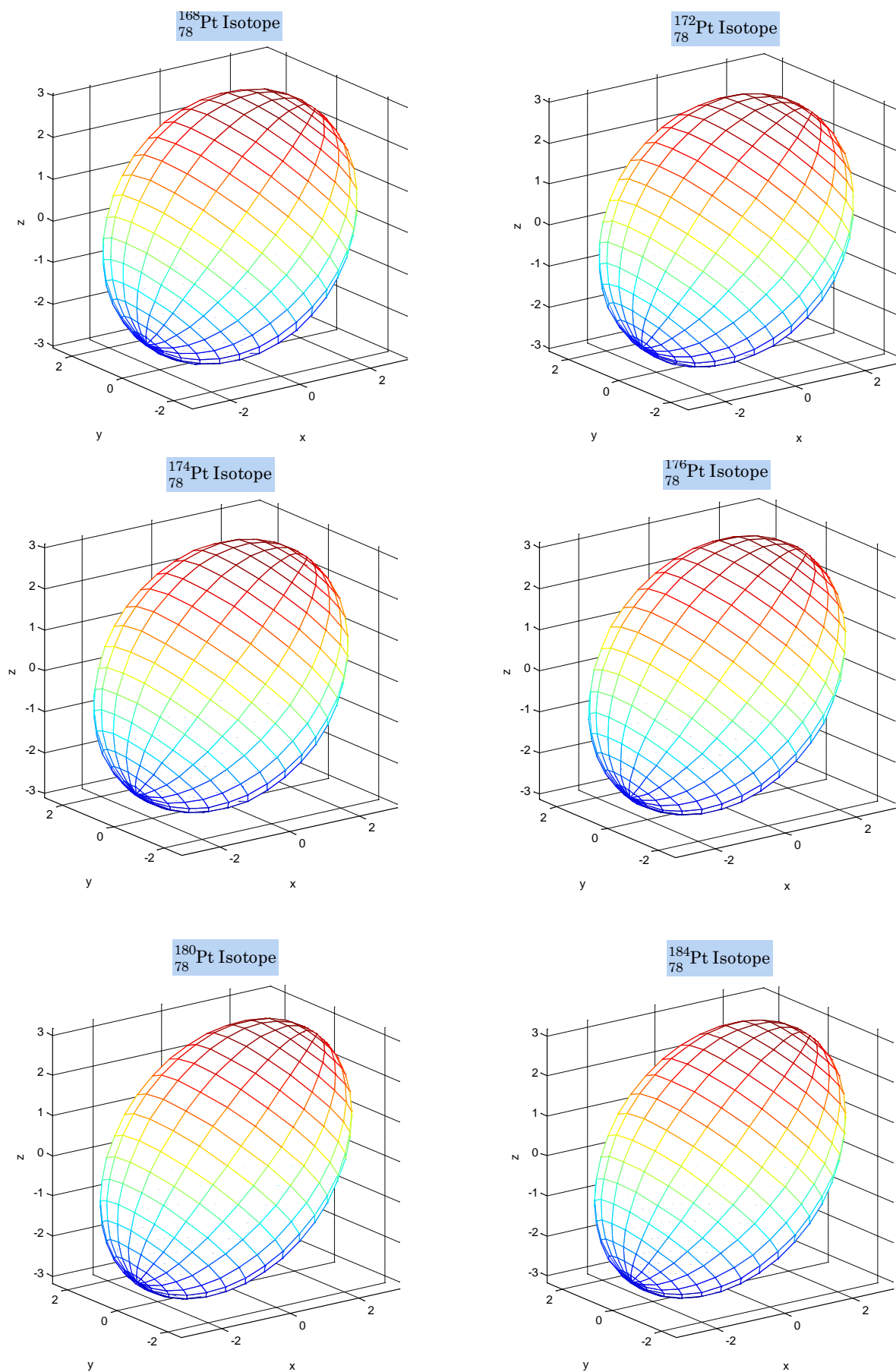


Figure (A-19): axially-symmetric quadrupole deformations, the prolate shape of Nucleus with $(x = y < z)$ (where z is the minor axis (b) (symmetric axis) and (x,y) are major axes (a) for Pt isotopes. **(to be continued)**

Appendix

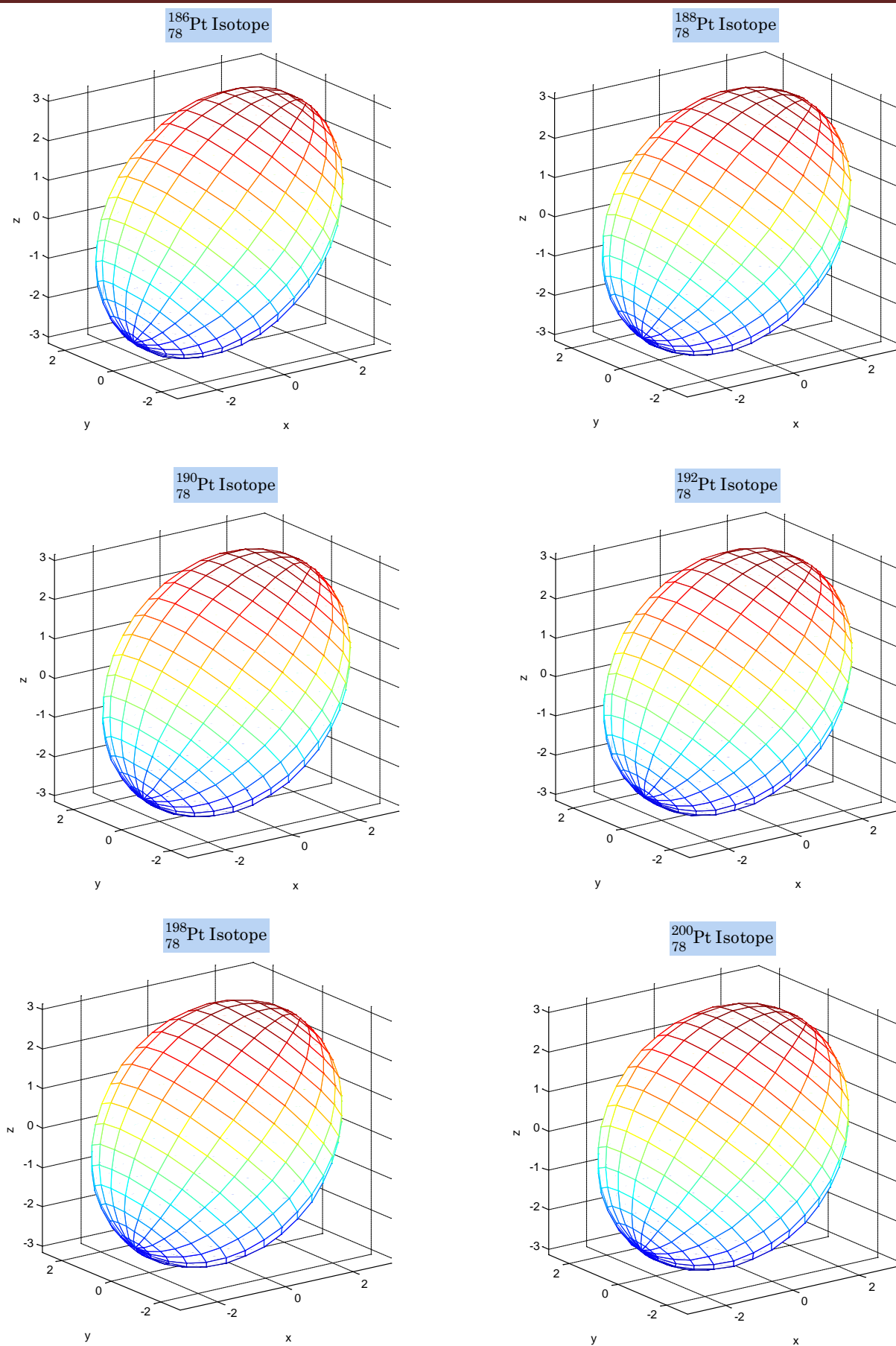


Figure (A-19): axially-symmetric quadrupole deformations, the prolate shape of Nucleus with $(x = y < z)$ (where z is the minor axis (b) (symmetric axis) and (x,y) are major axes (a) for Pt isotopes.

Appendix

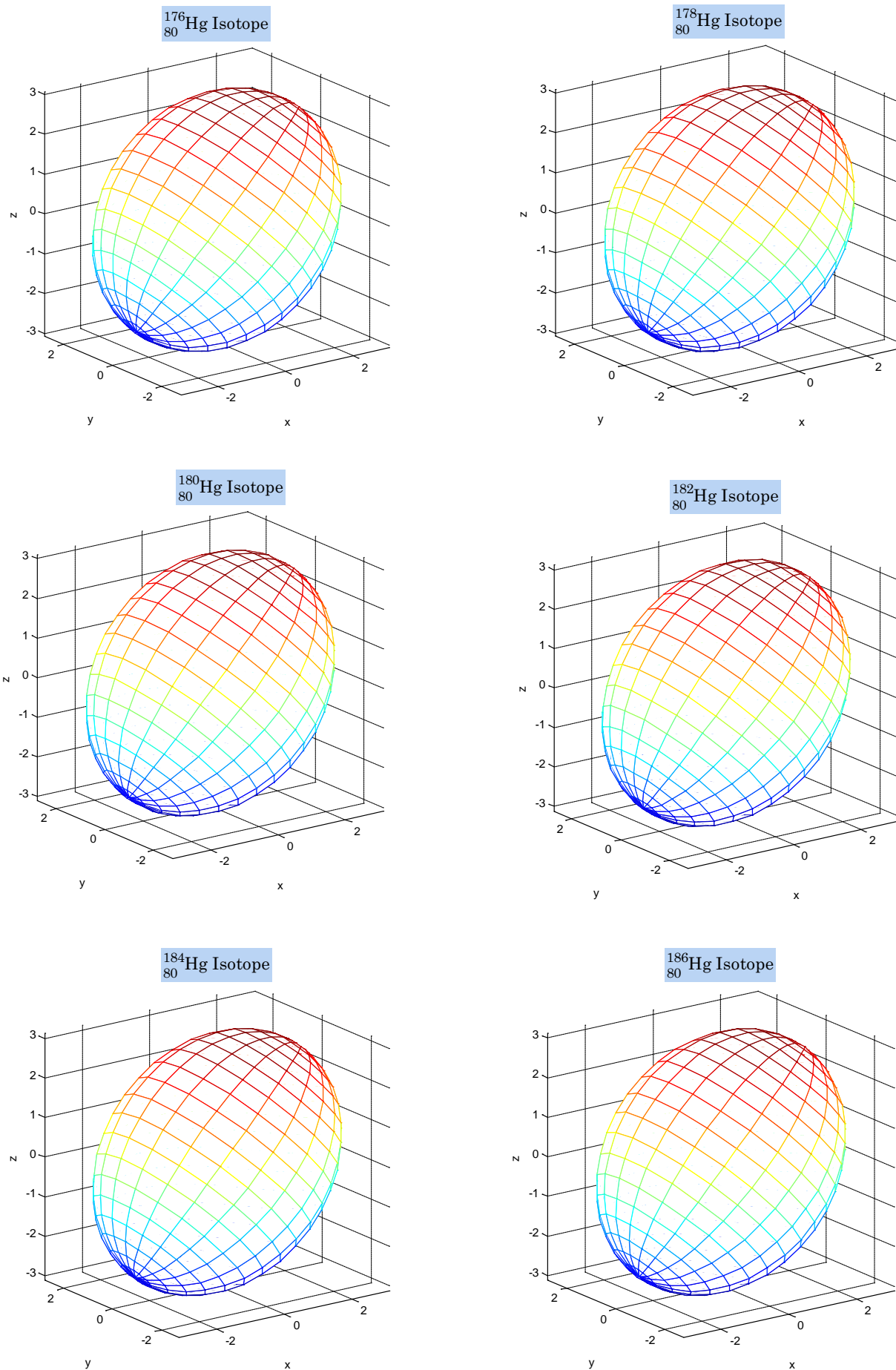


Figure (A-20): axially-symmetric quadrupole deformations, the prolate shape of Nucleus with ($x = y < z$) (where z is the minor axis (b) (symmetric axis) and (x,y) are major axes (a) for Hg isotopes.

Appendix

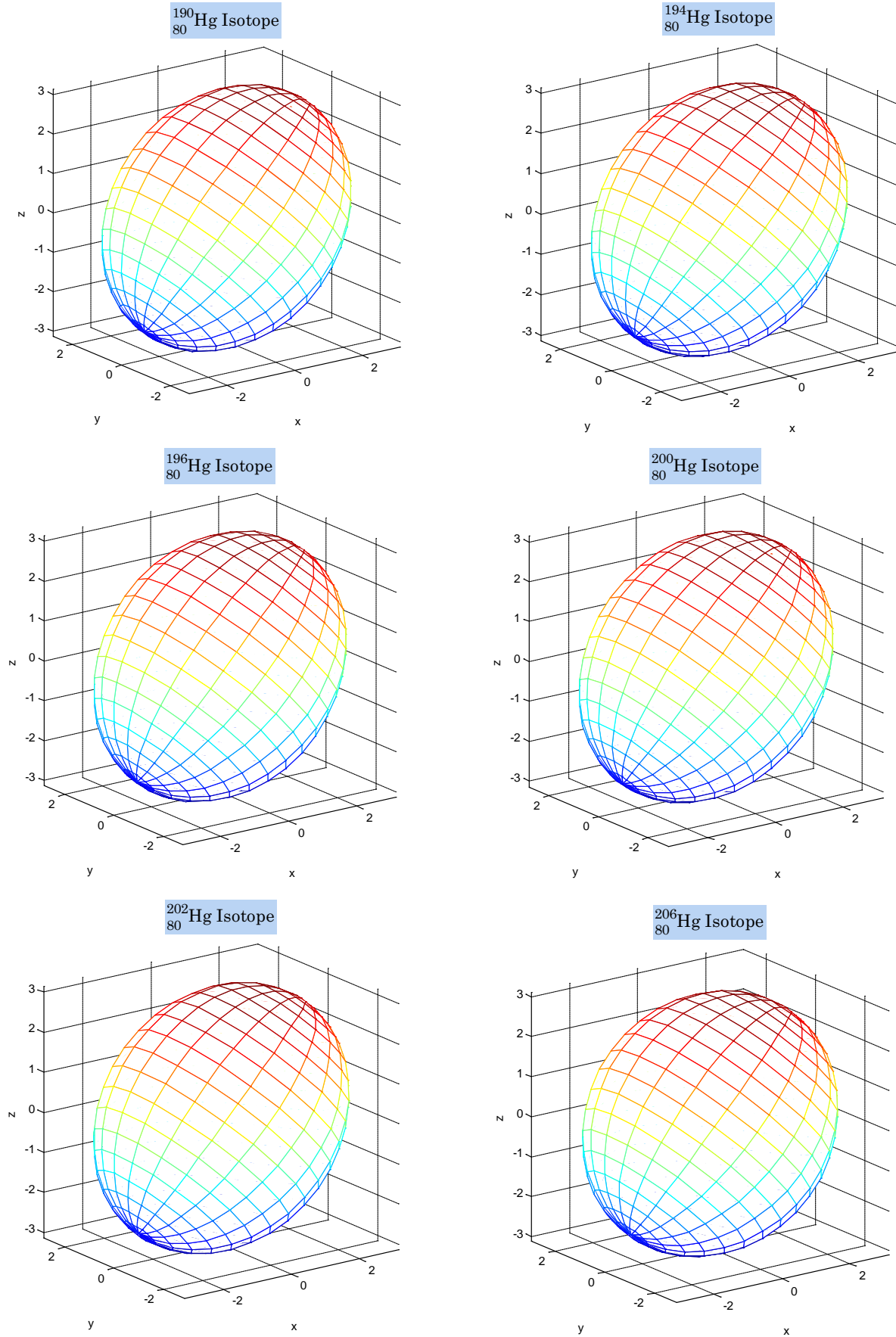


Figure (A-20): axially-symmetric quadrupole deformations, the prolate shape of Nucleus with $(x = y < z)$ (where z is the minor axis (b) (symmetric axis) and (x,y) are major axes (a) for Hg isotopes.

Appendix

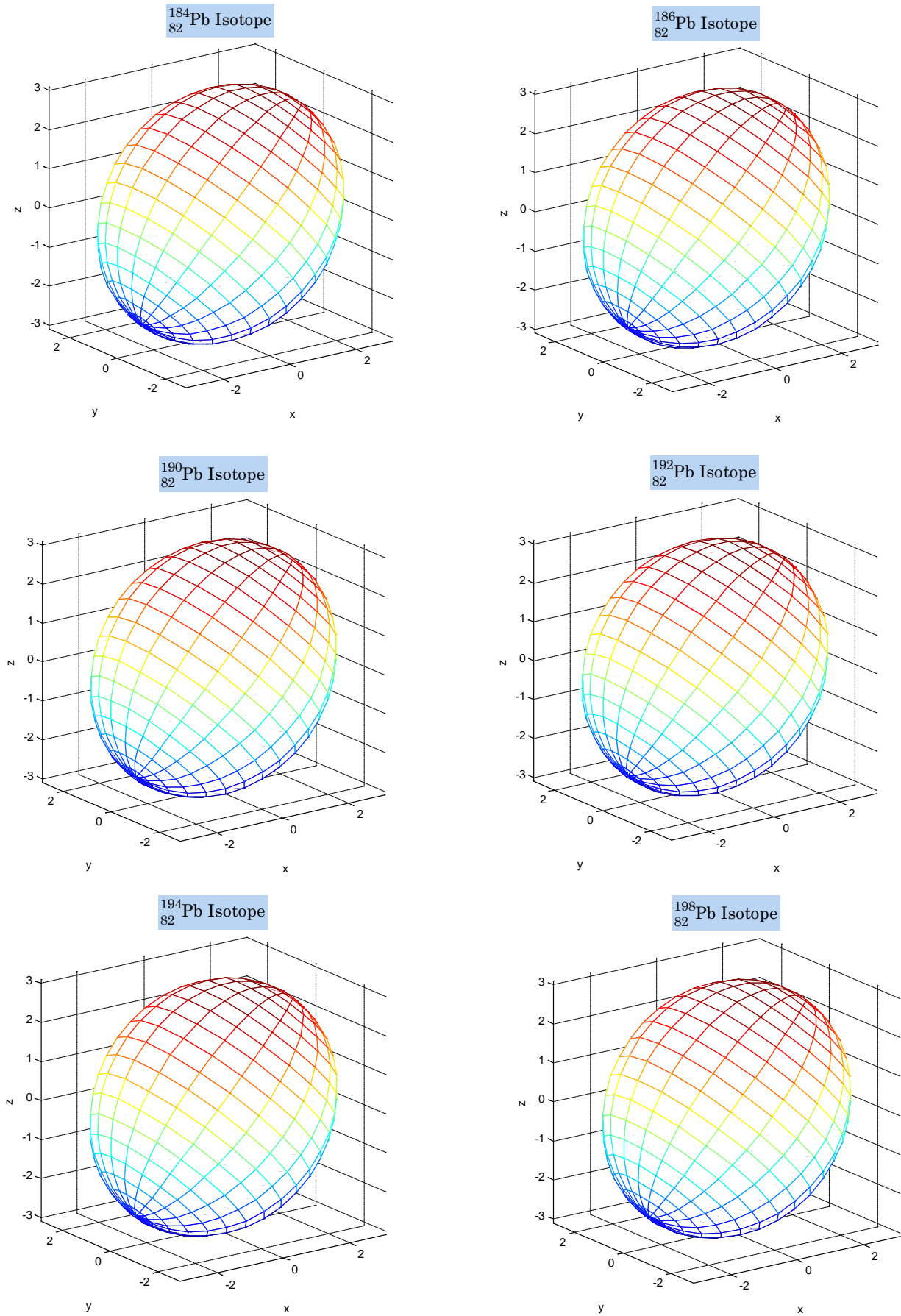


Figure (A-21): axially-symmetric quadrupole deformations, the prolate shape of Nucleus with $(x = y < z)$ (where z is the minor axis (b) (symmetric axis) and (x,y) are major axes (a) for Pb isotopes.

(to be continued)

Appendix

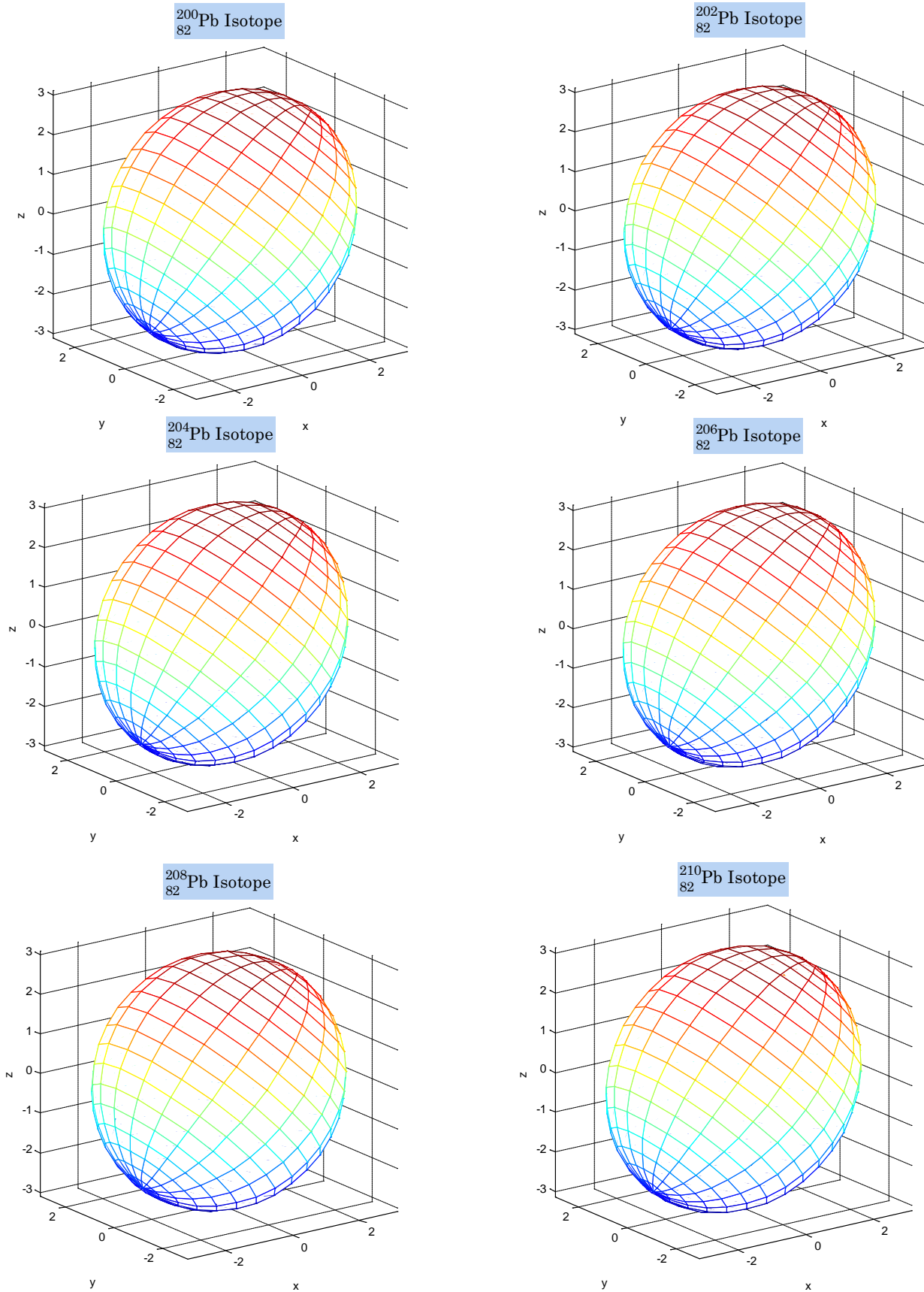


Figure (A-21): axially-symmetric quadrupole deformations, the prolate shape of Nucleus with $(x = y < z)$ (where z is the minor axis (b) (symmetric axis) and (x,y) are major axes (a) for Pb isotopes.

Appendix

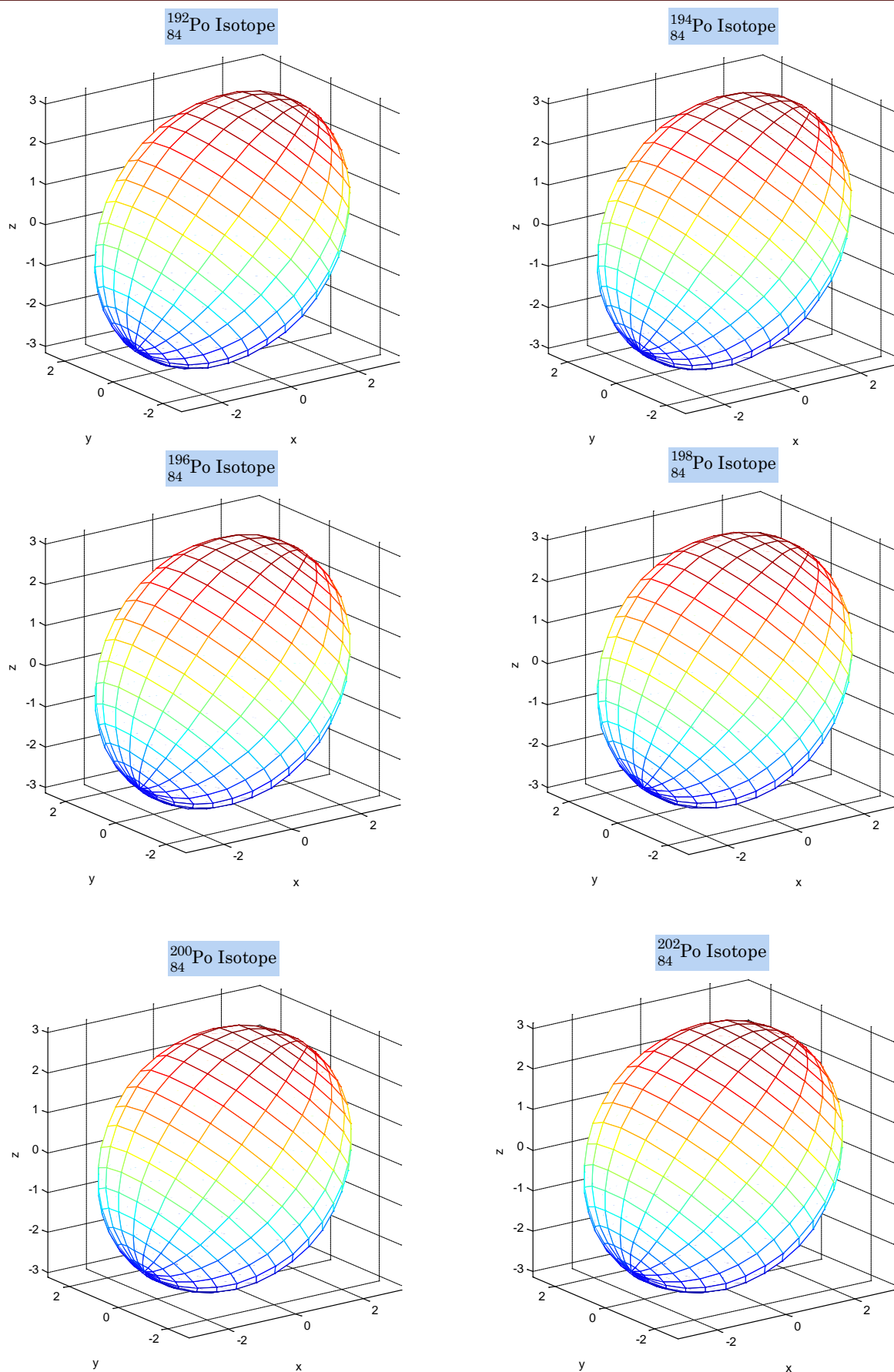


Figure (A-22): axially-symmetric quadrupole deformations, the prolate shape of Nucleus with $(x = y < z)$ (where z is the minor axis (b) (symmetric axis) and (x,y) are major axes (a) for Ba isotopes. **(to be continued)**

Appendix

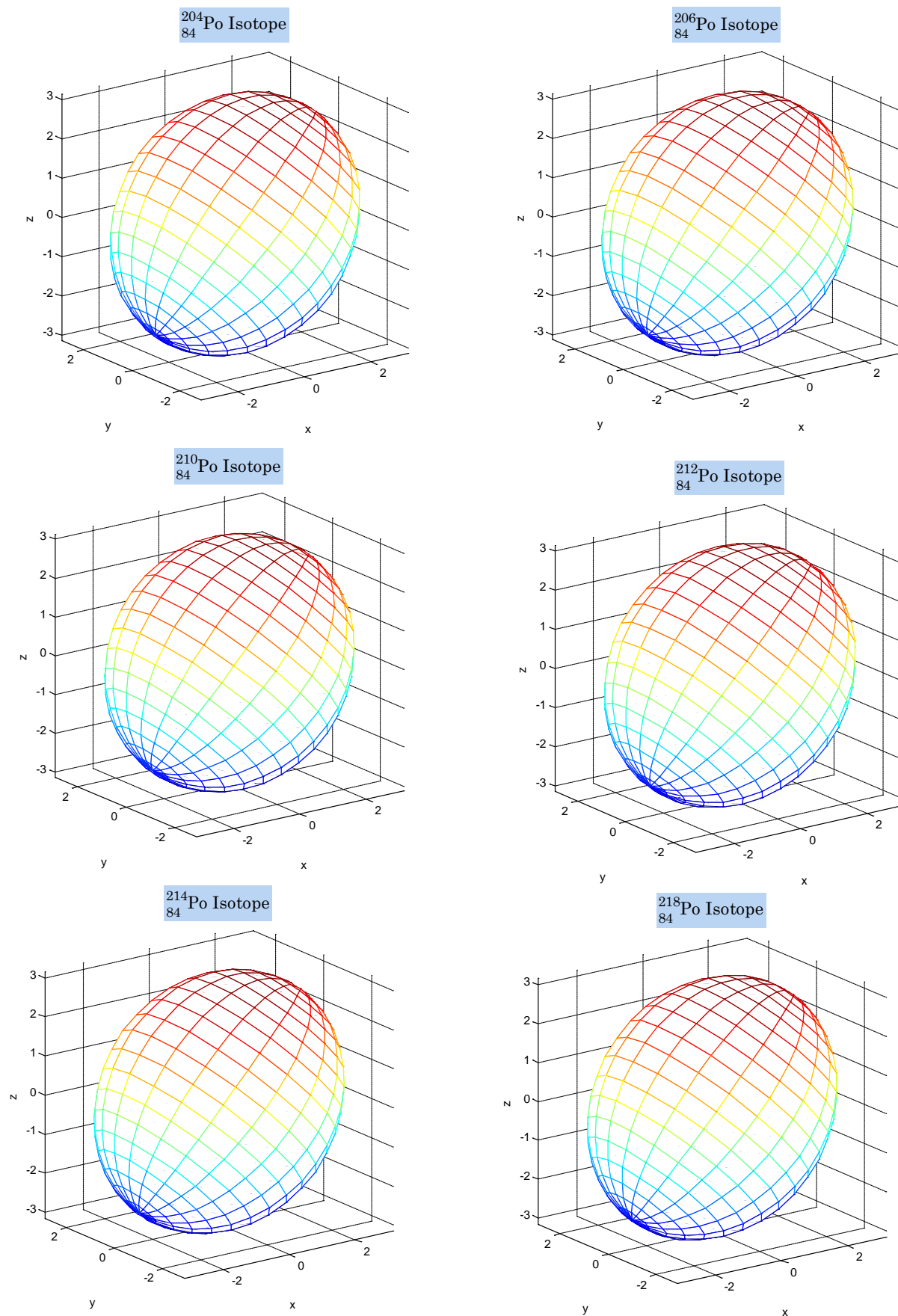


Figure (A-22): axially-symmetric quadrupole deformations, the prolate shape of Nucleus with $(x = y < z)$ (where z is the minor axis (b) (symmetric axis) and (x, y) are major axes (a) for Po isotopes.

Appendix

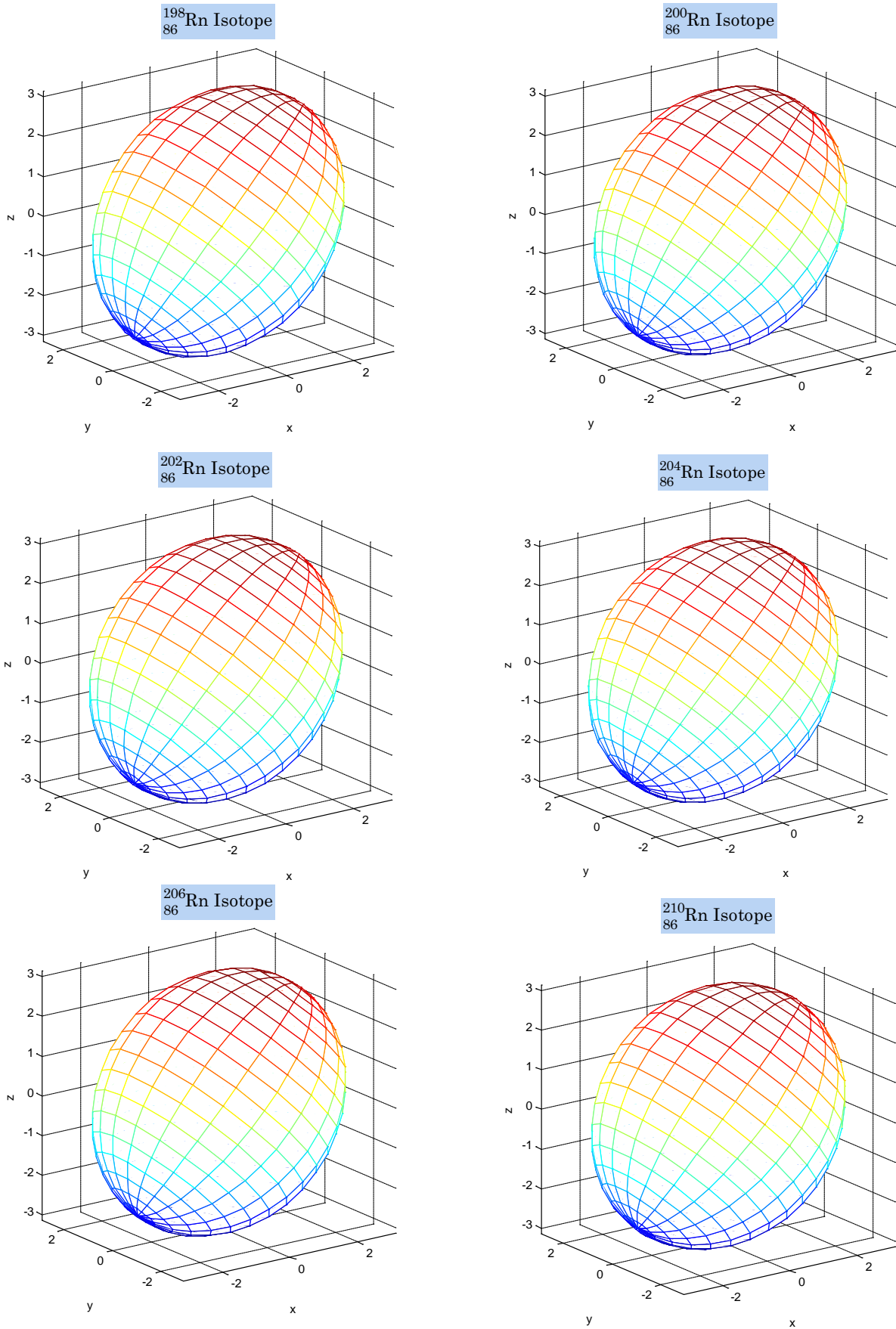
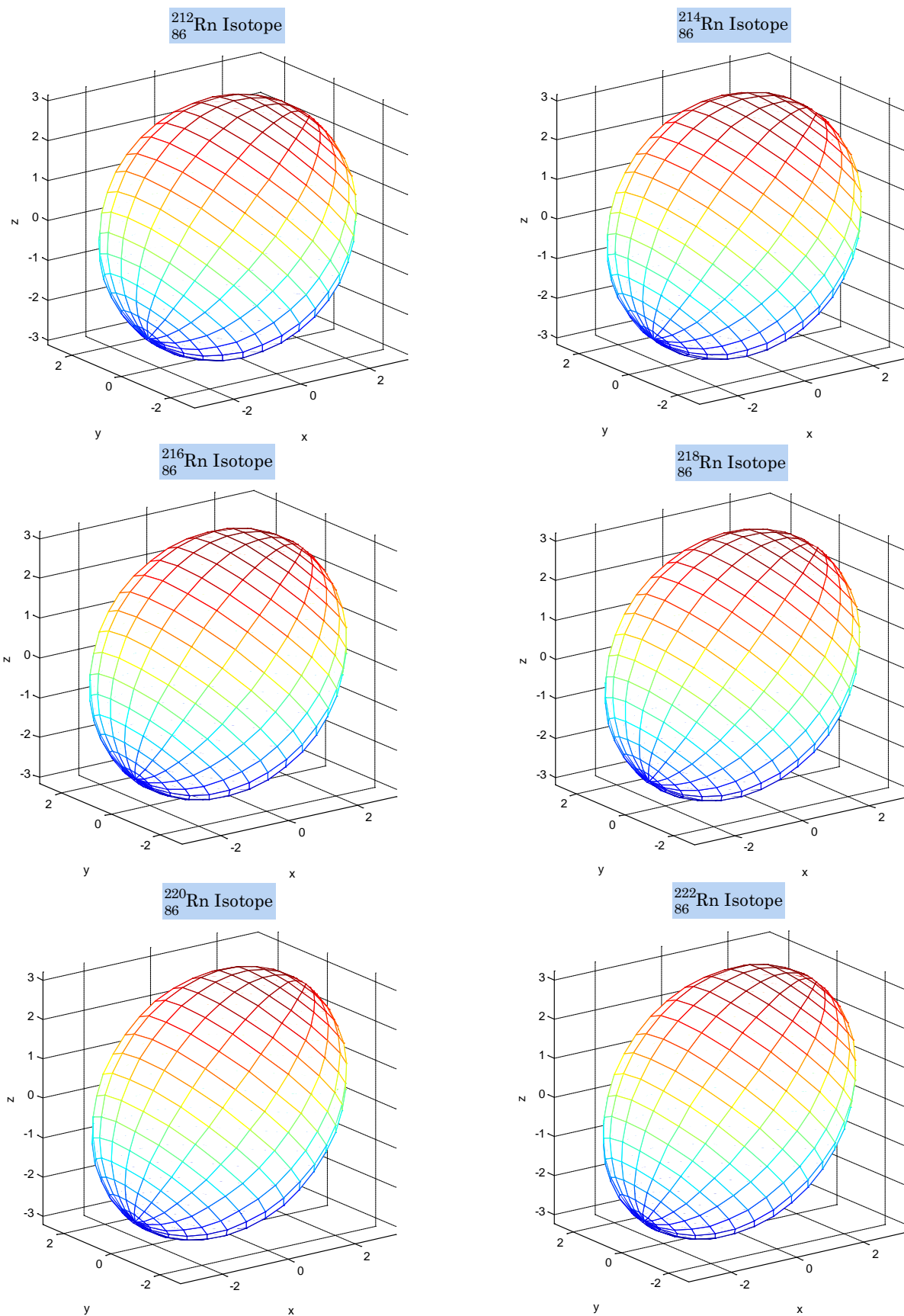


Figure (A-23): axially-symmetric quadrupole deformations, the prolate shape of Nucleus with $(x = y < z)$ (where z is the minor axis (b) (symmetric axis) and (x,y) are major axes (a) for Rn isotopes. **(to be continued)**

Appendix



Figure(A-23): axially-symmetric quadrupole deformations, the prolate shape of Nucleus with $(x = y < z)$ (where z is the minor axis (b) (symmetric axis) and (x,y) are major axes (a) for Rn isotopes.

Appendix

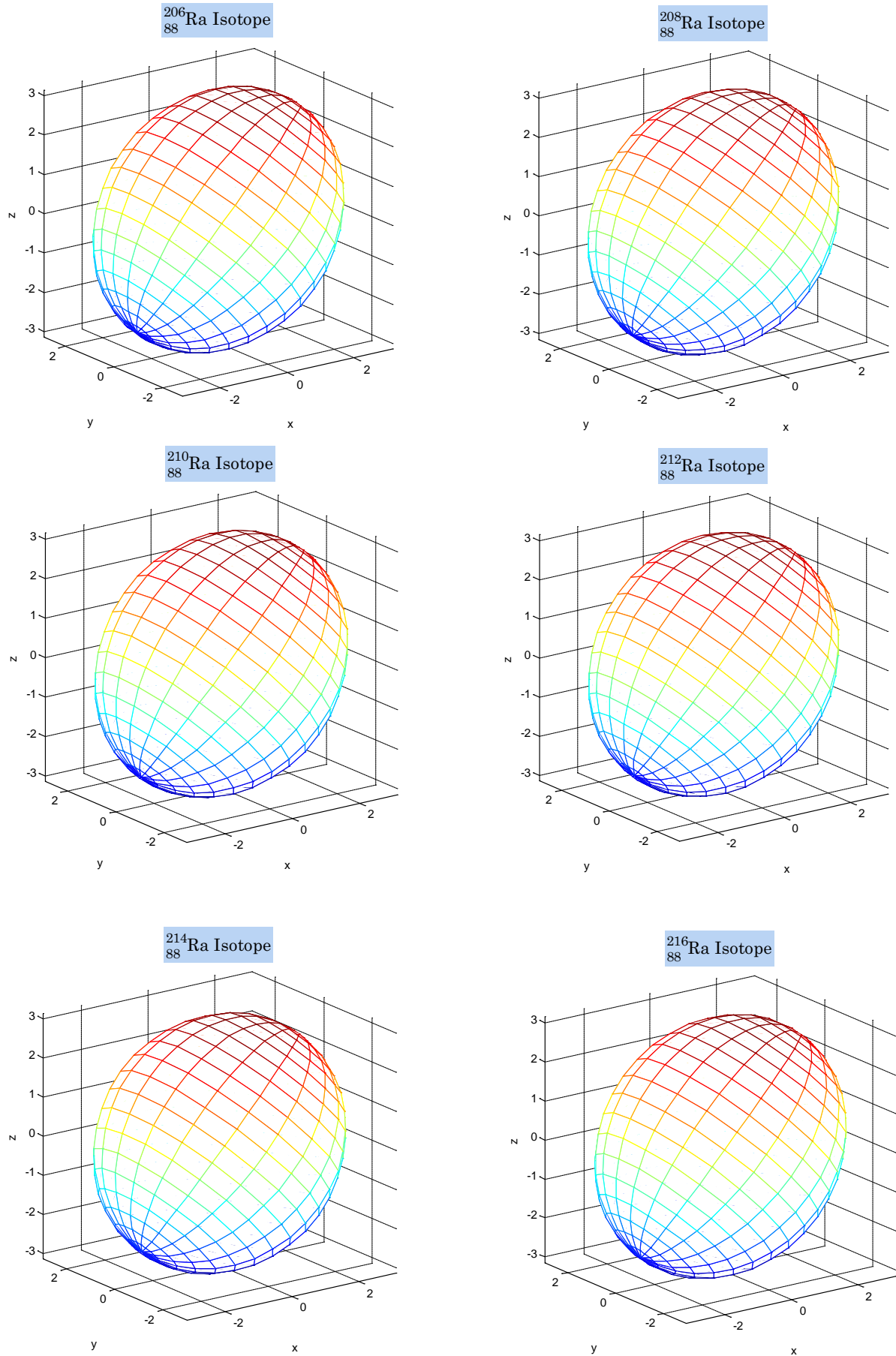
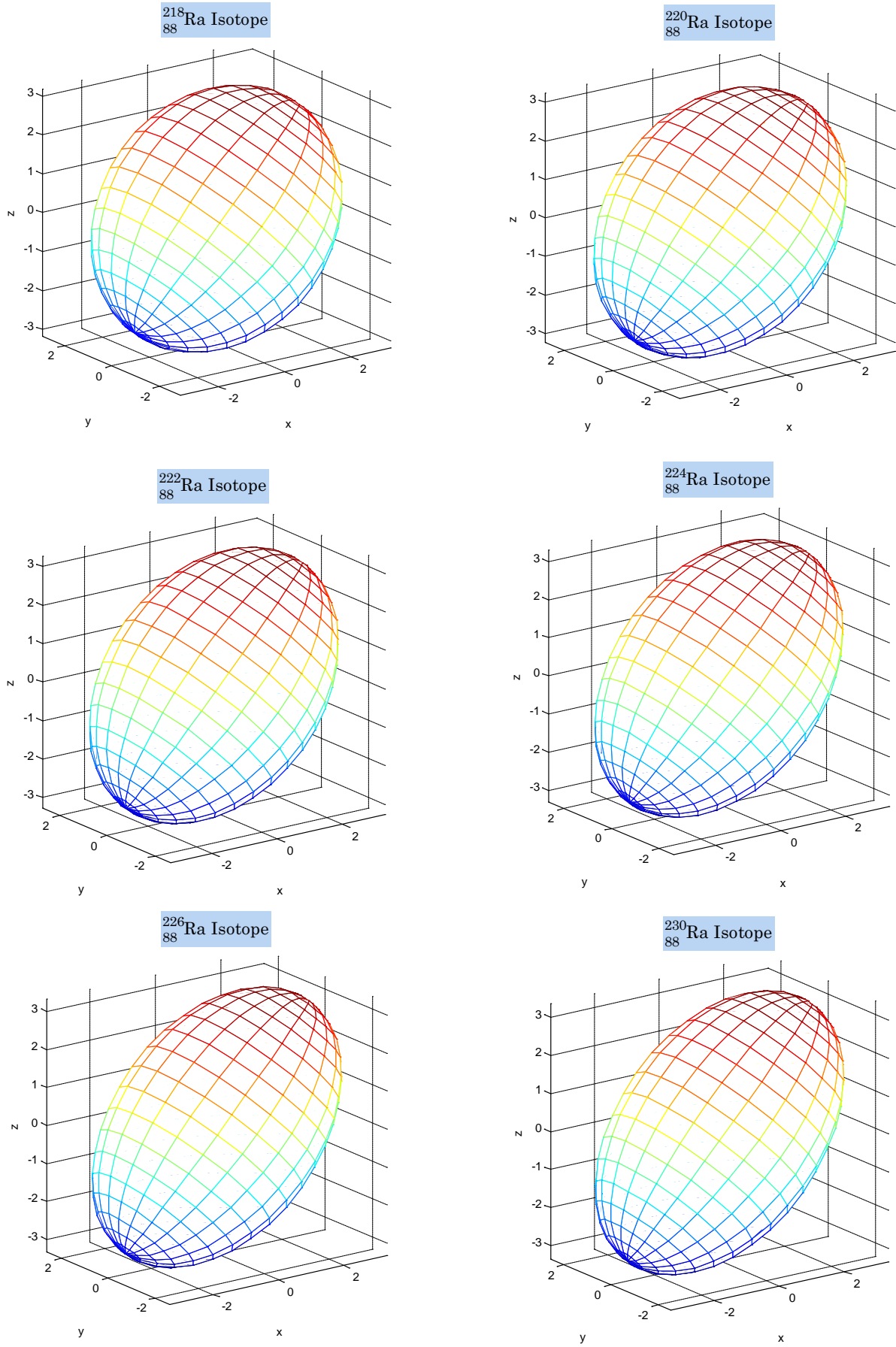


Figure (A-24): axially-symmetric quadrupole deformations, the prolate shape of Nucleus with $(x = y < z)$ (where z is the minor axis (b) (symmetric axis) and (x,y) are major axes (a) for Ra isotopes. **(to be continued)**

Appendix



Figure(A-24): axially-symmetric quadrupole deformations, the prolate shape of Nucleus with $(x = y < z)$ (where z is the minor axis (b) (symmetric axis) and (x,y) are major axes (a) for Ra isotopes.

Appendix

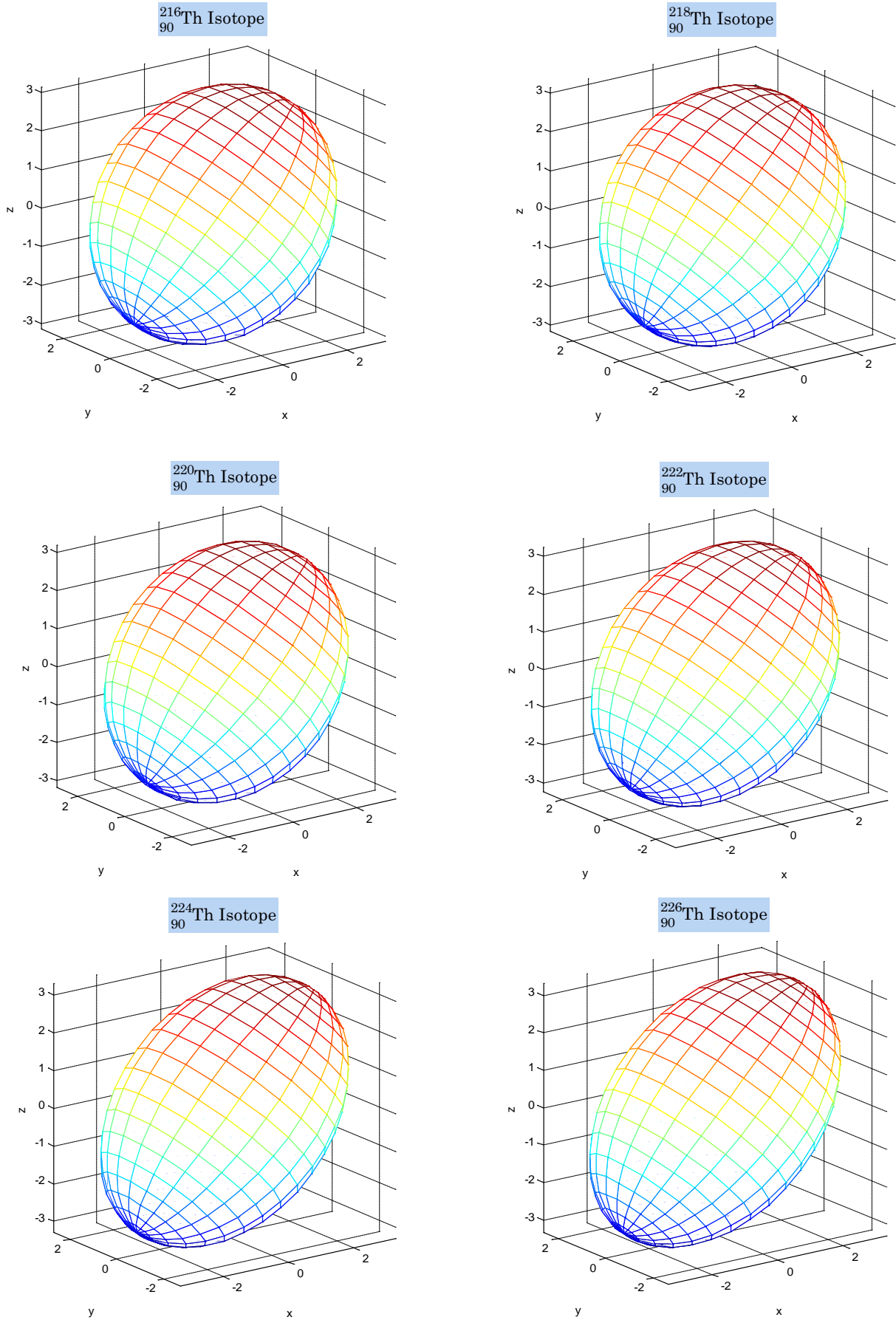


Figure (A-25): axially-symmetric quadrupole deformations, the prolate shape of Nucleus with $(x = y < z)$ (where z is the minor axis (b) (symmetric axis) and (x,y) are major axes (a) for Th isotopes. **(to be continued)**

Appendix

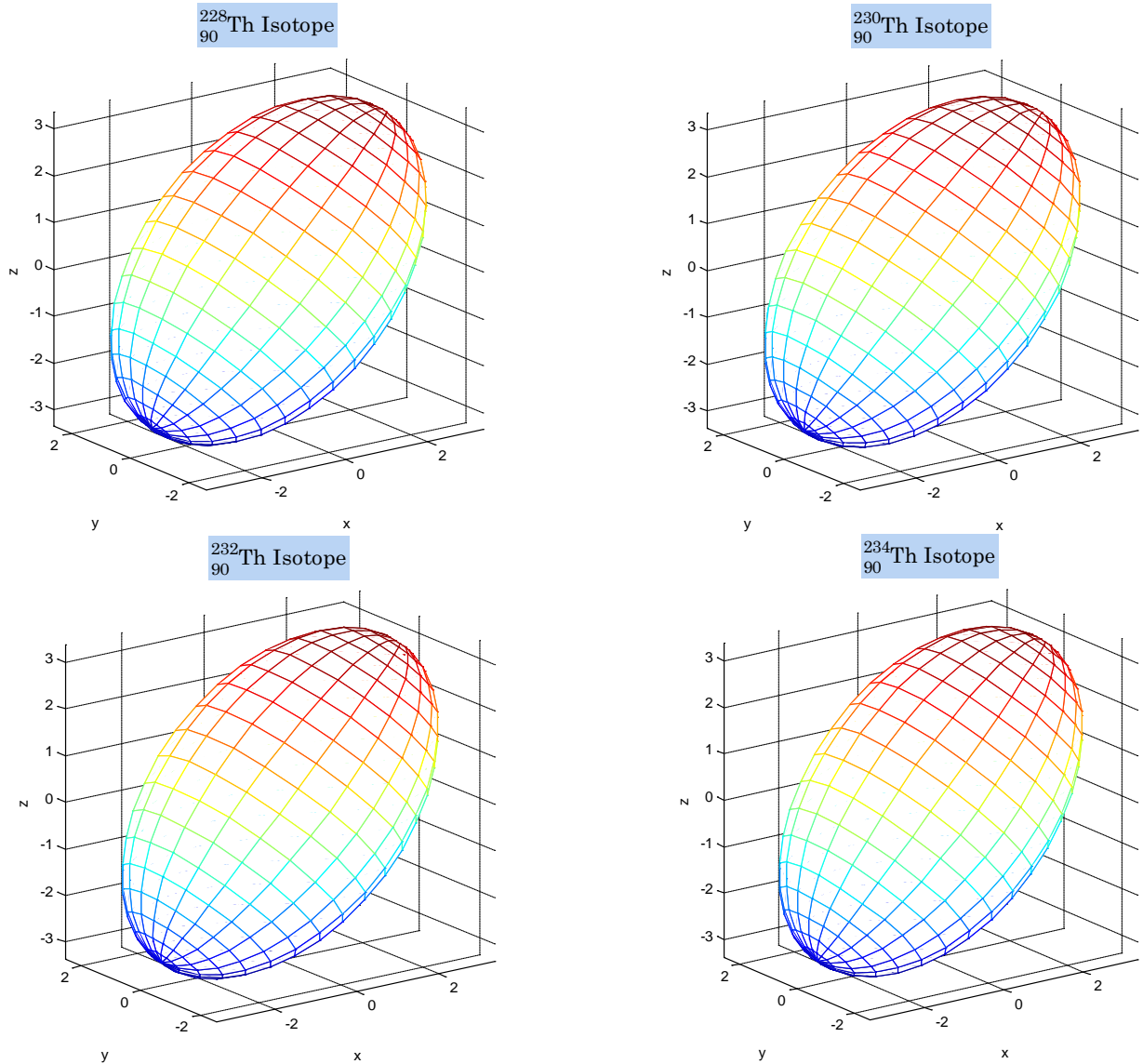


Figure (A-25): axially-symmetric quadrupole deformations, the prolate shape of Nucleus with $(x = y < z)$ (where z is the minor axis (b) (symmetric axis) and (x,y) are major axes (a) for Th isotopes.

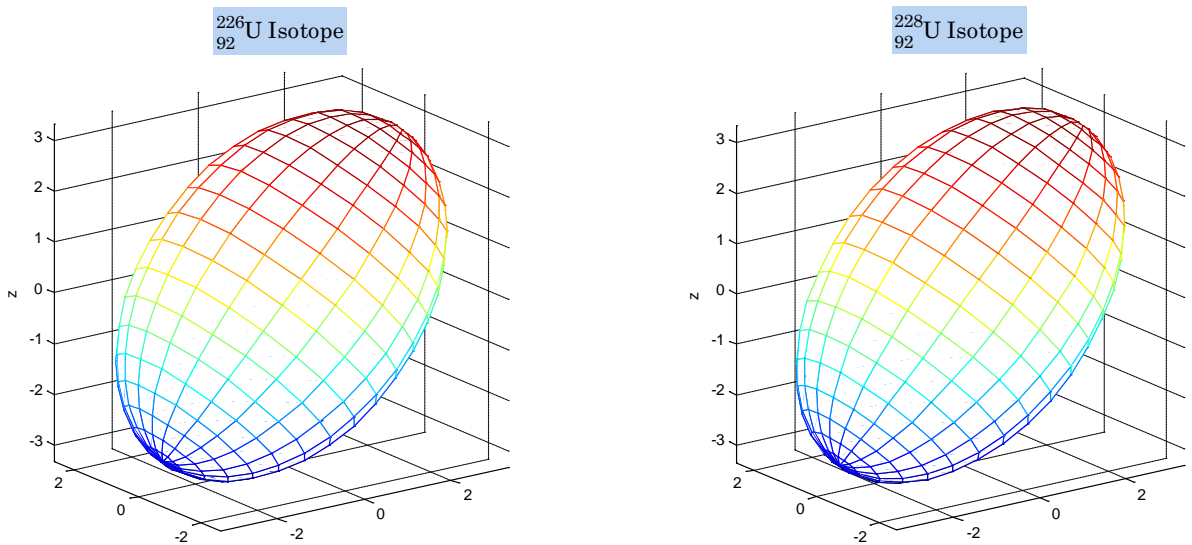
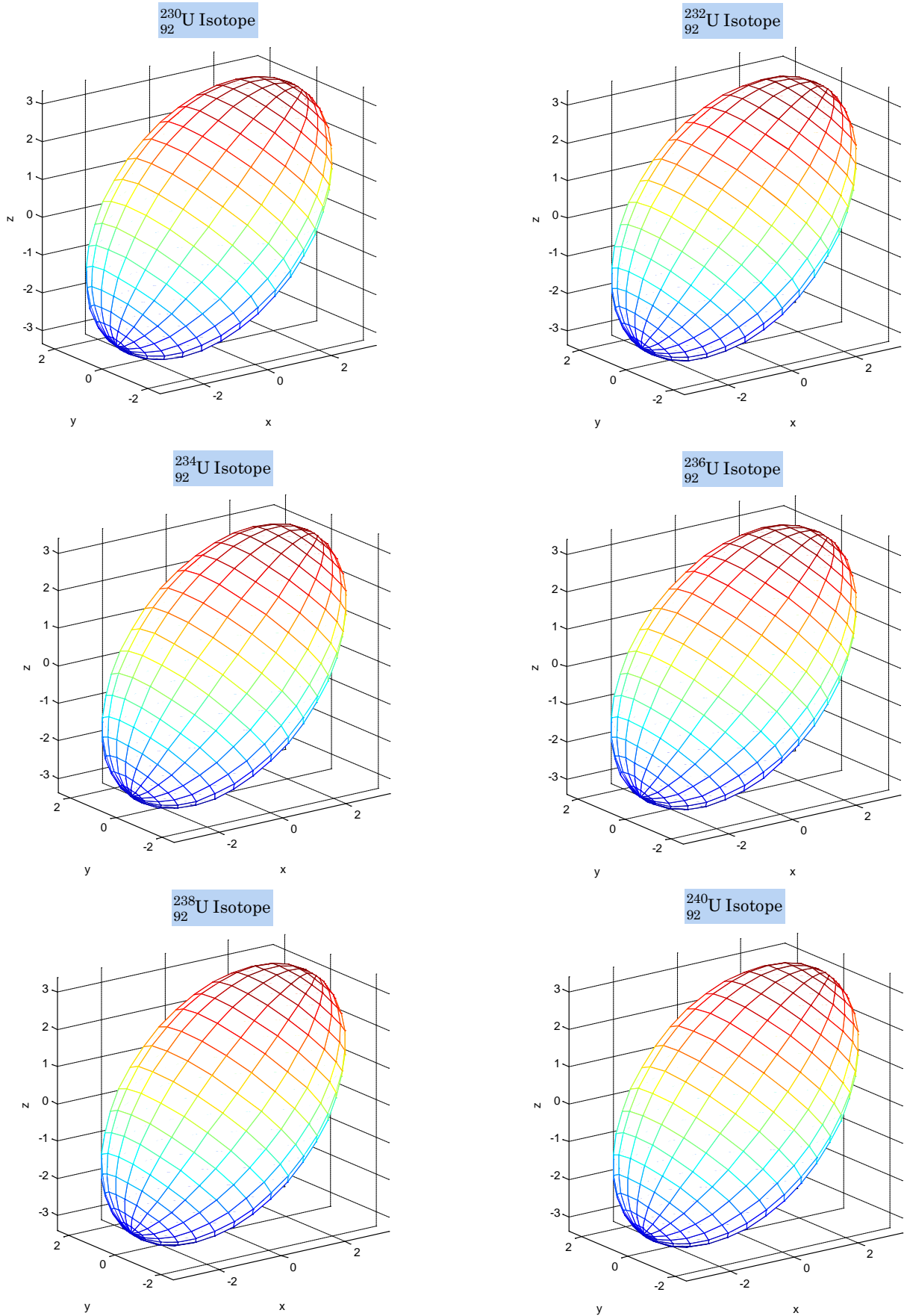


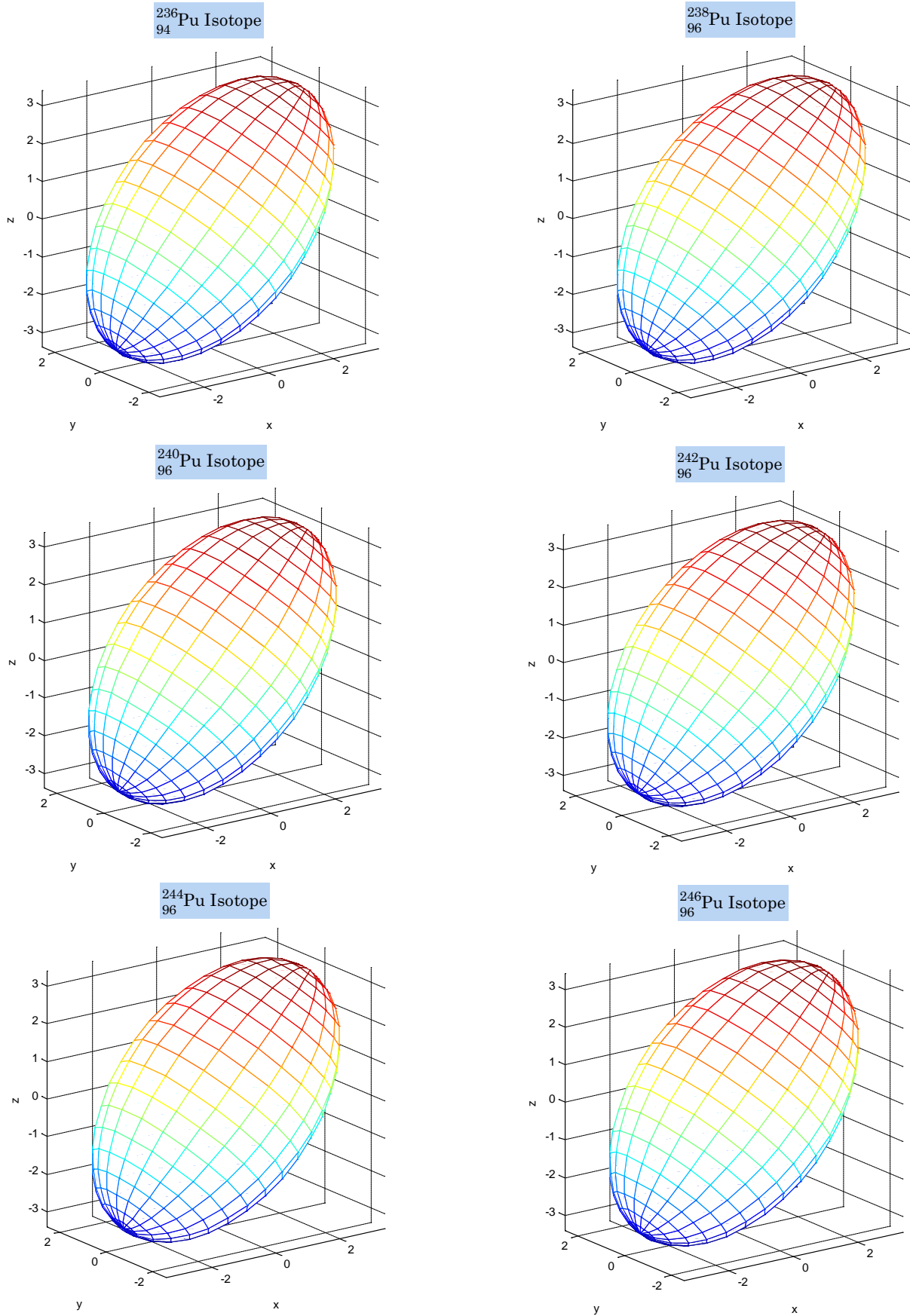
Figure (A-26): axially-symmetric quadrupole deformations, the prolate shape of Nucleus with $(x = y < z)$ (where z is the minor axis (b) (symmetric axis) and (x,y) are major axes (a) for U isotopes. **(to be continued)**

Appendix



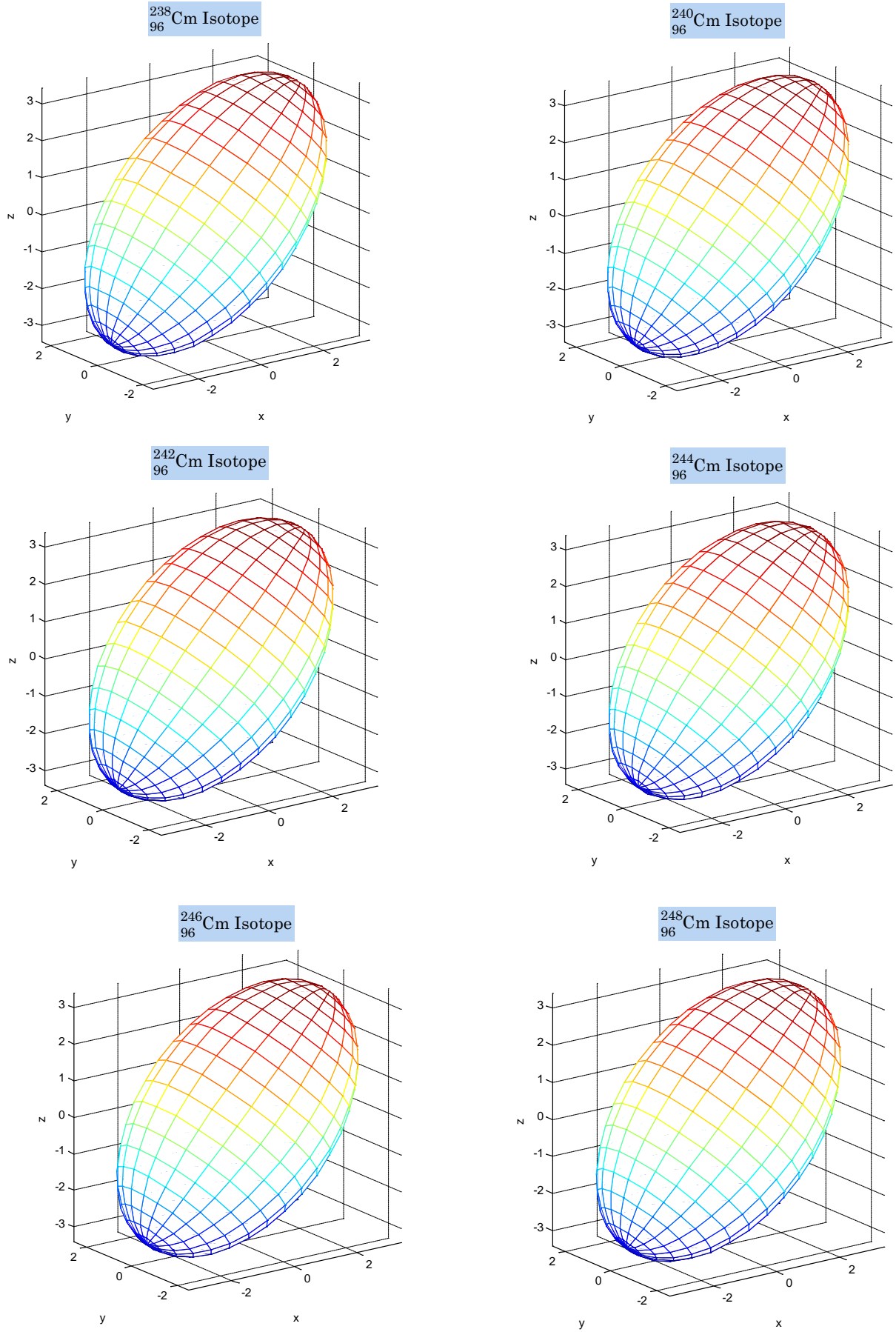
Figure(A-26): axially-symmetric quadrupole deformations, the prolate shape of Nucleus with $(x = y < z)$ (where z is the minor axis (b) (symmetric axis) and (x,y) are major axes (a) for U isotopes.

Appendix



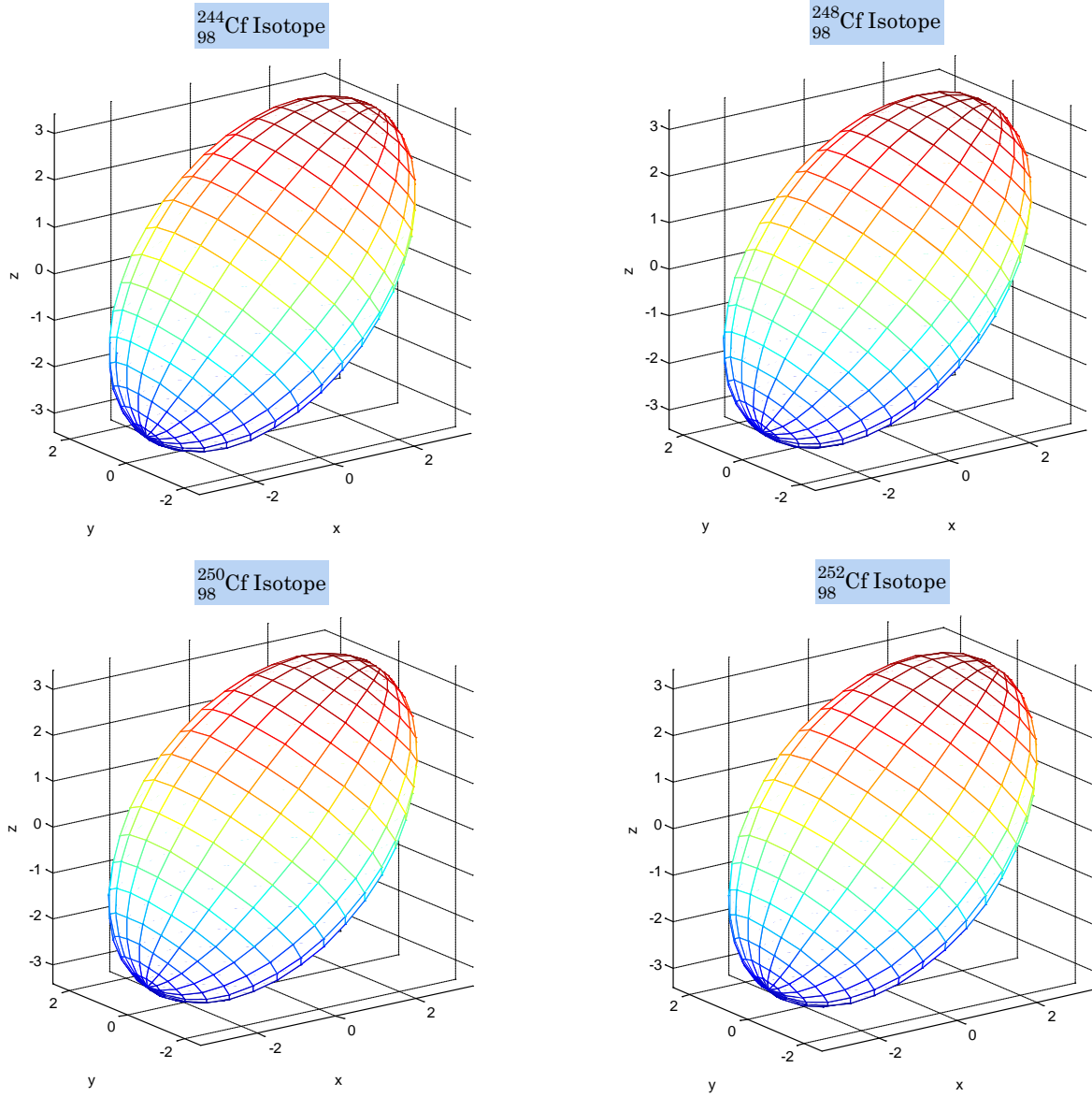
Figure(A-27): axially-symmetric quadrupole deformations, the prolate shape of Nucleus with $(x = y < z)$ (where z is the minor axis (b) (symmetric axis) and (x,y) are major axes (a) for Pu isotopes.

Appendix



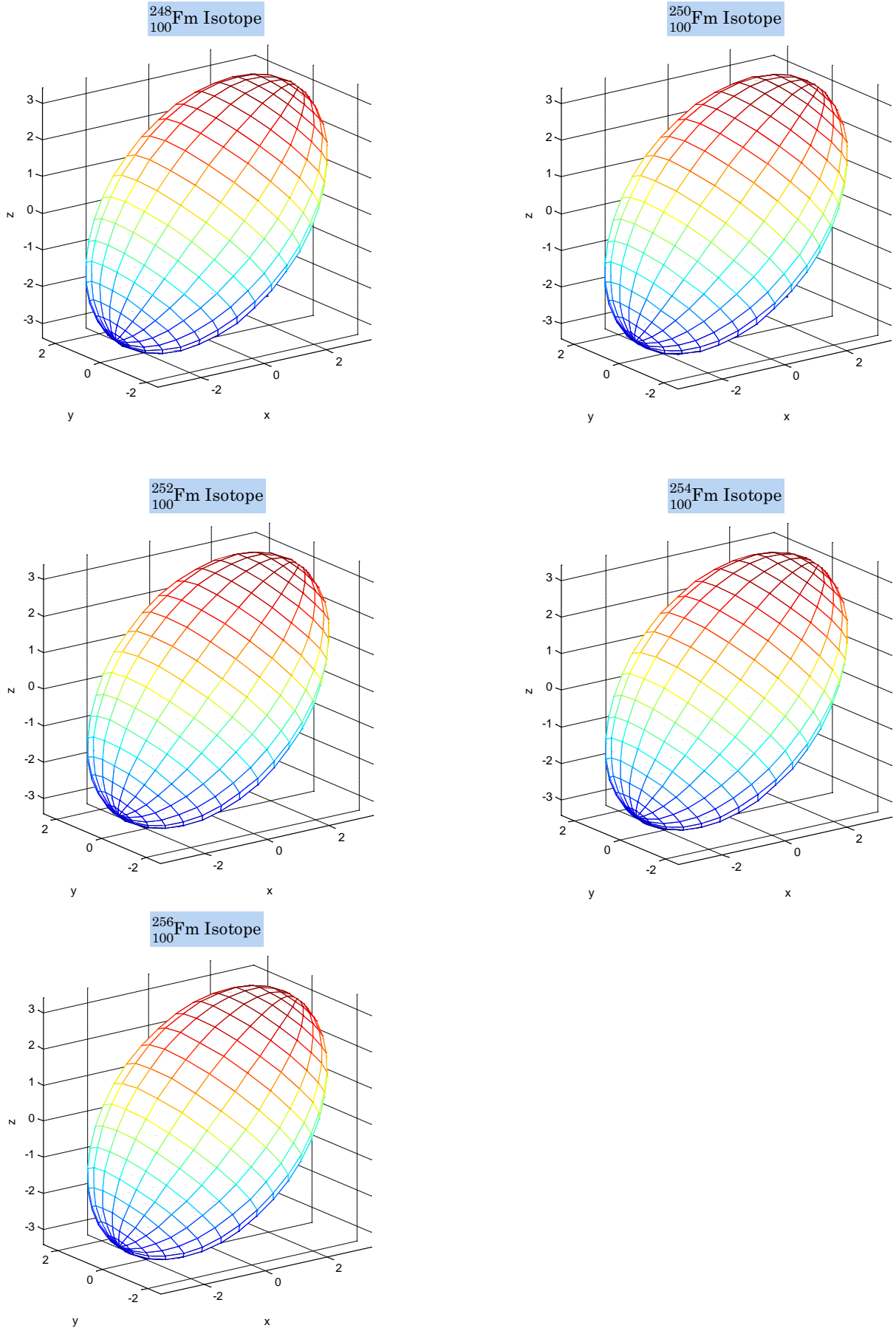
Figure(A-28): axially-symmetric quadrupole deformations, the prolate shape of Nucleus with ($x = y < z$) (where z is the minor axis (b) (symmetric axis) and (x,y) are major axes (a) for Cm isotopes.

Appendix



Figure(A-29): axially-symmetric quadrupole deformations, the prolate shape of Nucleus with $(x = y < z)$ (where z is the minor axis (b) (symmetric axis) and (x,y) are major axes (a) for Cf isotopes.

Appendix



Figure(A-30): axially-symmetric quadrupole deformations, the prolate shape of Nucleus with $(x = y < z)$ (where z is the minor axis (b) (symmetric axis) and (x,y) are major axes (a) for Fm isotopes.

الخلاصة

ركز البحث الحالي على دراسة أشكال النوى الزوجية- الزوجية ذات الأعداد الكتلية الأكبر من 100 ($A > 100$) ل(30) عنصر، والتي تضمنت دراسة معاملات التشوه (β_2) المشتقة من قيمة احتمالية الانتقال الكهربائي $B(E2) \uparrow$ المستندة على طاقة المستوي المتهيج الأول 2^+ (E_γ) ، وكذلك دراسة معاملات التشوه (δ) المشتقة من قيمة عزم رباعي القطب الكهربائي الذاتي (Q_0) وجذر مربع متوسط نصف القطر $\langle r^2 \rangle^{1/2}$.

ويتضح التنوع في أشكال النوى للنظائر المختارة وإختلافها من خلال رسم الأشكال ثنائية الأبعاد لنظائر العنصر الواحد ، إضافة الى رسم الأشكال ثلاثية الأبعاد المتماثلة محورياً للتمييز بينها وذلك بإستخدام المحاور شبه الرئيسية (a) وشبه الثانوية (b).

أن سلوك معاملات التشوه (β_2, δ) في النوى الزوجية - الزوجية يزودنا بالمعلومات الجيدة حول خصائص النوى السحرية ذات الأغلفة المغلقة فعلى سبيل المثال، عند حساب ورسم البارامترات لتلك النوى كدالة لعدد النيوترونات فإن الأشكال الكروية والقيم القليلة لهذه البارامترات سوف تظهر عند الأعداد السحرية للنيوترونات ($N = 50, 82, 126$).

أما من اجل المقارنة فإن قيم الانتقال الكهربائي المختزلة $B(E2) \uparrow$ للعمل الحالي والقيم المتنبأة (SSANM) تظهر لنا تبايناً طفيفاً بين هذه النتائج ، كون العمل الحالي يستند على إستخدام معادلة (GBF) (Global Best Fit) عند مقارنتها مع قيم (SSANM)، بالرغم من أنها تظهر نفس السلوك لمعظم العناصر المختارة.

أضافة الى ذلك تم حساب قيم (ΔR) (الفرق بين المحاور شبه الرئيسية a وشبه الثانوية b) باستخدام ثلاثة طرق، ووجد أن هذه النتائج كانت متقاربة الى حد ما.

أما قيم جذر متوسط مربع نصف القطر $r^2 > 1/2$ فقد تم مقارنتها مع القيم النظرية حيث كانت النتائج متوافقة بشكل كبير مع تلك القيم النظرية.

وفي نهاية البحث وجد أن جميع نوى النظائر للعناصر قيد الدراسة كانت مشوهة وذات أشكال بيضوية (prolate) ويكون هذا التشوه كبيراً في المناطق $(150 \leq A \leq 190)$ وكذلك $(A \leq 220)$ ، بإستثناء النظائر التي تمتلك عدد من النيوترونات أو البروتونات أو كلاهما مساوياً لعدد سحري فإن أشكال النوى تكون كروية متماثلة وذات زخم زاوي مساوي للصفر وتكون تلك النوى مستقرة بشكل خاص.

تم إجراء تلك الحسابات والرسومات بإستخدام برنامج الماتلاب النسخة (version 8.1) (2013).



جمهورية العراق
وزارة التعليم العالي والبحث العلمي
جامعة بغداد
كلية التربية للعلوم الصرفة / أبن الهيثم

"دراسة معاملات التشوه للعناصر ذات الأعداد الكتلية
الأكبر من 100 ($A > 100$) والمتضمنة (30) عنصراً"

رسالة مقدمة الى مجلس

كلية التربية للعلوم الصرفة / أبن الهيثم - جامعة بغداد
كجزء من متطلبات نيل درجة ماجستير علوم في الفيزياء

من قبل

حيدر عبد الزهرة زغير

(بكالوريوس 1995)

بإشراف

أ. م. د. سميرة أحمد ابراهيم